Spring 5-17-2010

Sea-Level Changes Along the U.S. Atlantic Coast: Implications for Glacial Isostatic Adjustment Models and Current Rates of Sea-Level Change

Simon E. Engelhart
University of Pennsylvania, simoneng@sas.upenn.edu

Sea-Level Changes Along the U.S. Atlantic Coast: Implications for Glacial Isostatic Adjustment Models and Current Rates of Sea-Level Change

Abstract
This study develops the first database of Holocene sea-level index points for the U.S. Atlantic coast using a standardized methodology. The database will help further understanding of the temporal and spatial variability in relative sea-level (RSL) rise, provide constraints on geophysical models and document ongoing crustal movements due to Glacial Isostatic Adjustment (GIA). I sub-divided the U.S. Atlantic coast into 16 areas based on distance from the center of the Laurentide Ice Sheet. Rates of RSL change were highest during the early Holocene and have been decreasing over time, due to the continued relaxation response of the Earth's mantle to GIA and the reduction of ice equivalent meltwater input around 7 ka. The maximum rate of RSL rise (c. 20 m since 8 ka) occurred in New Jersey and Delaware, which is subject to the greatest forebulge collapse. The rates of early Holocene (8 to 4 ka) rise were 3 - 5.5 mm a-1. I employed basal peat index points, which are subject to minimal compaction, to constrain models of GIA. I demonstrated that the current ICE-5G/6G VM5a models cannot provide a unique solution to the observations of RSL during the Holocene. I reduced the viscosity of the upper mantle by 50%, removing the discrepancy between the observations and predictions along the mid-Atlantic coastline. However, misfits still remain in Maine, northern Massachusetts and the Carolinas. Late Holocene (4 ka to present) RSL data are a proxy for crustal movements as the eustatic component was minimal during this time. Land subsidence is less than 0.8 mm a-1 in Maine, increasing to 1.7 mm a-1 in Delaware, and a return to rates lower than 0.9 mm a-1 in the Carolinas. This pattern results from the ongoing GIA due to the demise of the Laurentide Ice Sheet. I used these rates to remove the GIA component from tide gauge records to estimate a mean 20th century sea-level rise rate for the U.S. Atlantic coast of 1.8 ± 0.2 mm a-1. I identified a distinct spatial trend, increasing from Maine to South Carolina, which may be related to either the melting of the Greenland Ice Sheet, and/or ocean steric effects.

Degree Type
Dissertation

Degree Name
Doctor of Philosophy (PhD)

Graduate Group
Earth & Environmental Science

First Advisor
Benjamin P. Horton

Keywords
sea level, salt marsh, holocene, laurentide, climate, atlantic coast

Subject Categories
Earth Sciences

SEA-LEVEL CHANGES ALONG THE U.S. ATLANTIC COAST: IMPLICATIONS FOR GLACIAL ISOSTATIC ADJUSTMENT MODELS AND CURRENT RATES OF SEA-LEVEL CHANGE

Simon E. Engelhart

A DISSERTATION

in

Earth and Environmental Science

Presented to the Faculties of the University of Pennsylvania

in

Partial Fulfillment of the Requirements for the

Degree of Doctor of Philosophy

2010

Supervisor of Dissertation

_____

Dr. Benjamin P. Horton, Associate Professor, Earth and Environmental Science

Graduate Group Chairperson

_____

Dr. Arthur H. Johnson, Professor, Earth and Environmental Science

Dissertation Committee

Dr Frederick N. Scatena, Professor, Earth and Environmental Science

Dr Robert Giegengack, Professor, Earth and Environmental Science

Dr Torbjörn E. Törnqvist, Associate Professor, Tulane University

Sea-level changes along the U.S. Atlantic coast: Implications for Glacial Isostatic Adjustment Models and current rates of sea-level change

For Kate

ACKNOWLEDGEMENTS

I would firstly like to thank my supervisor Ben Horton. Ben's enthusiasm for understanding sea-level changes inspired me to study the topic as an undergraduate and continues to inspire me to this day. His encouragement, expertise, guidance and friendship, made this dissertation possible. A special debt of thanks must also go to Tor Törnqvist for his advice and constructive comments throughout my PhD. I would also like to thank my co-authors Dick Peltier and Bruce Douglas, who have provided invaluable advice and comments throughout the last five years.

I thank the entire faculty at the Department of Earth and Environmental Science, particularly my committee members, Fred Scatena and Bob Giegengack. Joan and Arlene have continually made my life easier providing administrative and organizational support.

A large component of any study is the people with which you share the experience. I would like to acknowledge the Sea-Level Research Laboratory, particularly Andrew "Derby" Kemp, Andrea Hawkes, Christopher Bernhardt and Candace Grandpre for informal discussions, help in the field and friendship. John Clark, Jamie Bedison and

Chuck Romanchock have been the best office mates you could ever wish to have.

I would like to acknowledge funding from the National Science Foundation, the Earthwatch Foundation, a Geological Society of America graduate student grant, the University of Pennsylvania Summer Stipend in Paleontology and research and teaching fellowships from the University of Pennsylvania. I particularly want to acknowledge the Thouron Family, who funded my first two years of graduate study.

Finally, I wish to thank my family, especially my Dad, whose emotional and financial support has allowed me to be in this position today. My fiancée Lucy has been the firm grounding on which this whole dissertation rests.

Finally, I am indebted to other researchers who have provided assistance throughout my PhD years including Roland Gehrels, Antony Long, Glenn Milne, Orson van de Plassche, Ian Shennan, Rob Thieler and Chris Vane.

ABSTRACT

SEA-LEVEL CHANGES ALONG THE US ATLANTIC COAST: IMPLICATIONS FOR GLACIAL ISOSTATIC ADJUSTMENT MODELS AND CURRENT RATES OF SEA-LEVEL CHANGE

Simon E. Engelhart

Benjamin P. Horton

This study develops the first database of Holocene sea-level index points for the U.S. Atlantic coast using a standardized methodology. The database will help further understanding of the temporal and spatial variability in relative sea-level (RSL) rise, provide constraints on geophysical models and document ongoing crustal movements due to Glacial Isostatic Adjustment (GIA). I sub-divided the U.S. Atlantic coast into 16 areas based on distance from the center of the Laurentide Ice Sheet. Rates of RSL change were highest during the early Holocene and have been decreasing over time, due to the continued relaxation response of the Earth's mantle to GIA and the reduction of ice equivalent meltwater input around 7 ka. The maximum rate of RSL rise (c. 20 m since 8 ka) occurred in New Jersey and Delaware, which is subject to the greatest forebulge collapse. The rates of early Holocene (8 to 4 ka) rise were 3 - 5.5 mm a^{-1}. I employed basal peat index points, which are subject to minimal compaction, to constrain models of GIA. I demonstrated that the current ICE-5G/6G VM5a models cannot provide a unique solution to the observations of RSL during the Holocene. I reduced the viscosity of the upper mantle by 50%, removing the discrepancy between the observations and predictions along the mid-Atlantic coastline. However, misfits still remain in Maine,

northern Massachusetts and the Carolinas. Late Holocene (4 ka to present) RSL data are a proxy for crustal movements as the eustatic component was minimal during this time. Land subsidence is less than 0.8 mm a^{-1} in Maine, increasing to 1.7 mm a^{-1} in Delaware, and a return to rates lower than 0.9 mm a^{-1} in the Carolinas. This pattern results from the ongoing GIA due to the demise of the Laurentide Ice Sheet. I used these rates to remove the GIA component from tide gauge records to estimate a mean 20th century sea-level rise rate for the U.S. Atlantic coast of 1.8 ± 0.2 mm a^{-1}. I identified a distinct spatial trend, increasing from Maine to South Carolina, which may be related to either the melting of the Greenland Ice Sheet, and/or ocean steric effects

List of Contents

List of Figures

Chapter Two

Chapter Five

List of Tables

Chapter Three

Chapter Five

CHAPTER ONE

INTRODUCTION

1.1 CONTEXT

International Geoscience Programme 495 (*Quaternary Land – Ocean Interactions: Driving Mechanisms and Coastal Responses*) seeks to understand the relative sea-level (RSL) changes since the Last Glacial Maximum (LGM). This aim can only be achieved if reliable reconstructions of RSL from around the globe are available. The U.S. Atlantic coast has a wealth of RSL research, commencing in the 1960s (e.g. Stuiver and Daddario, 1963; Bloom, 1963; Kaye and Barghoorn, 1964: Redfield, 1967; Belknap and Kraft, 1977; Field et al., 1979; Cinquemani et al., 1982; Pardi et al., 1984; van de Plassche, 1989; Gehrels and Belknap, 1993; Fletcher et al., 1993; Kelley et al., 1995; Barnhardt et al., 1995; Nikitina et al, 2000; Miller et al., 2009; Kemp et al., 2009) but the data has never been critically validated to ensure its accuracy.

To address this significant gap in our understanding, my research follows the consistent methodology developed by the IGCP projects such as 61 and 200 (e.g. Cinquemani et al., 1982; Greensmith and Tooley, 1982; Shennan, 1987) to produce validated records of Holocene RSL for the U.S. Atlantic coast from (un)published radiocarbon dated sea-level data. The U.S. Atlantic coast is important as it contains both near-field (formerly

ice covered) and intermediate-field (within the peripheral forebulge) sites, resulting in spatially variable RSL histories during the Holocne due to the different interplay of the eustatic and isostatic parameters (e.g. Clark et al., 1978; Lambeck, 1993; Milne et al., 2005).

Sites from the U.S. Atlantic coast constitute vital constraints upon the dynamical models of the Glacial Isostatic Adjustment (GIA) process (e.g. Peltier, 1996). GIA models have been used to understand the rheology of the earth (e.g. Peltier, 1996; Davis and Mitrovica, 1996; Shennan et al, 2002; Lambeck et al., 2004; Vink et al., 2007) and constrain ice equivalent meltwater input (Milne et al., 2002, 2005; Bassett et al., 2005; Peltier et al., 2005). Further, GIA models have been employed to filter tide gauge (e.g. Tushingham and Peltier, 1989; Peltier, 1996; Davis and Mitrovica, 1996) and satellite (Velicogna and Wahr, 2005, 2006; Velicogna, 2009) records of secular sea-level change so as to isolate the contribution to this signal due to climate warming. There is an urgent need for a sufficiently accurate model of the GIA process to inform the global data set currently being produced on the time dependence of the gravitational field of the planet by the Gravity Recovery and Climate Experiment (GRACE) (Cazenave et al., 2009). Geodetic constraints may be placed on GIA models by satellite techniques (e.g. Argus et al., 1999; Snay et al., 2007), but they lack the vertical precision of established geological methods (e.g. Shennan, 1989; Shennan and Horton, 2002) and cannot reconstruct changes prior to the 1990s.

1.2 THESIS AIMS

This thesis addresses three complementary aims with associated research questions:

1) To establish a quality controlled sea-level database from the Atlantic coast of the United States for the Holocene (11.7 ka to present).

There is an urgent need for a re-assessment of the quality of the observational evidence of former sea levels from the Atlantic coast of the United States, as well as concepts inherent in the interpretation of data. Previous research has failed to meet the fundamental criteria to produce an accurate sea-level database (Donnelly, 1998). This is important, as the rates of sea-level rise obtained during this period represent the fundamental basis for comparison with the historical and present day changes. Different types of sea-level indicators have different degrees of precision, but this is often not acknowledged (Zerbini, 2000) and common errors inherent to sea-level research are rarely quantified (e.g. Shennan, 1986).

The research questions are:

1. Can the previous sea-level research along the U.S. Atlantic coast meet the validation criteria to produce a sea-level index point?
2. What is the spatial and temporal distribution of the validated relative sea-level data?

3. Is there spatial heterogeneity within the observations of former RSL along the U.S. Atlantic coast, and if so, what is driving this variability?

4. Has RSL risen above present during the last 6 ka?

5. Can the temporal variation in the ice equivalent meltwater input be identified?

6. Can the effects of local processes such as compaction be isolated from the index points?

2) Apply the database to improve the accuracy of models of the GIA process along the U.S. Atlantic coast.

Models of the GIA process are currently employed to filter tide gauge (e.g. Peltier, 1996; Davis et al., 2008) and satellite (e.g. Velicogna and Wahr, 2005, 2006; Wahr, 2006; Velicogna, 2009) records of secular sea-level change so as to isolate the contribution to this signal due to climate warming. There is a need for a sufficiently accurate model of the GIA process, as the results from the GRACE mission are highly dependent on the removal of GIA trends to estimate increases in ocean volume (Cazenave et al., 2009). Whilst the current generation model (ICE-5G VM5a) provides an accurate fit to the observations from regions once covered by the Laurentide Ice Sheet (e.g. Hudson Bay), it is currently unknown whether this holds true for sites within the periphery of the ice sheet along the U.S. Atlantic coast. This is an independent test of the GIA model, as the data have not previously been used to constrain it.

The research questions are:

1. Can the current generation GIA model (ICE-5G VM5a) accurately predict the observations of Holocene RSLs from the U.S. Atlantic coast?
2. If a misfit between the model predictions and the observations is observed, is it systematic?
3. Can modifications to the earth and/or ice models reconcile any of the variance between observations and predictions?

3) Document current crustal motions of the U.S. Atlantic coast as a tool to further understand 20th century sea-level rise.

Background rates of RSL change in the late Holocene (4 ka to present) provide the baseline that changes in the 20th and 21st centuries must be superimposed upon (e.g. Velicogna and Wahr, 2006; Church and White, 2006; Rahmstorf et al., 2007; Jevrejeva et al., 2008). Late Holocene rates provide a regional perspective on spatial variability in RSL rise (e.g. Milne et al., 2009; Gehrels et al., in press). Crustal movements can be estimated from late Holocene RSL data as the ice equivalent meltwater input was zero or minimal, there are minimal tectonic effects on a passive margin and compaction can be reduced by utilizing basal peat. A comparison may be made between the crustal movements estimated by geological methods and global positioning systems.

The research questions to be answered are:

1. What are the late Holocene crustal motions associated with the removal of the Laurentide Ice Sheet?
2. Do the estimates of crustal motion have a spatial pattern along the U.S. Atlantic coast?
3. How do late Holocene rates compare with estimates from GPS observations?
4. Does the 20th century record of sea-level rise from the U.S. Atlantic coast exhibit spatial variability?

1.3 THESIS STRUCTURE

Chapter Two presents the scientific justification related to this research and associated background information. An overview of sea-level data since the LGM is provided to place this study into context. The methodology and terminology of reconstructing observations of Holocene RSL is outlined and compared to alternative methods of estimating RSL. These include GIA models, tide gauges, satellite altimetry, gravity measurments and global positioning systems.

Chapter Three describes the development of the U.S. Atlantic coast RSL database. The chapter aims to document the current state of knowledge concerning the RSL history of the U.S. Atlantic coast by validating published and unpublished radiocarbon dated sea-level indicators. The controls on spatial and temporal variability within the database

are discussed. The chapter provides a discussion of the advantages and limitations of the database. This paper is to be submitted to Quaternary Science Reviews.

Chapter Four demonstrates the application of observations of former RSL in constraining models of the GIA process. This chapter compares the database of Holocene RSL to the current state of the art GIA model of Dick Peltier (University of Toronto). Observed misfits between the model predictions and data are investigated and refined ice and earth models are presented. Further potential refinements are suggested which may lead to greater improvement in the variance between observed and modeled RSL. I will submit the publication to Geophysical Research Letters.

Chapter Five investigates the rates of glacial isostatic adjustment during the last 4 ka. Basal salt marsh peat from Maine to South Carolina is used as a proxy for the continuing glacial isostatic adjustment. The GIA observations are removed from 20th century tide gauge records to understand the acceleration in sea-level rise during this time period and to investigate spatial variability. This study has been accepted for publication in Geology on the 1st December 2009.

Chapter Six summarizes the main conclusions drawn from this research and makes recommendations for future relative sea-level studies on the US Atlantic coast.

CHAPTER TWO

Reconstructing Late Quaternary Relative Sea Level: Methodologies and Observations

2.1 INTRODUCTION

Observations of relative sea level (RSL) during the late Quaternary are significant to a number of disciplines in the Earth sciences (e.g. Alley et al., 2005; Rohling, 2008; Siddall et al., 2009). RSL data can be employed to provide information on the rheology of the Earth (Shennan et al., 2002; Lambeck et al., 2004; Peltier, 2004; Horton et al., 2005; Lambeck and Purcell, 2005; Milne et al., 2005; Vink et al., 2007; Brooks et al., 2008) and ice sheet reconstructions, including sources of meltwater input (Milne et al., 2002; Peltier and Fairbanks, 2006). Observations provide information on coastal evolution (e.g. Kraft, 1971; McLean, 1984; Barrie and Conway, 2002: Waller and Long, 2003; Behre, 2004; Massey and Taylor, 2007), as sea level serves as the base level for continental denudation (Summerfield, 1991). This further drives our understanding of the links between coastal processes and human development (e.g. Stanley, 1998; Richardson et al., 2005; Day et al., 2007; Turney et al, 2007).

The Database approach of reconstructing RSL since the Last Glacial Maximum (LGM) has been successful for the UK (e.g. Shennan, 1989; Shennan and Horton, 2002; Horton and Shennan, 2009; Shennan et al., 2009), northwest Europe (e.g. Vink et al., 2007), Mediterranean (Lambeck and Bard, 2000), Canada (e.g. Shaw et al. (2002), the

Caribbean (Toscano and Macintyre, 2003; Milne et al., 2005), South America (Rostami et al., 2000; Milne et al., 2005; Angulo et al., 2006), Southeast Asia (Horton et al., 2005; Woodroffe and Horton, 2005), China (Zong et al., 2004) and Australia (e.g. Larcombe, 1995) . These databases have been used to calibrate models of earth rheology (e.g. Peltier et al., 2002; Vink et al., 2007), constrain the source and magnitude of ice equivalent meltwater input (e.g. Shennan et al., 2002; Bassett et al., 2005; Milne et al., 2005); investigate the effects of sediment loading and compaction (e.g. Horton and Shennan, 2009), understanding the effects of tidal range change (e.g. Shennan et al., 2000; 2003), producing baseline rates of RSL rise to compare with 20th century rates (e.g. Shennan and Horton, 2002; Shennan et al., 2009) and constraining instrumental observations of crustal movements (e.g. Teferle et al., 2009).

While there have been previous attempts to produce a database for the U.S. Atlantic coast (e.g. Bloom, 1967; Newman et al., 1980, 1987; Cinquemani et al., 1982; Pardi and Newman, 1987; Gornitz and Seeber, 1990; Tushingham and Peltier, 1992; Peltier, 1996; Donnelly, 1998) the fundamental criteria to produce an accurate sea-level database have not been met. To address this I have collected over 50 fields of information for each sample within the U.S. Atlantic coast database to enable me to validate samples as sea-level index points. These include both data obtained from the authors (e.g. location, lab code, radiocarbon age plus error) as well as calculations and interpretations made by myself (e.g. calibrated age and error, indicative meaning of sample, total vertical

error). Conditional filters can be applied to these fields, such as possible contamination and stratigraphic context, to define those index points that I believe, from the published information, to be reliably related to past tide levels.

This chapter introduces the methodology and terminology used when reconstructing RSL in the U.S. Atlantic coast database. I provide a description of the four components that combine to produce the RSL history at any point on the globe and describe the different forms of RSL curves that are seen depending on the proximity to ice loading during the LGM. I outline the requirements for a sample to be validated as a sea-level index point and discuss potential errors induced when reconstructing RSL, including compaction, tidal range and chronology. Modern instrumental methods for reconstructing components of RSL and GIA modeling are discussed. Finally, I discuss the geological and geomorphological setting of my study area; the U.S. Atlantic coast.

2.2 RELATIVE SEA LEVEL

The processes that interact to produce a RSL curve at any one location on the surface of the Earth is commonly described by the following equation (Shennan, 2009):

$$\Delta\xi_{RSL}(\tau,\psi) = \Delta\xi_{eus}(\tau) + \Delta\xi_{iso}(\tau,\psi) + \Delta\xi_{tect}(\tau,\psi)+\Delta\xi_{local}(\tau,\psi) + \Delta\xi_{error}(\tau,\psi)$$

where τ and ψ represent time and space. $\Delta\xi_{eus}(\tau)$is the time-dependent eustatic function, $\Delta\xi_{iso}(\tau,\psi)$is the total isostatic effect of the glacial rebound process including both the ice (glacio-isostatic) and water (hydro-isostatic) load contributions, $\Delta\xi_{tect}(\tau,\psi)$ is any tectonic effects, while $\Delta\xi_{local}(\tau,\psi)$ represents the local process involved (Shennan and Horton, 2002). $\Delta\xi_{error}(\tau,\psi)$ is unknown but we attempt to minimize this component by employing proven methodologies.

2.2.1 Eustasy

The concept of eustasy was proposed by Eduard Seuss in 1888 to reflect global changes in sea level due to the changing ratio between water stored in the oceans and water stored on the continents as ice. This principle focused on the belief that any meltwater input to the oceans would be evenly distributed over the entire globe. With the development of radiocarbon dating (Libby, 1952) there was an increase in the collection of RSL data as scientists sought to identify the 'global eustatic curve' (e.g. Fairbridge, 1961). The development of geophysical models of RSL (e.g. Peltier et al., 1974, Farrell and Clark, 1976; Clark et al., 1978) and the understanding that gravitational effects were an important control on RSL (e.g. Clark and Lingle, 1977; Clark et al., 1978) highlighted that a global eustatic curve could not exist (Figure 2.1). Analysis of RSL data confirmed that the eustatic curve was an immeasurable factor at any one point on Earth (Kidson, 1986) and that it could only ever be inferred from sea-level data at multiple locations (e.g. Bassett et al., 2005).

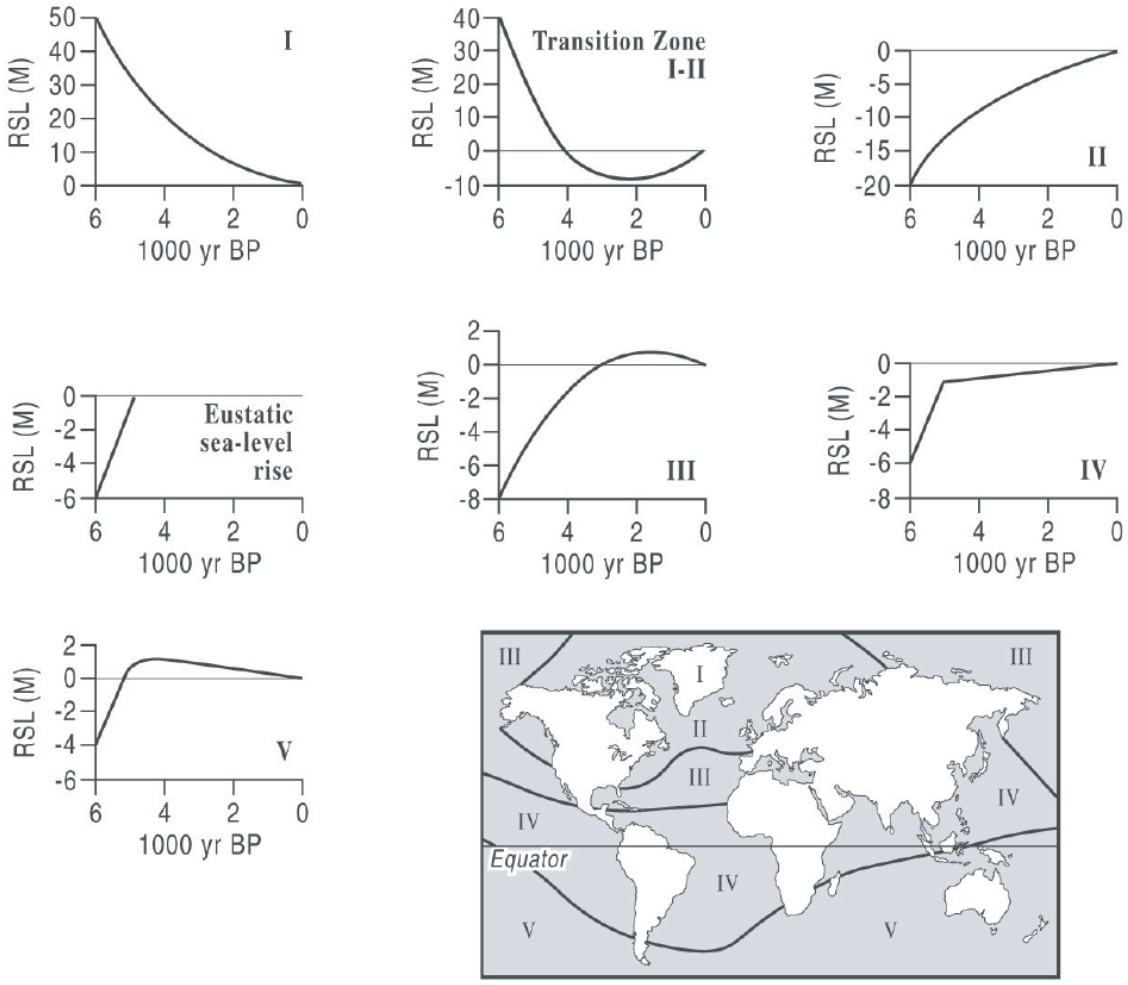

Figure 2.1 - Distribution of regional sea-level zones and typical relative sea-level curves predicted by Clark et al. (1978) using a gravitationally self consistent model of the GIA process.

Research has demonstrated that while the ice equivalent meltwater input has only a temporal component, changes in the gravitational attraction of melting and accreting ice sheets (e.g. Clark and Lingle, 1977) and rotational changes (e.g. Mörner, 1976), can result in spatially variable response to ice equivalent meltwater input, termed geoidal eustasy. Therefore, the ocean surface cannot be considered as a flat surface, but one with topography. This theory has been applied to 'fingerprint' the sources of meltwater input during the 20th century (e.g. Conrad and Hager, 1997; Mitrovica et al., 2001; Tamisiea et al., 2001) and to predict the effects of future melting scenarios (e.g. Mitrovica et al., 2009) (Figure 2.2).

The eustatic minimum coincides with the last glacial maximum (LGM), previously considered to be between 24 - 21 ka (Aharon, 1984; Fairbanks, 1989; Bard et al., 1990a, b; Pirazzoli, 1996; Fleming et al., 1998; Yokoyama et al., 2001; Clark and Mix, 2002; Peltier, 2002; Bird et al., 2005; Murray-Wallace, 2007; De Deckker and Yokoyama, 2009) when as much as 50 million km^3 of ice was transferred between the oceans and continents (e.g. Fleming et al., 1997; Yokoyama et al., 2000; Lambeck et al., 2002). However, there is conflicting evidence from an updated Barbados record that suggests that this should be 26 ka with 21 ka marking the commencement of deglaciation (Peltier and Fairbanks, 2006). Further, there is controversy surrounding the eustatic minimum itself, with estimates varying between 135 and 120 m (e.g. Bard et al., 1990; Yokoyama

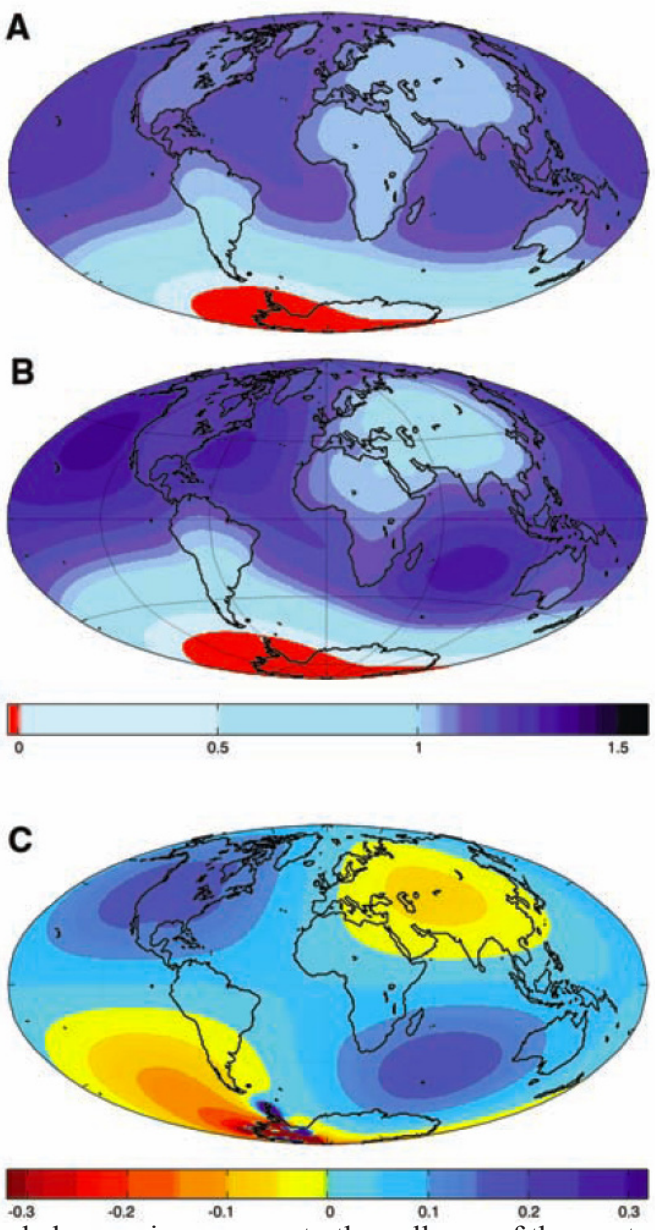

Figure 2.2 - Sea-level changes in response to the collapse of the western Antarctic ice sheet by using A) a standard sea-level theory and B) sea-level theory incorporating rotational feedback effects. C) The difference between the predictions using the two theories. Mitrovica et al. (2009).

et al., 2000; Peltier and Fairbanks, 2006). From deglaciation RSL rise proceeded at c. 6 mm a^{-1} (Fleming et al., 1998) before an increase to rates of c. 10 mm a^{-1} between 17 – 7 ka (Fleming et al., 1998). However, this rate was not constant but exhibited departures termed 'meltwater pulses' of up to 40 mm a^{-1} (Fairbanks, 1989, Alley et al., 2005; Peltier and Fairbanks, 2006). The sources of these meltwater pulses remain contentious. Peltier (2005) favors a Laurentian source for meltwater pulse 1a (c. 14.5 ka) whereas Clark et al. (2002) and Bassett et al. (2005) suggest that variability between models and observations during this time can be reduced with an Antarctic source. There is further controversy surrounding the termination of eustatic input during the late Holocene. Peltier (1998, 2002) proposes that meltwater input ceased c. 4 ka, whereas other research groups allow either 0.1 - 0.2 mm a^{-1} melting from 4 ka to 2 ka (e.g. Lambeck, 2002) or propose a scenario with continued melting to 1 ka (Fleming et al., 1998).

2.2.2 Isostasy

The first known documentation of postglacial land uplift is dated to A.D. 1491, when the inhabitants of the Swedish town of Östhammar reported that fishing boats could no longer reach the town "due to a growth of the land at the sea" (Ekman, 1991). The influence of istostasy on RSL histories was further understood from the depression of the surface of the earth by large continental ice sheets at the LGM. The response to this loading continues to the present day (e.g. Walcott 1972, Peltier et al., 1978). Therefore, different areas will experience variable RSL histories and can be classified as near-, intermediate-

and far-field regions (e.g. Clark et al., 1978). Near-field (e.g. Greenland, Canada, Northwest Scotland) regions are or were previously underneath ice masses, which caused the solid earth to subside. Following deglaciation, the solid earth uplifts as it regains isostatic equilibrium. At southern Greenland, the ice load was > 1.5 km thick (Bennike and Bjorck, 2002). As the depressed crust starts to uplift, RSL falls monotonically from the LGM to 2 ka (Long et al. 2003) (Figure 2.3). Long et al. (2003) demonstrated that the fall in RSL commenced from 108 m at 10.6 – 10.2 ka until it intersected present sea level at 3.5 ka. At 1.8 ka, RSL started to rise at c. 2 mm a^{-1} to the present. This rise is associated with the neoglaciation of Greenland, which caused the region to subside. In regions with thinner ice load (e.g. Arisaig, Scotland, < 1 km (Shennan et al., 2006)) the RSL curve can be distinctly non-monotonic. Shennan et al. (2005) showed an initial fall in RSL after the LGM due to rapid isostatic uplift (Figure 2.4). In the early to mid Holocene the isostatic process subsides to less than the eustatic input, resulting in a slight RSL rise. The declining eustatic function after 6 ka causes a further switch as RSL history is dominated by the continuing low rate of isostatic uplift.

Intemediate-field regions (e.g. southeast England, France, Delaware) are found at the periphery of the ice sheet where a forebulge is present due to the displacement of mantle material from near-field regions (e.g. Wu and Peltier, 1983). Therefore, areas within the periphery of the ice sheet were at a higher elevation with respect to the geoid at the LGM than they are at present. With the removal of the ice sheet, mantle material flowed from

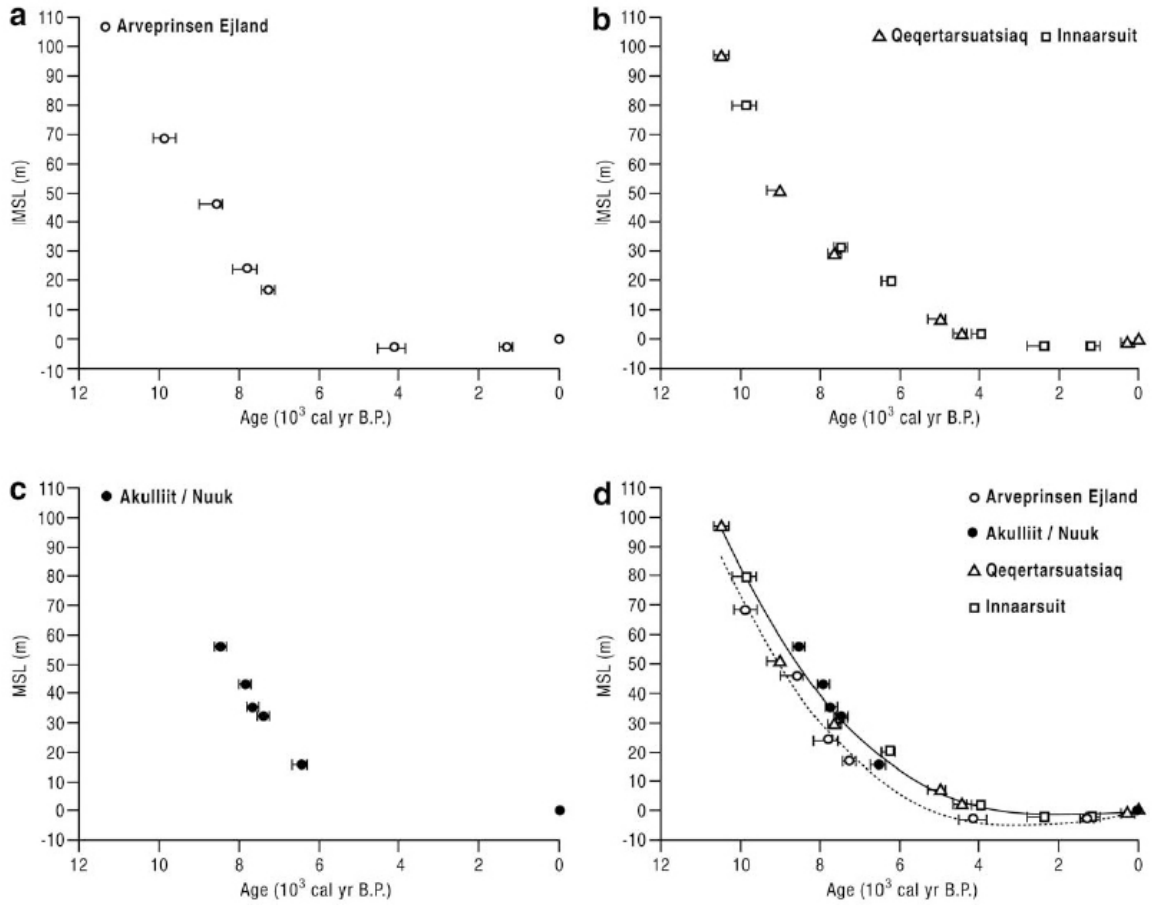

Figure 2.3 - Relative sea-level curves for four locations in southern Greenland. The trend lines summarizing the data are third-order polynomials. Long et al. (2003)

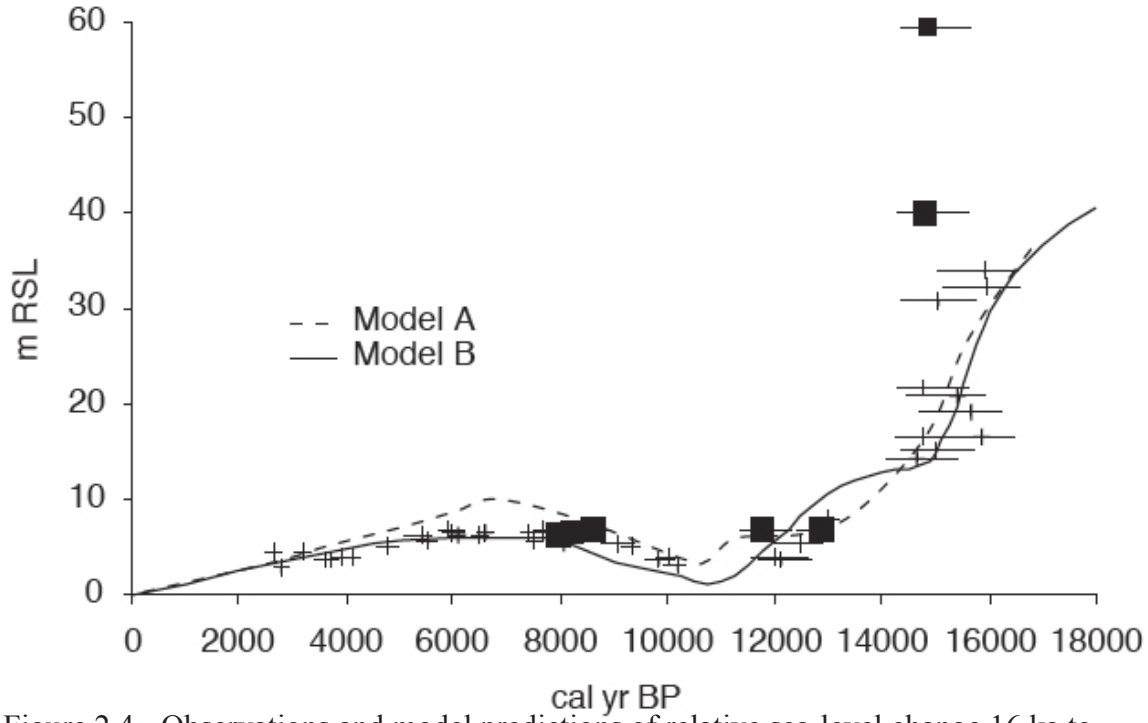

Figure 2.4 - Observations and model predictions of relative sea-level change 16 ka to present from Arisaig, Scotland. Relative sea level must lie at or below limiting dates, shown as solid black squares. Model predictions come from A) Shennan et al. (2000) and B) Peltier et al. (2002). Shennan et al. (2005).

the peripheral forebulge resulting in subsidence. As glaciation was a stepwise process and did not occur instantly, the movement of the mantle material varies over time and results in unique RSL curves at different intermediate-field areas (e.g. Tushingham and Peltier, 1992). RSL rise is expected to slow due to the exponential form of the forebulge collapse (e.g. Wu and Peltier, 1983).

Nikitina et al. (2000) presented a late Glacial RSL record (Figure 2.5) from the inner and outer Delaware estuary; an intermediate-field site. The record is well constrained by sea-level data from 7 ka to present. RSL rose at a decreasing rate through the mid and late Holocene. RSL rise decreased from 3.0 ± 0.2 mm a^{-1} from 7 – 5 ka, to 1.9 ± 0.1 mm a^{-1} from 4 – 1.25 ka. A further reduction is seen from 1.25 ka to present to 0.9 ± 0.07 mm a^{-1}.

Far-field areas are not directly affected by the ice loading or the peripheral forebulge. In these areas the effects of hydro-isostasy become dominant (e.g. Milne and Mitrovica, 2002). These effects consist of the subsidence of the oceanic crust due to water loading (e.g. Peltier et al., 2009), the levering effect of a reduced sea-level position on the edge of the continental shelf (e.g. Mitrovica and Milne, 2002) (Figure 2.6) and the movement of water to occupy areas of forebulge collapse within the ocean (equatorial ocean siphoning; Mitrovica and Peltier, 1991).

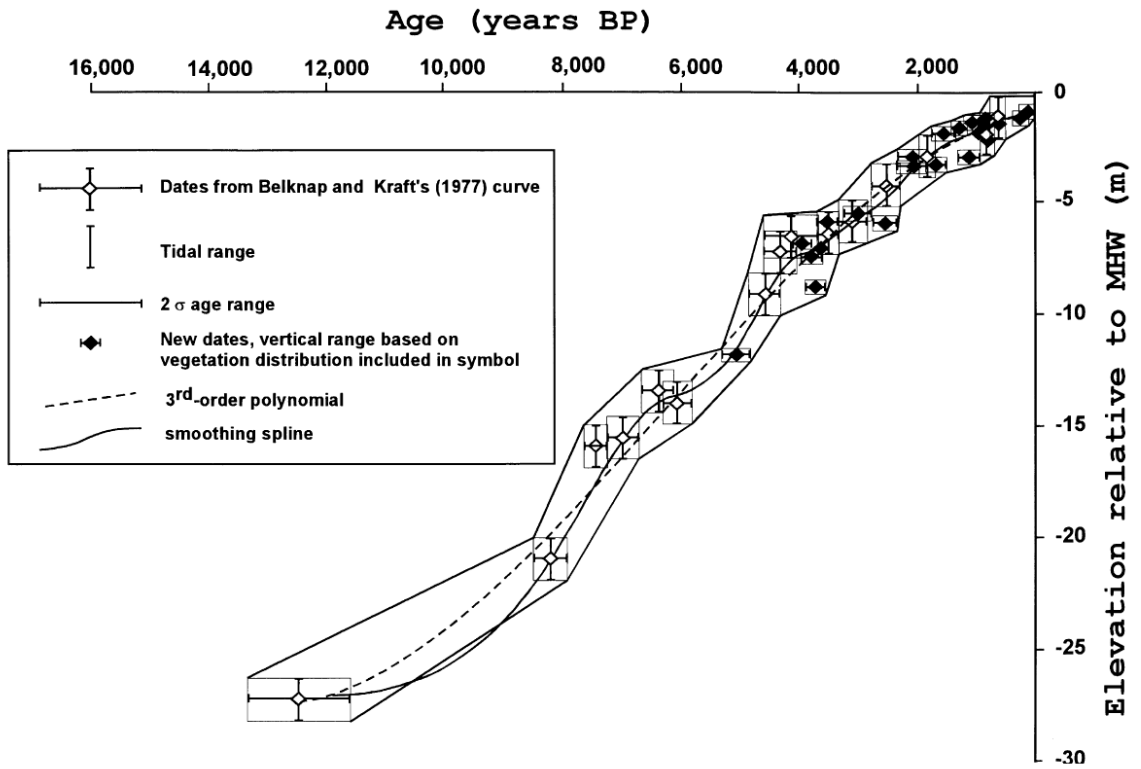

Figure 2.5 - Updated relative local sea-level curve for Delaware from Nikitina et al. (2000).

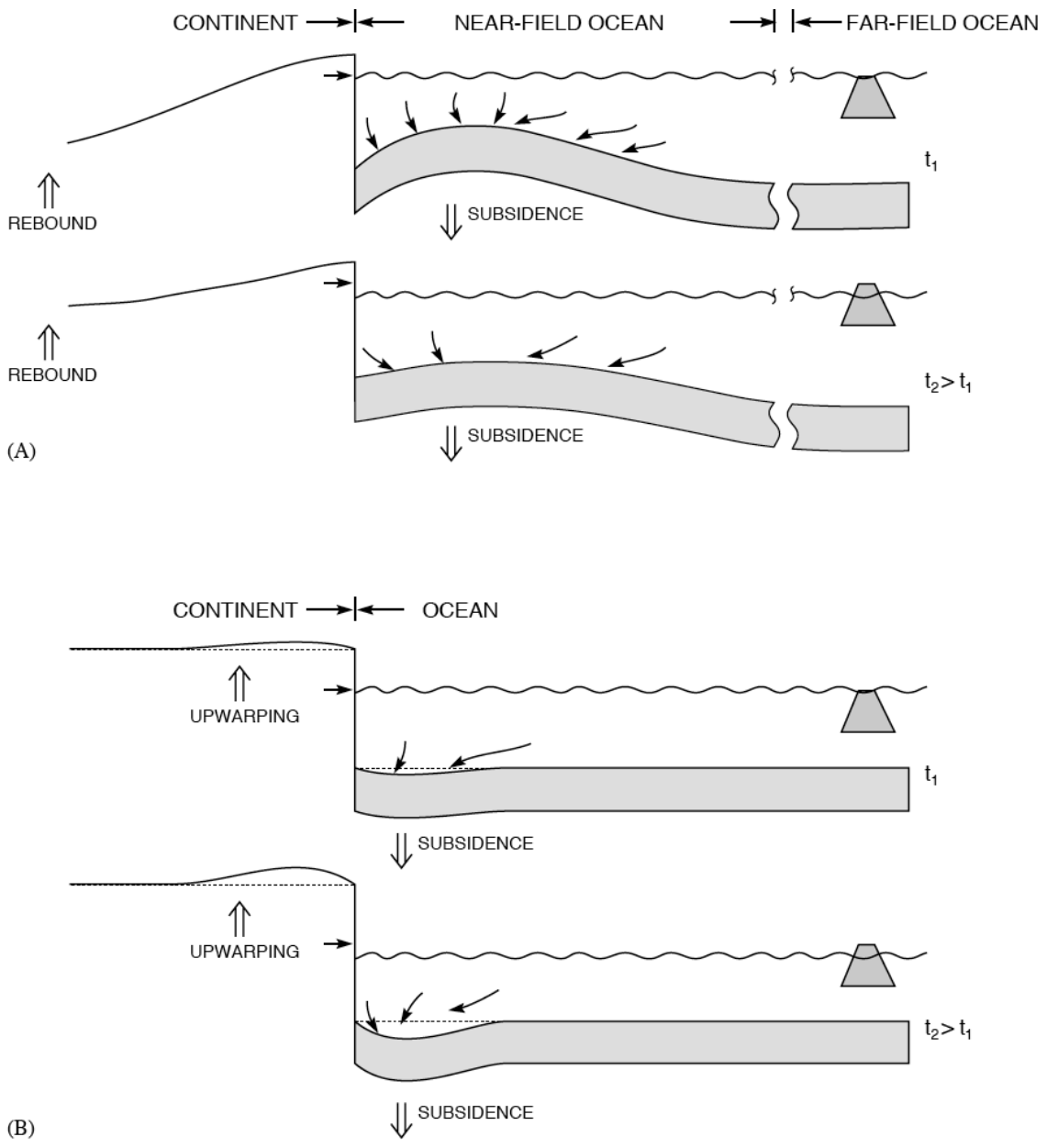

Figure 2.6 - A schematic illustrating the two physical mechanisms that dominate late Holocene sea-level change in far-field locations. A) Equatorial ocean siphoning and B) ocean induced loading of continental margins. Milne and Mitrovica (2002).

Far-field sites have commonly been chosen as locations for RSL reconstructions since deglaciation, as it was believed that this offered the opportunity to minimize contamination from the effects of isostasy and focus solely on the eustatic component. Records have been produced from a variety of sea-level indicators (e.g. corals, foraminifera) from the Sunda Shelf (Hanebuth et al., 2000), Tahiti (Bard et al., 1996; Montaggioni et al., 1997), the Huon Peninsula (Chappell, 1974; Chappell and Polach, 1991; Chappell et al., 1996), Australia (Thom and Chappell, 1975; Thom and Roy, 1985; Yokoyama et al., 2000) and the classic records from Barbados (Fairbanks 1989, Bard et al., 1990a, b; Peltier and Fairbanks, 2006). Hanebuth et al. (2000) presented a RSL record from 21 – 10 ka for the Sunda Shelf (Figure 2.7). The reconstruction is based on sediments from a delta plain, including mangrove and tidal flat deposits. The RSL data fills the gap from 21 – 14 ka, where there was previously a shortage of RSL data. Furthermore, it confirms the reconstructions of far-field sea level based on coral data. An initial slow rise in RSL from the termination of the LGM at 21 ka, is punctuated by a rapid increase of 16 m within 300 a (14.6 – 14.3 ka). This has previously been identified from the Barbados record (Fairbanks, 1989) and is termed meltwater pulse 1A.

However, recent research has suggested that many of these studies are not from areas ideal for inferring the eustatic signal (Milne and Mitrovica, 2008), due to sensitivity to ice model or mantle viscosity choices. Therefore, GIA models can guide field scientists to regions where the RSL history should closely approximate the eustatic function

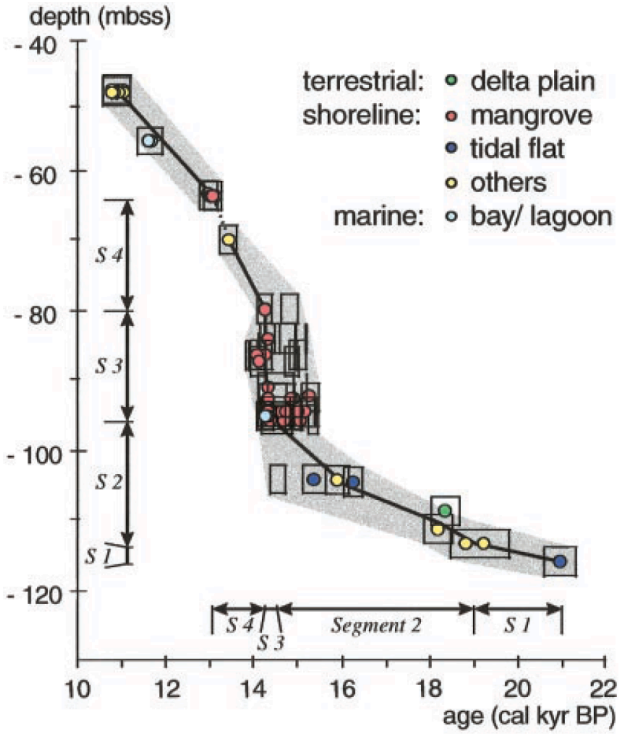

Figure 2.7 - Sea-level curve for the Sunda Shelf derived from shoreline facies. Hanebuth et al. (2000).

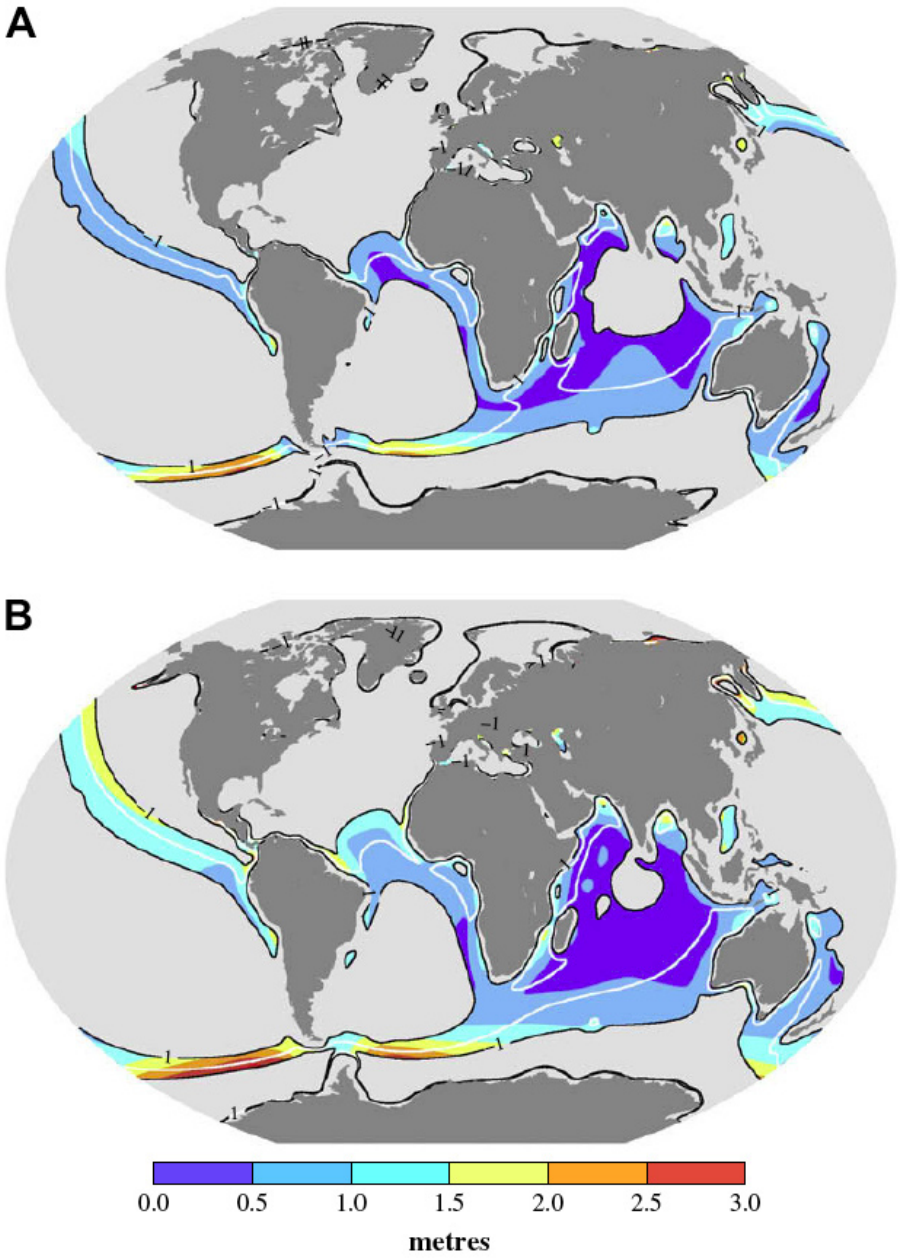

Figure 2.8 - Zones in which the RSL predictions lie within 1 m of the mean eustatic value at 6 ka. Frames A and B denote the results for the Bassett et al. (2005) and ICE-5G models, respectively. Milne and Mitrovica (2008).

at different points in time to test the current eustatic models (Figure 2.8) (Milne and Mitrovica, 2008).

2.2.3 Tectonics

One-third of the Earth's coastal margins lie along or near tectonically active plate boundaries (Nelson, 2007). Both geological (e.g. Atwater, 1989; Long and Shennan, 1994; Nelson et al., 1996) and instrumental (e.g. Pirazzoli, 1996; Scholz, 2002; Ota and Yamaguchi, 2004) methods have been applied to understand the patterns of deformation associated with active margins. Indeed, far-field records used to constrain the ice equivalent meltwater input including Barbados (e.g. Fairbanks, 1989), Tahiti (e.g. Bard et al., 1996) and Papua New Guinea (e.g. Chappell and Polach, 1991) must be corrected for the role of tectonics since the LGM. However, tectonic effects are considered to be negligible on passive margins such as the U.S. Atlantic coast during the late Quaternary (e.g. Szabo, 1985). Evidence for neotectonic activity as an explanation for differing RSL curves has also been rejected after careful consideration of the data (e.g. Gehrels and Belknap, 1993; van de Plassche et al., 2002).

2.2.4 Local

The total effect of local process at a site can be expressed schematically (Shennan and Horton, 2002):

$$\Delta\xi_{local}(\tau,\psi) = \Delta\xi_{tide}(\tau,\psi) + \Delta\xi_{sed}(\tau,\psi)$$

where$\Delta\xi_{tide}(\tau,\psi)$ is the total effect of tidal regime changes and the elevation of the sediment with reference to tide levels at the time of deposition, and $\Delta\xi_{sed}(\tau,\psi)$ is the total effect of sediment consolidation since the time of deposition.

The local effects on RSL are principally sediment compaction under its own and other sediment package's weight (e.g. Jelgersma, 1961; Kaye and Barghoorn, 1964) and changes in tidal regime due to differing paleogeographies in the past (e.g. Scott and Greenberg, 1983; Gehrels et al., 1995; Shennan et al., 2000, 2003). Sediment compaction (or consolidation) is a result of the reduction of void space within the sedimentary column (e.g. Greensmith and Tucker, 1986). Compaction will lower sea-level data from the elevation at which they formed, resulting in erroneous reconstructions (Shennan, 1986). Compaction is a complex process involving many variables (Pizzuto and Schwendt, 1997) such as the nature of the substrate and mass of overburden, which vary in time and space (Jelgersma, 1961; Kaye and Barghoorn, 1964; Törnqvist et al., 2008). The thickness of overburden has been shown to be a significant variable in data from the Missisippi Delta (Figure 2.9), suggesting millennial scale compaction rates up to 5 mm a^{-1} (Törnqvist et al., 2008).

Whilst models have been proposed to correct for the effects of compaction (e.g.

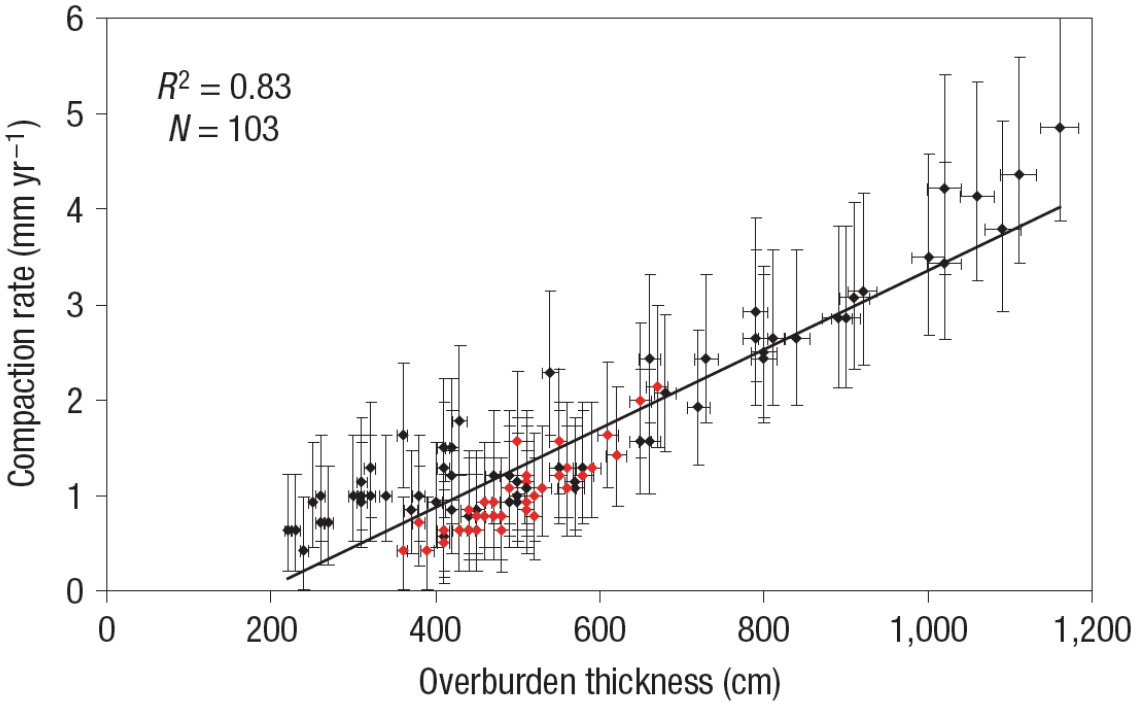

Figure 2.9 - Relationship between overburden thickness and compaction rate. Red data points represent sites with positive evidence for reduced compction due to a subsurface sand body. Horizontal error bars represent error due to angle of borehole. Vertical error bars are the elevational uncertainty. Törnqvist et al. (2008).

Skempton, 1970; Paul and Barras, 1998), the uncertainty associated with them has led to them rarely being applied (Shennan and Horton, 2002). To attempt to remove this error, base of basal peat have been used (e.g. Jelgersma, 1961; Kaye and Barghoorn, 1964; van de Plassche, 1979, 1982; Smith, 1985; Denys and Baeteman, 1995). These materials are compaction free because the underlying Pleistocene sands are practically unaffected by compaction (Jelgersma, 1961). However, there are a number of problems with basal peats. Firstly, it is important to assess whether sea level or local groundwater level is controlling formation. Kiden (1995) noted that data collected by Jelgersma (1961) appeared to plot anomalously high on an age/altitude graph relative to sea-level curves for the rest of the Netherlands. Van de Plassche (1979) concluded that basal peat samples could only be employed in sea-level reconstructions after a detailed study of the relief of the underlying Pleistocene sands. Samples should only be taken where there was a sufficient slope in the Pleistocene surface to avoid this groundwater-gradient effect (van de Plassche, 1979). Secondly, basal peats are rare and therefore any reconstructions reliant solely upon these data are liable to have significant gaps in the record. Finally, basal peats are often devoid of identifiable plant macrofossils or microfossils making it difficult to assess the relationship between the sample and sea level.

Sea-level researchers have therefore sub-divided samples based on potential for compaction, without assessing the absolute amount (e.g. Shennan et al., 2000). This method identifies samples as ‘base of basal’, ‘basal’ or ‘intercalated’ (Shennan et

al., 2000). Samples identified as basal come from within the unit overlying the uncompressible substrate but are not from the base of the unit and may be subject to some degree of compaction (Horton and Shennan, 2009). Intercalated samples are organic sediments underlain and overlain between different sedimentary units and are the most prone to compaction (Shennan, 1989).

Tidal range changes are important to reconstructions of RSL, as the methodology inherently assumes that tidal range has not varied through time (Shennan, 1980). Shennan (1980) acknowledged that this assumption reduces the value of the sea level indicators, but is necessary to allow for the use of sea-level data with different relationships to tidal levels. Models have been produced to assess the effects of tidal range change (e.g. Scott and Greenberg, 1983; Gehrels et al., 1995; Shennan et al., 2000; Shennan et al., 2003). Tidal range changes may stem from long-term changes in the tidal potential arising from variations in the orbital elements of the Sun and Moon, from changes in the shape or depth of ocean basins and/or the rate of global tidal dissipation (e.g. Woodworth et al., 1991). Various researchers have identified that shelf width and basin configuration (Redfield, 1958; Jardine, 1975; Cram, 1979; Woodworth et al., 1991) strongly influence tidal range. Changes in these paleogeographies may be due to long-term processes including RSL change, sediment supply and/or anthropogenic processes including dredging (Woodworth et al., 1991). It has been demonstrated that the effects of tidal range are most pronounced within estuaries with large tidal ranges, with a reduction

in the difference between mean tide level and mean high water spring tide of c 2.5 m in the Humber between 6 - 3 ka (Shennan and Horton, 2002). Scott and Greenberg (1983) used numerical modeling in the Bay of Fundy to infer a 1.2% increase in tidal range for every 1 m of sea-level rise between 7 and 2.5 ka. Gehrels et al. (1995) focused on the M2 tidal component and demonstrated that it was 73% of the modern value at 5 ka. Changes in tidal regime are currently beyond the scope of this study. However, the outputs from this research will increase the accuracy of paleogeographic maps for a current study of tidal range during the Holocene (David Hill, The Pennsylvania State University)

2.3 RECONSTRUCTING RELATIVE SEA LEVEL FROM THE U.S. ATLANTIC COAST

2.3.1 Sea-Level Index Points

A sea-level index point is a datum that can be utilized to show vertical movements of sea level. Index points as a concept were proposed and subsequently developed during the International Geoscience Programme (IGCP) Projects 61 and 200 (e.g. Cinquemani et al, 1982; Shennan, 1987).

For a sample to be considered an index point it must have three components: (1) a geographical location; (2) an altitude that can be related to a former water level; and (3) an age. If the location of a sample cannot be established to within 1 km, either through

GPS co-ordinates or identification from site maps then the sample cannot be considered a valid index point.

A sample must possess a systematic and quantifiable relationship to a tide level, which can be observed in the modern environment and, therefore, be used to estimate former sea level. This is formalized through the concept of the indicative meaning (e.g. Shennan, 1986; van de Plassche, 1986). It contains two components, the indicative range (the elevational range occupied by a sea-level indicator) and the reference water level (the relation of that indicator to a contemporaneous tide level, e.g. mean high water (MHW)). The reference water level does not have to be equal to a tide level, but can be offset (e.g. MHW + 0.2 m), a term known as the indicative difference. However, Shennan, (1986) stated that the reference water level should ideally be given as a mathematical expression of tidal parameters rather than a single tide level ± a constant, as the constant factor will indicate quite different tidal inundation characteristics for areas of different tidal range. A schematic of the indicative meaning is shown in Figure 2.10.

Index points can be produced from a wide array of sedimentary environments and geomorphic features where the relationship between the sample and a water level can be reliably established. In this thesis these include plant macrofossils, microfossils and geochemical data. Samples identified only as salt marsh in origin can be assigned an indicative meaning. This can be refined through the identification of plant macrofossils

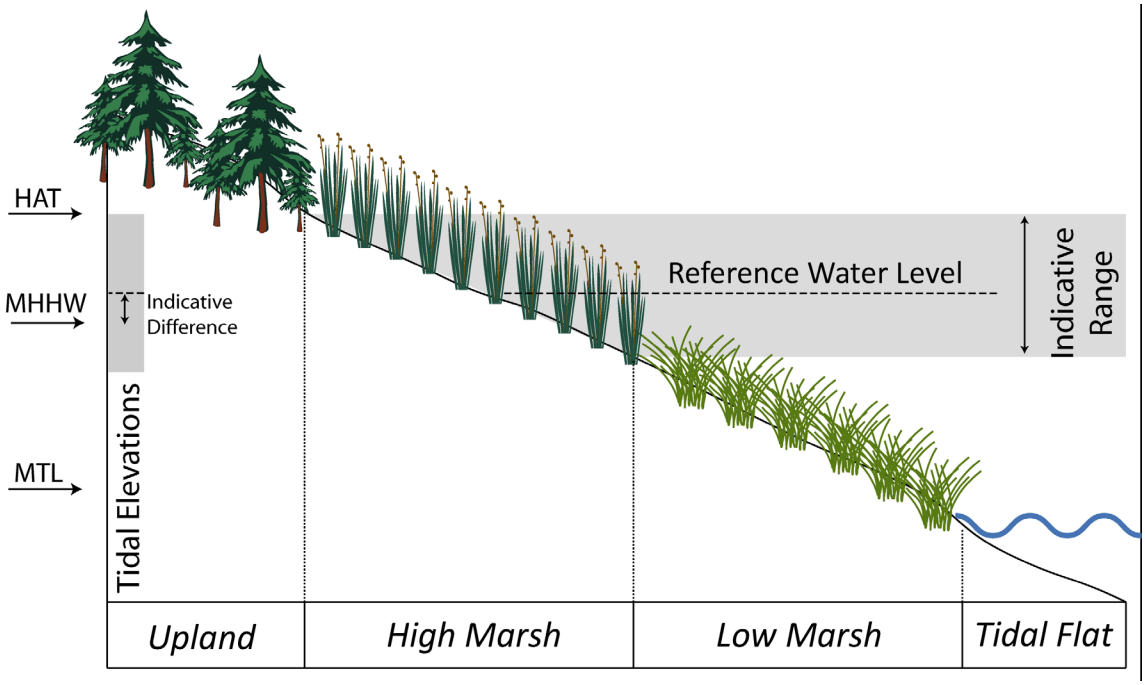

Figure 2.10 - Schematic representation of the Indicative Meaning. The concept of the Indicative Meaning formalizes the relationship between a sea-level indicator (e.g. high marsh vegetation) and a water level. It is defined as the elevational range occupied by a sea-level indicator (Indicative Range) in relation to a contemporaneous tide level (termed the Reference Water Level) such as MHW or HAT. The Indicative Difference is the elevation separating the reference water level and a tidal datum. Kemp (2009).

(e.g. van de Plassche et al., 1998). The low marsh is dominated by *Spartina alterniflora* (e.g. Gehrels, 1994). The high marsh has greater variation with plants including *Spartina patens*, *Distichlis spicata* and *Juncus* spp. (e.g. Gehrels, 1994; van de Plassche, 1998; Kemp et al., 2009). The most common microfossil groups used as a sea level indicator along the U.S. Atlantic coast are foraminifera (e.g. Edward et al., 2004), diatoms (e.g. Horton et al., 2006) and pollen (e.g. Roe and van de Plassche, 2005). The relationship of foraminifera to a water level can be identified as each species has its own optima and tolerances to inundation (e.g. Horton and Edwards, 2006). The utility of diatoms are enhanced when the assemblage shows a substantial change in the proportion of fresh, brackish and marine diatoms (e.g. Zong and Tooley, 1996). Pollen can be assigned an indicative meaning as high abundances of tree pollen are presumed to be terrestrial deposits, whilst samples with increasing content of small, inaperturate pollen and Chenopodiaceae are considered to be marine (e.g. Field et al., 1979). Stable carbon isotopes from bulk organic sediments may also be used (e.g. Törnqvist et al., 2004; Wilson et al., 2005; Lamb et al., 2007; Gonzalez and Törnqvist, 2009; Kemp et al., in press) as salt marsh plants are C4 and have a different ^{13}C signature to C3 terrestrial plants (e.g. Lamb et al., 2007; Kemp et al., in press)

Deposits beyond the influence of tidal range cannot be employed as sea-level indicators as an appropriate indicative meaning cannot be established. However, they can constrain RSL by acting as terrestrial limiting dates (e.g. Shennan et al., 2000), which

reconstructions of RSL must lie below. Similarly, most sub-tidal deposits have unclear indicative meanings (e.g. marine mollusks and bivalves) but can be employed as marine limiting dates when they are in-situ, which RSL reconstructions must plot above (e.g. Horton et al., 2009).

Reconstructing RSL is subject to a number of vertical errors. The indicative range of a sample is highly dependent on tidal range. For example, a high marsh deposit has an indicative range of highest astronomical tide to mean high water. At Oregon Inlet, North Carolina (0.3 m mean tidal range), a high marsh deposit would have an indicative range of ± 0.10 m At Eastport, Maine (5.6 m mean tidal range) the indicative range would be ± 0.63 m. This error can be significantly reduced in areas of high tidal range through quantitative techniques utilizing microfossils (e.g. Gehrels, 2000). The altitudinal error is composed of: (1) measurement of depth of a borehole; (2) leveling of the site to a benchmark; and (3) the accuracy of the benchmark to a geodetic datum (Shennan, 1986). The error due to depth measurement is largely unavoidable and due to the curvature of the coring rods, the angle of the borehole and any compaction due to the coring method. Errors due to leveling technique are minimized when high precision leveling techniques (e.g. Total Station) are utilized. However, this can become larger than 0.5 m when the sample elevation is presumed to be at mean high water (MHW) based on the modern salt marsh vegetation at the coring site. Benchmark reliability can be assessed from the National Geodetic Surveys benchmark classification and is usually ± 0.1 m (Horton et al.,

2009). Errors due to the methods of coring have also been incorporated (e.g. Woodroffe, 2006); hand coring may affect the measurement of depth by up to ± 0.05 m due to compaction of sediment during extrusion.

2.3.2 Chronological Issues in Relative Sea-Level Reconstructions

Radiocarbon dating (Libby, 1952) provides the chronological control within the U.S. Atlantic coast RSL database. The database contains samples from the late 1950s to the present day, a period over which there have been major developments and refinements to both the methods utilized in radiocarbon dating (e.g. Tuniz et al., 1998) and the calibration curves used to convert ^{14}C ages to sidereal years (e.g. Stuiver et al., 2004).

Early radiocarbon dates were produced using the liquid scintillation counting (LSC) (e.g. Hiebert and Watts, 1953) or gas proportional counting (GPC) techniques (e.g. Watt and Ramsden, 1964). These required a large amount of material to generate a date (>25 g for dry peat), and therefore early studies of RSL change since the LGM in Europe (e.g. Jelgersma, 1961, 1966, 1979; Tooley, 1974; 1978; van de Plassche, 1980; Kidson, 1982; Shennan, 1989; Shennan and Horton, 2002) and North America (e.g. Stuiver and Daddario, 1963; Bloom and Stuiver, 1963; Kaye and Barghoorn, 1964, Redfield, 1967; Kraft, 1971; Belknap and Kraft, 1977; Cinquemani et al, 1982) focused on using bulk organic material to establish sea-level index points (e.g. Shennan, 1986). However, there are a number of limitations associated with this technique. Firstly, the large thickness of

samples required (up to 0.6 m) results in the incorporation of organic material of widely different ages, resulting in potentially large but unknown age errors (e.g. Redfield and Rubin, 1962). Secondly, there is a concern that bulk-dated samples may be contaminated by allochthonous carbon, either by mechanical contamination or the penetration of younger roots (e.g. Törnqvist et al., 1992).

The development of the accelerator mass spectrometry (AMS) technique has reduced the minimum sample size required (e.g. Vogel et al., 1984). This has allowed individual plant macrofossils to be dated, which when correctly prepared, results in samples significantly less likely to be contaminated by the effects of younger or older carbon (Hatte and Jull, 2007). This has resulted in reduced age errors. However, care must be taken when selecting plant macrofossils for AMS dating, as it is dependent on the appropriate selection of material from the sediments. Dating of allochthonous plant material for instance, could result in erroneous RSL reconstructions. Therefore, AMS dating of plant macrofossils has focused on dating in-situ plant rhizomes, which have a strongly defined relationship to the marsh surface (e.g. van de Plassche et al., 1998; Kemp et al., 2009).

AMS dating has also greatly increased the range of datable sedimentary deposits (e.g. Hadjas et al., 1995; Jiang et al., 1997) and allowed age determinations to be made on small-sized calcareous material, including foraminifera, ostracods and mollusks; all of these are found within the U.S. Atlantic coast database. This has enabled marine limiting

dates to be constructed from a single, articulated shell, greatly improving the reliability of the sample. All marine samples however, must be corrected for the slow ocean turnover of ^{14}C, known as the marine reservoir effect (Jones et al., 1989). The correction can be up to 1200 years (Austin et al., 1995), but is more commonly 400 years within the mid- and low-latitudes; the standard correction in the marine calibration curve Marine04 (Hughen et al., 2004). Whilst data are currently sparse, it is also possible to calculate site-specific marine reservoir corrections (e.g. Reimer and Reimer, 2001). This correction is usually assumed to be constant through time. However, it has recently been shown that there are variations in this offset (e.g. McGregor et al., 2008).

One of the fundamental assumptions of AMS, GPC and LSC ^{14}C dating is that the production of atmospheric ^{14}C has remained constant in time and space. This was shown to be incorrect from samples of wood collected in the 17th century that contained greater than expected levels of ^{14}C (Vries, 1958). This was confirmed by analysis of the Bristlecone Pine tree-ring record (Suess, 1970). To correct for this, all radiocarbon dates in this study are calibrated to sidereal years using the CALIB 5.0.1 program (Stuiver et al. 2005) and either the IntCal04 (Reimer et al, 2004) or Marine04 (Hughen et al., 2004) calibration curves for terrestrial and marine samples, respectively. Calibration of radiocarbon ages generally results in an error in sidereal years twice that of the ^{14}C years (Bartlein et al., 1995). Radiocarbon dates can also be affected by isotopic fractionation. During photosynthesis, ^{12}C is preferentially absorbed by plants relative

to ^{14}C (van de Plassche, 1986) and, therefore, the ^{14}C content on the plants is deficient compared to the atmosphere in which they grew (Bowen, 1978; Olsson, 1979). The ^{13}C isotope can correct this, as the fractionation of ^{14}C relative to ^{12}C in the organic material is approximately twice that of the fractionation of ^{13}C relative to ^{12}C (e.g. Bowman, 1990).

2.4. GEOPHYSICAL AND INSTRUMENTAL METHODS FOR RECONSTRUCTING COMPONENTS OF RELATIVE SEA LEVEL FOR THE U.S. ATLANTIC COAST

2.4.1 GIA Models

The development of GIA models in the 1970s (e.g. Walcott, 1972; Farrell and Clark, 1976; Peltier and Andrews, 1976; Clark et al., 1978; Peltier, 1978) can be viewed as a conceptual revolution in RSL research (Pirazzoli, 1996). Current generation GIA models are based on mathematical analysis of the deformation of a viscoelastic Earth due to surface loading (Peltier, 1974). RSL predictions using this theory were first reported by Peltier and Andrews (1976), demonstrating the effects of the Pleistocene deglaciation. This early analysis presumed that the meltwater from the ice sheets would be equally distributed through the oceans. It was later demonstrated that the water forms an equipotential surface with the geoid (Farrell and Clark, 1976). The full theory of GIA was then employed to produce reconstructions of RSL from the LGM to present (Clark et al, 1978; Peltier et al., 1978). Despite the relative infancy of the science, these early

models were able to explain portions of the temporal and spatial variance seen in RSL records since deglaciation (e.g. Peltier, 1990).

GIA models are composed of an earth model and an ice model. The radial structure of the earth model is composed of a lithosphere (the thickness of which can be modified) and an upper and lower mantle (which can have altered viscosity). The structure is based on the preliminary reference earth model (PREM) proposed by Dziewonski and Anderson (1981). The upper mantle extends to the 670 km seismic discontinuity, with the lower mantle extending from this point to the core-mantle boundary. Whilst the radial profile of the earth model is well constrained by seismic data, the viscosity profile is not. Indeed, the GIA process itself has provided much of the information on the viscosity of the upper and lower mantle, as well as transition zones of differing viscosity (e.g. Peltier and Andrews, 1976; Sabadini et al., 1982; Wu and Peltier, 1983; Nakada and Lambeck, 1989; Ivins et al., 1993; Mitrovica et al, 1994; Kaufmann and Wolf, 1996; Mitrovica and Forte, 1997). The current generation earth models are based on the spherical, self-gravitating, compressible, Maxwell visco-elastic body form of the theory developed by Tushingham and Peltier (1991). The placement of load on this visco-elastic model results in horizontal pressure gradients in the mantle which results in flow (Allen and Allen, 1990). When the load is removed, the mantle flows back from the areas of elevated topography to the areas of depressed topography resulting in an exponential form of uplift due to the reduction in the horizontal pressure gradient over time (Allen and Allen, 1990).

The global ice model defines the global distribution of grounded ice thickness over time. It has developed from the initial ICE-1 model, which was a low-resolution (5° x 5°) model and did not include an Antarctic component (Peltier and Andrews, 1976). This was later modified to incorporate Antarctica in ICE-2 (Wu and Peltier, 1983). The development of ICE-3G increased the resolution (2° x 2°) and reduced the variance between the data and the models by a factor of 2 over ICE-2. This model continues to be widely used in sea-level research despite the availability of new models (e.g. Bassett et al., 2005; Milne et al., 2005). These refined models (e.g. ICE-4G, ICE-5G, ICE-6G) have similar total ice volumes, but the ice is placed in different locations. For example, ICE-5G incorportated a large ice dome over Keewatin (Figure 2.11) that was not present in ICE-4G (Peltier, 2004). There are also a number of local-scale, high resolution ice models (e.g. Greenland; Simpson et al., 2009), which can be employed for applications where extra resolution is required. GIA models have been applied on the U.S. Atlantic coast to validate refined earth and ice models (e.g. Peltier, 1996), investigate the effects of 3D earth models (e.g. Latychev et al., 2005; Davis et al., 2008), estimate the rate of 20th century sea-level rise (Peltier and Tushingham, 1989; Davis and Mitrovica, 1996; Peltier, 2001), fingerprint the melt from the Greenland ice sheet (e.g. Mitrovica et al., 2001; Tamisiea et al., 2001) and understand the steric contribution to sea-level rise (e.g. Wake et al., 2006)

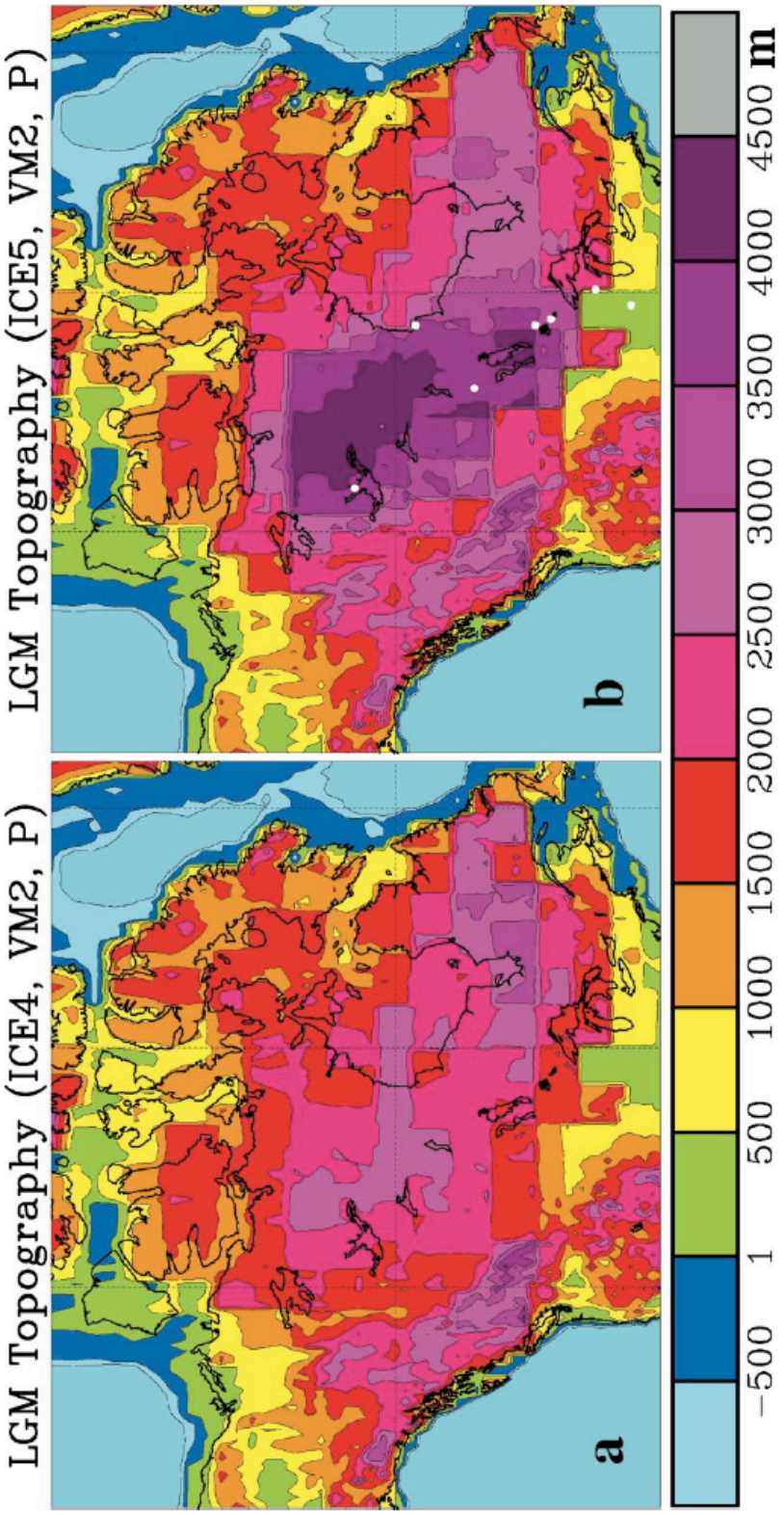

Figure 2.11 - a) Isostatically adjusted topography for the ICE-4G model over North America. b) Same as (a) but for the ICE-5G model. Peltier (2004).

GIA models have a number of limitations. Firstly, the inversion to calculate the viscosity parameters requires the construction of a realistic ice sheet to generate a load and test the observations of RSL versus the predictions. Therefore, it is difficult to assess the uniqueness and accuracy of a solution as multiple ice model and earth model combinations may produce the same result (e.g. Milne et al., 2006). Secondly, the most common assessment for the accuracy of a GIA model is RSL data (e.g. Tushingham and Peltier, 1991; Peltier, 1996; Shennan et al., 2000, 2002; Bassett et al., 2005). If reconstructions are erroneous, then the model's ability to make predictions is undermined. Therefore, high-quality datasets of RSL are required for calibration and testing of the models. The data from the U.S. Atlantic coast are an independent test of the model as they were not used to constrain it (e.g. Peltier, 1996)

2.4.2 Tide Gauges

Tide gauges provide an important instrumental measurement of RSL rise, which can extend back to the 17th century from select long records in Europe (e.g. Douglas, 2001; Woodworth and Player 2003; Jevrejeva et al., 2008). Tide gauges have demonstrated a global 20th century sea-level rise of 1.7 ± 0.3 mm a^{-1} (Church and White, 2006). The permanent service for mean sea level (PSMSL) collects data on tide gauges with global coverage (http://www.pol.ac.uk/psmsl).

At their simplest, tide gauge readings are taken on a graduated staff. Whilst this method

is accurate to only a few cm, it is still important to check the drift of automated tide gauges (Nerem and Mitchum, 2001). Most tide gauges in use today employ the stilling well (Douglas, 2001). A vertical 0.3 m pipe cones down to a 0.025 m orifice. The size of the hole prevents the tide gauge being effected by waves but does not interfere with the measurement of the tides, serving as a mechanical low pass filter (Douglas, 2001). In recent years, tide gauges have been updated to use echo sounding of the distance from a source (usually audio or radar) to the water level. Tide gauges are checked annually by geodetic surveys to ensure that no vertical changes associated with settling are contaminating the readings (Douglas, 2001).

A network of tide gauges covers the U.S. Atlantic coast, with the longest records obtained at The Battery, New York (1856 - present) (e.g. Douglas, 2008) and Key West, Florida (1846 - present) (e.g. Maul and Martin, 2003). NOAA and the USGS maintain the U.S. Atlantic coast tide gauges. Tide gauges were the primary data source for understanding 20th century sea-level acceleration prior to satellite techniques. Long-term (> 50 years data) tide gauge records have been employed to assess the onset of increased sea-level rise (e.g. Jevrejeva et al., 2008) and to identify its magnitude (e.g. Peltier and Tushingham, 1989; Douglas, 1991; Peltier, 1996; Church and White, 2006). Tide gauges have been analyzed to assess the 'fingerprint' of glacial melting from Greenland or Antarctica during the 20th century (e.g. Mitrovica et al., 2001; Tamisiea et al., 2001; Douglas, 2008). There is currently no consensus on this issue, with Douglas (2008) concluding that the tide gauges do not show a fingerprint of glacial melting, whilst

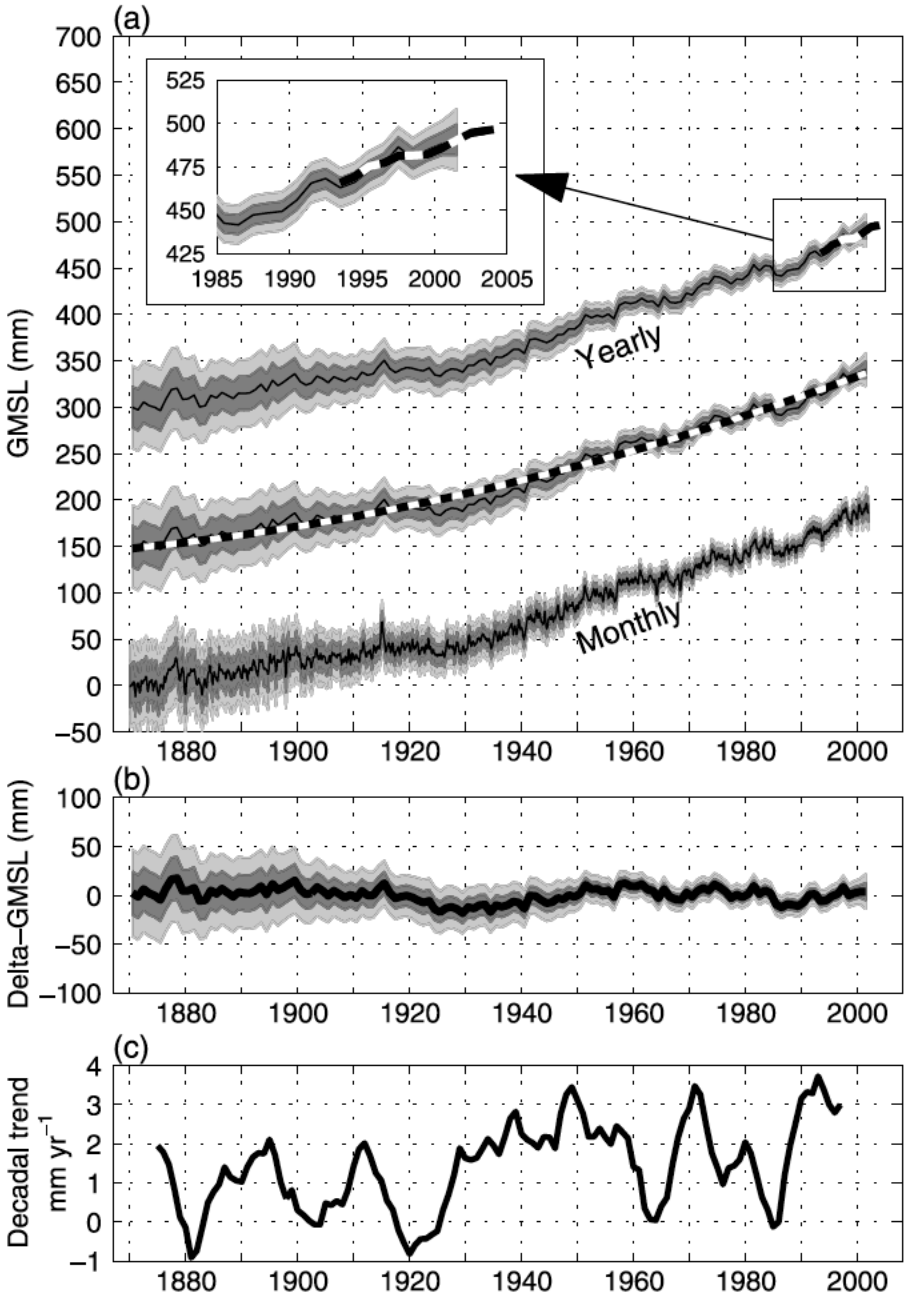

Figure 2.12 - a) Global mean sea level (GMSL) from the reconstruction for January 1870 to December 2001. b) Departures of GMSL from the quadratic fit to the data. c) Linear trends in sea level from the reconstructions for overlapping 10 year periods. Church and White (2006).

Mitrovica et al. (2001) believe the data allow for up to 0.6 mm a^{-1} contribution from Greenland. Tide gauges have also been used to understand the controlling mechanism of 20th century sea-level rise including the balance between the steric and meltwater components (e.g. Miller and Douglas, 2006; Wake et al., 2006).

Whilst tide gauges have provided valuable indications of global sea level (Figure 2.12) (e.g. Church and White, 2006), they are limited by their spatial distribution (e.g. Barnett, 1984; Groger and Plag, 1993), with the majority of long-term records in the northern hemisphere (e.g. Woodworth and Player, 2003). They are also contaminated by crustal movements that must be removed by either a GIA model (which may not be accurate) or from long-term geological records (which may not be available)(e.g. Douglas, 1995). This illustrates the need for TOPEX/Poseidon and JASON satellite altimeter data to provide a measure of global variations.

2.4.3 Satellite Altimetry

Satellite altimetry offers an additional method for measuring global sea-level rise. The first satellite altimeter was placed onboard the Geodynamics Explorer Ocean Satellite 3 (GEOS-3), launched in 1975 (Stanley, 1979). This initial experiment demonstrated that satellite altimetry could be employed to understand variations in the Gulf Stream (e.g. Douglas et al., 1983). The technology was advanced with the short-lived Seasat altimeter, which carried a microwave radiometer to correct for delays due to tropospheric

water vapor (e.g. Nerem and Mitchum, 2001). Further satellite altimeter missions were launched, including Geosat and ERS-1, but these did not meet the criteria outlined for measuring regional or global sea-level change (Nerem and Mitchum, 2001).

TOPEX/Poseidon was launched in 1992 as a joint project between the U.S.A. and France. Both the altimeter and orbit errors were improved over earlier missions, allowing the measurement of sea level accurate to c. 0.04 m (Nerem and Mitchum, 2001). The reduction in orbit errors are perhaps the most significant, due in part to the tracking of the satellite position by Satellite Laser Ranging (SLR), Doppler Orbitography and Radiopositiong Intergrated by Satellite (DORIS) and Global Positioning Systems (GPS) (e.g. Tapley et al., 1994; Nouel et al., 1994). TOPEX/Poseidon was followed by JASON-1. The longer than expected life of TOPEX/Poseidon allowed for simultaneous observations by both systems, preventing the need to use tide gauges to fill gaps between the two projects. This continous satellite altimetry data has been employed to show a rise in global sea-level of 3.3 ± 0.4 mm a^{-1} for the period 1993-2006 (Beckley et al., 2006). This was revised following a new methodology of interpreting altimetry data, to 3.11 ± 0.6 mm a^{-1} (Figure 2.13) for 1993-2008 (Ablain et al., 2009). This reduction can be attributed to a reduction in global sea-level rise by c. 2 mm a^{-1} between 2005 and 2008 (Ablain et al., 2009).

Measurements by TOPEX/Poseidon must, however, be calibrated against tide gauge

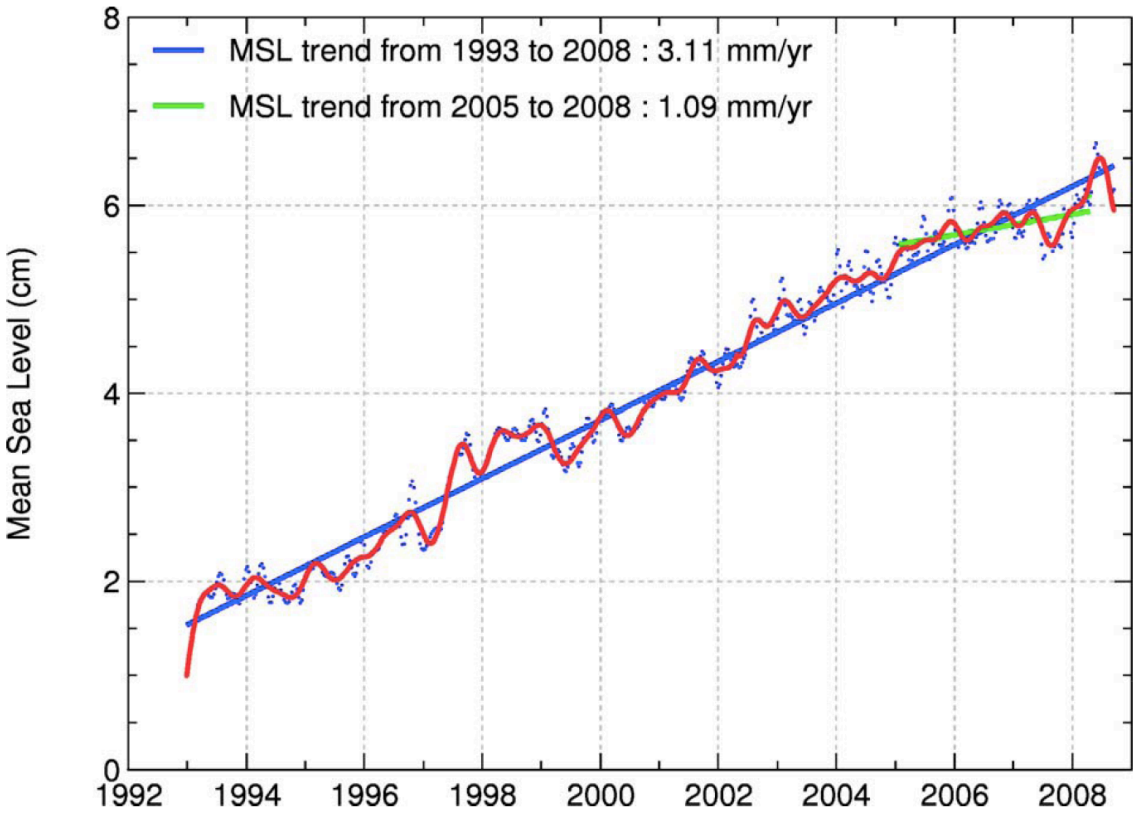

Figure 2.13 - Altimeter MSL from JASON-1 and TOPEX/Poseidon over the 1993-2007 period without GIA correction applied. Annual and semi-annual signals have been adjusted and a 60-day low-pass filter has been applied. Red curve is smoothed over a semi-annual period. Ablain et al. (2009).

records to check for instrumental drift (e.g. Mitchum, 1998). As most tide gauges do not have available SLR or DORIS data within 50 km, either global positioning system (GPS) measurements are used to correct for land motion (with low vertical precision due to short time series, as outlined below) or no correction is made at all (e.g. Nerem and Mitchum, 2001). This is a significant shortcoming of the methodology, which geological data and accurate models of GIA should be able to address.

2.4.4 Gravity

Satellites have primarily measured the Earth's gravity field for the past few decades, as gravitational forces largely determine their orbital motion (Wahr et al., 1998). However, early experiments such as Laser GEOdynamics Satellites (LAGEOS) used a high-earth orbit (c. 6000 km) to reduce the effects of non-gravitational forces, primarily from the atmosphere, that are of greater concern in low-orbit satellites (Wahr et al., 1998). However, this limits the resolution of the LAGEOS system to > 285 km (Wahr et al., 1988).

The Gravity Recovery and Climate Experiment (GRACE) was launched in March 2002 (Velicogna and Wahr, 2002) and has exceeded its estimated 5-year lifetime. The GRACE mission consists of two satellites in low-Earth orbit (450-500 km) and separated by 200 – 250 km. Each satellite ranges the other satellite using microwave phase measurements (Velicogna and Wahr, 2002). Each satellite contains accelerometers to remove the effects

of non-gravitational accelerations due to the low-earth orbit from the solutions. The residual of the ranges minus the non-gravitational accelerations gives the gravity field of the point of earth over which the satellites are passing. GRACE has a resolution of 200 km and can determine temporal variations in gravity every 30 days (Velicogna and Wahr, 2002).

The improved spatial and temporal resolution of GRACE has allowed it to reconstruct changes in ocean volume since 2003 (e.g. Cazenave et al., 2009). The raw GRACE-based ocean mass time series is dominated by an annual cycle caused by the annual exchange of water between land and oceans (Cazenave et al., 2000). Therefore, this signal must be removed to evaluate changes in ocean mass due to non-annual variability. The initial trend of ocean volume since 2003 from this modified dataset has a negative slope of -0.12 ± 0.06 mm a^{-1} (Figure 2.14). However, the result must be decontaminated to remove the effects of GIA. Different authors make different assumptions for the size of this effect (e.g. Willis et al., 2008; Peltier, 2009; Cazenave et al., 2009), varying from 1 – 2 mm a^{-1}. Based on an updated model incorporating the effects of rotational feedback, Peltier (2009) suggests that a correction closer to 2 mm a^{-1} is required for the ocean mass GIA correction. This leaves a residual 1.9 mm a^{-1} of ocean mass increase (Cazenave et al., 2009). GRACE has also been employed to measure the mass balance of ice sheets, indicating that Greenland melting increased from 137 Gt a^{-1} in 2002-2003 to 286 Gt a^{-1} in 2007-2009, and Antarctica melting accelerated from 104 Gt a^{-1} in 2002-2006 to 246 Gt a^{-1}

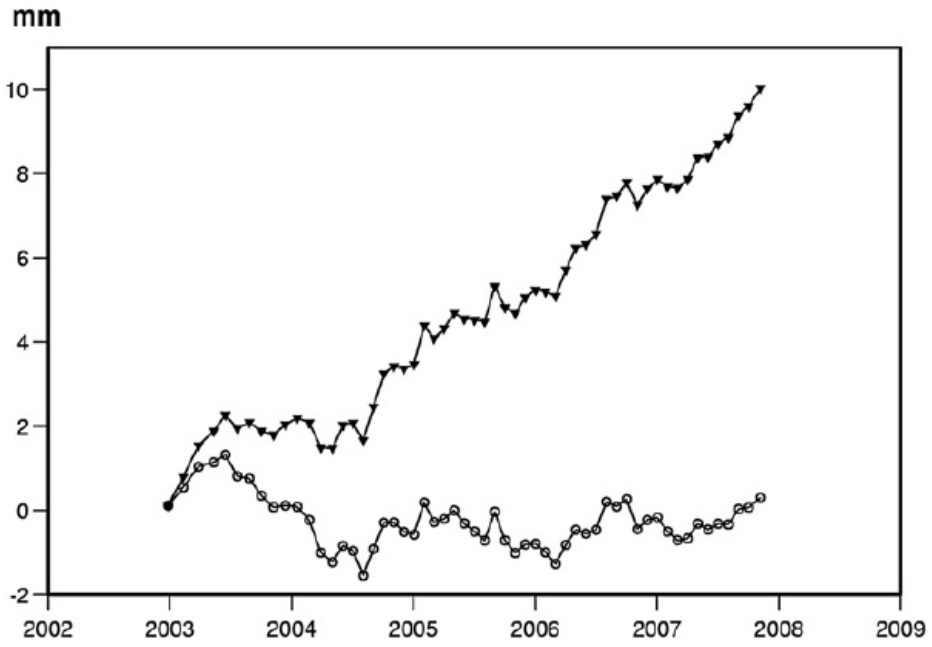

Figure 2.14 - Ocean mass change from GRACE over 2003-2008. The open circled curve is the raw time series. The black triangles curve corresponds to the GIA corrected time series. The raw data shows no trend over this time period. However, a strong trend is observed once the GIA correction is applied.Cazenave et al. (2009).

in 2006-2009 (Velicogna, 2009). This is equivalent to an acceleration in sea-level rise of 0.17 ± 0.05 mm/a^2 (Velicogna, 2009).

2.4.5 Global Positioning Systems

GPS have been employed to derive crustal velocities from the U.S. (e.g. Sella et al., 2007; Snay et al, 2007) and Europe (e.g. Bradley et al., 2009; Teferle et al., 2009). These crustal velocities have then been employed to remove the GIA component from tide gauge records to better understand 20th century sea-level rise (e.g. Snay et al., 2007). Snay et al. (2007) identified 37 tide gauges within 40 km of a geodetic station coupled to the International Terrestrial Reference Frame of 2000 (ITRF2000). They utilized six independent solutions to calculate the vertical motion at each site. Three of these solutions were then averaged to calculate a vertical motion plus a standard error. Using this method they calculated land level movement and hence after decontaminating the tide gauges, an average sea-level rise for North America of 1.8 ± 0.18 mm a^{-1} for the 20th century. When only tide gauges from the U.S. Atlantic coast were employed, this increased to 1.89 ± 0.29 mm a^{-1}. A spatial pattern was also observed, with highest rates at tide gauges between 35° and 40° N. However, it must be noted that the errors associated with the crustal movements are large due to the short time series of data (< 8 years) with a minimum of ± 1.26 mm a^{-1} and a maximum of ± 3.48 mm a^{-1} at the 2-sigma level. Comparison of continuous GPS estimates with absolute gravity (Mazzotti et al., 2007; Teferle et al., 2009) and very long baseline interferometry (VLBI) (MacMillan,

2004) suggest that the rates have a systematic positive bias (Teferle et al., 2009). They concluded that this might be due to a combination of errors in modeling satellite and receiver antenna phase centre variations, the use of reference frames and the differences between global and regional solutions (Teferle et al., 2009).

2.5 GEOLOGY AND GEOMORPHOLOGY OF THE U.S. ATLANTIC COAST

My study area stretches from Maine to South Carolina, a distance of greater than 1800 km. The development of the Atlantic continental margin system commenced in the late Permian with the propagation of the Arctic-North Atlantic rift system (Manspeizer et al., 1978; Ziegler, 1982). Further rifting followed, before the first oceanic crust was produced in the early Middle Jurassic (Klitgord and Schouten, 1986). With the continued sea-floor spreading, the Atlantic Ocean basin spread to over 200 km wide by 170 Ma and development of ocean circulation patterns commenced (Jansa, 1986). Due to the size of the study area, the coastline exhibits a number of different geomorphological settings. These are due to both the differences in underlying geology (e.g. Thornbury, 1965) and the spatially variable response to loading by the Laurentide Ice Sheet since the LGM (e.g. Clark et al., 1978; Dyke and Prest, 1987; Tushingham and Peltier, 1991; Peltier, 1996; Dyke, 2004).

The northern Atlantic coast was ice covered at the LGM and geomorphological features

due to glaciation, such as end moraines and ice thrust masses indicate that Connecticut, Rhode Island and southern Massachusetts regions were positioned at or near the ice sheet terminus (Dyke and Prest, 1987; Dyke, 2004). The well-developed eskers and contemporaneous ice flow lineaments in northern Massachusetts and Maine indicate a position behind the LGM ice margin (Dyke and Prest, 1987; Dyke, 2004). The geomorphology of this coastline is shaped by its ice history. Moraines, drowned river mouths and glacial outwash formations are common features (Sherman, 2005).

In contrast, the southern Atlantic coastline was not covered by the Laurentide Ice Sheet. As a result, the geomorphology of this region is shaped by the underlying geology, composed of Cretaceous, Triassic and Quaternary coastal plain formations (e.g. Thornbury, 1965). Barrier islands are the predominant feature along this coastline. The barriers in New York, New Jersey and on the Delmarva peninsula are separated from the mainland by wide bays and are continous, except where they are dissected by drowned river valleys such as the Delaware estuary (Sherman, 2005). Whilst the North Carolina barrier islands are considered part of the same complex (Fisher, 1982), they are elongate and primarily controlled by an underlying geological high (Walker and Coleman, 1987). The North Carolina barriers are separated from the mainland by large sounds (Riggs, 2002)). The South Carolina barrier islands are considered a separate complex with broader barriers and more inlets.

2.5.1 Maine

In Maine, there is over 5,970 km coastline, the majority of which is resistant rocky shoreline (Jacobson et al., 1987). However, there are also areas of erodible coastline, including 79 km^2 of salt marsh (Jacobson et al., 1987). These soft coastal features are dominated by glacial tills and the Presumpscot Formation, a glacio-marine unit deposited during the demise of the Laurentide Ice Sheet (Thompson, 2001). These have been classified as back-barrier, transitional, fluvial and bluff-toe marshes (Kelley et al., 1988). These marshes tend to be small in size and form in between rocky headlands where they are protected by barriers or fluvial systems (Kelley, 1987). A change in the distribution of salt marshes occurs around Penobscot Bay. There are more individual marshes to the north east than to the south west, but the former marshes are reduced in size compared to the latter marshes, which occupy 68% of the total salt marsh area (Jacobson et al., 1987). The coast of Maine is macrotidal with ranges greater than 4 m.

2.5.2 Massachusetts

The surficial geology of the Boston area is marked by a pre-Wisconsinan drift, which forms a cover over most of the irregular bedrock surfaces (LaForge, 1932; Mencher et al., 1968; Kaye, 1976; Kaye, 1982; Newman and Rosen, 1990). The younger sequence that overlays this drift relates to the last glaciation. A marine deposit overlays this as the land was inundated by a marine transgression following the withdrawal of the Laurentide Ice Sheet. Moving to the south to Cape Cod, the surficial geology is dominated by the effects

of the outflow of the Laurentide ice sheet. Two terminal moraines form the connection of Cape Cod to the mainland (Oldale and Barlow, 1986). Moving north along the cape, eolian deposits have been reshaped during the Holocene as sea level rose through this period (Winkler, 1992). The availability of sand on the northern shore has allowed for the development of barrier beaches, which protect extensive salt marshes such as those at Barnstable Harbor (Redfield and Rubin, 1962; van Heteren et al., 2000). The tidal range varies from greater than 3 m at Boston to less than 1 m at Woods Hole on the southern portion of Cape Cod.

2.5.3 Connecticut

The coastline of Connecticut borders Long Island Sound to the south and Block Island Sound to the north. The shape of the Connecticut coastline is controlled predominantly by the crystalline bedrock (Lewis and DiGiacomo-Cohen, 2000) with gently dipping coastal plain strata to the north in Block Island Sound (Needell and Lewis, 1984). It has been suggested that neotectonic faulting has been occurring within Connecticut (Thompson et al., 2000) with punctuated evidence for large prehistoric earthquakes. However, research from the Eastern Border Fault identifies that previous research suggesting up to 1 m of offset from neotectonic faulting was incorrect (van de Plassche et al., 2002). Two glacial deposits, dating to pre-late-Wisconsinan and late-Wisconsinan, unconformably overlie the crystalline bedrock and coastal plain strata (Donner, 1964; Rampino and Sanders, 1981). Tidal range increases westward into Long Island Sound

from c. 1 m at New London to c. 2.25 m at Bridgeport.

2.5.4 New York

New York is underlain by Grenville rocks, which are exposed at the surface in the Adirondack mountains (Isachsen et al., 2000). Holocene coastal deposits are limited in extent to the Hudson Highlands, the Manhattan Prong and Long Island. The bedrock geology of the Hudson Highlands is formed by Proterozoic rocks deformed during the Grenville orogeny (Isachsen et al., 2000). The bedrock geology of the Manhattan Prong is comprised of metamorphic rocks, including the Fordham Gneiss and the Manhattan Schist. These rocks were folded and metamorphosed during the Taconian orogeny and strongly control the shape of the land surface (Isachsen et al., 2000). Long Island marks the most northerly point on the U.S. Atlantic coast where coastal plain deposits lie above sea level (Isachsen et al., 2000). Long Island is bounded by a number of late Wisconsinan end marines. The oldest of these, the Ronkonkoma-Amangansett-Shinnecock moraine, lies across central and south Long Island and marks the maximum extent of late Wisconsinan glaciation (Lewis and DiGiacomo-Cohen, 2000). The more northerly moraine runs across northern Long Island before extending across Block Island Sound as small islands (Plum Island and Fishers Island) before reaching into southern Rhode Island. Tidal range varies from c. 0.75 m at Montauk at the tip of Long Island to c. 1.5 m at The Battery on Manhattan.

2.5.5 New Jersey

Coastal plain sediments dominate New Jersey. The majority of the coastline is younger than Tertiary in age (Outer Coastal Plain) with Cretaceous and Triassic sediments limited to the extreme north of the coastline (Inner Coastal Plain). The maximum extent of the late Wisconsinan glaciation extended no further south than Sandy Hook, therefore the move south to New Jersey marks a movement away from surficial geology dominated by glacial sediments. Instead, the coastal deposits are composed of thin veneers of late Quaternary sediments composed of beach, dune, swamp and marsh sediments (Lewis and Kummel, 1915). The general geomorphic system of the New Jersey barrier island coastline can be classified as the broad flank of continental platform that is being transgressed by sea-level rise. An inland drainage system is incising into the older pre-Holocene stratigraphy (Psuty, 1986). Tides on the Atlantic coast of New Jersey have a range of c. 1.5 m with an increase once you enter the Delaware estuary at Cape May to c. 1.75 m.

2.5.6 Delaware

The coastline of Delaware is split between the open Atlantic coastline, which has a similar barrier island geomorphology to New Jersey to the south, and the Delaware Estuary. The Delaware estuary and open Atlantic Ocean are underlain by Tertiary sand deposits including the Chesapeake Group and the Rancocas formation (Spojlaric and Jordan, 1966). The Delaware estuary formed as the ancestral Delaware River valley was

drowned by rising sea level during the late Quaternary (Knebel et al., 1988; Fletcher et al., 1993). The tributaries of this paleoriver system ran approximately parallel to the coastline and through downcutting, formed steep, high relief valley systems (Kraft, 1971; Kraft et al., 1987). As the transgression continued, the rising sea level moved first into the paleo valley systems, resulting in a thick sequences of salt-marsh sediments (Kraft et al., 1987; Fletcher et al., 1990; Fletcher et al., 1993). Tidal range increases from c. 1.5 m at the mouth of the estuary at Lewes to c. 1.75 m within the inner estuary at Reedy Point.

2.5.7 Maryland and Virginia

The coastline of Virginia and Maryland is composed of sand deposits of assorted ages. Southeastern Maryland and the Eastern Shore of Virginia are composed of Quaternary sands, which are either undivided or belong to the Nassawadox and Omar formations (Virginia Division of Mineral Resources, 1993). The deposits on the eastern side of the Chesapeake Bay in Maryland are also composed of Quaternary sands, whilst the coastal plain deposits to the east of the Bay are composed of Paleocene and Miocene sand deposits from the Calvert and Aquia formations (Cleaves et al., 1968). Tidal range on the open Atlantic coast of Maryland and Virginia ranges from c. 0.75 m at Ocean City, MD, to c. 1.5 m at Wachapreague, VA. Within the Chesapeake Bay tides are largest at the mouth of the Bay (c. 0.9 m) and decrease towards the inner Bay (c. 0.5 m).

2.5.8 North Carolina

The coast of North Carolina can be split into two geological provinces, a northern section from the Virginia border to the southern Pamlico Sound and a southern section from Cape Lookout to Cape Fear. The northern section occupies the Cenozoic Albemarle embayment, which is bounded to the north and south by the Norfolk Arch (Foyle and Oertel, 1997) and Cape Lookout respectively. The southern portion is underlain by the Paleozoic Carolina Platform, a structural high in the basement rocks (Riggs and Belknap, 1988). Regional stratigraphic studies have identified broad areas of uplift (e.g. Winker and Howard, 1977; Marple and Talwani, 2004) of 0.14 - 1.8 mm a^{-1}. The barrier island system of the Outer Banks has a significant effect on tidal ranges within the Albemarle and Pamlico Sounds, with tidal ranges greater at the inlets (c. 0.4 m at Oregon Inlet) and smaller tidal ranges within the sounds (c. 0.2 m at Manteo). Tidal ranges along the open coastline range from c. 1.1 m at Duck on the northern coast to c. 1.4 m at Wilmington on the southern coast.

2.5.9 South Carolina

From Winyah Bay north to the South Carolina and North Carolina border, the geology is dominated by the Pleistocene Socastee formation, composed primarily of sand with some clays and muds (Newell et al., in review). Along the coast, there are isolated pockets of Holocene material from the Chenier plain and the deltas of the Suwannee and Chattahoochee Rivers (Newell et al., in review). South of Winyah Bay, the geology

is mixed between lobes of Quaternary tidal marsh deposits, the Pleistocene age Wando formation and the Holocene chenier plain and delta deposits of the Suwannee and Chattahoochee Rivers (Newell et al., in review). Tidal range along the South Carolina coast is c. 1.75 m.

2.6 SUMMARY

Relative sea-level at any place and time can be explained by a combination of eustatic, isostatic, tectonic and local factors. Eustatic controls on RSL are primarily driven by the transfer of water from the continents to the oceans during deglaciation. The effects are not similar around the globe, due to the redistribution of water, termed geoidal eustasy. Isostasy stems from the direct effects of the removal of ice sheets from the continents (glacio-isostasy) in near-field and intermediate-field locations, and through water loading (hydro-isostasy) from the melting ice sheets in far-field locations. This study concentrates on areas within the near- and intermediate-field. Tectonic effects can be important controls on RSL, but are negligible on the U.S. Atlantic coast over the Holocene. Local factors including sediment compaction and tidal range change may have significant influence on RSL reconstructions. RSL reconstructions also provide a means to investigate these and to correct for them.

A sea-level index point is a datum that can be used to show vertical movements of sea

level when information about the geographic position, environment, indicative meaning, altitude and age are established. They are the primary source of information on RSL in this study. I will use plant macrofossils, microfossils and geochemical information to assess the relationship of a sample to a tidal level. RSL research is subject to a number of inherent errors that are rarely accounted for. In this study, I assess the full vertical error term from a variety of factors including the estimate of elevation and the technique used to collect samples. The chronological control in this study is radiocarbon dating. A full assessment of the errors associated with this technique including sample selection, method of calculating the marine reservoir effect and calibration of dates is considered.

Finally, I discussed the geophysical and instrumental methods that have previously been utilized on the U.S. Atlantic coast. Applications of the data will focus on the refinement of GIA models and understanding background rates of RSL rise during the late Holocene and their application in further understanding 20th century sea-level rise. GIA models use an earth and ice model coupled to gravitational effects to make predictions of RSL. They can provide site-specific reconstructions for anywhere on Earth but their accuracy must be assessed by high-quality RSL data. In this thesis tide gauges are the primary means for understanding the acceleration of sea level in the 20th century. However, they are contaminated by GIA and have an uneven spatial distribution. I estimate the GIA trend using late Holocene basal peat data and remove this from the tide gauge records to investigate spatial variability in 20th century sea-level rise. GPS provides a

potential solution for calculating ongoing crustal motions but is currently limited by short time series of data, resulting in low vertical precision. I compare the rates of crustal subsidence produced by GPS to my estimates from late Holocene RSL data.

The aim of my research is to provide the first validated database of the Holocene RSL history for the U.S. Atlantic coast. I have collated data from published and unpublished sources to construct a database of RSL. I have validated this database and assigned indicative meanings to commonly employed sample types. Samples that meet all of the criteria for inclusion as a SLI but cannot be assigned an indicative meaning have been employed as marine or terrestrial limiting dates.

CHAPTER THREE

Holocene Relative Sea Levels of the Atlantic Coast of the United States

3.1 ABSTRACT

We have constructed a validated database of Holocene relative sea-level (RSL) data from both published and unpublished records for the Atlantic coast of the United States. The database contains 473 index points that constrain the position of relative sea level (RSL) with associated error terms and 347 limiting dates that identify the minima and maxima of former sea levels. The database has good temporal coverage from 6 ka to present; however the early Holocene record is predominantly defined by limiting dates. We sub-divide the database into 16 areas based on distance from the center of the Laurentide Ice Sheet. Spatially, index points are present between Maine and South Carolina, although there are no data for Georgia and on the Atlantic coast of Florida.

There are no index points above present during the Holocene. Rates of RSL change were highest during the early Holocene and have been decreasing over time, due to the continued relaxation response of the Earth's mantle to GIA and the reduction of ice equivalent meltwater input in the early Holocene. The maximum rate of relative sea-level rise (c. 20 m since 8 ka) occurred in the mid-Atlantic region (New Jersey and Delaware), which is subject to the greatest ongoing forebulge collapse. The rates of early

Holocene (8 to 4 ka) rise were 3 – 5.5 mm a^{-1} with late Holocene (4 ka to present) rates of rise ≥ 1.2 mm a^{-1}. There is a reduction in rates of rise to the north and south of this region. A comparison of RSL rise from the U.S. Atlantic coast over the last 4 ka and last 2 ka indicates no change in rate within the error terms of the regression. This implies that any meltwater input between 4 ka and 2 ka was minimal.

**To be submitted as: Engelhart, S.E. and Horton, B.P. Holocene relative sea levels of the Atlantic coast of the United States. Quaternary Science Reviews.*

3.2 INTRODUCTION

Observations of relative sea level (RSL) are significant to a number of disciplines in the Earth sciences (e.g. Alley et al., 2005; Rohling et al., 2008; Siddall et al., 2009). They provide information regarding coastal evolution (e.g. Kraft, 1979; McLean, 1984; Barrie and Conway, 2002; Waller and Long, 2003; Behre, 2004; Massey and Taylor, 2007) and the links between coastal processes and human development (e.g. Stanley, 1998; Richardson et al., 2005; Day et al., 2007; Turney and Brown, 2007). RSL change through the Holocene serves as the background rates for 21st century sea-level rise (e.g. Velicogna and Wahr, 2006; Church and White, 2006; IPCC, 2007; Rahmstorf et al., 2007; Jevrejeva et al., 2008) and provide a much needed regional perspective on spatial variability in RSL (e.g. Milne et al., 2006; Milne et al., 2009; Shennan et al., 2009; Engelhart et al., 2009; Gehrels, in press).

Sea-level records from the Holocene extending to the Last Glacial Maximum (LGM) are able to provide insight into the magnitude of continental ice volume (Fairbanks, 1989; Chappell and Polach, 1991; Bard et al., 1996, Hanebuth et al., 2000; Yokoyama et al., 2000; Milne et al., 2002; Milne et al., 2005; Peltier and Fairbanks, 2006; Milne and Mitrovica, 2008; Stocchi et al., 2009) and assist in the determination of the timing and abruptness of deglaciation through an approximation of the global ice equivalent eustatic function (Nakada and Lambeck, 1989; Fleming et al., 1998, Lambeck, 2002; Peltier,

2002; Milne et al., 2005). The application of RSL data has been further expanded to constrain the size, fingerprint and source of meltwater pulses (Clark et al., 2002; Bassett et al., 2005; Peltier, 2005). RSL observations are further influenced by the ongoing Glacial Isostatic Adjustment (GIA) and can, therefore, constrain models of this process (Tushingham and Peltier, 1991, 1992; Peltier, 1996, Shennan et al., 2000; Peltier et al., 2002; Shennan et al, 2002; Milne et al., 2005; Horton et al., 2005; Brooks et al. 2008; Massey et al., 2008). GIA will differ based on the ice loading history of a region, which results in regionally different RSL histories in formerly ice covered, near field areas (e.g. Shaw et al., 2002; Shennan et al., 2005), intermediate field regions at the periphery of the ice sheets (e.g. Nikitina et al., 2000; Edwards, 2006) and far field locations not directly affected by ice sheet loading (e.g. Chappell and Polach, 1991; Hanebuth et al., 2000). At the local scale, RSL observations can identify the effects of tidal range change through time (e.g. Gehrels et al., 1995; Shennan et al., 2000; Shennan et al., 2003) and coastal subsidence due to the compaction of the Holocene strata (Jelgersma, 1961; Bloom, 1964, Kaye and Barghoorn, 1964; van de Plassche, 1980; Edwards, 2006; Long et al., 2006; Törnqvist et al., 2008; Horton and Shennan, 2009).

In this paper, we construct a database of validated RSL observations for the Holocene (11.7 ka to present) from the Atlantic coast of the United States. There is a wealth of RSL data for this region including: (1) the initial applications of salt-marsh peat to constrain RSL (e.g. Redfield and Rubin, 1962; Stuiver and Daddario, 1963); (2) understanding the

contributions from glacial- and hydro-isostatic processes (e.g. Belknap and Kraft, 1977; Miller et al., 2009); (3) investigating small-scale fluctuations in late Holocene RSL (e.g. van de Plassche, 1991; Fletcher et al., 1993); and (4) the production of high-resolution (cm to m vertical resolution, annual to centennial age resolution) records of RSL for the past millennia (e.g. Gehrels et al., 2002; Kemp et al., 2009). The database is constructed from published and unpublished sea-level observations. The data are sub-divided into geographical areas based on distance from the center of the Laurentide Ice Sheet (e.g. Peltier, 2004; Engelhart et al., 2009) and contains near-field and intermediate-field sites from Maine to South Carolina. We calibrated all dates using the latest calibration curves (Hughen et al., 2004; Reimer et al, 2004) and reservoir corrections (Reimer and Reimer, 2001). We calculated indicative meanings (van de Plassche, 1986) for all sample types and evaluated the errors associated with each index point. To illustrate this methodology we present a detailed example from New Jersey.

3.3 THE U.S. ATLANTIC COAST

The study area stretches from Maine to South Carolina (Figure 3.1), a distance of more than 1,800 km. The Atlantic coast of the U.S. is a passive margin (e.g. Klitgord et al., 1988) that has not been subject to major tectonic influences over the late Quaternary (e.g. Szabo, 1985) and shows little evidence for neotectonic activity (e.g. Gehrels and Belknap, 1993; van de Plassche et al., 2002). Due to the size of the study area, the

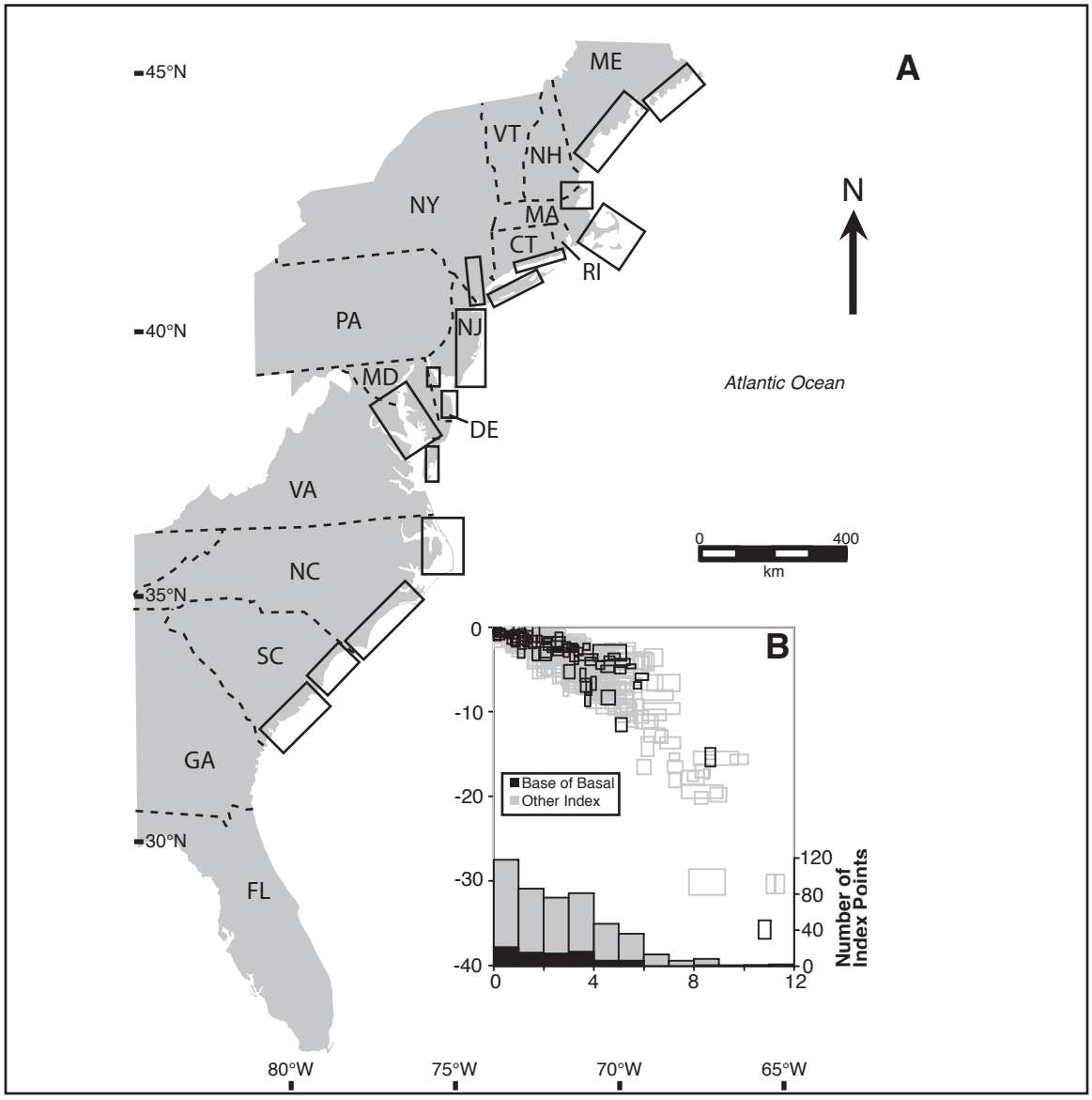

Figure 3.1 - A) Location map of the U.S. Atlantic coast showing the study area from Maine to South Carolina. The 16 areas with a Holocene RSL history are identified by black rectangles. B) Calibrated age versus relative sea level (m MSL) for all the index points. These are sub-divided into base of basal and other index points. The index points are plotted as boxes including the age and vertical error terms. Insert: histogram of the temporal distribution of base of basal and other index points over the Holocene.

coastline exhibits a number of different geomorphological settings. These are due to both the differences in underlying geology (e.g. Thornbury, 1965) and the spatially variable response to loading by the Laurentide Ice Sheet since the LGM (e.g. Clark et al., 1978; Dyke and Prest, 1987; Tushingham and Peltier, 1991; Peltier, 1996; Dyke, 2004).

The geomorphology of the northern Atlantic coast from Maine to Connecticut includes drowned river mouths, moraines and glacial outwash (Sherman, 2005). Salt marshes are small and located between rock headlands and behind barriers (e.g. Kelley et al., 1988, Wood et al, 1989). Triassic and Cretaceous coastal plain formations are mainly located offshore (e.g. Thornbury, 1965; Isachsen et al, 2000). This region was ice covered at the LGM and glacial features such as extensive end moraines and ice thrust masses indicate that Connecticut and southern Massachusetts were positioned at or near the terminus of the ice sheet (Clark, 1980; Dyke and Prest, 1987; Dyke, 2004). In northern Massachusetts and Maine, well-developed eskers and contemporaneous ice flow lineament indicate a position behind the LGM ice margin (Belknap, 1987; Dyke and Prest, 1987; Thompson, 2001; Dyke, 2004).

Two barrier island complexes dominate the geomorphology of the middle and southern Atlantic coastline from New York to North Carolina and in South Carolina (Fisher, 1982). The northern complex shows some differences in form, with the New York, New Jersey and Delmarva barriers separated from the mainland by wide bays and dissected by

drowned river valleys such as the Chesapeake Bay (Fenneman, 1938; Thornbury, 1965; Sherman, 2005). The North Carolina system is marked by thin, elongate barriers that are structurally controlled by the underlying geology (Walker and Coleman, 1987). The South Carolina barrier islands are broader with an increased number of inlets (Fisher, 1968; Sherman, 2005; Harris et al., 2005). Back barrier marshes are common and the shallow slope behind the barriers (Riggs and Ames, 2003) promotes the development of spatially extensive marsh systems (e.g. Riggs, 2002; Kemp et al., 2009). The underlying geology is Cretaceous, Triassic and Quaternary coastal plain formations (e.g. Thornbury, 1965). The Laurentide Ice Sheet did not cover this region and, thus, this is the region of forebulge collapse (Dyke and Prest, 1987; Dyke, 2004).

The tidal range of the Atlantic coast of the U.S. is predominantly mesotidal (NOAA, 2007). Tidal range in the Gulf of Maine and Bay of Fundy is greater than 2.5 m, with areas of macrotidal regime in the north of this system. South of Maine, the tidal range is 1.0 – 2.5 m, with localized areas of microtidal ranges, such as the Inner Chesapeake Bay and the sounds of North Carolina (< 0.5 m).

3.4 MATERIALS AND METHODS

We have followed the consistent methodology developed by International Geological Correlation Projects (IGCP) such as 61, 200 and 495 (e.g. Cinquemani et al., 1982;

Greensmith and Tooley, 1982; Shennan, 1987; Gehrels and Long, 2007; Horton et al., 2009) to construct the database. We have collated data from both published and unpublished sources. To be defined as a sea-level index point a sample must meet the following three criteria: (1) the location of the sample is known to within 1 km (Shennan, 1989); (2) the age of the sample is calibrated to sidereal years using the latest calibration curves (Shennan and Horton, 2002); and (3) the relationship between the sample and a known water level can be defined (van de Plassche, 1986). This relationship, known as the indicative meaning, comprises a reference water level (e.g. mean high water (MHW)) and the indicative range (the elevational range over which the sample may occur). We have defined the indicative meanings of samples within the database (Table 3.1) using modern vegetation zonations (e.g. van de Plassche, 1991; Gehrels, 1994) and microfossils (e.g. Gehrels, 1994; Edwards et al., 2004; Roe and van de Plassche, 2005; Horton et al., 2006) distributions, which may be supported by $\delta^{13}C$ values (e.g. Andrews et al., 1998; Gonzalez and Tornqvist, 2009; Kemp et al., in press). The largest indicative ranges belong to those samples, which can only be identified as salt marsh in origin (Highest Astronomical Tide (HAT) to Mean Tide Level (MTL)). However, where samples have floral and/or faunal indications of a high marsh environment (Table 3.1), the indicative range is reduced (HAT to MHW). We have retained the reference water level and indicative range where authors have used microfossil-based quantitative techniques (e.g. transfer functions)(e.g. Gehrels, 1999; Kemp et al., 2009). For samples where an indicative meaning cannot be defined, we are able to produce limiting points. Terrestrial

Sample Type	Evidence	Example	Reference Water Level	Indicative Range
Salt marsh	Organic deposit with unidentified salt marsh plant macros	Stuiver and Daddario (1963)	(HAT+MTL)/2	HAT-MTL
	Organic deposit with $\delta^{13}C < 25$*	Gonzalez and Törnqvist (2009)	(HAT+MTL)/2	HAT-MTL
High salt marsh	Organic deposit with foraminiferal assemblage dominated by high marsh taxa (e.g. *Jadammina macrescens*)	Gehrels (1994)	(HAT+MHW)/2	HAT-MHW
	Organic deposit with diatom assemblage dominated by oligohalobous and mesohalobous taxa	Culver et al. (2006)	(HAT+MHW)/2	HAT-MHW
	Organic deposit with high marsh plant macrofossils (e.g. *Spartina* patens, *Distichlis spicata*)	van de Plassche (1991)	(HAT+MHW)/2	HAT-MHW
Low salt marsh	Organic deposit with foraminiferal assemblage dominated by low marsh taxa (e.g. *Miliammina fusca*)	Edwards et al. (2004)	(MHW+MTL)/2	MHW-MTL
	Organic deposit with low marsh plant macrofossils (e.g. *Spartina alterniflora*)	van de Plassche (1991)	(MHW+MTL)/2	MHW-MTL
Marine limiting	Clastic deposit with identifiable in-situ marine shells (e.g. *Crassostrea virginica*) or foraminiferal assemblage dominated by calcareous taxa (e.g. *Elphidium* spp.)	Bratton et al. (2003) Miller et al. (2009)	MHW	Anywhere at or below RWL
Terrestrial limiting	In-Situ Tree stumps	Bloom (1963)	MTL	Anywhere at or above RWL
	Undifferentiated peat (may be supported by $\delta^{13}C > 25$*)	Horton et al. (2009)		
	Organic deposit with freshwater diatoms e.g. dominated by Halophobous taxa	Horton et al. (2009)		

* Must be supported by other litho- or bio-stratigraphic evidence

Table 3.1 - Indicative meanings for the different sample types within the database. The associated evidence that is required to classify the sample as an index point or limiting date and supporting references are shown. HAT = Highest Astronomical Tide, MHW = Mean High Water, MTL = Mean Tide Level, RWL = Reference Water Level

limiting dates are composed of freshwater peat and in-situ tree stumps, and must have formed above sea level (Shennan and Horton, 2002). Marine limiting dates, such as articulated marine shells and calcareous foraminiferal assemblages, must have formed below sea level (Horton et al., 2009). These data points have their error terms subtracted and added, respectively, from their reference water levels (Shennan and Horton, 2002).

Relative sea level is estimated for each index point using the equation (Shennan, 1982):

$$\text{Relative Sea Level} = \text{Elevation}_{\text{sample}} - \text{Reference Water Level}_{\text{sample}} \quad [1]$$

where elevation and reference water level for the index point are expressed relative to the national geodetic datum (North American Vertical Datum (NAVD) 88) and subsequently corrected to mean sea level (MSL).

Every index point has an error calculated from a variety of factors (Table 3.2) that are inherent to sea-level research (Shennan, 1986; Woodroffe, 2006). These include an error for the angle of borehole, which is calculated as ± 1% of the overburden of the index point (Törnqvist et al., 2008). We include an error associated with surveying the index point to NAVD88. This can be as low as ± 0.05 m with high precision leveling methods utilizing advanced surveying equipment (e.g. Gehrels, 1999), but can increase to greater than ± 0.5 m when estimated from salt-marsh floral zones (e.g. Redfield and

Error	Description	Example	Magnitude
Measuring Altitude	Precision Surveying e.g. Total Station to Benchmark	Shennan (1986)	± 0.05 m
	Position in tidal frame estimated from high marsh vegetation	This publication	Surface height presumed to be MHW; error = ± (HAT-MHW)/2
	Offshore coring related to MSL	Shennan (1989)	± Tidal Range
Benchmark Error	NGS Benchmark	Horton et al. (2009)	± 0.1 m
Measurement Errors	Angle of Borehole	Törnqvist et al. (2008)	± 1% overburden
	Sampling Error	Shennan (1986)	± 0.01 m
Sample Errors	Thickness of sample	Shennan (1986)	± 50% of sample thickness
Tidal Error	Sample equidistant to two tide gauges when calculating RWL	Shennan (1986)	± Difference in tidal datum's used at the two gauges
Compaction due to coring method	Hand Corer	Woodroffe (2006)	± 0.05 m
	Vibracorer, Piston Corer	Shennan and Horton (2002)	± 0.05 m plus extra error based on information provided by author

Table 3.2 - Individual error terms that are considered for each sample and contribute to the total error term. The reference for each error term is provided. NGS = National Geodetic Survey, HAT = Highest Astronomical Tide, MHW = Mean High Water, MSL = Mean Sea Level, RWL = Reference Water Level

Rubin, 1962). We include an error to account for the stability of the benchmark (National Geodetic Survey classification). The sample thickness is also incorporated into the error term. For older bulk peat samples, this may be as large as ± 0.3 m (e.g. Bloom, 1963). The total error for each index point is subsequently calculated from the expression (Shennan, 1982; Shennan et al., 2000):

$$E_h = (e^2_1 + e^2_2 + e^2_n)^{1/2} \quad [2]$$

where $e_1 \ldots e_n$ are the individual sources of error.

Reconstructions of RSL may also be influenced by the compaction of sediment (e.g. Jelgersma, 1961; Bloom, 1964; Kaye and Barghoorn, 1964; van de Plassche, 1980), which may lower the elevation of an index point. We do not model the compaction of the pre-Holocoene surface and rock strata, presuming this to be compaction free. We investigate the potential effects of compaction by separating the index points into: 'base of basal'; 'basal'; and 'intercalated' (e.g. Shennan, 1989; Törnqvist et al., 2008; Horton and Shennan, 2009). We define base of basal samples as those that were collected from within 0.05 m of the presumed uncompressible substrate (e.g. Pleistocene Sands) and are less than 0.1 m thick. Such samples are presumed to be compaction free (e.g. Jelgersma, 1961). Basal samples were recovered from within the sedimentary unit that overlies the uncompressible substrate, but not from the base. These samples may be subject to some

degree of compaction (Horton and Shennan, 2009). Intercalated samples are organic sediments that were underlain and overlain by different sedimentary units and, thus, are potentially the most prone to compaction (Shennan, 1989).

All sample ages in the database were estimated using radiocarbon dating. The majority of samples are organic sediment (salt and fresh water marshes) or shells of marine gastropods, bivalves and foraminifera. The database contains samples that were dated by accelerator mass spectrometry, gas proportional counting and liquid scintillation counting. We do not make a correction for the possible contamination of bulk peat samples (e.g. Törnqvist et al., 1992). Every sample was calibrated to sidereal years using CALIB 5.0.1 (Stuiver et al., 2005). We used a laboratory multiplier of 1 with 95% confidence limits and the IntCal04 dataset (Reimer et al., 2004) for terrestrial samples and the Marine04 (Hughen et al., 2004) dataset for marine samples. Information on the necessary reservoir correction was taken either from the Marine Reservoir Database (Reimer and Reimer, 2001) or from published values (e.g. Colman et al., 2002). Where this information was not available, the standard marine reservoir correction value in Marine04 was used (Hughen et al., 2004). All index points are presented as calibrated years BP (ka) with the zero point as A.D. 1950.

We plot index points as boxes instead of crosses (e.g. Gehrels, 1994; Donnelly et al., 2004; Gonzalez and Tornqvist, 2009). We sub-divided the database into 16 areas based

on distance from the center of the Laurentide Ice Sheet, which is estimated to be over Western Hudson Bay (Peltier, 2004). To illustrate the influence of GIA along the Atlantic coast of the U.S. we calculate rates of RSL change for the last 4 ka after removing the 20th century RSL rise (Engelhart et al., 2009). We eliminate the 20th century component by extrapolating to MSL in 1900 AD from the nearest reliable tide gauge. We do not include any correction for the potential effects of equatorial ocean siphoning (e.g. Gehrels, in press). The rate of sea-level rise is calculated from a linear regression over the last 4 ka, which is forced through zero (Shennan and Horton 2002).

3.4.1 Example of a late Holocene basal sea-level index point from New Jersey

Core EF/07/10 (39.49 °N, 74.42 °W) was extruded from a modern salt marsh at the Edwin B. Forsythe National Wildlife Refuge in New Jersey in the mid-Atlantic region of the U.S. Atlantic coast (Figure 3.2a). The modern marsh was dominated by stunted *Spartina alterniflora* with a patchy presence of the high marsh species *Distichlis spicata* and *Spartina patens*. Two transects of cores across the marsh (Figure 3.2c) revealed a spatially consistent stratigraphy. The peat was less than 0.3 m thick at the salt marsh/ terrestrial boundary and increased to over 5 m thick at the most seaward core.

Core EF/07/10 was surveyed using a total station (±0.05 m leveling error) to a NGS benchmark with first order vertical precision (±0.10 m benchmark error). The core has a surface elevation of 0.48 m NAVD88 and extended to a depth of -4.02 m NAVD88. The

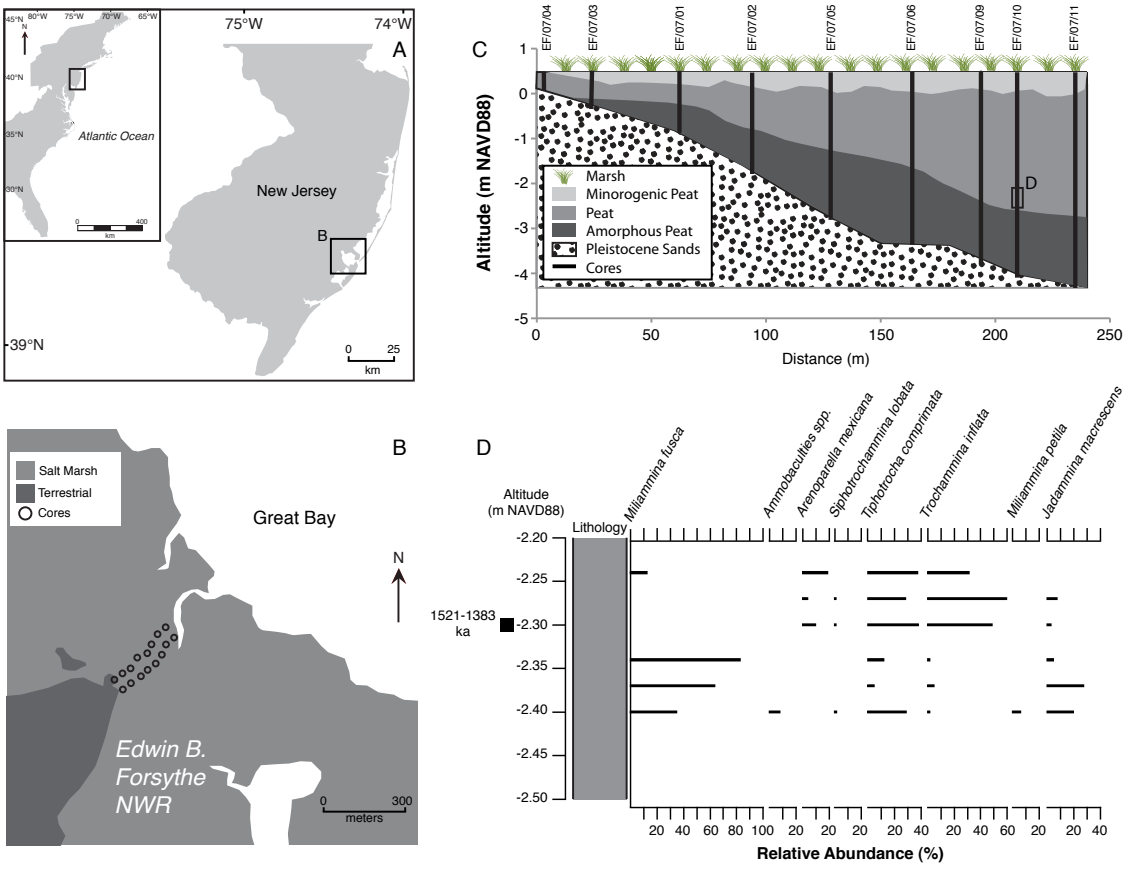

Figure 3.2 - A) Location of the New Jersey study site within the United States of America. B) Local study area map of the Edwin B. Forsythe National Wildlife Refuge on Great Bay, New Jersey. The locations of cores used to ascertain the stratigraphy are shown. C) Stratigraphy for a transect of eight cores across the marsh. D) Foraminiferal assemblages of six samples surrounding a dated rhizome of *Spartina patens* at -2.3 m NAVD88 in core EF/07/10. The sample age is calibrated to sidereal years.

core terminated in a sand unit including some pebble-sized grains, which we interpret as a former Pleistocene surface (Psuty, 1986). The lower 1.70 m (-4.02 to 2.32 m NAVD88) was composed of biodegraded, amorphous peat, which is devoid of identifiable plant macrofossils and foraminifera. In contrast, the peat in the upper 2.8 m of the core (-2.32 to 0.48 m NAVD88) contained large numbers of identifiable high salt marsh plant rhizomes and rootlets, and abundant agglutinated foraminifera. The top 0.50 m of the core (-0.02 to 0.48 m NAVD88) had an increasing minerogenic content that is probably the consequence of ditching during the early 20th century (e.g. Headlee and Carroll, 1920; Teal and Peterson, 2009). A sample of sub-surface high marsh *Spartina patens* rhizome (0.01 m thick) was selected for dating 2.78 m below the surface (±0.03 m borehole error) at -2.30 m NAVD88 (±0.01 m sampling error), which yielded a date of 1.521-1.383 ka (1550 ± 25 14C a). The $\delta^{13}C$ of the sample of -14.4 $^{0}/_{00}$ is within the expected range associated with C4 plants such as *Spartina patens* (Chmura and Aharon, 1995; Lamb et al., 2006; Johnson et al., 2007). Samples were analyzed for their foraminiferal content to further assess the depositional environment (Figure 3.2d). The bottom three samples from -2.40 to -2.34 m NAVD88 suggest a low marsh with the assemblage dominated by the agglutinated foraminifera *Miliammina fusca* (e.g. Gehrels, 1994; Edwards et al., 2004; Kemp et al., 2009). The foraminifera indicate that between -2.34 and -2.30 m, there was a change to a middle to high marsh environment as illustrated by high abundances of *Tiphotrocha comprimata* and *Trochammina inflata* (e.g. Gehrels, 1994; De Rijk and Troelstra, 1997; Edwards et al., 2004). The combination of plant macrofossils,

foraminifera and geochemical data suggest that the radiocarbon dated sample formed in a high marsh environment. The dated sample was, therefore, assigned a reference water level of the midpoint between MHW and HAT (0.73 m NAVD88) and an indicative range of [MHW to HAT]/2 (±0.25 m). The sample lies within a peat unit overlying the Pleistocene substrate, but it was not sampled within 0.05 m of the boundary, thus it is considered a basal peat index point. The calculation of RSL and the error term for this index point is (this is then converted to mean sea level):

$$\begin{aligned} \text{RSL} &= -2.30\ \text{m}_{\text{elevation}} - 0.73\ \text{m}_{\text{Reference Water Level}} \\ &= -3.03\ \text{m} \end{aligned} \quad [3]$$

$$\begin{aligned} \text{Error} &= \Sigma(0.25\ \text{m}^2_{\text{indicative range}} + 0.005\ \text{m}^2_{\text{thickness}} + 0.05\ \text{m}^2_{\text{levelling}} + 0.01\ \text{m}^2_{\text{sampling}} \\ &\quad + 0.1\ \text{m}^2_{\text{benchmark}} + 0.03\ \text{m}^2_{\text{borehole}})^{1/2} \\ &= \pm 0.28\ \text{m} \end{aligned} \quad [4]$$

3.5 HOLOCENE RELATIVE SEA-LEVEL HISTORY OF THE U.S. ATLANTIC COAST

Validation of the database resulted in 820 radiocarbon dated samples covering the Holocene, consisting of 473 index points, 189 marine limiting samples and 158 terrestrial limiting samples (Table 3.3, Appendix One). Figure 3.1b demonstrates considerable

Region	GPS Coordinates (decimal degrees)	Index Points	Base of Basal Index Points	Basal Index Points	Intercalated Index Points	Marine Limiting Dates	Terrestrial Limiting Dates	Late Holocene RSL Rate (mm a^{-1})	References
1. Eastern Maine	44.43 – 44. 68 ºN 67.41 – 68.01 ºW	45	20	12	13	0	0	0.7 ± 0.1	Stuiver and Borns (1975), Belknap et al. (1989), Gehrels and Belknap (1993), Gehrels et al. (1996), Gehrels (1999)
2. Southern Maine	43.29 – 44.12 ºN 68.84 – 70.57 ºW	56	7	12	37	7	2	0.7 ± 0.5	Bloom (1963), Stuiver and Borns (1975), Belknap et al. (1989), Kelley et al.(1992), Barnhardt et al. (1995), Kelley et al. (1995), Gehrels et al. (1996), Gehrels et al. (2002)
3. Northern Massachusetts	42.27 – 42.75 ºN 70.80 – 71.04 ºW	7	5	1	1	1	5	0.6 ± 0.1	Redfield and Rubin (1962), Kaye and Barghoorn (1964), Redfield (1967), Field et al. (1979), Newman et al. (1980), Oldale et al. (1993), Donnelly (2006)
4. Southern Massachusetts	41.25 – 41.71 ºN 70.31 – 70.99 ºW	17	0	12	5	5	10	1.2 ± 0.2	Redfield and Rubin (1962), Stuiver et al. (1963), Emery et al. (1967), Redfield (1967), Field et al. (1979), Oldale and O'Hara (1980), Gutierrez et al. (2003)
5. Connecticut	41.26 – 41.33 ºN 71.86 – 72.85 ºW	54	12	9	33	0	15	1.1 ± 0.1	Redfield and Rubin (1962), Bloom (1963), Emery et al. (1967), Cinquemani et al. (1982), Nydick et al. (1995), van de Plassche (1991), van de Plassche et al. (1998), van de Plassche et al. (2002), Donnelly et al. (2004)
6. New York	40.72 – 41.61 ºN 73.88 – 74.01 ºW	51	0	51	0	3	11	1.2 ± 0.2	Olson and Broecker (1961), Pardi et al. (1984), Slagle et al. (2006)
7. Long Island	40.60 – 41.20 ºN 72.20 – 73.80 ºW	19	0	16	3	0	4	0.8 ± 0.3	Olson and Broecker (1961), Redfield and Rubin (1962), Emery et al. (1967), Redfield (1967), Field et al. (1979), Pardi and Newman (1980), Cinquemani et al. (1982), Pardi et al. (1984)
8. New Jersey	39.20 – 40.45 ºN 74.16 – 74.70 ºW	46	0	26	20	6	7	1.3 ± 0.2	Stuiver and Daddario (1963), Emery and Garrison (1967), Field et al. (1979), Cinquemani et al. (1982), Pardi et al. (1984), Psuty (1986), Donnelly et al. (2001), Donnelly et al. (2004), Miller et al. (2008), Engelhart et al. (this publication)
9. Inner Delaware	38.90 – 39.05 ºN 75.30 – 75.46 ºW	28	13	8	7	2	6	1.7 ± 0.2	Belknap (1975), Belknap and Kraft (1977), Fletcher et al. (1993), Ramsey and Baxter (1996), Nikitina et al. (2000)
10. Outer Delaware	38.64 -38.79 ºN 75.07 – 75.11 ºW	50	9	32	9	4	4	1.7 ± 0.2	Belknap (1975), Kraft (1976), Belknap and Kraft (1977), Rogers and Pizzuto (1994), Ramsey and Baxter (1996), Nikitina et al. (2000), Leorri et al. (2006)
11. Inner Chesapeake	38.05 – 38.88 ºN 76.20 – 76.42 ºW	7	0	7	0	5	0	1.3 ± 0.2	Cinquemani et al. (1982), Colman et al. (2002), Kearney (1996)
12. Eastern Shore	37.12 – 37.80 ºN 85.53 – 79.53 ºW	15	4	5	6	5	4	0.9 ± 0.3	Newman and Rusnak (1965), Finkelstein and Ferland (1987), van de Plassche (1990), Engelhart et al. (2009)
13. Northern North Carolina	35.24 – 36. 02 ºN 75.55 – 75.65 ºW	32	9	23	0	12	4	1.0 ± 0.1	Emery and Wigley (1967), Sears (1973), Benton (1980), Mallinson et al. (2005), Stanton (2008), Horton et al. (2009), Kemp et al. (2009), Riggs and Ames (unpublished)
14. Southern North Carolina	34.11 – 34.96 ºN 76.39 – 77.92 ºW	15	0	15	0	2	2	0.7 ± 0.1	Redfield (1967), Field et al. (1979), Cinquemani et al. (1982), Spaur and Snyder (1999), Culver et al. (2007), Horton et al. (2009), Riggs and Ames (unpublished)
15. Northern South Carolina	33.20 – 33.58 ºN 79.00 – 79.40 ºW	10	1	9	0	0	2	0.8 ± 0.1	Cinquemani et al. (1982), Gayes et al. (1992)
16. Southern South Carolina	32.10 – 32.90 ºN 79.90 – 81.00 ºW	21	0	21	0	0	2	0.6 ± 0.1	Cinquemani et al. (1982)

Table 3.3 - A summary of the RSL data for the 16 areas. The GPS coordinates for the areas are shown. The total number of index points are sub-divided into base of basal, basal and intercalated. The number of marine limiting and terrestrial limiting dates are illustrated. The late Holocene (4 ka to present) rate and 2-sigma error derived from the linear regression for each region are presented. The sources of data used in this publication are listed.

scatter within the database as a result of the spatially variable GIA across the Atlantic coast of the U.S.; this is greater than 10 m at 6 ka. The data demonstrate that RSL has not risen above present from southern Massachusetts to South Carolina during the Holocene. Temporally, the majority of the index points occur within the last 6 ka, with less than 7% of the index points older than 6 ka (Figure 3.1b, insert). Base of basal index points account for 22% of the database. The database is sub-divided into 16 areas from Maine to South Carolina; there are no index points from Georgia or the Atlantic coast of Florida.

3.5.1 Northeastern Atlantic Region

The RSL histories of the Northeastern Atlantic states are shown in Figure 3.3. The record from **eastern Maine (#1)** documents the RSL history since 6 ka. The base of basal index points support a non-linear rise in RSL over the last 6 ka. However, it is difficult to assess the rate of rise in the mid Holocene (from 6 – 4 ka) due to scatter in the index points. RSL rose by 0.7 mm a^{-1} from 4 ka to present and may have reached present day levels by c.1.5 ka. The database for **southern Maine (#2)** provides a RSL history for most of the Holocene. It contains the largest number of index points in any one region within the database (56). Multiple marine limiting dates indicate that a RSL lowstand occurred between 11 – 8 ka and this must have been higher than –26 m MSL. The oldest index point at 7.4 – 7.0 ka shows RSL was -15.3 ± 0.4 m MSL. The rise from this index point to the cluster of other data at 6 ka is constrained by marine limiting points and

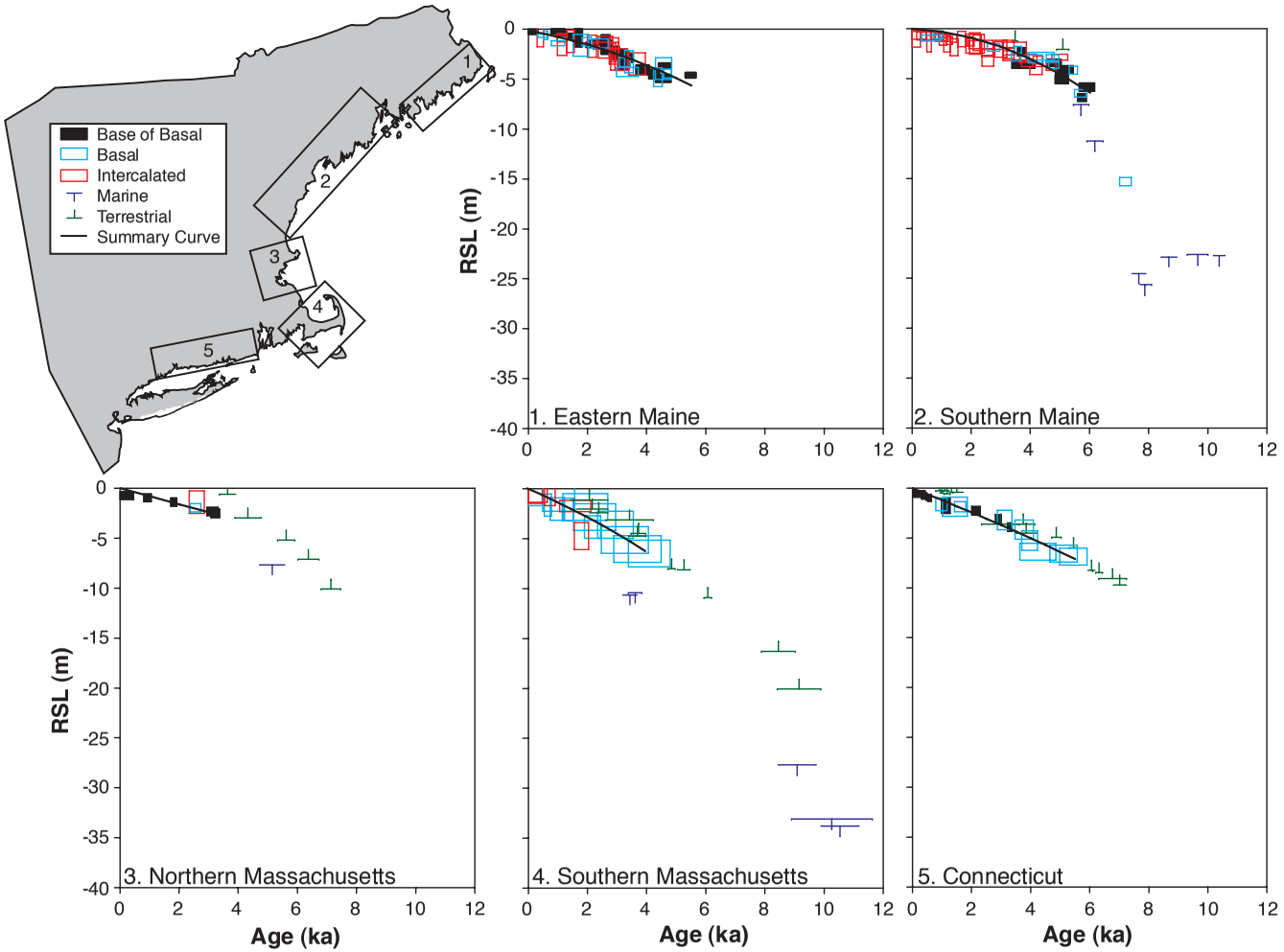

Figure 3.3 - Sea-level index points for 16 areas along the U.S. Atlantic coast plotted as calibrated age versus relative sea level (m MSL). The index points are represented as boxes including the age and vetical error terms. A summary curve is calculated for each area with a 2nd order polynomial through the center points of base of basal or basal data.

indicates a rise of c. 3.5 mm a^{-1}, with a reduction in the rate to c. 1.6 mm a^{-1} between 6 – 4 ka. RSL rose at a further reduced rate of 0.7 mm a^{-1} between 4 ka and present.

The **northern Massachusetts (#3)** reconstruction spans the interval from 7.5 ka to present. The early to mid Holocene RSL history is documented solely by limiting dates (7.5 – 3.5 ka), indicating that RSL was below -10 m at 7.5 – 6.8 ka. The seven index points are all late Holocene in age with the oldest index point at 3.4 – 3.1 ka, which suggests RSL was -2.5 ± 0.4 m MSL. The rate of rise to the present is 0.6 mm a^{-1}. The **southern Massachusetts (#4)** record covers the whole Holocene. The limiting points indicate RSL was above -33.8 m MSL at 11.2 – 9.9 ka and between -27.7 and -20.1 m MSL at c. 9 ka, from where it rose to the first basal index point of -6.5 ± 1.3 m at 4.8 – 3.4 ka. RSL rose by 1.2 mm a^{-1} from 4 ka to present, although precision is compromised by large vertical (> ± 1.0 m) and age errors (> ± 250 a). The RSL history of **Connecticut (#5)** documents the early Holocene to present. The record is constrained from 7 – 6 ka by terrestrial limiting dates, which places RSL below -9.7 m MSL at 7.2 – 6.8 ka. A basal index point demonstrates that RSL was -6.9 ± 0.8 m MSL at 5.9 – 5.0 ka. Further basal index points suggest RSL rose by c. 1.7 mm a^{-1} between 6 – 4 ka, reducing to 1.1 mm a^{-1} from 4 ka to present.

3.5.2 Mid-Atlantic Region

Mid-Atlantic RSL histories are shown in Figure 3.4. The **New York (#6)** record spans

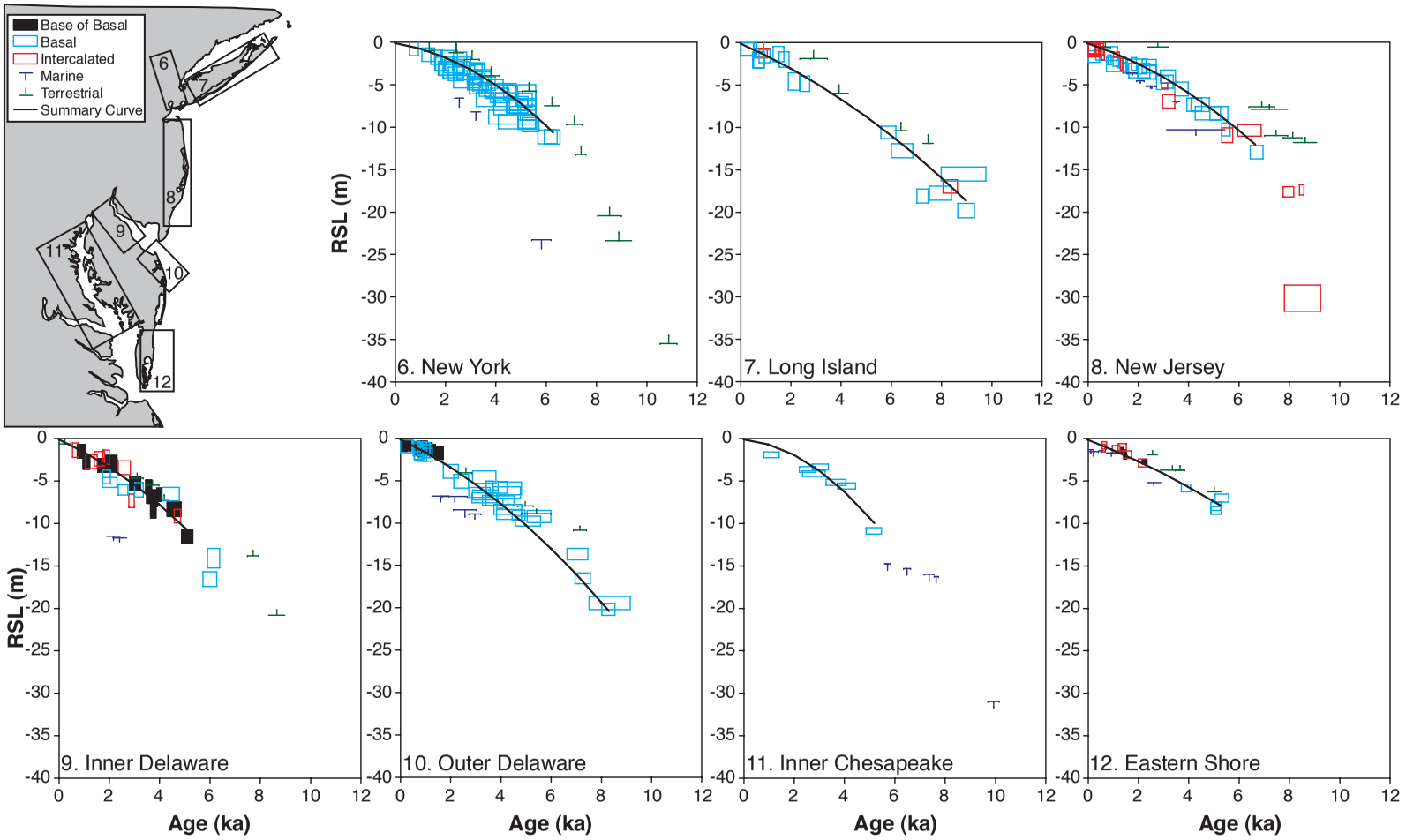

Figure 3.4 - Sea-level index points for 16 areas along the U.S. Atlantic coast plotted as calibrated age versus relative sea level (m MSL). The index points are represented as boxes including the age and vetical error terms. A summary curve is calculated for each area with a 2nd order polynomial through the center points of base of basal or basal data.

the interval from 11 ka to present. Terrestrial limiting dates place RSL below -35.5 m MSL at 11.2 – 10.5 ka, below -23.4 m MSL at 9.4 – 8.4 ka and below -13.2 m MSL at 7.6 – 7.2 ka. The first index point at 6.6 – 5.9 ka suggests a RSL of -11.2 ± 0.8 m MSL. RSL rose by c. 2.5 mm a^{-1} from this index point to 4 ka; a rate of 1.2 mm a^{-1} from 4 ka to present. The **Long Island (#7)** sea-level data provide constraints on RSL from 9.8 ka. The early Holocene record contains five index points, which show a scatter of c. 5 m between a basal sample at 9.8 – 8.0 ka and 9.3 – 8.6 ka. We infer that RSL rose by c. 2 mm a^{-1} from 10 ka to 4 ka and by 0.8 mm a^{-1} between 4 ka and present. The **New Jersey (#8)** reconstruction provides information on RSL from the early Holocene to present. RSL rises from an intercalated index point at -30.2 ± 1.5 m MSL at 9.2 – 7.8 ka, through two further intercalated index points of -17.4 ± 0.6 m MSL at 8.6 – 8.4 ka and -17.6 ± 0.6 m MSL at 8.2 – 7.7 ka. The rate of RSL rise from 9.2 – 4 ka was c. 4 mm a^{-1} with a lower rate of 1.3 mm a^{-1} from 4 ka to present.

The **Inner Delaware (#9)** record covers the period from the early Holocene to present. A terrestrial limiting date constrains RSL to lower than -20.8 m MSL at 9.0 – 8.3 ka with a rise to the first two basal index points, which place RSL at -16.5 ± 0.9 m MSL at 6.3 – 5.7 ka. RSL rose from this time to 4 ka at c. 5.5 mm a^{-1} and at 1.7 mm a^{-1} from 4 ka to present. RSL information is available for the **Outer Delaware (#10)** area from the early Holocene to present. At 8.5 – 8.0 ka, a basal index point suggests RSL was -20.2 ± 0.7 m MSL. RSL rose by c. 3 mm a^{-1} from 8.5 – 4 ka and at a reduced rate of 1.7 mm a^{-1} from

4 ka to present. The **Inner Chesapeake (#11)** reconstruction provides a near-complete Holocene RSL history. The record from 10.1 – 6 ka consists of marine limiting dates that indicate RSL was above -31 m MSL at 10.1 – 9.7 ka and above -15 m MSL at 5.8 – 5.6 ka. The oldest base of basal index point documents that RSL was -10.9 ± 0.4 m MSL at 5.5 – 4.8 ka. RSL rose by c. 2.1 mm a^{-1} from 5.5 – 4.8 ka to 4 ka and by 1.3 mm a^{-1} from 4 ka to present. The RSL record from the **Eastern Shore of Virginia (#12)** provides information on RSL from the mid Holocene to present. The basal index points indicate that RSL was -8.5 ± 0.5 m MSL at 5.3 – 4.9 ka and rose at c. 1.5 mm a^{-1} to 4 ka. The rate of RSL rise decreased to 0.9 mm a^{-1} from 4 ka to present.

3.5.3 Southern Atlantic Region

The RSL histories for the Southern Atlantic coast are highlighted in Figure 3.5. The **northern North Carolina (#13)** area includes the oldest index point in the database (11.6 – 11.2 ka). RSL rose by c. 4 mm a^{-1} from 11.6 – 4 ka. The reconstruction is constrained to ± 5 m by a suite of marine and terrestrial limiting dates between 8.9 – 8.5 ka and 2.8 – 2.5 ka. The late Holocene record includes seven base of basal and 19 basal index points that suggest a rate of RSL rise of 1.0 mm a^{-1} from 4 ka to present. The RSL record for **southern North Carolina (#14)** covers the complete Holocene. A terrestrial limiting date indicates that RSL was below -25 m MSL at 12.6 – 10.8 ka. The oldest basal index point places RSL at -8.0 ± 0.6 m MSL between 7.2 – 5.9 ka. RSL rose by 1.7 mm a^{-1} to 4 ka and by 0.7 mm a^{-1} from 4 ka to present. The **northern South Carolina (#15)** sea-

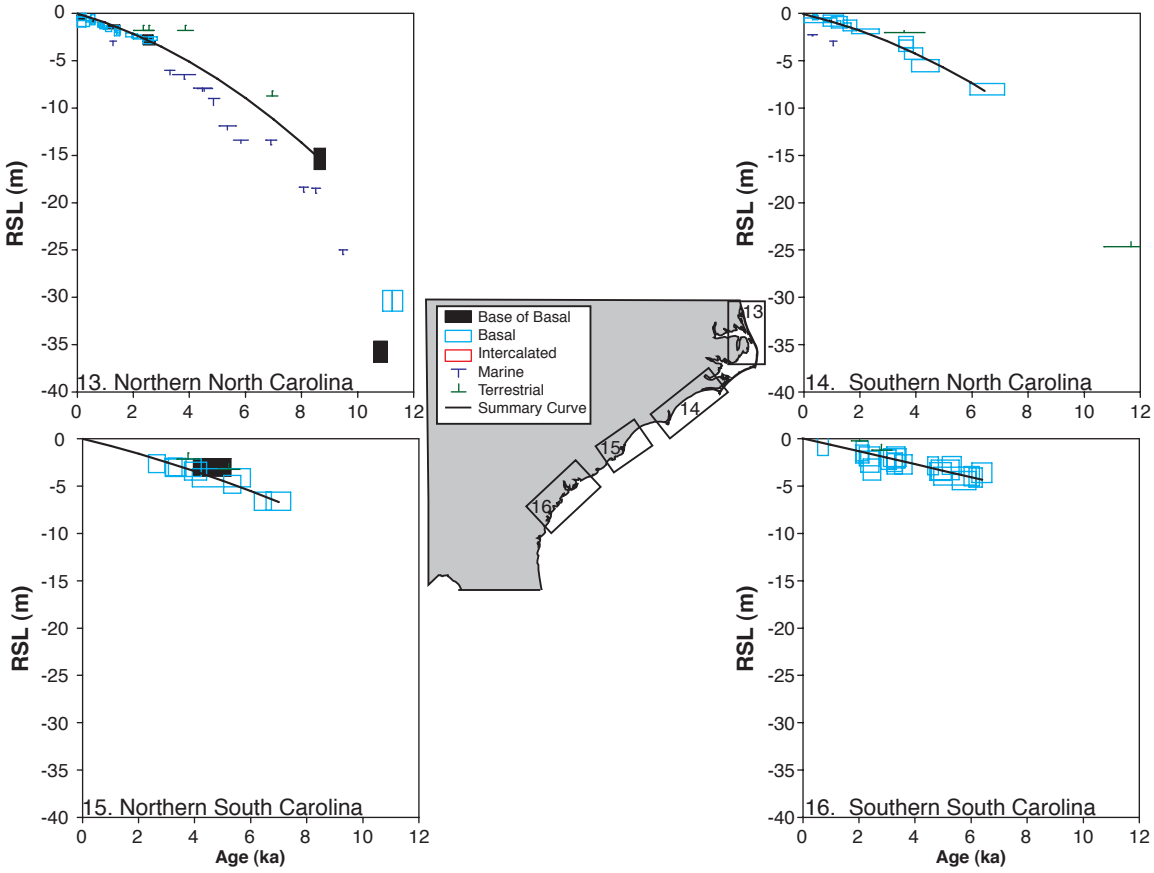

Figure 3.5 - Sea-level index points for 16 areas along the U.S. Atlantic coast plotted as calibrated age versus relative sea level (m MSL). The index points are represented as boxes including the age and vetical error terms. A summary curve is calculated for each area with a 2nd order polynomial through the center points of base of basal or basal data.

level data cover the early Holocene to 2 ka. RSL was -6.6 ± 1.0 m MSL at 7.4 – 6.6 ka. RSL rose by c. 1.3 mm a^{-1} from this time to 4 ka and by 0.8 mm a^{-1} from 4 ka to present. The RSL history of **southern South Carolina (#16)** provides information from the mid Holocene to present. The oldest basal index point indicates that RSL was -3.6 ± 1.0 m MSL at 6.7 – 6.0 ka. RSL rose by 0.6 mm a^{-1} to 4 ka, with no evidence for a change in rate from 4 ka to present.

3.6 DISCUSSION

3.6.1 Holocene RSL History of the U.S. Atlantic Coast

The database of Holocene RSL for the Atlantic coast documents a decreasing rate of RSL rise through time. The rate of RSL rise prior to 4 ka for the 16 study areas range from 1.3 – 5.5 mm a^{-1}, compared to 0.6 – 1.7 mm a^{-1} from 4 ka to present. Similar observations from northwest Europe also suggest RSL rise started to decline during the early and mid Holocene (e.g. Shennan and Horton, 2002; Behre et al., 2007; Yu et al, 2007). This decrease in RSL rise coincides with a significant decrease in ice equivalent eustatic input by 7 ka (Milne et al., 2005), which is linked with the disappearance of the Laurentide ice Sheet (e.g. Dyke and Prest, 1987; Renssen et al, 2009; Widmann, 2009). The Laurentide Ice Sheet was the major source of meltwater input in the early Holocene, as the majority of the Fennoscandinavian Ice Sheet had disappeared by c. 9 - 10 ka (e.g. Rinterknecht et al., 2006; Widmann, 2009) and the western Antarctic Ice Sheet did not start to thin until

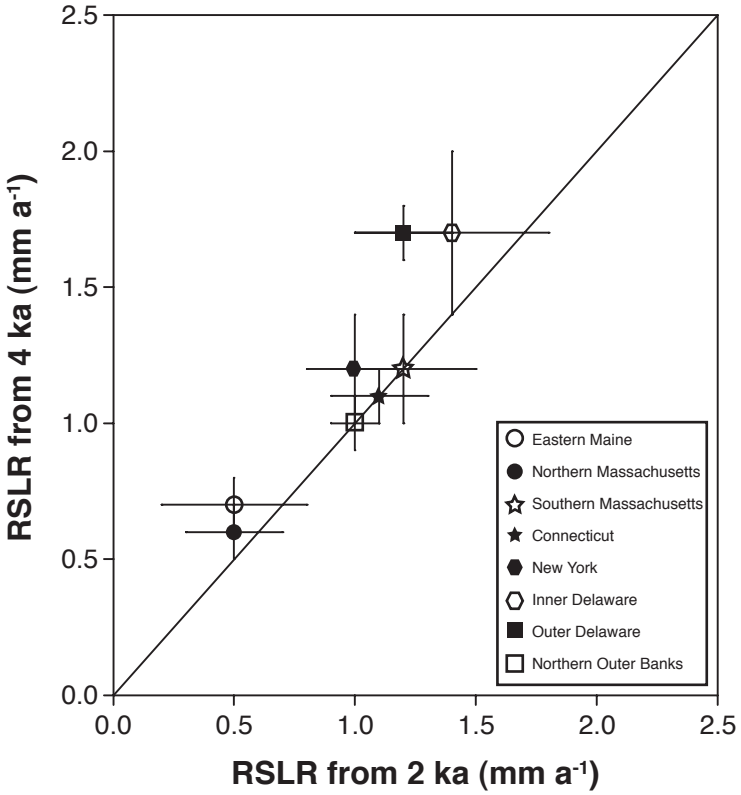

Figure 3.6 - Rates of relative sea-level rise for the last 4 ka plotted on the y-axis and the last 2 ka on the x-axis. The 2-sigma linear regression errors are plotted. The black line marks the 1:1 relationship.

after 7 ka (e.g. Stone et al., 2003). During the late Holocene (4 ka to present), meltwater input has been proposed to be zero (e.g. Peltier, 1998, 2002; Peltier et al., 2002), 0.1 – 0.2 mm a^{-1} from 4 ka to 2 ka (e.g. Lambeck, 2002) or continued melting to 1 ka (Fleming et al., 1998). The database can be used to address this controversy. A comparison between linear rates of rise over the last 4 ka and 2 ka for eight areas highlights similar rates of rise within the error terms of the regression (Figure 3.6), which suggests minimal change in meltwater input over this time.

The database of the Atlantic coast of the U.S. indicates significant spatial variability (Figure 3.7). This variability is driven by the removal of the Laurentide Ice Sheet and the continuing movement towards isostatic equilibrium (e.g. Peltier, 1996). As ice retreated from the near field regions (Figure 3.7a) of Connecticut and Rhode Island by 17 ka (Dyke, 2004), the land mass started to uplift as mantle material flowed from the peripheral forebulge (e.g. Peltier, 1974). Subsequently, near-field areas switched from uplift to subsidence as areas to the north and northwest deglaciated and mantle material further flowed towards Hudson Bay (the center of the former ice sheet) to accommodate the uplift (e.g. Peltier, 1996, 2004). The trends of late Holocene RSL rise within the Northeastern Atlantic region further demonstrate the spatial variation. Lower rates of rise are identified in the northern areas including both Maine sites and northern Massachusetts (0.7 and 0.6 mm a^{-1} respectively) compared to the more southerly Connecticut and southern Massachusetts (1.1 and 1.2 mm a^{-1}, respectively)

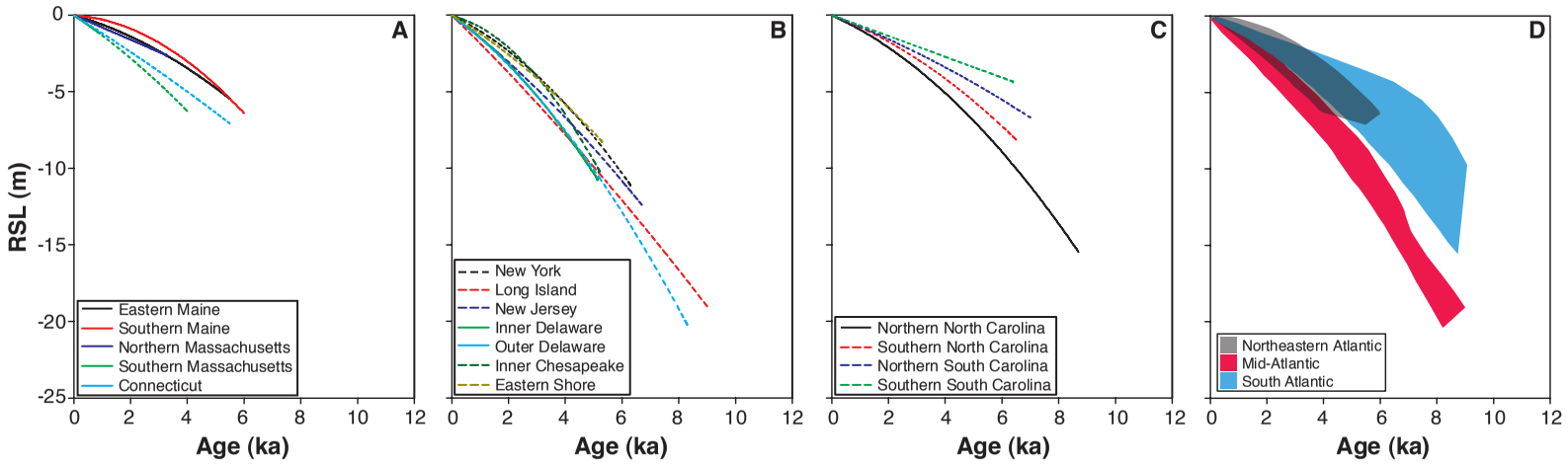

Figure 3.7 - Summary curves for each of the 16 areas sub-divided into A) Northeastern Atlantic, B) Mid-Atlantic and C) South Atlantic regions. Solid lines indicate that the 2nd order polynomial was fitted only to base of basal samples. Dashed lines indicate that the 2nd order polynomial was fitted to base of basal plus basal index points, or solely to basal index points. D) Relative sea-level envelopes for the three regions.

The mid-Atlantic and South Atlantic regions of the U.S. Atlantic coast were at the periphery of the ice sheet (intermediate-field locations) (Dyke and Prest, 1987). When the Laurentide Ice Sheet was at its full extent, the depressed land mass resulted in mantle material moving south (e.g. Wu and Peltier, 1983). This created an area of uplift known as the peripheral forebulge (e.g. Daly, 1934). With the removal of the ice sheet, this mantle material flowed back north resulting in a collapsing forebulge. The highest rate of RSL rise in Delaware and New Jersey of c. 20 m over the last 8 ka (Figure 3.7b), indicates that the maximum extent of the forebulge is not at the former edge of the ice sheet but up to 200 km away from it. This agrees with previous research from GIA models (e.g. Peltier, 2001; Davis et al., 2008). The South Atlantic region has been subject to lower rates of subsidence than the mid-Atlantic (Figure 3.7c) as the effect of the forebulge diminishes with increased distance from the Laurentide Ice Sheet (e.g. Milne et al., 2005). This is illustrated by the late Holocene rates of rise. From Long Island to northern North Carolina, rates of rise are all ≥ 0.8 mm a^{-1}, in contrast to southern North Carolina and South Carolina where rates of rise are ≤ 0.8 mm a^{-1}.

3.6.2 Data Resolution and Spatial Area

Our regional approach sub-divides the U.S. Atlantic coast into 16 areas based on the distance from the Laurentide Ice Sheet. We separate Maine into two areas as the eastern Maine sites are 50 km further from the center of the Laurentide Ice Sheet than southern

Maine. Previous research has shown that small changes in distance can have a large effect on rates of RSL rise (e.g. Davis et al., 2008). We also partition Massachusetts into southern and northern areas rather than assuming that Massachusetts was responding homogenously to GIA (e.g. Redfield and Rubin, 1962; Oldale and O'Hara, 1980). This is supported by Donnelly (2006) who identifies greater similarities between the northern Massachusetts and Maine RSL records than with the southern Massachusetts record. In agreement with Leorri et al. (2006), we also sub-divide the Delaware sites into the Inner and Outer portions of the estuary (supported by different early Holocene rates of 5.5 and 3.0 mm a^{-1}, respectively). A similar partitioning is made for the Inner Chesapeake and Eastern Shore of Virginia sites, further supported by differing late Holocene RSL rise (1.3 and 0.9 mm a^{-1}, respectively).

A limitation of the current database is its inability to produce high-resolution (centimeter to meter scale vertical and annual to centennial age resolution) records of vertical changes in RSL. The index points have an average age error of ±250 a (range: 29 – 1031 a). The range in age errors can be attributed to the variation in material used for dating, the dating technique and the nature of the calibration curve. For example, index points collected between 1960 and 1990 consisted of bulk peat samples, often greater than 0.3 m thick with assay calculated by conventional methods (e.g. Redfield and Rubin, 1962), which results in large age errors (often > ± 500 a). In comparison, index points collected in the last c. 15 years are comprised of dates on plant macrofossils (e.g. van de Plassche

et al., 1998) using the AMS technique, which allows for smaller sample sizes and, thus, commonly produced precise age errors (< ± 100 a). The vertical error ranges from 0.19 – 1.53 m (mean: ±0.66m). The magnitude of the error is dominated by the technique used to estimate the elevation of a sample and the indicative range of the sample. Earlier studies (e.g. Stuiver and Daddario, 1963) presumed an elevation of MHW based on the presence of high marsh vegetation in their study area. Whilst the high marsh does commonly form at MHW, it can extend up to HAT, therefore introducing an error often greater than 0.5 m. The error from the indicative range is coupled to the tidal range. For example, a peat identified as high marsh from Eastport, Maine, would have an indicative range of ±0.63 m (5.6 m mean tidal range), compared to ± 0.10 m at Oregon Inlet, North Carolina (0.3 m mean tidal range). The database, therefore, cannot resolve small-scale (< 0.5 m, < 200 a) fluctuations in RSL that have been suggested from local studies in Maine (e.g. Gehrels et al., 2002), Connecticut (e.g. van de Plassche, 1991; Nydick et al., 1995), New York (e.g. Rampino and Sanders, 1981) and Delaware (e.g. Fletcher et al., 1993; Leorri et al., 2006). Further this limits the analysis of the sea-level change associated with the 8.2 ka climate event (e.g. Barber et al., 1999; Törnqvist et al., 2004; Kendall et al., 2008)

A further limitation of the current database is the temporal and spatial distribution of index points. There is an absence of early Holocene index points, with only 7% of the index points older than 6 ka. This has limited the ability to assess the effects of

compaction in the U.S. Atlantic coast database. Compaction is expected, as fibrous peat is particularly prone to consolidation (e.g. Yamaguchi et al., 1985; Hobbs, 1986, Mitchell and Soga, 2005). However, there is no apparent difference in the elevation among base of basal, basal and intercalated index points in the database. The thickness of overburden has been shown to be a significant variable in assessing compaction (e.g. Shennan et al, 2000; Edwards, 2006; Törnqvist et al., 2008; Horton and Shennan, 2009). The mid and late Holocene index points that dominate the U.S. database come from uninterrupted sequences of peat, which have low sediment overburdens (< 5 m). Similarly, Gehrels (2005), Horton et al. (2009) and Kemp et al. (2009) suggest there is little compaction within the upper c. 2 m of unbroken salt marsh sediments. The lack of data in Georgia and Florida, results in a disconnect between the database and other available RSL data from the Caribbean (e.g. Fairbanks, 1989; Toscano and Macintyre, 2003; Milne et al. 2005) and Gulf Coast (e.g. Blum et al., 2001;Tornqvist et al., 2004, 2006; Gonzalez and Tornqvist, 2009). Addressing the temporal and spatial variations in the database is a vital area for future research.

3.7 CONCLUSIONS

We have reassessed the radiocarbon dated RSL record of the Atlantic Coast of the United States of America to produce a database of 473 index points that indicate the position of former RSL and 347 limiting dates that define the maximum upper and lower limits of

RSL. We have produced indicative meanings for each index point from microfossil and plant macrofossil sea-level indicators and quantified the error term associated with the reconstructions. The database has excellent temporal coverage since 6 ka. Limiting data provide constraints for the early Holocene record. We sub-divided the coastline into 16 areas based on distance from the Laurentide Ice Sheet. RSL rise is well documented from Maine to South Carolina, but there is an absence of index points from Georgia and the Atlantic coast of Florida.

The Holocene RSL rise for the U.S. Atlantic coast is controlled by the interplay between the ice equivalent meltwater input and GIA. There are no index points above present from Maine to South Carolina. The decreasing rate of meltwater input in the early Holocene is reflected in a decrease in the rate of rise from 3 – 5 mm a^{-1} (8 – 4 ka) to 1.2 – 1.7 mm a^{-1} (4 ka – present) in New Jersey and Delaware. The eustatic signal overlays the spatial variability induced by the removal of the Laurentide Ice Sheet, with the greatest rates of RSL rise in New Jersey and Delaware (c. 20 m at 8 ka); the area of greatest forebulge collapse. RSL rise is reduced to the north and south of these two areas. We highlighted that the rates of RSL rise for the last 2 ka and last 4 ka are similar within the error term, which suggests that any meltwater input was minimal.

CHAPTER FOUR

Holocene Relative Sea Levels of the U.S. Atlantic Coast: Implications for Glacial Isostatic Adjustment Models

4.1 ABSTRACT

The relative sea-level (RSL) data from the U.S. Atlantic coast are an independent constraint on the accuracy of glacial isostatic adjustment (GIA) models. We have constructed a quality-controlled database of Holocene sea-level index points for the U.S. Atlantic coast. The observations show spatial variability related to the removal of the Laurentide Ice Sheet and document a decreasing rate of RSL rise through the Holocene. RSL rise during the Holocene was highest in the mid-Atlantic region because of the collapse of the peripheral forebulge. Predictions of RSL for these areas are generated using two ice models (ICE-5G and ICE-6G) coupled to an existing model of mantle viscosity (VM5a). We identified significant misfits from Massachusetts to South Carolina using ICE-5G with the VM5a viscosity profile; ICE-6G provides some improvement for areas from northern Massachusetts to New York but misfits remain elsewhere. Decreasing the upper mantle viscosity by 50% removes the discrepancy between observations and predictions along the mid-Atlantic coastline from southern Massachusetts to the inner Chesapeake Bay. There is no improvement from the Eastern Shore of Virginia to South Carolina, and the previously good agreement with data from Maine disappears. We believe that further refinement of the earth and ice models may be

able to resolve these misfits.

**To be submitted as: Engelhart, S.E., Horton, B.P. and Peltier, W.R. Holocene relative sea levels of the U.S. Atlantic coast: implications for glacial isostatic adjustment models. Geophysical Research Letters.*

4.2 INTRODUCTION

Models of glacial isostatic adjustment (GIA) provide vital constraints on the mass loss of Greenland and Antarctica (e.g. Velicogna and Wahr, 2006; Velicogna, 2009; Cazenave et al., 2009; Peltier, 2009) and the 20th century acceleration in sea-level rise (e.g. Peltier and Tushingham, 1989; Douglas, 1991; Peltier, 1996; Davis and Mitrovica, 1996; Davis et al., 2008). GIA models influence studies of geodesy, as measurements of gravity, earth rotation, site positions and reference frames all must account for changing water and ice loads (e.g. Nakada and Okuno, 2003; Cazenave et al., 2009; Gross and Poutanen, 2009). GIA models have been further employed to understand sediment loading and its associated subsidence (e.g. Ivins et al., 2007) and to provide paleogeographic maps for reconstructions of tidal range change (e.g. Shennan et al., 2000, 2003).

Ongoing crustal motion due to GIA can be identified by Global Positioning Systems (GPS) (e.g. Wolf et al., 2006; Sella et al., 2007; Snay et al., 2007; Teferle et al., 2009;Argus and Peltier, submitted), Satellite Laser Ranging (SLR) (e.g. Argus et al., 1999), Doppler Orbitography by Radiopositioning Integrated on Satellite (DORIS) (e.g. Wolf et al., 2006), Very Long Baseline Interferometry (VLBI) (e.g. Argus et al., 1999) and the Gravity Recovery and Climate Experiment (GRACE) (e.g. Peltier, 2009). However, observations of RSL during deglaciation are vital to constrain models, because they provide a measure of paleo GIA. Such RSL data have been used to

better understand the viscosity of the upper mantle (e.g. Peltier, 1996), lower mantle (e.g. Mitrovica and Peltier, 1992; Mitrovica and Peltier, 1995), and thickness of the Earth's lithosphere (e.g. Tushingham and Peltier, 1992; Shennan et al., 2000), as well as providing information on continental ice volume (e.g. Milne et al., 2002; Peltier and Fairbanks, 2006) and ice equivalent meltwater input (e.g. Milne et al., 2005; Yu et al., 2007).

RSL observations from the Atlantic coast of the U.S.A. during the Holocene provide an independent constraint on the GIA models, because they have been tuned to different datasets from Canada and far-field locations (e.g. Peltier, 1996; Peltier et al., 2002; Peltier and Fairbanks, 2006). The early GIA models did not fit the observational data from the U.S. Atlantic coast (e.g. Clark et al., 1978; Tushingham and Peltier, 1991), with the predictions lying below the observations. The combination of ICE-4G and the 'M2' viscosity profile, however, resulted in the first agreement between the models and observational data (Peltier, 1996); although this dataset was not subject to validation. Recent advances have resulted in new ice models, including ICE-5G (Peltier, 2004) and ICE-6G (Peltier et al., submitted), and the incorporation of rotational feedback (e.g. Peltier, 1994, 1996; 1998, 1999; 2009; Milne and Mitrovica, 1996) have been made. It is unknown whether these developments have eliminated the previously good agreement between observations and predictions from the U.S. Atlantic coast.

To address the above, we have developed a validated database of observations of Holocene RSLs from the U.S. Atlantic coast (Engelhart and Horton, in preparation) to constrain GIA models. Indeed an accurate GIA model is important for defining the location and amplitude of the peripheral forebulge (e.g. Davis and Mitrovica, 1996; Peltier and Jiang, 1996). To account for spatial variations in response to deglaciation, we have subdivided the data into 16 geographical regions based on distance from the center of the Laurentide Ice Sheet (e.g. Peltier, 2004; Engelhart et al., 2009). We proceed to compare the observations to the model predictions, composed of the ICE-5G 1.3e and ICE-6G 1.0 ice models. We attempt to eliminate the misfit between observations and models by modifying the upper mantle viscosity (VM5a/b)

4.3 METHODS

4.3.1 Geological Data

A sea-level index point is a datum that can be employed to show vertical movement of sea level (e.g. van de Plassche, 1986; Shennan, 1986). There are three criteria that all data must meet to be considered an index point, namely: a location; age; and a defined relationship between the sample and a tidal level (Shennan, 1986; van de Plassche, 1986). We constrain this relationship, known as the indicative meaning, using the distribution of microfossils (e.g. Gehrels, 1994; Horton et al., 2006) and/or identifiable plant macrofossils of salt marsh vegetation (e.g. Redfield, 1972; Niering and Warren,

1980), supported by $\delta^{13}C$ values from the radiocarbon-dated sediments (e.g. Andrews et al., 1998; Gonzalez and Törnqvist, 2009; Kemp et al., in press). A sample specific error term is calculated for each sample, including a variety of factors that are inherent to sea-level research (Shennan, 1986; Engelhart and Horton, in preparation). These include the sample thickness, the method of elevation estimation, sediment compaction due to coring and the accuracy of the benchmark used to calculate the altitude of the sample to North American Vertical Datum 88 (NAVD88). We do not consider the effects of possible changes in tidal range. The influence of compaction is reduced by only utilizing base of basal and basal peat samples (salt-marsh peat that directly overlies uncompressible substrate). For samples that cannot be directly related to former sea level, we can produce marine (e.g. marine shells) and terrestrial (e.g. freshwater peat) limiting dates. These are important constraints on models of GIA, as the dates must lie above or below predictions of former sea level, respectively (e.g. Shennan and Horton, 2002).

All the samples within the database were radiocarbon dated and calibrated to sidereal years using CALIB 5.0.1 (Stuiver et al., 2005). A laboratory multiplier of 1 was used, and all radiocarbon assays are presented with 2 sigma age errors. Samples with a terrestrial source were calibrated using the IntCal04 data set (Reimer et al., 2004). Marine samples were calibrated with the Marine04 data set (Hughen et al., 2004) with an appropriate marine reservoir correction (e.g. Reimer and Reimer, 2001).

4.3.2 Model Data

The model analyses are based on the full gravitationally self-consistent form of GIA (e.g. Peltier, 2007) and include the effects of rotational feedback (e.g. Peltier et al., 2009). The RSL predictions are based on the ICE-5G ice model v. 1.3e (Peltier, 2004) and the newly published ICE-6G (Peltier et al., submitted). Both ice models are coupled to the VM5a viscosity model (Peltier and Drummond, 2008) that reduces the misfit between predicted and observed horizontal motions of the North American plate (Argus and Peltier, submitted). VM5a was modified from VM2, the model originally inferred on the basis of a Bayesian inversion of all the available GIA data that could be invoked to constrain the radial profile of mantle viscosity (Peltier, 1996; Peltier and Drummond, 2008). Importantly, VM2 has a perfectly elastic lithosphere of thickness 90 km, whereas VM5a includes a 60 km thick perfectly elastic upper layer, beneath which exists a 40 km thick layer with a viscosity of 10^{22} Pa s. We modify the VM5a model by reducing the upper mantle viscosity from $0.5 * 10^{21}$ Pa s to $0.25 * 10^{21}$ Pa s.

4.4 RESULTS

We present Holocene RSL data consisting of 339 basal peat index points, 52 marine limiting dates and 78 terrestrial limiting dates. This is a subset of the complete Holocene dataset for the U.S. Atlantic coast (Engelhart and Horton, in preparation), as we are not considering intercalated index points. These are sub-divided into 16 areas (Figure 4.1).

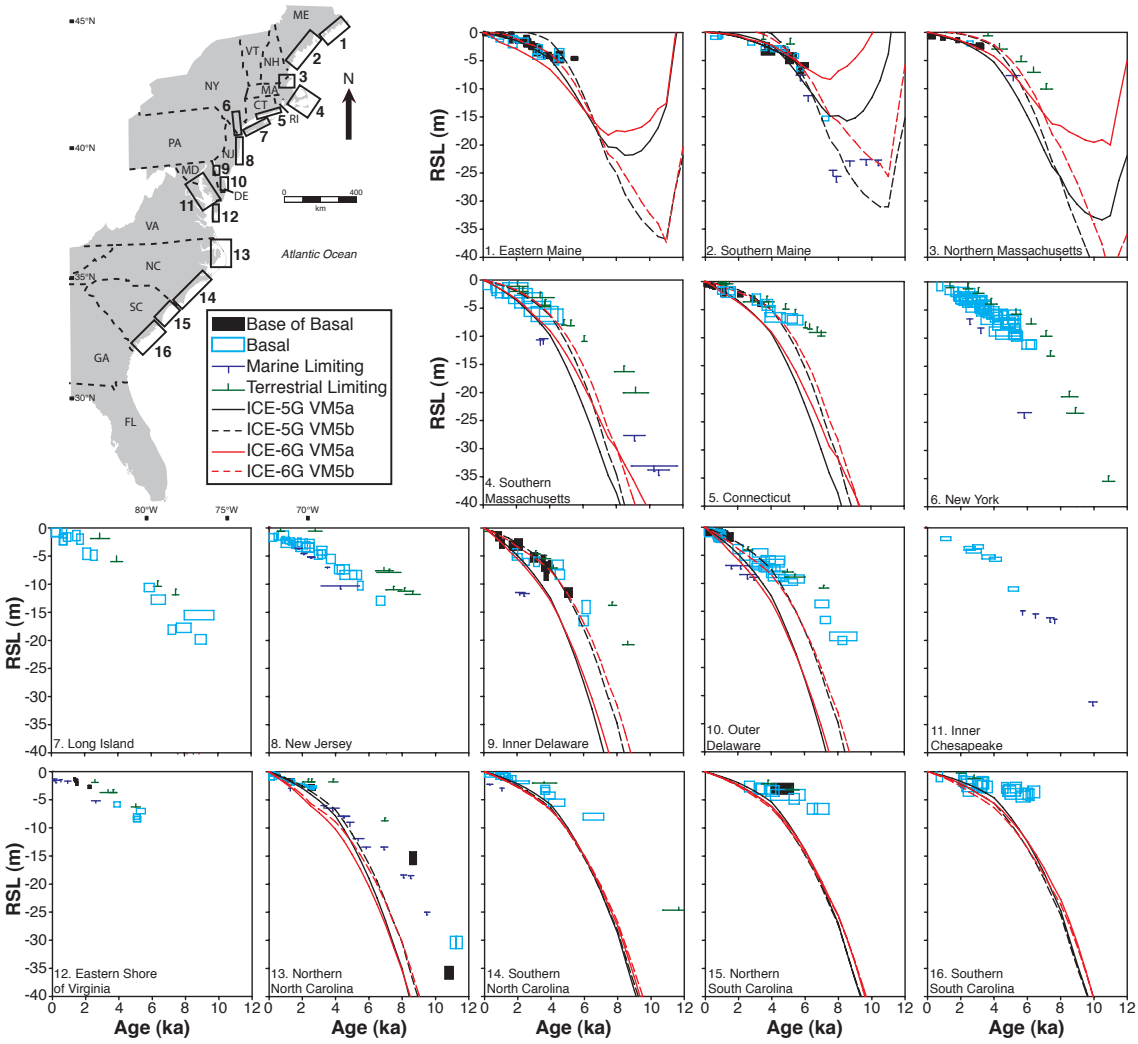

Figure 4.1 - Age-altitude plots of RSL observations and model predictions for 16 different areas from Maine to South Carolina on the U.S. Atlantic coast. Index points are plotted as boxes with the full vertical and age error and are relative to modern mean sea level. Predictions shown are from the ICE-5G (black line) and ICE-6G (red line) ice models, coupled to either the original VM5a (solid lines) or the modified VM5b (dashed lines) viscosity profiles. Where index points are not available, the model should plot above marine limiting dates and below terrestrial limiting dates.

The database has good spatial coverage from Maine to South Carolina, but there is an absence of index points in Georgia and on the Atlantic coast of Florida. The RSL records during the early and mid Holocene consist of index points supported by terrestrial and marine limiting dates. There are no index points above present during the Holocene. Rates of RSL change were highest during the early Holocene and have been decreasing over time. The maximum rate (c. 20 m since 8 ka) occurred in New Jersey and Delaware, the area of greatest ongoing forebulge collapse.

The ICE-5G VM5a model is in good agreement with the data in eastern Maine (#1) and southern Maine (#2) for the last 6 ka (Figure 1). The model does not invalidate marine limiting dates from southern Maine that indicates a sea-level lowstand between 8 and 11 ka. For the remaining study areas (#3 to #16), the model fits the observations in the late Holocene (0-3 ka) but with increasing age, there is a systematic disagreement between the model and data. The misfit is most pronounced between New York and northern North Carolina (#6 to #13), with observations of RSL c. 10 m higher than model predictions at 6 ka (e.g. Connecticut, #5). The predictions are invalidated by marine limiting dates at southern Massachusetts (#4), New Jersey (#8), Inner Chesapeake (#11) and northern North Carolina (#13).

The ICE-5G VM5b model raises the Holocene RSL predictions. This is, however, at the expense of the agreement between the model and data in eastern Maine (#1),

southern Maine (#2) and northern Massachusetts (#3), with predicted highstands during the last 3 ka that are not supported by the observations. The change in viscosity profile significantly improves the fit between data and model predictions from southern Massachusetts to the Eastern Shore of Virginia (#4 to #12). The model predictions agree with the data at all these sites to 4 ka, with the fit extending into the mid-Holocene (e.g. Connecticut #5, New York #6 and Inner Delaware #9). However, early Holocene marine limiting dates in southern Massachusetts (#4), Inner Chesapeake (#11) and northern North Carolina (#13) invalidate the model. Varying the viscosity profile does not change the model predictions in North Carolina and South Carolina (#13-#16) and therefore the misfit remains; at northern South Carolina (#15) observation are c. 10 m higher than predictions at 7 ka.

The ICE-6G VM5a is an improvement over ICE-5G VM5a for northern Massachusetts to New York (#3 to #6) because model predictions of Holocene RSL are higher. However, the new ice model removes the agreement between model and observations in Maine. The model under-predicts RSL in eastern Maine (#1) and over-predicts in southern Maine (#2). There is little difference between the ICE-6G and ICE-5G results from Long Island to southern South Carolina (#7 to #16), with the exception of the Eastern Shore of Virginia (#12) and northern North Carolina (#13). At these two sites, ICE-6G VM5a is the worst of the four models, under predicting RSL at 4 ka by ~5 m.

ICE-6G VM5b provides the best agreement between models and data in the mid-Atlantic from southern Massachusetts to the inner Chesapeake (#4 to #11). It also resolves the highstand predicted at eastern Maine (#1) by ICE-5G VM5b. The highstands, however, remains at southern Maine (#2) and northern Massachusetts (#3). Utilizing the VM5b instead of VM5a viscosity model does not resolve the misfit between the model and the data for ICE-6G at the Eastern Shore of Virginia (#12) and northern North Carolina (#13) areas. It also does not affect the predictions for the three most southerly sites (#14-16). This indicates a systematic error in all four model predictions for these locations.

4.5 DISCUSSION

Decreasing the upper mantle viscosity in VM5a to produce VM5b results in a significant improvement in the quality of fit along the U.S. Atlantic coast, which is particularly noticeable in the area of forebulge collapse. This has been observed for earlier model iterations, where increasing the upper mantle/lower mantle contrast ratio from 1:1 to 1:4 resulted in a decrease in the variance between the models and data (Tushingham and Peltier, 1992). However, by reducing the value of both the upper mantle and the transition zone, we have violated the McConnell spectrum (McConnell, 1968). If this adjustment remains necessary to fit the U.S. Atlantic coast RSL data, then it suggests that lateral heterogeneity of the upper mantle may be on a spatial scale large enough to affect GIA.

Whilst the VM5b viscosity profile results in a significant improvement in the agreement between the model and the data at most sites, there are two remaining issues. Firstly, the incorporation of the VM5b viscosity profile causes late Holocene highstands of sea level in eastern and southern Maine (#1 and #2) and northern Massachusetts (#3). These are not observed in the data. VM5b causes these highstands to exist as the softening of the upper mantle and transition zone causes a time dependent shift of the boundary between uplift and subsidence. However, the highstand at eastern Maine is not present when the new ICE-6G model is used with the VM5b viscosity profile due to a change in the thickness of proximal ice load. Therefore, the highstands in southern Maine (#2) and northern Massachusetts (#3) may be eliminated through further thickening of the ice load in proximity to these two locations.

Changing the upper mantle viscosity profile has no effect on the RSL predictions in the southern region because the RSL data from this southernmost region are apparently controlled by significantly deeper structure. Changing the ice model also has no effect because both the ice models directly employed in this investigation have very similar total mass and cover exactly the same surface area of the North American continent. This indicates that further modification of the upper mantle viscosity profile or ice model are unlikely to improve the fit to the data. Therefore, we must consider that changes to other parameters in the earth model may be necessary to fit the data.

Previous researchers have suggested that changes in lower mantle viscosity (e.g. Davis and Mitrovica, 1996), lithospheric thickness (e.g. Tushingham and Peltier, 1992) and incorporating lateral heterogeneity in the mantle (e.g. Latychev et al., 2005; Davis et al., 2008) may be able to resolve the disagreement between models and observations of RSL along the U.S. Atlantic coast. The lower mantle viscosity is strongly constrained by emergent shorelines in Hudson Bay (e.g. Peltier, 1994; Mitrovica and Peltier, 1995; Forte and Mitrovica, 1996; Peltier, 1998; Mitrovica and Forte, 2004). Davis et al. (2008) investigated the effects of solely incorporating lateral heterogeneity of the lower mantle and demonstrated that it increased the rates of ongoing GIA. Further, it has been acknowledged that ice marginal sites are sensitive to changes in lithospheric thickness, whilst near-field sites are not (Tushingham and Peltier, 1992). However, the proposed value of 245 km to improve the fit (Tushingham and Peltier, 1992) is a factor of 2 greater than the values normally considered for lithospheric thickness (e.g. Peltier, 2004). Finally, a further softening of the transition zone may be able to further improve the fit, but if true, this would exacerbate the issue of fitting the McConnell spectrum.

4.6 CONCLUSIONS

We have constructed a validated database of sea-level observations for the Holocene consisting of 339 basal peat index points and 130 limiting dates. We have demonstrated that the ICE-5G VM5a model cannot resolve the observations of RSL along the U.S.

Atlantic coast with the model systematically underpredicting RSL in the early and mid Holocene. The variance between the model and the observations can be significantly reduced in the mid-Atlantic from southern Massachusetts to the inner Chesapeake by a 50% reduction in the upper mantle viscosity (VM5b). However, the misfit remains in both northern (southern Maine and northern Massachusetts) and southern (Eastern Shore of Virginia to southern South Carolina) areas. Changes to the ice model may be able to resolve the misfit in the northern sector by thickening the proximal ice load. We believe that the southern misfits may be resolved by further refinement of the earth model.

CHAPTER FIVE

Spatial Variability of Late Holocene and 20th Century Sea-Level Rise along the Atlantic Coast of the United States

5.1 ABSTRACT

Accurate estimates of global sea-level rise in the pre-satellite era provide a context for 21st century sea-level predictions, but the use of tide-gauge records is complicated by the contributions from changes in land level due to glacial isostatic adjustment (GIA). We have constructed a rigorously quality-controlled database of late Holocene sea-level indices from the U.S. Atlantic Coast, exhibiting subsidence rates of less than 0.8 mm a^{-1} in Maine, increasing to rates of 1.7 mm a^{-1} in Delaware, and a return to rates less than 0.9 mm a^{-1} in the Carolinas. This pattern can be attributed to ongoing GIA due to the demise of the Laurentide Ice Sheet. Our data allow us to define the geometry of the associated collapsing proglacial forebulge with a level of resolution unmatched by any other currently available method. The corresponding rates of relative sea-level rise serve as "background" rates on which future sea-level rise must be superimposed. We further employ the geological data to remove the GIA component from tide-gauge records to estimate a mean 20th century sea-level rise rate for the U.S. Atlantic Coast of 1.8 ± 0.2 mm a^{-1}, which is similar to the global average. However, we find a distinct spatial trend in the rate of 20th century sea-level rise, increasing from Maine to South Carolina. This is the first evidence of this phenomenon from observational data alone. We suggest this may

be related to either the melting of the Greenland Ice Sheet, and/or ocean steric effects.

**Published as: Engelhart, S.E., Horton, B.P., Douglas, B.C., Peltier, W.R. and Törnqvist, T.E., 2009. Spatial Variability of Late Holocene and 20th Century Sea-Level Rise Along the Atlantic coast of the United States. Geology, 37, 1115-1118*

5.2 INTRODUCTION

Global sea-level rise is the result of an increase in the volume of the ocean, which evolves from changes in ocean mass due to melting of continental glaciers and ice sheets, and expansion of ocean water as it warms. To extract the 20th century rates of sea-level rise from satellite altimeters and long-term tide-gauge records, corrections must be applied for vertical land movements that are primarily associated with the glacial isostatic adjustment (GIA) of the solid Earth.

There are various approaches to develop estimates of sea-level rise for the 20th century. Firstly models of GIA have been constructed and then later employed by a number of authors, which produce global sea-level rise estimates of c. 1.8 mm a^{-1} (Peltier and Tushingham, 1989; Douglas, 1991, 1997; Peltier, 2001; Church and White, 2006), although the U.S. Atlantic Coast shows considerable variation in the rate of sea-level rise with respect to this global average depending upon the GIA model employed (Peltier and Tushingham, 1989; Peltier, 1996; Davis and Mitrovica, 1996; Peltier, 2001). Secondly, global positioning systems (GPS) have been used that suggest a rate of c. 1.9 mm a^{-1} for the Atlantic Coast (Snay et al., 2007), which is essentially identical to the result reported in Peltier (1996), but the errors associated with this technique are currently large due to the short time series of the GPS data. A third method of correcting for land movements is to use geological data. Salt-marsh sedimentary sequences enable the reconstruction of

relative sea-level change over a much longer period. This data-based technique improves on model-based approaches, because subtle tectonic effects are incorporated into both the geological and 20th century rates. Gornitz (1995) estimated a 20th century sea-level rise of 1.5 ± 0.7 mm a^{-1} for the U.S. Atlantic Coast. However, this geological database included sea-level index points up to 6 ka, thus sea-level rise rates included meltwater contributions from the remnants of the major ice sheets (Peltier, 2002). Peltier (2001) demonstrated that the Gornitz (1995) result was a significant underestimate because it was based upon a linear least squares fit to the data over a range of time sufficiently long that sea level could not be assumed to be rising linearly.

5.3 METHODOLOGY

5.3.1 Construction of a Sea-Level Index Point

To be a validated sea-level index point, a sample must have a location, an age, and a defined relationship between the sample and a tidal level (Shennan, 1986; van de Plassche, 1986). We constrain this relationship, known as the indicative meaning (van de Plassche, 1986), using zonations of modern vegetation (Redfield, 1972; Niering and Warren, 1980; Lefor et al., 1987; Gehrels, 1994), the distribution of microfossils (Gehrels, 1994) and/or $\delta^{13}C$ values from the radiocarbon-dated sediments (Andrews et al., 1998; Törnqvist et al., 2004). We calculate the total vertical error of each index point from a variety of errors that are inherent to sea-level research (Shennan, 1986), including

thickness of the sample, techniques of depth measurement, compaction of the sediment during sampling and leveling of the sample to the nationwide geodetic datum, NAVD 88 (Supplementary Information A). These errors exclude any influence of the possible change of tidal range through time. Each validated index point in the database was radiocarbon dated and we present such assays as calibrated years BP using CALIB 5.0.1 (Stuiver et al., 2005). We used a laboratory multiplier of 1 with 95% confidence limits and employed the IntCal04 data set (Reimer et al., 2004).

5.3.2 Geological Records

We assume the ice-equivalent meltwater input 4 ka to AD 1900 is either zero (Peltier and Tushingham, 1991; Douglas, 1995; Peltier, 1996, 2002) or minimal (Milne et al., 2005; Church et al., 2008). Along the passive margin of the U.S. Atlantic Coast, it is widely accepted that the tectonic component is negligible. We have significantly reduced the influence of compaction by only utilizing basal peat samples (salt-marsh peat that directly overlies uncompressible substrate; Jelgersma, 1961). Therefore, any changes observed in relative sea level are almost entirely from vertical land movements due to GIA. To calculate the late Holocene rate of relative sea-level rise (RSLR) for each location, we excluded the 20th century sea level contribution by expressing all ages with respect to AD 1900 and adjusted the sea-level axis to mean sea level in AD 1900 (Supplementary Information B). We estimated the rate of late Holocene RSLR by running a linear regression over the last 4 ka with two sigma errors (Shennan and Horton, 2002).

5.3.3 Tide Gauge Records

We identified 10 suitable tide-gauge records along the U.S. Atlantic Coast with a nearby geological record of late Holocene RSLR with negligible influence of non-GIA subsidence, such as groundwater withdrawal (Sun et al., 1999). All records are at least 50 years in length to minimize contamination by interannual and decadal variability (Douglas, 1991). A single standard error was calculated for all the gauges, which included a thorough consideration of tide-gauge record length (Supplementary Information C).

5.4 ANALYSIS

We produced a late Holocene database of validated sea-level index points from new, unpublished and published records of basal peats of the U.S. Atlantic Coast. The validated database contains 212 basal sea-level index points for the last 4 ka from 19 locations that stretch from Maine (45ºN) to South Carolina (32ºN) (Figure 5.1). There is an absence of index points from Georgia and Florida. Relative sea level has risen along the entire U.S. Atlantic Coast during the late Holocene with no evidence of former sea levels above present during this time period within our validated database. There is a large vertical scatter (over 5 m at 4 ka), because the entire coastline has been subject to spatially variable GIA-induced subsidence from the collapse of the proglacial forebulge (Peltier, 1994). From eastern Maine (45ºN) to northern Massachusetts (42ºN), relative sea level has risen less than 3.5 m during the last 4 ka, with rates of RSLR lower than

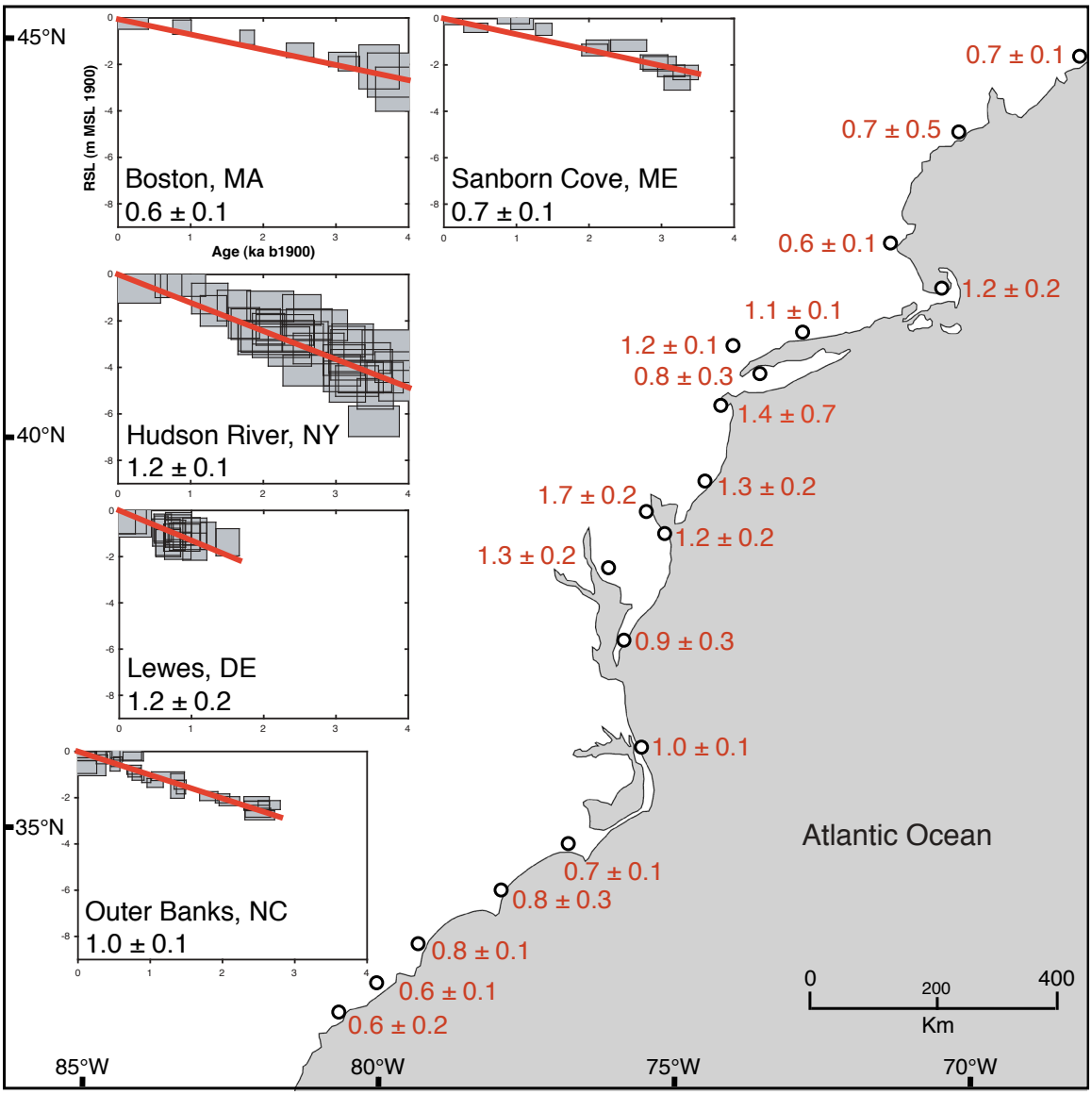

Figure 5.1. Rate of late Holocene relative sea-level rise with two sigma errors for 19 locations along the U.S. Atlantic coast. Inset plots are examples of locations with sea-level index points plotted as calibrated age versus change in RSL relative to MSL in 1900 (m). The red line is the linear regression for each site. Rates and errors shown to 1 decimal place.

0.8 mm a^{-1} (Figure 5.1, Table 5.1). Along the mid-Atlantic coastline from Cape Cod, Massachusetts (41.5ºN) to the northern Outer Banks, North Carolina (35.9ºN), late Holocene RSLR of 1 mm a^{-1} is met or exceeded at nine of eleven locations. The highest rates of RSLR are recorded in New Jersey, Delaware and Maryland, where all rates are greater than 1.2 mm a^{-1}. The maximum RSLR of 1.7 ± 0.2 mm a^{-1} is recorded in the inner Delaware estuary. RSLR decreases to less than 0.9 mm a^{-1} from Beaufort, North Carolina (34.7ºN) to Port Royal, South Carolina (32.4ºN). The southern North Carolina and South Carolina sites all show similar records of RSLR (0.5 - 0.8 mm a^{-1}).

All tide-gauge locations along the U.S. Atlantic Coast show an acceleration in the rate of RSLR between the late Holocene geological data and the 20th century tide gauges (Figure 5.2). Subtracting the late Holocene RSLR from the tide gauges yields an average 20th century sea-level rise rate of 1.8 ± 0.2 mm a^{-1}. This corresponds closely to the global average for the past century (Peltier and Tushingham, 1989; Douglas, 1991, 1997; Peltier, 2001; Church and White, 2006). Despite the errors of the tide gauge and geological data, there is a north to south increase in the rate of 20th century sea-level rise. The lowest rate of 1.2 ± 0.6 mm a^{-1} occurs near the northern end of the study area at Portland, Maine, while to the south it doubles to 2.6 ± 0.3 mm a^{-1} (Charleston, South Carolina) (Figure 5.2); a range of 1.4 mm a^{-1}.

Site #	Site Name	Late Holocene RSLR (mm a^{-1})	Rate from Nearest GPS Station (mm a^{-1})	References
1	Sanborn Cove, Maine	0.7 ± 0.1	1.9 ± 2.0 (1)	Gehrels and Belknap, 1993; Gehrels, 1999
2	Phippsburg, Maine	0.7 ± 0.5	-0.2 ± 3.2 (2)	Gehrels et al., 1996
3	Boston, Massachusetts	0.6 ± 0.1	2.3 ± 1.2 (2)	Newman et al., 1980; Donnelly, 2006
4	Barnstable, Massachusetts	1.2 ± 0.2	N/A	Redfield and Rubin, 1962; Stuiver et al., 1963
5	Clinton, Connecticut	1.1 ± 0.1	N/A	Cinquemani et al., 1982; van de Plassche, 1991; Nydick et al., 1995; van de Plassche et al., 2002
6	Hudson River, New York	1.2 ± 0.1	0.6 ± 3.0 (2)	Newman et al., 1980, Pardi et al., 1984
7	Northern Long Island, New York	0.8 ± 0.3	1.6 ± 3.0 (2)	Cinquemani et al., 1982; Pardi et al., 1984
8	Sandy Hook, New Jersey	1.4 ± 0.7	2.2 ± 1.4 (1)	Cinquemani et al., 1982
9	Atlantic City, New Jersey	1.3 ± 0.2	N/A	Stuiver and Daddario, 1963; Cinquemani et al., 1982; Pardi et al., 1984; Psuty, 1986
10	Inner Delaware Estuary, Delaware	1.7 ± 0.2	2.9 ± 2.0 (2)	Belknap, 1975; Belknap and Kraft, 1977; Nikitina et al., 2000
11	Lewes, Delaware	1.2 ± 0.2	1.1 ± 2.3 (1)	Elliot, 1972; Belknap, 1975; Belknap and Kraft, 1977; Fletcher et al., 1993; Ramsey and Baxter, 1996; Nikitina et al., 2000
12	Blackwater, Maryland	1.3 ± 0.2	2.2 ± 2.3 (1)	Cinquemani et al., 1982
13	Eastern Shore, Virginia	0.9 ± 0.3	3.5 ± 1.6 (2)	Engelhart and Kemp, unpublished
14	Outer Banks, North Carolina	1.0 ± 0.1	N/A	Cinquemani et al., 1982; Horton et al., 2009
15	Beaufort, North Carolina	0.7 ± 0.1	N/A	Cinquemani et al., 1982; Spaur and Snyder, 1999; Horton et al., 2009
16	Wilmington, North Carolina	0.8 ± 0.3	N/A	Cinquemani et al., 1982
17	Georgetown, South Carolina	0.8 ± 0.1	N/A	Cinquemani et al., 1982
18	Charleston, South Carolina	0.6 ± 0.1	1.6 ± 1.7 (1)	Cinquemani et al., 1982
19	Port Royal, South Carolina	0.6 ± 0.2	N/A	Cinquemani et al., 1982

Table 5.1 - Location of the 19 sites along the U.S. Atlantic Coast and the rate of late Holocene (last 4 ka) relative sea-level rise (RSLR) derived from geological data. The references for the geological data are shown. GPS rates of vertical motion are from (1) Snay et al. (2007) and (2) Sella et al. (2007). Geological and GPS rates are shown with two sigma errors. Positive and negative values from the geological and GPS data refer to subsidence and uplift, respectively.

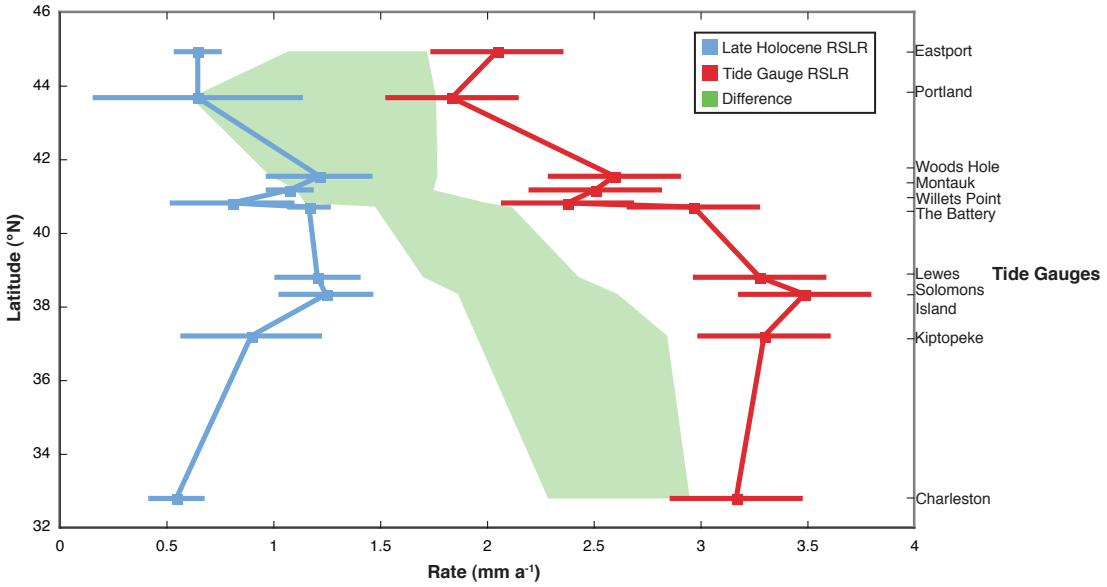

Figure 5.2. Detrending of 20th century tide gauge relative sea-level rise (RSLR) with rates of late Holocene relative sea-level rise for 10 locations along the U.S. Atlantic coast. Mean and two sigma error of sea-level trends are plotted against latitude.

5.5 DISCUSSION

The geological data constrain the form of the ongoing forebulge collapse along the U.S. Atlantic Coast. This is apparent when the rates of late Holocene RSLR are plotted against the distance from the center of mass loading of the Laurentide Ice Sheet (Figure 5.3). Vertical motions from continental North America GPS measurements (Sella et al., 2007) and GIA models (Peltier, 2004) propose the center of ice loading is west of Hudson Bay. Sella et al. (2007) calculated maximum vertical velocities of +10 mm a^{-1}, with rates generally decreasing with distance away from Hudson Bay. Interpolation of the GPS observations suggest the "hinge line" separating uplift from subsidence is offshore of the Maine coastline, whereas the geological data from two locations in this study suggest Maine is experiencing GIA related subsidence of 0.7 mm a^{-1} with a maximum uncertainty of 0.5 mm a^{-1}. Snay et al. (2007) also identified subsidence rates within Maine of 1.9 ± 1.0 mm a^{-1} using coastal GPS stations but with significant spatial variation; two GPS measurements from Maine suggest uplift (+1.0 ± 1.2 mm a^{-1} and +0.3 ± 1.0 mm a^{-1} vertical velocity).

Snay et al. (2007) estimated the maximum rate of subsidence (3.1 ± 3.5 mm a^{-1}) occurs within Maryland. Similarly, the geological data show late Holocene RSLR increasing from eastern Maine to a maximum within the mid-Atlantic but of a smaller magnitude (Maryland 1.3 ± 0.2 mm a^{-1}; Delaware, 1.7 ± 0.2 mm a^{-1}; New Jersey, 1.4 ± 0.7 mm a^{-1}).

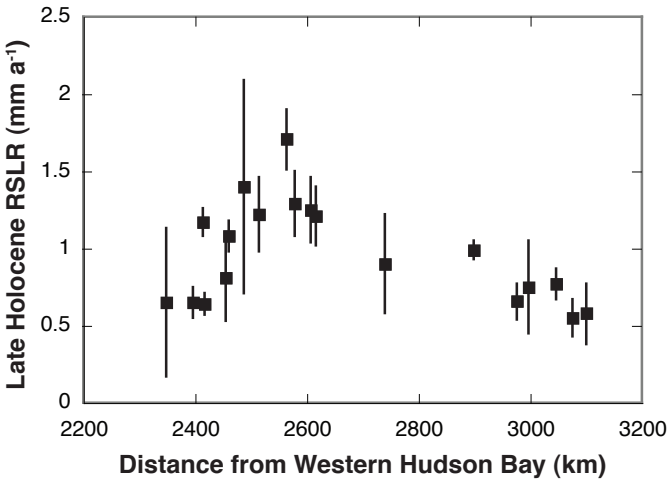

Figure 5.3. Rate of late Holocene relative sea-level rise with two sigma errors for 19 locations along the U.S. Atlantic coast plottted as a function of distance from western Hudson Bay (km).

The geological rates of subsidence decline rapidly with distance from Hudson Bay along the U.S. Atlantic Coast compared to the GPS observations. The GPS observations suggest that high rates of subsidence from the collapse of the forebulge extend into Virginia and the Carolinas (Sella et al., 2007; Snay et al., 2007). For example, the geological data within Chesapeake Bay, Virginia, estimate subsidence of 0.9 ± 0.3 mm a^{-1} compared to nearby GPS observations of 3.5 ± 1.6 mm a^{-1} (Sella et al., 2007) and 2.6 ± 1.2 mm a^{-1} (Snay et al., 2007). Although the GPS data agree with the general form of the forebulge collapse revealed by the geological data, there are significant spatial variations. The GPS data are limited by the short time series with a maximum length of eight years on the U.S. Atlantic Coast between Maine and South Carolina (Snay et al., 2007), which results in large errors. The errors of the GPS data quoted above are at the one sigma level; if two sigma errors are used, the geological and GPS rates concur. Furthermore, it has been noted elsewhere that continuous GPS measurements may be systematically biased (too positive), potentially due to inadequate modeling of antenna phase center variations and/or the use of current terrestrial reference frames (Teferle et al., 2009).

Removing the GIA signal from the tide-gauge records with our geological observations of subsidence reveals that the rate of 20th century sea-level rise increased from north to south. A similar slope has been identified by GIA modeling (Peltier, 1996) but this is the first evidence from observational data alone. There may be a significant contribution to the 20th century sea-level changes from Greenland Ice Sheet mass balance changes

(Marcos and Tsimplis, 2007) and/or ocean steric effects (Domingues et al., 2008). The effects of Greenland mass loss on the U.S. Atlantic Coast would result in a similar north to south increase in sea-level rise (Conrad and Hager, 1997). Estimates of Greenland mass loss from GRACE since AD 2002 vary between 100 and 270 Gt a^{-1}, which is equivalent to a sea-level rise of c. 0.4–0.7 mm a^{-1} (Velicogna and Wahr, 2006; Peltier, in press). Rignot et al. (2008) suggested that Greenland is currently losing mass at the equivalent sea-level rise rate of c. 0.6 mm a^{-1}. Steric effects may also play an important role in 20th century sea-level change (Miller and Douglas, 2004; Wake et al., 2006; Church et al., 2008). Church et al. (2008) propose significant spatial variation in ocean thermal expansion for the upper 700 m along the U.S. Atlantic Coast with areas possessing negative and positive thermal contributions to sea-level rise over the period 1993–2003. Wake et al. (2006) analyzed hydrographic data sets of the Atlantic Coast and identified a large steric effect for the southern portion of the coastline that would influence 20th century RSLR, but Miller and Douglas (2006, 2007) concluded that there were only minor steric contributions to sea-level rise during the 20th century, north of Cape Hatteras.

The geological data documents the continued response of the U.S. Atlantic Coast to the collapsing Laurentide forebulge at a significantly improved resolution. Furthermore, we have demonstrated that the removal of the variation imposed on the tide gauges by this ongoing deformation cannot fully explain the spatial variations seen within the

tide-gauge records. Therefore, care should be taken when employing tide-gauge records as a validation of GIA models (Davis and Mitrovica, 1996; Davis et al., 2008). The database of late Holocene sea levels provides a new tool both for testing hypotheses relating to this spatial variability, as well as refining models of ocean dynamical effects. From analyzing climate models, Yin et al. (2009) found that a dynamic, regional rise in sea level is induced by a weakening meridional overturning circulation in the Atlantic Ocean (superimposed on the global mean sea-level rise). The application of a comparable methodology to de-trend relative sea-level records from Canada (e.g., Gehrels et al., 2004), the U.S. Gulf Coast (e.g., Törnqvist et al., 2004) and the Caribbean (e.g., Toscano and Macintyre, 2003) using geological data will further elucidate the spatial variability of 20th century sea-level rise.

5.6 SUPPLEMENTARY MATERIALS

5.6.1 Supplementary Information A: Sea-Level Index Points

The standardized methodology for reconstructing former sea levels from low energy, sedimentary environments has been established during the International Geological Correlation Programs (IGCP) (van de Plassche, 1986; Shennan and Horton, 2002; Edwards, 2006). To be a validated sea-level index point (SLI), a sample must have a location, an age and a known relationship between the sample and a known tidal level and the indicative meaning (Shennan, 1986; van de Plassche, 1986). The indicative

meaning is constructed of two parameters, the reference water level (e.g. mean higher high water (MHHW)) and the indicative range (the vertical range over which the sample could occur). To constrain the indicative meaning of the index points in the U.S. Atlantic database, we have used published zonations of modern vegetation (Redfield, 1972; Niering and Warren, 1980; Lefor et al., 1987; Gehrels, 1994) and the distribution of microfossils (Gehrels, 1994) supported by $\delta^{13}C$ values from the radiocarbon-dated sediments (Andrews et al., 1998; Törnqvist et al., 2004). As an example, where we have a floral and/or faunal indication that a sample was formed within a salt marsh environment but cannot be identified as specifically high or low marsh, the index point is conservatively estimated to have formed between MHHW and mean tide level (Törnqvist et al., 2004). For samples where we have a positive identification of plant macrofossil species, we can reduce the indicative range. Where authors have used microfossils to quantitatively assess the relationship between the sample and former sea level, these predictions of the indicative meaning have been retained. In practice, over 70% of the samples in the database can only be identified as salt-marsh deposits.

The relative sea level of the sea-level index points is calculated using the equation:

$$\text{Relative Sea Level} = \text{Elevation}_{\text{sample}} - \text{Reference Water Level}_{\text{sample}}$$

where the elevation and reference water level are expressed in meters relative to the national datum, NAVD 88, and subsequently corrected to local mean sea level (MSL).

For each sample, we calculated the vertical error of the index point from a variety of factors that are inherent to sea-level research (Shennan, 1986). Further errors are incorporated including the type of coring equipment used, techniques of depth measurement and the compaction of the sediment during penetration (Woodroffe, 2006). We also included an error estimate associated with the leveling of the sample with respect to NAVD 88. For high precision leveling using modern techniques, this can be as low as ±0.05 m but can rise as high as ±0.5 m for less precise methods. A further error is included due to the leveling of the sample to local tide levels. This is typically ±0.1 m but may be much larger, particularly when samples are collected offshore (Shennan, 1986). The errors in this study do not include the effects of tidal range change through time; we assume that this influence is minimal (Gehrels et al., 1995). The total error (Eh) for each sample is then calculated from the expression:

$$E_h = (e^2_1 + e^2_2 \ldots + e^2_n)^{1/2}$$

Where $e_1 \ldots e_n$ are the individual sources of error.

A further source of error in sea-level reconstruction is sediment consolidation, that is, compression of a sedimentary package by its own weight or the weight from overlying sediment (Kaye and Barghoorn, 1964). The significance of sediment consolidation was recognized from early studies of North American (Bloom, 1964; Kaye and Barghoorn,

1964) and European (Jelgersma, 1961; Streif, 1971; van de Plassche, 1980) salt marshes. If consolidation is not corrected for, then index points will be lowered from their original elevation and the rate and magnitude of relative sea-level rise will be overestimated. However, correcting for the compaction of sediments is a complex process involving many variables (Pizzuto and Schwendt, 1997). Therefore, we have reduced the influence of compaction by only employing basal peat samples, which are deposited directly on the presumed compaction-free substrate (Kaye and Barghoorn, 1964).

Every SLI in the validated database (Figure 5.4, Figure 5.5, Figure 5.6, Figure 5.7, Figure 5.8) was radiocarbon dated and calibrated using CALIB 5.0.1 (Stuiver et al., 2005). We used a laboratory multiplier of 1 with 95% confidence limits and employed the dataset IntCal04 (Reimer et al., 2004). The database contains samples that were dated by Accelerator Mass Spectrometry (AMS), Gas Proportional Counting (GPC) and Liquid Scintillation Counting (LSC). Sample material in the database varies from dates on bulk peat to dates on identifiable salt marsh rhizomes.

5.6.2 Supplementary Information B: Late Holocene Rates of Relative Sea-Level Rise

We have used validated geological observations from basal peat over the last 4 ka (the late Holocene) to reconstruct background rates of sea-level rise. We assume that the ice-equivalent meltwater input over the last 4 ka is either zero (Douglas, 1995; Peltier, 1996,

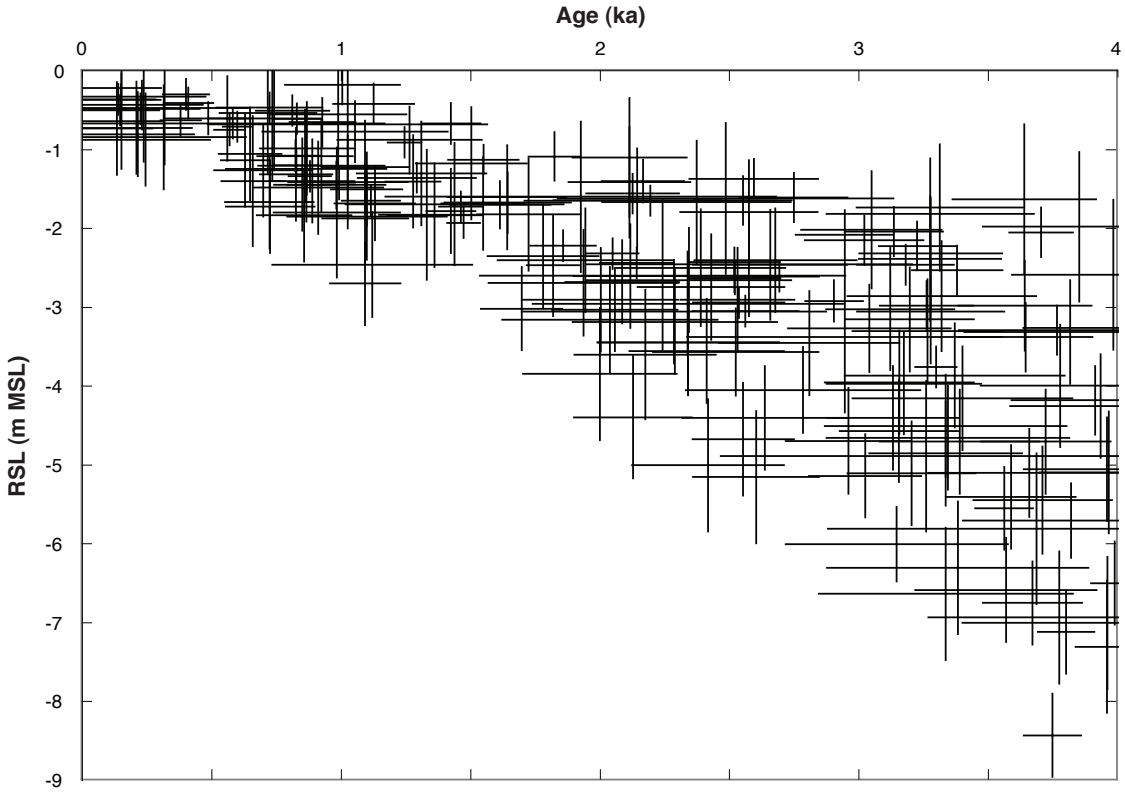

Figure 5.4 - All 212 radiocarbon dated basal index points, covering the last 4 ka. The data demonstrates the considerable scatter caused by the differential GIA along the Atlantic Coast.

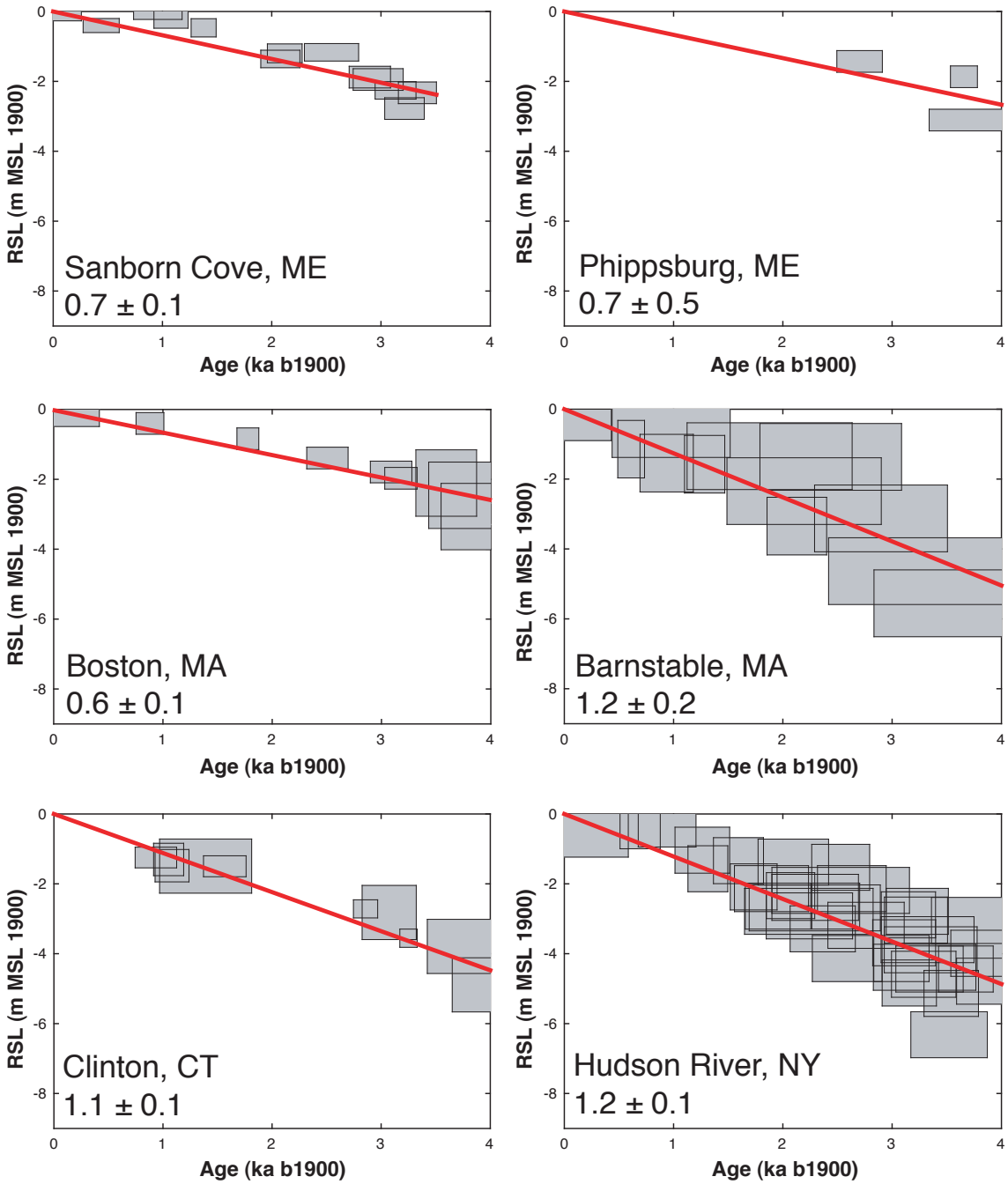

Figure 5.5 - Six locations along the U.S. Atlantic Coast with three or more basal sea-level index points and the late Holocene rates of RSL rise. Sea-level index points are plotted as calibrated age versus change in RSL relative to MSL in AD 1900 (m). The red line is the linear regression for each site. Rates and errors shown to 1 d.p. Data sources for sea level index points are referenced in Table 5.1.

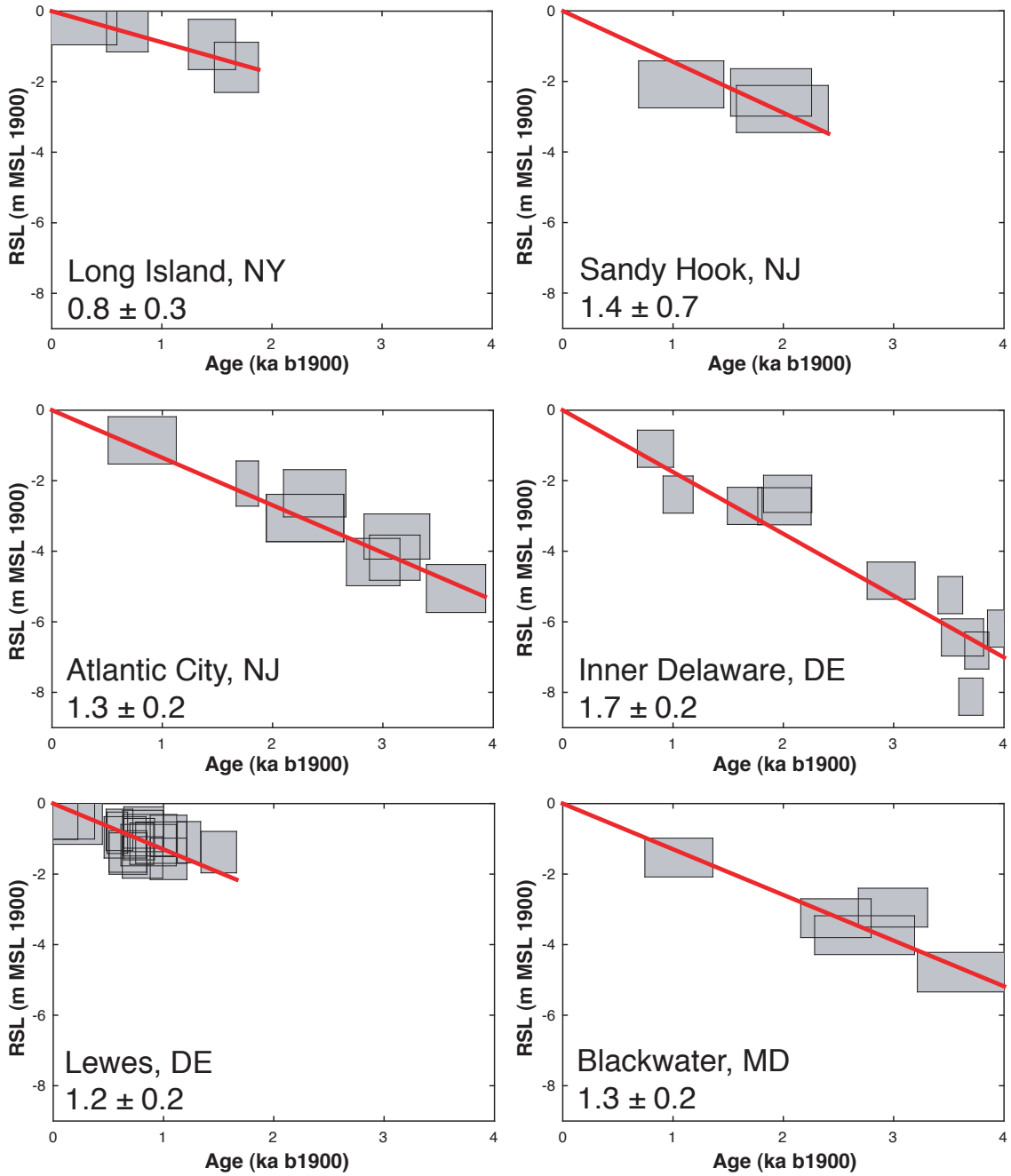

Figure 5.6 - Six locations along the U.S. Atlantic Coast with three or more basal sea-level index points and the late Holocene rates of RSL rise. Sea-level index points are plotted as calibrated age versus change in RSL relative to MSL in AD 1900 (m). The red line is the linear regression for each site. Rates and errors shown to 1 d.p. Data sources for sea level index points are referenced in Table 5.1.

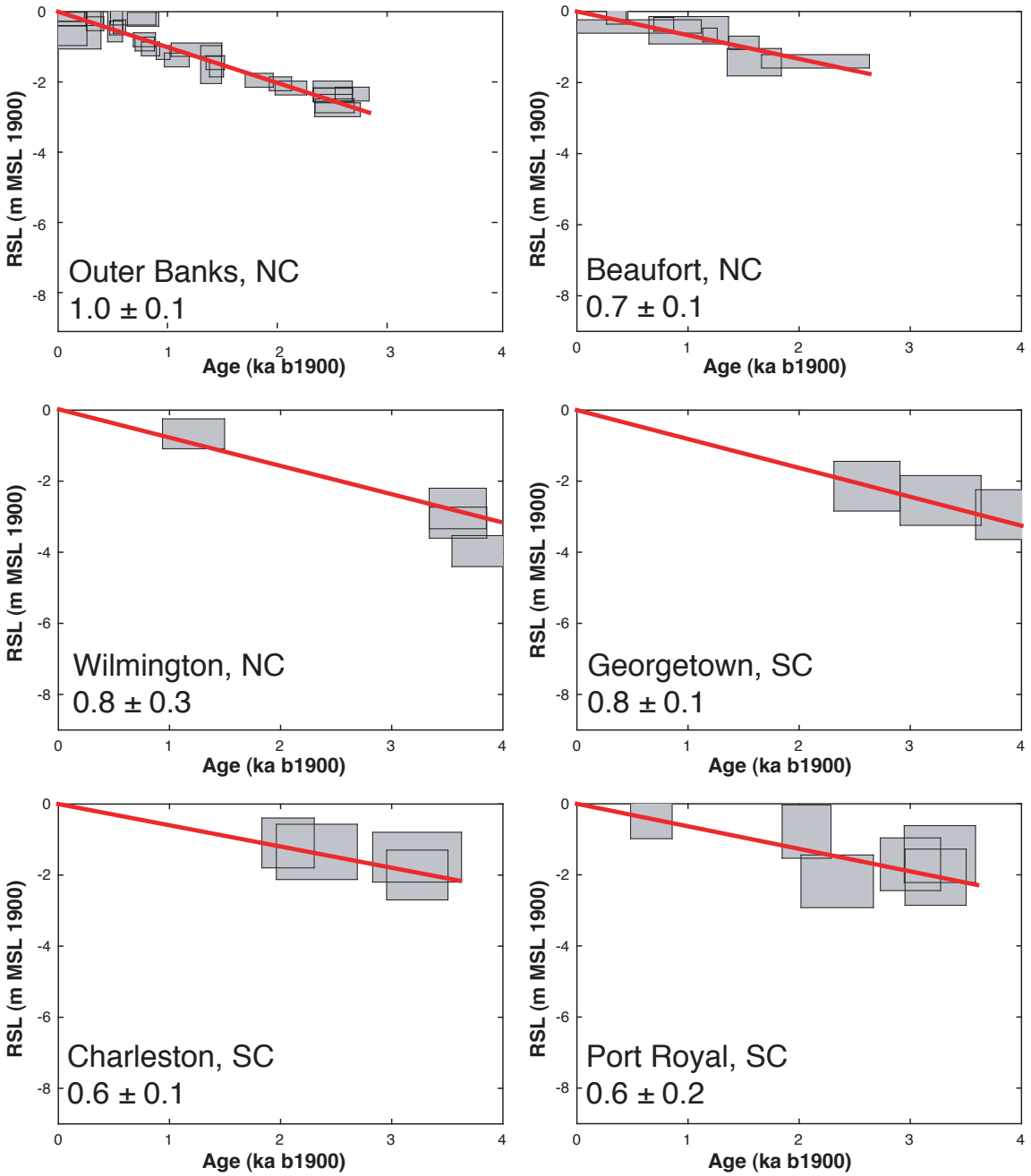

Figure 5.7 - Six locations along the U.S. Atlantic Coast with three or more basal sea-level index points and the late Holocene rates of RSL rise. Sea-level index points are plotted as calibrated age versus change in RSL relative to MSL in AD 1900 (m). The red line is the linear regression for each site. Rates and errors shown to 1 d.p. Data sources for sea level index points are referenced in Table 5.1.

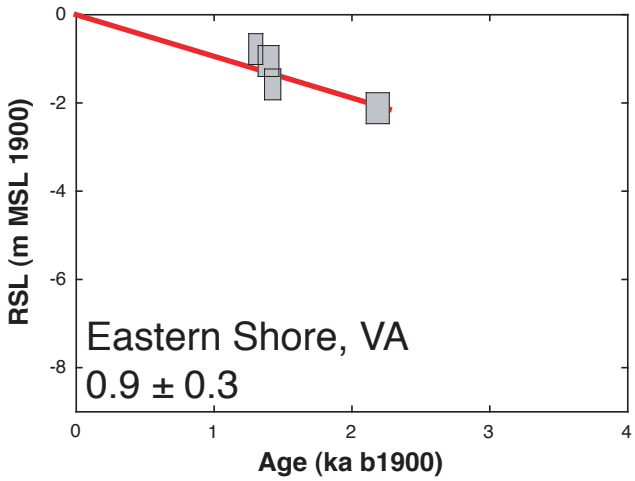

Figure 5.8 - Eastern Shore of Virginia with three or more basal sea-level index points and the late Holocene rates of RSL rise. Sea-level index points are plotted as calibrated age versus change in RSL relative to MSL in AD 1900 (m). The red line is the linear regression for each site. Rates and errors shown to 1 d.p. Data sources for sea level index points are referenced in Table 5.1.

2002) or minimal (Milne et al., 2005). A meltwater input of 1 m during the late Holocene (Church et al., 2008) would reduce the estimate of subsidence by 0.25 mm a^{-1}. We also assume that the tectonic component is small, except in close proximity to the Cape Fear Arch, North Carolina, which has experienced uplift (Marple and Talwani, 2004).

When calculating the background rate of relative sea-level rise, it is necessary to remove the modern component, as this will overestimate the background rate due to the sea-level rise experienced during the 20th century (c. 0.2 – 0.3 m along the U.S. Atlantic coast). In this study, we remove this modern sea level rise by using the nearest reliable tide gauge rate to extrapolate to MSL in 1900 AD. We then express all dates with respect to 1900 AD. At all sites the linear regression is run over the last 4 ka and is forced through zero. Regression errors are at the 95% confidence level. This contrasts with previous work (Gornitz, 1995; Peltier, 1996) that reported the error as the standard deviation and not the standard error.

5.6.3 Supplementary Information C: Uncertainty Of Sea-Level Trends From Tide Gauge Data

We identified 10 suitable tide gauge records along the U.S. Atlantic Coast from the Permanent Service for Mean Sea Level (Woodworth and Player, 2003) that are at least 50 years in length and where the influence of non-GIA subsidence, such as groundwater withdrawal, is minimal. The tide gauge record at The Battery, New York, is truncated to only include data from the 20th century.

Formal uncertainties of trends of relative sea-level (RSL) obtained from tide gauge data are usually a few tenths of a mm per year for records longer than about 50 years. These formal uncertainties are optimistic, since tide gauge records do not satisfy the criteria for a linear regression, i.e., that the data consist of a trend plus Gaussian random noise. The records also contain interannual and longer variations of high amplitude that can negate the underlying trend of sea level for even many decades in some cases (Douglas, 2001). As glacial isostatic adjustment (GIA) is considered to be the dominant control on the variation in the tide gauge records, we can assess the appropriate error term by running a linear regression through the rates from long-term tide-gauge records, going from areas of isostatic uplift in Canada to the proposed peak of GIA in the mid-Atlantic (Figure 5.9). It is apparent that these rates lie along a straight line with little variation. Therefore, we can run a linear regression through these rates to produce a single estimate of the error for the tide gauges along the U.S. Atlantic Coast of ± 0.3 mm a^{-1}.

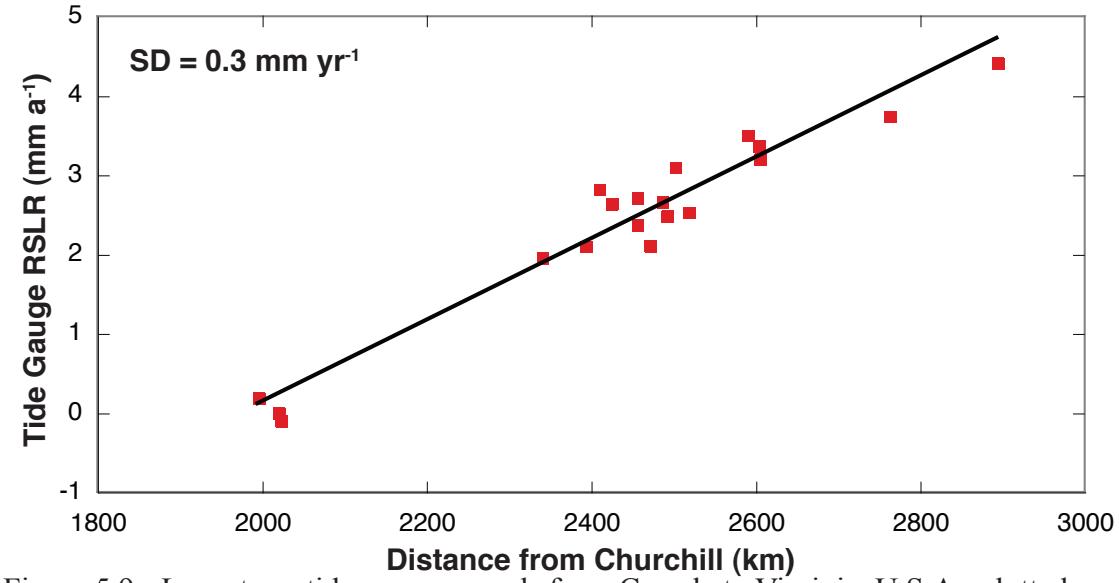

Figure 5.9 - Long-term tide gauge records from Canada to Virginia, U.S.A., plotted against distance from Churchill, Canada. The regression line demonstrates the methodology used to ascertain an appropriate error for the tide gauges.

CHAPTER SIX

Conclusions

6. INTRODUCTION

The overarching goal of this research was to assemble the first US Atlantic coast database of validated sea-level observations for the Holocene and to apply them to further understand the spatial and temporal variability of Holocene relative sea level (RSL), constrain models of the Glacial Isostatic Adjustment (GIA) process and to document the ongoing crustal movements.

6.1 HOLOCENE RELATIVE SEA LEVELS OF THE ATLANTIC COAST OF THE UNITED STATES

RSL observations provide valuable information for a number of Earth science disciplines. They can be used to further understand the evolution of coastlines and the links between human development and the coastal system. A greater understanding of the regional signal of RSL rise is required, as the effects of 21st century sea-level rise will not be equal across the Earth. I have developed a database of validated Holocene sea-level observations for the U.S. Atlantic coast. I have applied this to answer the research questions outlined in the introduction.

1) Can the previous sea-level research along the US Atlantic coast meet the validation criteria to produce a sea-level index point?

Yes. To validate each sample in the database I have collected over 50 fields of information. For each validated index points I have identified the location, age and indicative meaning. I assigned indicative meanings to sample types based on published information on the zonations of plant macrofossils, microfossils and geochemical data. Using this methodology, I have validated 473 index points and 347 limiting dates for the US Atlantic coast. The data includes both conventional and AMS radiocarbon dates. Dated material includes bulk peat, plant macrofossils and marine shells. Indicative meanings were established for all sample types within the database.

2) What is the spatial and temporal distribution of the validated relative sea-level data?

The database has good spatial coverage from Maine to South Carolina but there is an absence of index points from Georgia and the Atlantic coast of Florida. The majority of index points in the database (93%) are within the last 6 ka. The early Holocene record is predominantly constrained by marine and terrestrial limiting dates.

3) Is there spatial heterogeneity within the observations of former RSL along the US Atlantic coast, and if so, what is driving this variability

Yes. There is spatial variability induced by the removal of the Laurentide Ice Sheet, with the greatest rates of RSL rise in New Jersey and Delaware (c. 20 m since 8 ka); the area of greatest forebulge collapse. RSL rise is reduced to the north (< 16 m since 7 ka) as mantle material flowing towards Hudson Bay has been replaced by mantle material emanating from the collapsing forebulge. RSL rise is lower to the south (< 10 m since 7 ka) as the influence of the peripheral forebulge declines with distance from the center of the former ice mass.

4) Has RSL risen above present during the last 6 ka?

Observations of RSL above present in the mid and late Holocene are important because they define the boundary between intermediate- and far-field regions. There is no evidence that RSL has risen above present during the last 6 ka from Maine to South Carolina, confirming that this region is near- and intermediate-field.

5) Can the temporal variation in the ice equivalent meltwater input be identified?

Yes. The decreasing rate of meltwater input in the early Holocene associated with the disappearance of the Laurentide Ice Sheet is identified in the database. For example, this decrease is highlighted for New Jersey and Delaware, where the rate of rise decreased from 3 – 5 mm a^{-1} (8 – 4 ka) to 1.2 – 1.7 mm a^{-1} (4 ka – present). Analysis of the rates of RSL rise from 2 ka to present and 4 ka to present indicated that these are similar within the error terms of the regression. This suggests that any meltwater input was minimal

during the last 4000 years.

6) Can the effects of local processes such as compaction be isolated from the index points?

No. The absence of early Holocene index points has limited our ability to assess the effects of compaction in the US Atlantic coast database. Whilst compaction is expected, this is not identified by a difference in the elevation among base of basal, basal and intercalated index points. The thickness of overburden has been shown to be a significant variable in assessing compaction. However, the mid and late Holocene index points that dominate the US database come from unbroken sequences of peat, which have low overburdens.

6.2 HOLOCENE RELATIVE SEA LEVELS OF THE U.S. ATLANTIC COAST: IMPLICATIONS FOR GLACIAL ISOSTATIC ADJUSTMENT MODELS

There is a requirement for accurate models of the glacial isostatic adjustment (GIA) process as they provide constraints on geodetic measurements of climate change. Mass loss from Greenland is currently measured using GRACE, which must be corrected for GIA effects. GIA models are also employed to understand coastal evolution during the Holocene including the development, and subsequent subsidence, of deltas and providing paleobathymetries to reconstruct tidal range changes. However, whilst geodetic techniques can provide information on the present day changes due to GIA, observations

of RSL are required to extend this understanding back into the Holocene. I applied a GIA model to the U.S. Atlantic coast database to answer the research questions below.

1) Can the current GIA model (ICE-5G VM5a) accurately predict the observations of Holocene RSLs from the US Atlantic coast?

No. The ICE-5G VM5a model is in good agreement with the data in eastern Maine and southern Maine for the last 6 ka. The model does not invalidate marine limiting dates from southern Maine that indicates a sea-level lowstand between 8 and 11 ka. For the remaining study areas, the model fits the observations in the late Holocene (0-3 ka) but cannot reconcile the early and mid Holocene observations.

2) If a misfit between the model predictions and the observations is observed, is it systematic?

A misfit is observed in the data. With increasing age, there is a systematic disagreement between the model and data. The misfit is most pronounced between New York and northern North Carolina, with observations up to ~10 m higher than model predictions at 6 ka (e.g. Connecticut). The predictions invalidate marine limiting dates in southern Massachusetts, New Jersey, Inner Chesapeake and northern North Carolina.

3) Can modification to the earth and/or ice models reconcile any of the variance between observations and predictions?

Yes. Reducing the viscosity of the upper mantle by 50% (VM5b) reconciles most of the differences between the observations and models in the mid Holocene for the mid-Atlantic region. However, this is at the expense of the previously good fit in Maine where highstands are predicted but not observed. Using an updated ice model with a thicker proximal ice load removes the predicted highstand at eastern Maine, suggesting that further modifications to the ice model may resolve the present misfit between VM5b and the observations at southern Maine and northern Massachusetts. VM5b cannot reconcile the difference between the observations in North Carolina and South Carolina, suggesting that these areas are responding to deeper mantle structure.

6.3 SPATIAL VARIABILITY OF LATE HOLOCENE AND 20TH CENTURY SEA-LEVEL RISE ALONG THE ATLANTIC COAST OF THE UNITED STATES

Corrections must be applied to data obtained from tide gauges and satellite altimeters to remove the influence of GIA. The effects of GIA are not consistent along the U.S. Atlantic coast, with spatial variability driven by the removal of the Laurentide Ice Sheet. Without this correction, it is not possible to assess the global sea-level rise as the result of the increasing volume in ocean mass due to the expansion of water as it warms and from melting of continental glaciers and ice sheets.

1) What are the late Holocene crustal motions associated with the removal of the Laurentide Ice Sheet?

From eastern Maine (45ºN) to northern Massachusetts (42ºN), crustal subsidence is lower than 0.8 mm a^{-1}. Along the mid-Atlantic coastline from Cape Cod, Massachusetts (41.5ºN) to the northern Outer Banks, North Carolina (35.9ºN), crustal subsidence of 1 mm a^{-1} is met or exceeded at nine of eleven locations. The highest rates of crustal subsidence are recorded in New Jersey, Delaware and Maryland, where all rates are greater than 1.2 mm a^{-1}. The maximum subsidence of 1.7 ± 0.2 mm a^{-1} is recorded in the inner Delaware estuary. Subsidence decreases to less than 0.9 mm a^{-1} from Beaufort, North Carolina (34.7ºN) to Port Royal, South Carolina (32.4ºN). The southern North Carolina and South Carolina sites all show similar records of subsidence (0.5 - 0.8 mm a^{-1}).

2) Do the estimates of crustal motion have a spatial pattern along the US Atlantic coast?

Yes. The geological data constrain the form of the ongoing forebulge collapse along the US Atlantic coast. This is apparent when the rates of late Holocene RSL rise are plotted against the distance from the center of mass loading of the Laurentide Ice Sheet. With increasing distance from the ice sheet center, the rate of RSL rise increases from 0.7 mm a^{-1} in Maine to a peak of 1.7 mm a^{-1} in the Delaware Estuary, the zone of greatest forebulge collapse. The rates of RSL rise then start to fall with increasing distance from the ice sheet.

3) How do late Holocene rates compare with estimates from GPS observations?

The GPS observations agree with the late Holocene rates within both the estimate's error terms at the 2-sigma level. The errors of the GPS measurements are currently large due to the short time series of the data (< 8 years). Currently, geological measurements of crustal motion are more precise than those measured by GPS. The general form of the forebulge collapse shown by both methods is broadly similar but there are significant spatial variations. For example, whilst the geological data indicates that the zone of greatest forebulge collapse is located over Delaware, New Jersey and Maryland, the GPS data suggest that this continues into North Carolina.

4) Does the 20th century record of sea-level rise from the US Atlantic coast exhibit spatial variability?

Yes. Despite the errors of the tide gauge and geological data, there is a north to south increase in the rate of 20th century sea-level rise. The lowest rate of 1.2 ± 0.6 mm a^{-1} occurs near the northern end of the study area at Portland, Maine, while to the south it doubles to 2.6 ± 0.3 mm a^{-1} (Charleston, South Carolina); a range of 1.4 mm a^{-1}. A similar slope has been identified by GIA modeling but this is the first evidence from observational data alone. There may be a significant contribution to the 20th century sea-level changes from Greenland Ice Sheet mass balance changes and/or ocean steric effects.

6.4 AREAS OF FUTURE RESEARCH

The development of the US Atlantic coast database has identified future research avenues. These can be sub-divided into research on the existing database and research that will require further data collection.

6.4.1 Tidal Modeling

If the tidal range has not remained constant through time, sea-level chronologies based upon tide level indicators will differ from the 'true' sea-level curve (Gehrels et al., 1995). Primarily, RSL changes affect shelf width and bathymetric depths, and hence reflection and amplification of tide waves and the distribution of frictional dissipation of the tidal energy that is transported from the deep oceans to the shallow shelf regions. Secondly, coastline location changes, also a function of RSL change and sediment deposition, affect tidal characteristics by modifying the nearshore morphology and frictional environment (e.g. Uehara et al., 2006). Therefore, it is likely that tidal range will change through time, perhaps significantly.

Accurate paleogeographies are required to estimate past tidal ranges. However, these paleogeographies are usually provided by GIA models, which cannot currently fit the US Atlantic coast observations. The new database will be able to constrain the GIA models to produce more accurate paleogeographies. Further, my data will be used to ground

truth the paleogeographies to ensure that the coastline reconstruction does not identify areas as terrestrial or marine, where data is present to suggest otherwise.

6.4.2 Compaction

Following deposition, sediment consolidation will lower index points from their original elevation and, unless corrected for, will lead to an over-estimate of the rate and magnitude of RSL rise (Shennan and Horton, 2002). These effects can be particularly severe for intercalated sediments. There is no suitable model of autocompaction (e.g. Pizzuto and Schwendt, 1997). However, it has been identified that overburden, depth to basement and the total thickness of the Holocene sediment package are controlling variables (e.g. Törnqvist et al., 2008; Horton and Shennan, 2009).

Our current analysis has suggested that there is little compaction in the database but this needs to be quantitatively assessed. Within the database, I have collected information on overburden, depth to basement and total Holocene sediment thickness. I will employ the refined GIA model, which will be modified to fit base of basal peat data where available to provide a compaction-free record of RSL. I will calculate the residuals for each index point within the database and perform statistical analysis to identify if compaction is a significant effect, and if so, what the controlling variables are.

6.4.3 Effects of Sample Type on Radiocarbon Dated Index Points

The development of AMS radiocarbon dating has resulted in a shift towards utilizing individual salt marsh plant macrofossils (e.g. van de Plassche et al., 1998) as age control on index points. However, greater than 50% of the US Atlantic coast database contains samples that were dated by conventional methods on bulk samples of salt marsh peat (e.g. Redfield and Rubin, 1962). This may be problematic, as bulk samples have been shown to provide different ages to plant macrofossils due to mechanical contamination and root penetration (e.g. Törnqvist et al., 1992). For each sample in the database, I have recorded the method of radiocarbon dating (AMS or conventional) and whether the sample dated was a plant macrofossil or a bulk organic sediment. Therefore, it will be possible to compare these data and the effect on RSL reconstructions.

6.4.4 Spatial and Temporal Data Distribution

I have identified that there are spatial and temporal limitations to the current US Atlantic coast database. Temporally, there is a shortage of index points prior to 6 ka. Further collection of data from this time period is necessary. However, salt marsh peats are difficult to locate and sample on the continental shelf. Research should initially focus on areas in the database where these samples have been identified including the southern shore of Long Island and Delaware as there is the potential to refine the error ranges associated with the samples through high-precision leveling and applications of microfossils.

There are currently no index points from Georgia or the Atlantic coast of Florida. These are important areas as they link the near and intermediate field regions of the US Atlantic coast with the far field region of the Caribbean. Further, they contain numerous long-term, reliable tide gauges that require the removal of the GIA component to further inform on the spatial variability in 20th century sea-level rise.

6.4.5 Geophysical Modeling

I have demonstrated that the GIA models can be modified to improve the fit to the observations. However, misfits still remain between the model and the observations that need to be rectified. It is unlikely that a unique solution can be found and, therefore, it is necessary to investigate the possible effects of all parameters on the RSL history of the U.S. Atlantic coast. I will investigate modifications to the earth parameters that have previously been suggested by other researchers including the lower mantle viscosity, lithospheric thickness, incorporation of lateral heterogeneity in the mantle and a softening of the transition zone.

6.4.6 Fingerprints of Glacial Melting

I have identified a slope in the rate of sea-level rise from north to south along the U.S. Atlantic coast using geologically derived rates of RSL rise and tide gauges. This has previously been suggested as indicative of a fingerprint from the melting of the Greenland

Ice Sheet (e.g. Mitrovica et al., 2001). However, steric effects may also play an important role in 20th century sea-level rise (e.g. Wake et al., 2006). I will apply the latest steric corrections to the tide gauge data to remove this influence. If a residual slope remains, Dick Peltier (University of Toronto) will model the fingerprint of Greenland melting and enable me to investigate the magnitude of 20th century Greenland melting.

6.4.7 Assimilation with the Gulf Coast and Caribbean Databases

Databases of Holocene RSL change similar to mine are currently being compiled by Torbjörn Törnqvist (Tulane University) and Maggie Toscano (Smithsonian Institute) for the Gulf Coast and Caribbean, respectively. This is important as the final database will then contain RSL records from near-, intermediate- and far-field locations. Comparison with GIA models over a large spatial scale with differing RSL histories may enable the formulation of a unique model solution to fit all the observations. Further, it will allow us to expand the area for which we have calculations of late Holocene crustal movements.

Appendix One

U.S. ATLANTIC COAST RELATIVE SEA-LEVEL DATABASE

Site	Latitude	Longitude	Labcode	Material	^{14}C age ± 1σ	δ^{13}C	Calibrated age range	RSL (m MSL)	Error (m)	Reference
Eastern Maine										
Index Points										
Sanborn Cove	44.683	67.406	AA-8210	HHM Plant	4795 ± 80	-28	5661-5319	-4.60	0.25	Gehrels (1999)
Sanborn Cove	44.683	67.406	AA-8211	S. alt	4075 ± 75		4822-4422	-3.67	0.24	Gehrels (1999)
Sanborn Cove	44.683	67.406	AA-8941	S. alt	3010 ± 70	-15.7	3370-2996	-2.58	0.25	Gehrels (1999)
Sanborn Cove	44.683	67.406	AA-8942	Plant frag	2540 ± 110	-28.7	2845-2349	-1.38	0.24	Gehrels (1999)
Sanborn Cove	44.683	67.406	AA-27620	Twig	1070 ± 90	-30	1230-786	-0.19	0.25	Gehrels (1999)
Sanborn Cove	44.683	67.406	AA-27621	Twig	195 ± 45	-28.4	308-0	-0.23	0.25	Gehrels (1999)
Sanborn Cove	44.683	67.406	AA-27622	Plant frag	1210 ± 80	-26.5	1284-972	-0.43	0.25	Gehrels (1999)
Sanborn Cove	44.683	67.406	AA-27623	Plant frag	1540 ± 60		1531-1313	-0.68	0.25	Gehrels (1999)
Sanborn Cove	44.683	67.406	AA-27624	Plant frag	2170 ± 50	-28.4	2328-2010	-1.41	0.27	Gehrels (1999)
Sanborn Cove	44.683	67.406	AA-27625	Plant frag	2120 ± 60		2308-1950	-1.57	0.25	Gehrels (1999)
Gouldsboro	44.429	68.011	BETA-63981	HM peat	4030 ± 70	-29.8	4818-4296	-4.92	0.39	Gehrels et al. (1996)
Gouldsboro	44.429	68.011	BETA-64579	HM peat	2730 ± 80	-26.3	3063-2729	-2.06	0.34	Gehrels et al. (1996)
Gouldsboro	44.429	68.011	SI-6541	HHM peat	3580 ± 75	-24.6	4088-3650	-4.05	0.45	Gehrels et al. (1996)
Jasper Beach	44.629	67.382	BETA-52183	HM peat	3150 ± 70	-24	3557-3209	-2.87	0.45	Gehrels and Belknap (1993)
Jasper Beach	44.629	67.382	BETA-52184	HM peat	2880 ± 80	-26	3253-2795	-2.49	0.45	Gehrels and Belknap (1993)
Sanborn Cove	44.683	67.406	BETA-52185	HM peat	3860 ± 60	-27	4425-4091	-4.50	0.45	Gehrels and Belknap (1993)
Sanborn Cove	44.683	67.406	BETA-52187	HM peat	2800 ± 70	-26	3137-2759	-2.42	0.45	Gehrels and Belknap (1993)
Gouldsboro	44.430	68.010	SI-6543	HM peat	1775 ± 50	-23.1	1821-1565	-0.80	0.94	Belknap et al. (1989)
Gouldsboro	44.430	68.010	SI-6544	HM peat	2550 ± 50	-27.6	2759-2467	-1.55	0.94	Belknap et al. (1989)
Gouldsboro	44.430	68.010	SI-6545	HM peat	3045 ± 65	-18.2	3396-3040	-3.11	0.94	Belknap et al. (1989)
Sanborn Cove	44.683	67.406	BETA-57808	S. alt	490 ± 70	-19.4	654-324	-0.62	0.19	Gehrels (1999)
Sanborn Cove	44.683	67.406	BETA-57809	S. alt + S. rob	1070 ± 90	-16.8	1230-786	-1.42	0.24	Gehrels (1999)
Gouldsboro	44.429	68.011	SI-6536	HHM peat	570 ± 50	-25.1	653-519	-0.61	0.45	Gehrels et al. (1996)
Gouldsboro	44.429	68.011	SI-6537	HHM peat	2010 ± 60	-25.7	2123-1827	-1.25	0.45	Gehrels et al. (1996)
Gouldsboro	44.429	68.011	SI-6538	HM peat	2325 ± 65	16.8	2696-2150	-1.43	0.45	Gehrels et al. (1996)
Jasper Beach	44.629	67.382	BETA-52182	HM peat	3170 ± 140	-27	3716-2978	-4.30	0.45	Gehrels and Belknap (1993)
Sanborn Cove	44.683	67.406	BETA-52186	HM peat	3090 ± 60	-23	3446-3084	-3.32	0.45	Gehrels and Belknap (1993)
Jasper Beach	44.629	67.382	PITT-0964	HM peat	4165 ± 30		4829-4583	-4.44	0.45	Gehrels and Belknap (1993)
Addison	44.608	67.753	SI-6199	HM peat	4095 ± 100	-23	4853-4299	-3.94	1.10	Belknap et al. (1989)
Addison	44.608	67.753	SI-6204	HM peat	3170 ± 60	-26.6	3557-3255	-3.26	1.10	Belknap et al. (1989)
Addison	44.608	67.753	SI-6208	HM peat	1840 ± 110	-26.9	2041-1521	-1.62	1.10	Belknap et al. (1989)
Gouldsboro	44.430	68.010	SI-6542	HM peat	3940 ± 50	-16.6	4523-4239	-4.83	0.94	Belknap et al. (1989)
Gouldsboro	44.429	68.011	BETA-61775	HHM peat	2380 ± 70	-16.2	2716-2208	-1.66	0.34	Gehrels et al. (1996)
Gouldsboro	44.429	68.011	BETA-63980	HHM peat	1230 ± 70	-26.3	1288-984	-0.95	0.34	Gehrels et al. (1996)
Addison	44.608	67.753	SI-6201	HM peat	2960 ± 75	-21.1	3345-2927	-3.04	1.10	Belknap et al. (1989)
Addison	44.608	67.753	SI-6200	HM peat	3415 ± 110	-23.4	3963-3405	-3.49	1.10	Belknap et al. (1989)
Addison	44.608	67.753	SI-6207	HHM peat	2595 ± 80	-18.5	2860-2366	-1.80	1.10	Belknap et al. (1989)
Addison	44.608	67.753	SI-6206	HHM peat	2730 ± 75	-17.9	3059-2733	-2.40	1.10	Belknap et al. (1989)
Addison	44.608	67.753	SI-6205	HM peat	2815 ± 50	-18.8	3066-2792	-3.00	1.10	Belknap et al. (1989)
Addison	44.608	67.753	SI-6210	HM peat	365 ± 70	-22.8	521-295	-0.67	1.10	Belknap et al. (1989)
Addison	44.608	67.753	SI-6209	HM peat	1525 ± 75	-28.2	1558-1296	-1.22	1.10	Belknap et al. (1989)
Addison	44.608	67.753	SI-6534	HM peat	1245 ± 70	-27.1	1296-990	-1.53	1.10	Belknap et al. (1989)
Addison	44.608	67.753	SI-6530	HM peat	2150 ± 50		2311-2001	-1.70	1.10	Belknap et al. (1989)
Addison	44.608	67.753	SI-6531	HM peat	2780 ± 65	-22.4	3062-2758	-1.97	1.10	Belknap et al. (1989)
Gouldsboro	44.430	68.010	SI-6539	HM peat	2740 ± 55		2954-2754	-2.34	0.94	Belknap et al. (1989)
Terrestrial Limiting										
Gouldsboro	44.430	68.020	BETA-64580	Fresh peat	9730 ± 60	-29.4	11251-10801	-3.53	0.17	Gehrels et al. (1996)
Gouldsboro	44.430	68.020	BETA-64581	Fresh peat	9490 ± 80	-27.6	11121-10561	-2.05	0.17	Gehrels et al. (1996)
Gouldsboro	44.430	68.010	SI-5417	Marsh peat	1490 ± 45		1515-1301	0.50	0.85	Belknap et al. (1989)
Gouldsboro	44.430	68.010	SI-5425	Wood	1465 ± 50		1512-1290	1.29	0.85	Belknap et al. (1989)
Southern Maine										
Index Points										
Phippsburg	43.752	69.822	BETA-50161	LM peat	4980 ± 60	-19.1	5893-5601	-6.88	0.39	Gehrels et al. (1996)
Phippsburg	43.752	69.822	AA-8939	HM peat	4270 ± 70	-15.9	5039-4581	-3.42	0.34	Gehrels et al. (1996)
Phippsburg	43.752	69.822	PITT-0965	HHM peat	4480 ± 95		5441-4857	-4.11	0.39	Gehrels et al. (1996)
Phippsburg	43.752	69.822	PITT-0967	HHM peat	3470 ± 150		4147-3389	-3.55	0.39	Gehrels et al. (1996)
Phippsburg	43.752	69.822	PITT-0968	HHM peat	3435 ± 45		3830-3584	-2.31	0.39	Gehrels et al. (1996)
Wells	43.292	70.573	SI-6623	HM peat	5135 ± 70		6171-5663	-5.85	0.39	Kelley et al. (1995)
Wells	43.292	70.573	SI-6626	HM peat	4380 ± 55		5274-4842	-5.09	0.39	Kelley et al. (1995)
Phippsburg	43.742	69.832	AA-8212	LM peat	4945 ± 75	-25.7	5896-5494	-6.47	0.39	Gehrels et al. (1996)
Phippsburg	43.752	69.822	AA-8937	HM peat	990 ± 60	-15.4	1053-745	-0.60	0.38	Gehrels et al. (1996)
Phippsburg	43.752	69.822	AA-8938	HM peat	2675 ± 70		2960-2544	-1.87	0.38	Gehrels et al. (1996)
Phippsburg	43.752	69.822	BETA-52188	HM peat	3760 ± 60	-17.1	4400-3928	-3.01	0.39	Gehrels et al. (1996)
Damariscotta	43.964	69.571	SI-6617	HHM peat	6295 ± 55	-27.8	7413-7021	-15.31	0.41	Gehrels et al. (1996)
Wells	43.292	70.573	PITT-0907	BM peat	4255 ± 55		4967-4617	-3.60	0.39	Gehrels et al. (1996)
Wells	43.292	70.573	AA-8208	BM peat	4235 ± 70	-25.7	4965-4539	-2.95	0.38	Gehrels et al. (1996)
Wells	43.292	70.573	PITT-0917	BM peat	3900 ± 145		4815-3927	-2.75	0.40	Gehrels et al. (1996)
Wells	43.292	70.573	PITT-0918	BM peat	3265 ± 70		3680-3362	-2.85	0.39	Gehrels et al. (1996)
Wells	43.292	70.573	PITT-0920	BM peat	3340 ± 55		3700-3446	-2.10	0.34	Gehrels et al. (1996)
Wells	43.292	70.573	AA-8209	BM peat	4735 ± 70		5591-5319	-4.15	0.39	Gehrels et al. (1996)
Wells	43.340	70.541	PITT-0902	LM peat	705 ± 165		966-330	-0.91	0.30	Kelley et al. (1995)
Phippsburg	43.742	69.832	AA-8940	HM peat	2770 ± 65		3060-2754	-1.69	0.38	Gehrels et al. (1996)
Morse River	43.752	69.822	SI-6555	HM peat	2865 ± 70	-23	3211-2797	-2.00	0.84	Belknap et al. (1989)
Morse River	43.752	69.822	SI-6546	HM peat	155 ± 45	-18.9	286-0	-1.00	0.84	Belknap et al. (1989)
Morse River	43.752	69.822	SI-6547	HM peat	2540 ± 55	-17	2759-2367	-2.91	0.84	Belknap et al. (1989)
Morse River	43.752	69.822	SI-6549	HHM peat	540 ± 60	-17.4	653-503	-1.49	0.84	Belknap et al. (1989)
Morse River	43.752	69.822	SI-6550	HM peat	1305 ± 60	-18.6	1310-1074	-1.48	0.84	Belknap et al. (1989)
Morse River	43.752	69.822	SI-6551	HHM peat	1505 ± 80	-19	1554-1286	-1.85	0.84	Belknap et al. (1989)
Morse River	43.752	69.822	SI-6553	LM peat	2115 ± 50	-18.7	2305-1949	-1.48	1.08	Belknap et al. (1989)
Penobscot Bay	44.176	68.825	GX-11006	HM peat	2145 ± 125	-19	2451-1821	-1.51	0.94	Belknap et al. (1989)
Penobscot Bay	44.176	68.825	GX-11007	HM peat	3255 ± 150	-27.7	3863-3079	-2.26	0.94	Belknap et al. (1989)
Wells	43.292	70.573	PITT-0906	LM peat	2225 ± 60		2350-2066	-1.40	0.76	Kelley et al. (1995)
Wells	43.292	70.573	PITT-0909	HM peat	3065 ± 75		3447-3063	-2.60	0.39	Kelley et al. (1995)
Wells	43.292	70.573	PITT-0912	LM peat	3585 ± 60		4080-3704	-3.50	0.30	Gehrels et al. (1996)
Wells	43.292	70.573	PITT-0916	HM peat	2010 ± 40		2104-1876	-1.34	0.39	Kelley et al. (1995)
Wells	43.340	70.541	PITT-0896	HM peat	300 ± 50		489-155	-0.73	0.39	Gehrels et al. (1996)
Wells	43.340	70.541	PITT-0897	HM peat	1090 ± 50		1168-924	-1.27	0.39	Gehrels et al. (1996)
Wells	43.340	70.541	PITT-0900	LM peat	4335 ± 60		5265-4729	-2.85	0.30	Gehrels et al. (1996)
Wells	43.292	70.573	SI-6618	HM peat	1470 ± 55		1516-1290	-0.95	0.39	Kelley et al. (1995)
Wells	43.292	70.573	SI-6619	HM peat	3080 ± 70		3445-3079	-1.56	0.39	Kelley et al. (1995)
Wells	43.292	70.573	SI-6620	HM peat	3865 ± 55		4424-4098	-3.14	0.39	Kelley et al. (1995)

Wells	43.292	70.573	SI-6621	HM peat	1345 ± 55		1361-1145	-1.17	0.39	Kelley et al. (1995)
Wells	43.292	70.573	SI-6622	LM peat	1755 ± 55		1816-1550	-1.03	0.76	Kelley et al. (1995)
Wells	43.292	70.573	SI-6624	LM peat	2495 ± 80		2740-2362	-1.92	0.76	Kelley et al. (1995)
Wells	43.292	70.573	SI-6625	HM peat	3780 ± 55		4404-3982	-4.19	0.39	Kelley et al. (1995)
Wells	43.292	70.573	SI-6627	HM peat	3105 ± 70		3467-3081	-2.24	0.39	Kelley et al. (1995)
Wells	43.292	70.573	SI-6628	HM peat	3705 ± 50		4226-3898	-2.92	0.39	Kelley et al. (1995)
Wells	43.292	70.573	SI-6629	HHM peat	4220 ± 60		4871-4539	-3.79	0.39	Kelley et al. (1995)
Wells	43.292	70.573	Beta-44061	Sp	980 ± 55		1046-744	-0.67	0.38	Kelley et al. (1995)
Wells	43.292	70.573	Beta-44062	Sp	2100 ± 55		2303-1929	-1.58	0.38	Kelley et al. (1995)
Wells	43.292	70.573	Beta-44063	Sp	2520 ± 60		2749-2365	-2.38	0.39	Kelley et al. (1995)
Wells	43.292	70.573	Beta-44064	Sp	3510 ± 60		3964-3638	-3.01	0.39	Kelley et al. (1995)
Wells	43.292	70.573	BETA-106461	Saltmarsh peat	270 ± 60	-25.4	492-0	-0.64	0.39	Gehrels et al. (2002)
Wells	43.292	70.573	AA-33346	Saltmarsh peat	465 ± 60		633-319	-0.71	0.39	Gehrels et al. (2002)
Wells	43.292	70.573	AA-33347	Saltmarsh peat	825 ± 45	-22.8	900-672	-0.69	0.39	Gehrels et al. (2002)
Wells	43.292	70.573	AA-33348	Saltmarsh peat	1020 ± 55		1055-795	-0.88	0.39	Gehrels et al. (2002)
Wells	43.292	70.573	AA-33349	Saltmarsh peat	1105 ± 45	-13.5	1168-930	-0.83	0.39	Gehrels et al. (2002)
Wells	43.292	70.573	BETA-106462	Saltmarsh peat	1140 ± 60	-25.4	1228-932	-0.89	0.39	Gehrels et al. (2002)
Marine Limiting										
Kennebec River	43.701	69.824	BETA-63124	M. edu	7490 ± 90		8104-7634	-25.62	3.02	Barnhardt et al 1995
Kennebec River	43.701	69.824	BETA-63125	M. edu	7310 ± 70		7900-7514	-25.62	3.02	Barnhardt et al 1995
Kennebec River	43.707	69.794	OS-1862	M. bal	8610 ± 40		9379-8977	-26.62	3.02	Barnhardt et al 1995
Kennebec River	43.707	69.794	OS-1860	M. bal	8710 ± 35		9456-9068	-26.62	3.02	Barnhardt et al 1995
Saco Bay	43.533	70.217	PITT-0739	A. isl	785 ± 35		488-146	-54.31	3.02	Kelley et al 1992
Saco Bay	43.533	70.217	PITT-0741	H. arc	5915 ± 155		6624-5878	-51.51	3.02	Kelley et al 1994
Cape Small	43.700	69.767	PITT-0744	M. are	9000 ± 100		9998-9310	-22.61	3.02	Kelley et al 1997
Cape Small	43.700	69.767	PITT-0745	M. are	9630 ± 75		10577-10191	-22.71	3.02	Kelley et al 1998
Cape Small	43.700	69.767	PITT-0746	M. mod	9700 ± 65		10646-10230	-22.91	3.02	Kelley et al 1999
Cape Small	43.700	69.767	PITT-0747	M. are	9260 ± 100		10220-9576	-24.71	3.02	Kelley et al 2000
Cape Small	43.700	69.767	PITT-0748	M. edu	8250 ± 80		8962-8416	-22.86	3.02	Kelley et al 2001
Cape Small	43.700	69.767	PITT-0749	M. are	9235 ± 60		10171-9623	-23.91	3.02	Kelley et al 2002
Cape Small	43.700	69.767	PITT-0585	M. are	9090 ± 95		10091-9465	-24.26	3.02	Kelley et al 2003
Cape Small	43.700	69.767	PITT-0586	M. are	9250 ± 110		10216-9550	-24.36	3.02	Kelley et al 2004
Cape Small	43.700	69.767	PITT-0587	M. are	7270 ± 105		7904-7438	-24.51	3.02	Kelley et al 2005
Cape Small	43.683	69.917	PITT-0753	A. isl	1300 ± 35		914-636	-37.91	3.02	Kelley et al 2008
Cape Small	43.683	69.917	PITT-0754	M. are	2570 ± 50		2326-1924	-39.01	3.02	Kelley et al 2009
Cape Small	43.683	69.917	PITT-0755	M. are	2950 ± 210		3161-2049	-42.11	3.02	Kelley et al 2010
Cape Small	43.800	69.850	PITT-0756	A. isl	8270 ± 75		8974-8440	-46.11	3.02	Kelley et al 2011
Casco Bay	43.717	70.167	PiTT-0737	M. are	9130 ± 70		10089-9519	-24.11	3.02	Kelley et al 2012
Penobscot Bay	44.414	68.857	BETA-69336	M. are	8730 ± 70		9487-9037	-27.40	3.02	Barnhardt et al 1995
Penobscot Bay	44.414	68.857	BETA-69337	M. are	8730 ± 60		9484-9058	-27.40	3.02	Barnhardt et al 1995
Fox Island	44.119	68.869	GX-11004	M. are	5880 ± 105	2	6455-5911	-11.25	0.80	Belknap et al. 1989
Fox Island	44.119	68.869	GX-11005	M. are	5430 ± 100	1.6	5975-5453	-7.60	0.80	Belknap et al. 1989
Terrestrial Limiting										
Penobscot Bay	44.176	68.825	GX-11008	Wood	3700 ± 200	-26.3	4780-3484	-0.52	0.80	Belknap et al. (1989)
Wells	43.320	70.580	PITT-0962	stump	4535 ± 35		5313-5051	-1.23	0.26	Kelley et al. (1995)
Wells	43.320	70.580	PITT-0963	stump	3260 ± 40		3574-3390	-1.23	0.26	Kelley et al. (1995)
Wells	43.320	70.580	W-396	white pine stump	2980 ± 180		3559-2757	2.83	0.73	Bloom (1963)
Wells	43.320	70.580	W-508	white pine stump	2810 ± 200		3436-2366	3.90	0.73	Bloom (1963)
Wells	43.320	70.580	PITT-0913	wood	4480 ± 60		5309-4887	-2.06	0.16	Kelley et al. (1995)
Northern Massacusetts										
Index Points										
Romney Marsh	42.428	70.989	BETA-134753	Jg and Sp	3050 ± 50	-18	3376-3080	-2.52	0.41	Donnelly (2006)
Romney Marsh	42.428	70.989	BETA-134755	Ds	2950 ± 60	-15	3328-2948	-2.33	0.41	Donnelly (2006)
Romney Marsh	42.428	70.989	BETA-134756	Jg, Sr and Sp	1900 ± 40	-23.8	1927-1727	-1.38	0.40	Donnelly (2006)
Romney Marsh	42.428	70.989	OS-24172	Jg and Sp	260 ± 50	-20.8	468-0	-0.73	0.40	Donnelly (2006)
Romney Marsh	42.428	70.989	BETA-138707	Sp	1040 ± 40	-15.7	1058-804	-0.95	0.40	Donnelly (2006)
Romney Marsh	42.428	70.989	BETA-134754	Sp	2510 ± 50	-14.7	2744-2366	-1.94	0.40	Donnelly (2006)
Boston	42.500	71.100	O-1119	Salt marsh peat	2550 ± 115		2854-2348	-1.40	1.13	Kaye and Barghoorn (1964)
Marine Limiting										
Boston	42.351	71.075	O-1475	Estuarine Silt	4450 ± 130		5567-4727	-7.66	0.27	Kaye and Barghoorn (1964)
Jeffreys Ledge	42.640	70.450	WHG-709	Marine shells	4660 ± 65		4960-4540	-58.05	3.18	Oldale et al. (1993)
Jeffreys Ledge	42.655	70.415	WHG-706	Marine shells	7500 ± 75		8027-7673	-61.06	3.19	Oldale et al. (1993)
Terrestrial Limiting										
Boston	42.346	71.080	O-1124	Sedge peat	3850 ± 130		4784-3878	-2.95	0.26	Kaye and Barghoorn (1964)
Boston	42.351	71.075	O-1118	Fresh peat	5600 ± 140		6729-6021	-7.12	0.27	Kaye and Barghoorn (1964)
Neponset River	42.270	71.050	I-2215	Undiff peat	1310 ± 95		1387-989	2.04	0.96	Redfield (1967)
Neponset River	42.270	71.050	I-2216	Undiff peat	1360 ± 105		1517-1017	1.74	0.96	Redfield (1967)
Neponset River	42.270	71.050	I-2217	Undiff peat	1860 ± 100		2034-1542	1.43	0.96	Redfield (1967)
Neponset River	42.270	71.050	W-1451	Undiff peat	2100 ± 200		2660-1648	1.31	0.96	Redfield (1967)
Neponset River	42.270	71.050	W-1452	Undiff peat	2790 ± 200		3381-2365	0.70	0.96	Redfield (1967)
Neponset River	42.270	71.050	W-1453	Undiff peat	3110 ± 200		3823-2793	0.22	0.96	Redfield (1967)
Boston	42.400	71.100	C-417	Fresh peat	5717 ± 550		7669-5315	-6.33	0.27	Redfield and Rubin (1962)
Gloucester Point	42.750	70.800	H-1376	Undiff peat	2450 ± 110		2763-2185	0.80	0.95	Newman et al. (1980)
Gloucester Point	42.750	70.800	H-1367	Undiff peat	3550 ± 130		4226-3482	-0.95	0.95	Newman et al. (1980)
Gloucester Point	42.750	70.800	H-1366	Undiff peat	3375 ± 120		3920-3364	-0.60	0.95	Newman et al. (1980)
Gloucester Point	42.750	70.800	H-1375	Undiff peat	3625 ± 125		4377-3595	-1.56	0.95	Newman et al. (1980)
Gloucester Point	42.750	70.800	H-1372	Undiff peat	4225 ± 135		5277-4419	-2.49	0.95	Newman et al. (1980)
Gloucester Point	42.750	70.800	H-1356	Undiff peat	4900 ± 130		5912-5324	-5.20	0.95	Newman et al. (1980)
Gloucester Point	42.750	70.800	H-1359	Undiff peat	6280 ± 150		7464-6798	-10.09	0.96	Newman et al. (1980)
Southern Massachusetts										
Index Points										
Barnstable	41.710	70.370	W-1092	Spartina peat	3400 ± 300		4496-2284	-6.04	1.34	Redfield and Rubin (1962)
Barnstable	41.700	70.360	W-971	Spartina peat	2800 ± 250		3556-2340	-3.61	1.34	Redfield and Rubin (1962)
Barnstable	41.700	70.360	W-973	Spartina peat	3660 ± 250		4801-3391	-6.48	1.34	Redfield and Rubin (1962)
Barnstable	41.730	70.300	Y-1186	Salt peat	1400 ± 80		1518-1150	-2.06	1.12	Stuiver et al. (1963)
Barnstable	41.730	70.300	Y-1189	Salt peat	2200 ± 100		2451-1905	-3.83	1.12	Stuiver et al. (1963)
Barnstable	41.710	70.370	W-1094	Spartina peat	1040 ± 300		1568-488	-0.91	1.34	Redfield and Rubin (1962)
Barnstable	41.710	70.370	W-1095	Spartina peat	1850 ± 300		2684-1174	-1.83	1.34	Redfield and Rubin (1962)
Barnstable	41.710	70.370	W-1096	Spartina peat	2240 ± 300		2951-1539	-2.83	1.34	Redfield and Rubin (1962)
Barnstable	41.710	70.370	W-1098	Spartina peat	3060 ± 300		4057-2469	-5.12	1.34	Redfield and Rubin (1962)

Barnstable	41.730	70.320	Y-1187	Salt peat	710 ± 80		784-540	-1.63	1.12	Stuiver et al. (1963)
Barnstable	41.730	70.300	Y-1188	Salt peat	240 ± 80		480-0	-0.56	1.12	Stuiver et al. (1963)
Barnstable	41.730	70.320	Y-1190	Salt peat	1060 ± 100		1231-743	-2.03	1.12	Stuiver et al. (1963)
Centerville	41.633	70.333	W-582	Spartina peat	1640 ± 240		2116-1064	-1.73	0.56	Redfield and Rubin (1962)
Barnstable	41.700	70.317	W-637	Spartina peat	190 ± 150		476-0	-0.12	1.34	Redfield and Rubin (1962)
Barnstable	41.700	70.360	W-675	Spartina peat	770 ± 100		915-555	-0.33	1.34	Redfield and Rubin (1962)
Barnstable	41.700	70.360	W-677	Spartina peat	400 ± 100		642-0	-0.03	1.34	Redfield and Rubin (1962)
Barnstable	41.700	70.360	W-678	Spartina peat	1880 ± 100		2044-1560	-4.74	1.34	Redfield and Rubin (1962)
Marine Limiting										
Nantucket Sound	41.550	70.467	BETA-122519	Mercenaria	3790 ± 70	0	3838-3394	-10.43	0.71	Gutierrez et al. (2003)
Nantucket Sound	41.550	70.467	BETA-122520	Mercenaria	3640 ± 90	0	3683-3203	-10.63	0.71	Gutierrez et al. (2003)
Marthas Vineyard	41.300	71.000	W-2013	C. vir	9300 ± 250		10561-9405	-37.42	3.15	Oldale and O'Hara (1980)
Marthas Vineyard	41.408	70.739	W-3786	Mercenaria	7570 ± 250		9726-8452	-27.65	0.75	Oldale and O'Hara (1980)
Marthas Vineyard	41.317	70.922	W-3766	shell hash	5150 ± 200		5841-4867	-34.38	0.78	Oldale and O'Hara (1980)
Marthas Vineyard	41.368	70.867	W-3787	shell hash	4470 ± 500		5722-3260	-26.75	0.75	Oldale and O'Hara (1980)
Marthas Vineyard	41.443	70.722	I-9944	shell hash	3710 ± 80		3758-3318	-15.11	0.71	Oldale and O'Hara (1980)
Marthas Vineyard	41.443	70.722	I-9945	shell hash	3560 ± 95		3597-3069	-14.61	0.71	Oldale and O'Hara (1980)
Marthas Vineyard	41.243	70.927	W-3782	Mercenaria	1340 ± 200		1222-484	-32.17	0.77	Oldale and O'Hara (1980)
Marthas Vineyard	41.302	70.992	W-3763	C. vir	9740 ± 250		11167-9901	-33.77	0.77	Oldale and O'Hara (1980)
Marthas Vineyard	41.317	70.992	W-3769	C. vir	9710 ± 300		11201-9681	-35.78	0.78	Oldale and O'Hara (1980)
Marthas Vineyard	41.303	70.992	W-3764	C. vir	9470 ± 500		11623-8895	-33.07	0.77	Oldale and O'Hara (1980)
Terrestrial Limiting										
Centerville	41.633	70.333	W-586	Fresh peat	5500 ± 300		6955-5607	-3.74	0.53	Emery et al. (1967)
Falmouth	41.550	70.633	Y-1663	Fresh peat	3420 ± 120		3975-3401	-4.74	0.53	Emery et al. (1967)
Barnstable (Brewster)	41.817	70.085	W-2494	Fresh peat	4700 ± 300		6174-4572	-8.52	3.14	Field et al. (1979)
Nantucket Sound	41.583	70.383	OS-18551	plant fragments	4600 ± 50	-27.4	5468-5054	-8.12	0.70	Gutierrez et al. (2003)
Nantucket Sound	41.583	70.383	OS-18548	wood	5290 ± 45	-26.5	6190-5938	-10.91	0.71	Gutierrez et al. (2003)
Nantucket Sound	41.550	70.467	OS-18556	Undiff peat	4130 ± 45	-26.5	4823-4529	-9.71	0.71	Gutierrez et al. (2003)
Nantucket Sound	41.583	70.400	OS-18549	Undiff peat	4280 ± 35	-26.8	4961-4727	-8.02	0.70	Gutierrez et al. (2003)
Nantucket Sound	41.550	70.467	OS-18550	Undiff peat	4490 ± 40	-26.5	5300-4978	-11.71	0.71	Gutierrez et al. (2003)
Nauset Bay	41.840	69.970	I-1967	Undiff peat	2300 ± 105		2705-2059	-2.39	0.57	Redfield (1967)
Nauset Bay	41.840	69.970	I-1968	Undiff peat	3460 ± 100		3975-3475	-4.46	0.57	Redfield (1967)
Barnstable	41.730	70.380	W-1093	Oak wood	4860 ± 350		6395-4629	-4.85	0.54	Redfield and Rubin (1962)
Barnstable	41.700	70.317	W-639	Fresh peat	500 ± 150		736-0	1.46	0.53	Redfield and Rubin (1962)
Barnstable	41.730	70.380	W-1099	Fresh peat	3170 ± 300		4230-2622	-3.11	0.22	Redfield and Rubin (1962)
Centerville	41.633	70.333	W-570	chaemocypris log	2130 ± 200		2707-1633	-2.00	0.26	Redfield and Rubin (1962)
Centerville	41.633	70.333	W-584	Fresh peat	2040 ± 240		2703-1421	-1.10	0.53	Redfield and Rubin (1962)
Marthas Vineyard	41.450	70.937	W-3386	Fresh peat	8230 ± 300		9895-8417	-20.07	0.73	Oldale and O'Hara (1980)
Marthas Vineyard	41.482	70.860	W-3394	Fresh peat	7600 ± 250		9028-7880	-16.28	0.72	Oldale and O'Hara (1980)
Connecticut										
Index Points										
Guildford	41.278	72.650		Sp	1070 ± 80	-10	1175-795	-1.61	0.63	Nydick et al. (1995)
Hammock River	41.266	72.515	GrN-14518	Sp/Ds	1710 ± 60		1812-1422	-1.86	0.51	van de Plassche (1991)
Barn Island	41.332	71.864	OS-26454	Sp/Jg	265 ± 30		434-0	-0.52	0.31	Donnelly et al. (2006)
Barn Island	41.332	71.864	OS-29654	Sp/Jg			256-0	-0.57	0.31	Donnelly et al. (2006)
Barn Island	41.332	71.864	OS-27765	Sp/Jg	240 ± 35		428-0	-0.63	0.31	Donnelly et al. (2006)
Barn Island	41.332	71.864	OS-26452	Sp/Jg	305 ± 40		476-292	-0.73	0.31	Donnelly et al. (2006)
Barn Island	41.332	71.864	OS-29653	Sp	330 ± 35		479-307	-0.82	0.31	Donnelly et al. (2006)
Barn Island	41.332	71.864	OS-27764	Sp	540 ± 40		643-509	-0.91	0.31	Donnelly et al. (2006)
Barn Island	41.332	71.864	OS-33644	Sp	475 ± 40		622-466	-0.94	0.31	Donnelly et al. (2006)
Barn Island	41.332	71.864	OS-29652	Sp	570 ± 35		650-524	-1.03	0.31	Donnelly et al. (2006)
Branford	41.261	72.849	UtC-9139	Ds	3092 ± 31	-18.1	3381-3221	-3.92	0.45	van de Plassche et al. (2002)
Branford	41.250	72.860	UtC-9140	Ds	2814 ± 34	-14.2	3018-2796	-3.08	0.45	van de Plassche et al. (2002)
Branford	41.256	72.839	UtC-9262	Ds	2124 ± 37	-15.8	2301-1995	-2.25	0.45	van de Plassche et al. (2002)
Gulf Pond	41.200	73.000	QC-1016	Salt peat	1515 ± 185		1863-1019	-1.87	0.97	Cinquemani et al. (1982)
Indian River	41.200	73.000	QC-1010	Salt peat	3645 ± 95		4236-3702	-5.27	0.97	Cinquemani et al. (1982)
Indian River	41.200	73.000	QC-1012	Salt peat	3500 ± 120		4089-3473	-4.17	0.97	Cinquemani et al. (1982)
Indian River	41.200	73.000	QC-1017	Salt peat	2970 ± 100		3372-2876	-3.20	0.97	Cinquemani et al. (1982)
Guildford	41.277	72.641		Plant frags	1220 ± 80	-14.3	1288-978	-1.79	0.78	Nydick et al. (1995)
Oyster Creek	41.260	72.350	QC-1013	Salt peat	4780 ± 175		5909-4983	-6.87	0.84	Cinquemani et al. (1982)
Oyster Creek	41.260	72.350	QC101413BC	Salt peat	3850 ± 235		4856-3638	-6.37	0.84	Cinquemani et al. (1982)
Oyster Creek	41.260	72.350	QC-1014A	Salt peat	4460 ± 155		5580-4648	-6.57	0.84	Cinquemani et al. (1982)
Branford	41.251	72.856	UtC-10439	Ds	1560 ± 40	-15.1	1536-1360	-1.57	0.45	van de Plassche et al. (2002)
Branford	41.251	72.856	UtC-10440	Ds	1133 ± 37	-15.5	1171-961	-1.20	0.45	van de Plassche et al. (2002)
Guildford	41.269	72.681		Sa	1170 ± 50	-14.5	1240-964	-1.44	0.66	Nydick et al. (1995)
Guildford	41.269	72.681		Sp	370 ± 60	-10	511-307	-1.11	0.63	Nydick et al. (1995)
Guildford	41.278	72.650		Sp	90 ± 70	-10	282-0	-0.77	0.63	Nydick et al. (1995)
Guildford	41.278	72.650		Sp	160 ± 60	-10	296-0	-0.80	0.63	Nydick et al. (1995)
Guildford	41.277	72.641		Sp	1020 ± 80	-9.7	1166-738	-1.40	0.63	Nydick et al. (1995)
Guildford	41.277	72.641		Sp	1780 ± 70	-10	1867-1547	-2.03	0.63	Nydick et al. (1995)
Guildford	41.269	72.681		Sa	100 ± 70	-12	282-0	-0.35	0.52	Nydick et al. (1995)
Guildford	41.269	72.681		Sa	590 ± 60	-13.8	664-522	-0.73	0.52	Nydick et al. (1995)
Guildford	41.278	72.650		Sa	10 ± 60	-13.8	268-0	-0.22	0.52	Nydick et al. (1995)
Guildford	41.278	72.650		Sa	440 ± 60	-10	615-315	-0.43	0.52	Nydick et al. (1995)
Guildford	41.278	72.650		Sa	600 ± 80	-13.8	680-508	-0.62	0.52	Nydick et al. (1995)
Guildford	41.277	72.641		Sa	210 ± 60	-13.2	428-0	-0.35	0.52	Nydick et al. (1995)
Guildford	41.277	72.641		Sa	660 ± 70	-10.8	722-532	-0.63	0.52	Nydick et al. (1995)
Guildford	41.277	72.641		Sa	1720 ± 70	-13.8	1821-1419	-1.48	0.52	Nydick et al. (1995)
Hammock River	41.265	72.508	2178-13	Ds	340 ± 50	-14	498-306	-1.04	0.45	van de Plassche et al. (1998)
Hammock River	41.265	72.508	2181-13	Ds	1100 ± 30	-14	1063-937	-1.48	0.45	van de Plassche et al. (1998)
Hammock River	41.265	72.508	2002-F	Ds	500 ± 30	-13	616-502	-1.23	0.45	van de Plassche et al. (1998)
Hammock River	41.265	72.508	2164-1	Ds	1120 ± 30	-15	1166-956	-1.39	0.45	van de Plassche et al. (1998)
Hammock River	41.265	72.508	2173-6.5	Ds	380 ± 30	-26	505-319	-1.03	0.45	van de Plassche et al. (1998)
Hammock River	41.265	72.508	2789-6.5	Ds	170 ± 40	-13	296-0	-0.51	0.45	van de Plassche et al. (1998)
Hammock River	41.265	72.508	2179-13	Sa	390 ± 30	-14	510-320	-0.53	0.26	van de Plassche et al. (1998)
Hammock River	41.265	72.508	2180-13	Sa	520 ± 50	-13	647-497	-0.67	0.26	van de Plassche et al. (1998)
Hammock River	41.265	72.508	1999-F	Sa	1460 ± 40	-13	1410-1296	-1.26	0.26	van de Plassche et al. (1998)
Hammock River	41.265	72.508	2000-F	Sa	1370 ± 50	-22	1371-1179	-1.09	0.26	van de Plassche et al. (1998)
Hammock River	41.265	72.508	2003-F	Sa	440 ± 30	-14	534-342	-0.56	0.26	van de Plassche et al. (1998)
Hammock River	41.265	72.508	2005-F	Sa	340 ± 40	-4	488-308	-0.27	0.26	van de Plassche et al. (1998)
Hammock River	41.265	72.508	2004-F	Sa	530 ± 50	-14	648-502	-0.41	0.26	van de Plassche et al. (1998)
Hammock River	41.265	72.508	2166-6.5	Sa	130 ± 40	-15	280-0	0.17	0.26	van de Plassche et al. (1998)
Hammock River	41.265	72.508	2167-6.5	Sa	180 ± 40	-14	304-0	-0.07	0.26	van de Plassche et al. (1998)

Hammock River	41.266	72.515	GrN-14519	Sp	1800 ± 35		1823-1617	-2.15	0.53	van de Plassche (1991)
Hammock River	41.266	72.515	GrN-14520	Sa	1890 ± 30		1895-1733	-1.57	0.76	van de Plassche (1991)
Terrestrial										
Mystic	41.370	71.950	W-1082	Undiff peat	2850 ± 260		3608-2348	-3.60	0.40	Redfield and Rubin (1962)
Kittam's Point	41.250	72.810	Y-840	Wood	910 ± 120		1066-574	0.36	0.48	Bloom (1963)
New Haven	41.300	72.750	W-945	Undiff peat	5900 ± 200		7242-6304	-9.08	0.51	Redfield and Rubin (1962)
Stiles Brickyard	41.340	72.880	Y-843	Wood	6810 ± 170		7982-7338	-4.37	0.56	Bloom (1963)
Guildford	41.269	72.681		Wood	720 ± 90		899-533	-0.08	0.48	Nydick et al. (1995)
Guildford	41.270	72.660	Y-855	Wood	1180 ± 80		1276-956	0.03	0.48	Bloom (1963)
Hammock River	41.265	72.508	GrN-14515	Sedge peat	3950 ± 60		4569-4161	-3.80	0.22	van de Plassche et al. (1989)
Hammock River	41.265	72.508	GrN-14514	Sedge peat	4295 ± 45		5031-4713	-4.93	0.22	van de Plassche et al. (1989)
Hammock River	41.265	72.508	GrN-14513	Sedge peat	4700 ± 40		5581-5319	-5.97	0.22	van de Plassche et al. (1989)
Hammock River	41.265	72.508	GrN-14512	Sedge peat	5300 ± 60		6267-5933	-7.28	0.23	van de Plassche et al. (1989)
Hammock River	41.265	72.508	GrN-14511	Sedge peat	5880 ± 70		6881-6503	-7.35	0.23	van de Plassche et al. (1989)
Hammock River	41.265	72.508	GrN-14510	Sedge peat	5520 ± 60		6436-6206	-8.48	0.23	van de Plassche et al. (1989)
Hammock River	41.265	72.508	Y-1056	sedge peat	4780 ± 130		5888-5062	-7.11	0.48	Bloom (1963)
Hammock River	41.265	72.508	Y-1057	sedge peat	3540 ± 130		4220-3478	-4.50	0.49	Bloom (1963)
Hammock River	41.265	72.508	Y-1058	sedge peat	3450 ± 160		4149-3363	-3.60	0.49	Bloom (1963)
Hammock River	41.265	72.508	Y-1074	sedge peat	6130 ± 90		7248-6794	-9.69	0.50	Bloom (1963)
Hammock River	41.265	72.508	Y-1175	sedge peat	3020 ± 90		3437-2955	-1.56	0.51	Bloom (1963)
Hammock River	41.265	72.508	Y-1176	sedge peat	3220 ± 90		3685-3245	-2.27	0.50	Bloom (1963)
Hammock River	41.265	72.508	Y-1177	Wood	4880 ± 120		5899-5325	-4.77	0.50	Bloom (1963)
Hammock River	41.160	72.310	Y-1055	Undiff peat	7060 ± 100		8151-7673	-8.94	0.50	Bloom (1963)
Hammock River	41.265	72.508	2177-13	Sr	210 ± 30	-26	306-0	0.43	0.17	van de Plassche et al. (1998)
Hammock River	41.265	72.508	2792-13	Sr	370 ± 40	-25	505-315	0.01	0.17	van de Plassche et al. (1998)
Hammock River	41.265	72.508	2786-13	Sr	1020 ± 40	-22	1052-798	-0.26	0.17	van de Plassche et al. (1998)
Hammock River	41.265	72.508	2182-13	Sr	1250 ± 40	-25	1276-1076	-0.57	0.17	van de Plassche et al. (1998)
Hammock River	41.265	72.508	2001-F	Sr	1410 ± 40	-9	1381-1279	-0.42	0.16	van de Plassche et al. (1998)
Hammock River	41.265	72.508	2163-1	Sr	1170 ± 50	-28	1240-964	-0.26	0.17	van de Plassche et al. (1998)
Hammock River	41.265	72.508	2165-1	Sr	1100 ± 30	-27	1063-937	-0.48	0.17	van de Plassche et al. (1998)
Hammock River	41.265	72.508	2168-6.5	Sr	230 ± 40	-27	428-0	0.36	0.17	van de Plassche et al. (1998)
Hammock River	41.265	72.508	2169-6.5	Sr	240 ± 50	-26	462-0	0.30	0.17	van de Plassche et al. (1998)
Hammock River	41.265	72.508	2170-6.5	Sr	220 ± 40	-27	426-0	0.22	0.17	van de Plassche et al. (1998)
Hammock River	41.265	72.508	2171-6.5	Sr	430 ± 50	-27	540-318	0.14	0.17	van de Plassche et al. (1998)
Hammock River	41.265	72.508	2172-6.5	Sr	420 ± 50	-13	535-317	0.09	0.17	van de Plassche et al. (1998)
Hammock River	41.265	72.508	2174-6.5	Sr	440 ± 40	-26	541-331	0.00	0.17	van de Plassche et al. (1998)
Hammock River	41.265	72.508	2175-6.5	Sr	520 ± 30	-27	627-507	-0.08	0.17	van de Plassche et al. (1998)
Hammock River	41.265	72.508	2176-6.5	Sr	520 ± 30	-26	627-507	-0.14	0.17	van de Plassche et al. (1998)
Hammock River	41.265	72.508	2790-6.5	Sr	350 ± 50	-26	500-308	0.20	0.17	van de Plassche et al. (1998)
Hammock River	41.265	72.508	2794-6.5	Sr	480 ± 50	-26	634-334	-0.14	0.17	van de Plassche et al. (1998)
Menunketesuck River	41.280	72.480	GrN-15007	Sedge peat	5280 ± 40		6184-5940	-8.22	0.24	van de Plassche et al. (1989)
Hammock River	41.266	72.515	GrN-15556	Sr	85 ± 45		270-0	0.58	0.32	van de Plassche (1991)
Hammock River	41.266	72.515	GrN-15557	Pa	740 ± 40		735-569	0.15	0.32	van de Plassche (1991)
Hammock River	41.266	72.515	GrN-15595	Pa	1580 ± 110		1715-1291	-0.40	0.30	van de Plassche (1991)
Hammock River	41.266	72.515	GrN-15596	Pa	890 ± 60		924-698	0.20	0.30	van de Plassche (1991)
New York										
Index Points										
Cedar Pond Brook Marsh	41.225	73.967	QC-770	Salt peat	800 ± 100		928-560	-0.76	0.81	Pardi et al. (1984)
Cedar Pond Brook Marsh	41.225	73.967	QC-711	Salt peat	3630 ± 110		4282-3640	-5.21	0.82	Pardi et al. (1984)
Cedar Pond Brook Marsh	41.225	73.967	QC-772	Salt peat	1740 ± 100		1873-1415	-1.76	0.81	Pardi et al. (1984)
Cedar Pond Brook Marsh	41.225	73.967	QC-712	Salt peat	1940 ± 110		2285-1607	-2.56	0.81	Pardi et al. (1984)
Cedar Pond Brook Marsh	41.225	73.967	QC-773	Salt peat	2650 ± 100		2995-2367	-2.56	0.81	Pardi et al. (1984)
Cedar Pond Brook Marsh	41.225	73.967	QC-810	Salt peat	3030 ± 100		3447-2951	-3.31	0.82	Pardi et al. (1984)
Cedar Pond Brook Marsh	41.225	73.967	QC-709	Salt peat	2220 ± 120		2688-1898	-3.34	0.82	Pardi et al. (1984)
Cedar Pond Brook Marsh	41.225	73.967	QC-774	Salt peat	3090 ± 110		3557-2979	-3.46	0.81	Pardi et al. (1984)
Cedar Pond Brook Marsh	41.225	73.967	QC-811	Salt peat	2700 ± 120		3160-2462	-3.61	0.82	Pardi et al. (1984)
Constitution Island	41.411	73.948	QC-227	Salt peat	4230 ± 120		5265-4423	-7.51	0.81	Pardi et al. (1984)
Constitution Island	41.406	73.942	QC-692	Salt peat	4660 ± 140		5654-4892	-9.46	0.83	Pardi et al. (1984)
Constitution Island	41.406	73.948	QC-1039	Salt peat	2160 ± 130		2469-1823	-1.80	0.82	Pardi et al. (1984)
Constitution Island	41.406	73.942	QC-695	Salt peat	2440 ± 100		2753-2315	-3.06	0.83	Pardi et al. (1984)
Constitution Island	41.411	73.948	QC-226	Salt peat	2320 ± 100		2713-2117	-3.71	0.80	Pardi et al. (1984)
Constitution Island	41.406	73.942	QC-693	Salt peat	3210 ± 110		3700-3084	-4.86	0.84	Pardi et al. (1984)
Constitution Island	41.411	73.948	QC-276	Salt peat	4110 ± 100		4861-4317	-5.96	0.80	Pardi et al. (1984)
Constitution Island	41.406	73.942	QC-694	Salt peat	3760 ± 120		4512-3782	-6.26	0.84	Pardi et al. (1984)
Marlboro Marsh	41.611	73.966	QC-341	Salt peat	2330 ± 240		2942-1742	-3.11	0.80	Pardi et al. (1984)
Marlboro Marsh	41.611	73.966	QC-340	Salt peat	3010 ± 120		3448-2872	-4.11	0.80	Pardi et al. (1984)
Marlboro Marsh	41.611	73.966	QC-343	Salt peat	4390 ± 220		5583-4437	-5.81	0.80	Pardi et al. (1984)
Marlboro Marsh	41.611	73.966	QC-705	Salt peat	4260 ± 130		5283-4441	-7.21	0.81	Pardi et al. (1984)
Marlboro Marsh	41.611	73.966	QC-686	Salt peat	4570 ± 110		5580-4482	-8.31	0.83	Pardi et al. (1984)
Oscawana I Tidal Marsh	41.229	73.931	QC-228	Salt peat	1870 ± 90		1997-1569	-2.51	0.80	Pardi et al. (1984)
Oscawana I Tidal Marsh	41.229	73.931	QC-221B	Salt peat	4570 ± 120		5580-4878	-6.61	0.80	Pardi et al. (1984)
Oscawana I Tidal Marsh	41.229	73.931	QC-264	Salt peat	4500 ± 100		5448-4860	-6.81	0.80	Pardi et al. (1984)
Roa Hook	41.299	73.947	QC-1043	Salt peat	4450 ± 200		5586-4540	-7.64	0.83	Pardi et al. (1984)
Roa Hook	41.299	73.947	QC-512	Salt peat	4120 ± 350		5580-3718	-8.81	0.81	Pardi et al. (1984)
Roa Hook	41.299	73.947	QC-509	Salt peat	4550 ± 130		5580-4866	-9.31	0.80	Pardi et al. (1984)
Roa Hook	41.299	73.947	QC-569	Salt peat	2490 ± 120		2844-2314	-1.95	0.80	Pardi et al. (1984)
Roa Hook	41.299	73.947	QC-568	Salt peat	3170 ± 170		3799-2949	-4.02	0.80	Pardi et al. (1984)
Roa Hook	41.292	73.947	QC-1041	Salt peat	3190 ± 160		3828-2978	-4.31	0.81	Pardi et al. (1984)
Roa Hook	41.299	73.947	QC-510	Salt peat	3140 ± 170		3816-2878	-4.81	0.80	Pardi et al. (1984)
Roa Hook	41.299	73.947	QC-721	Salt peat	3320 ± 110		3840-3342	-5.56	0.81	Pardi et al. (1984)
Roa Hook	41.299	73.947	QC-723	Salt peat	3910 ± 130		4812-3978	-6.76	0.81	Pardi et al. (1984)
Stoney Point	41.244	73.968	QC-505	Salt peat	3100 ± 110		3564-2996	-3.21	0.80	Pardi et al. (1984)
Stoney Point	41.244	73.968	QC-506	Salt peat	3740 ± 200		4798-3576	-5.81	0.80	Pardi et al. (1984)
Piermont Tidal Marsh	41.025	73.900	QC-737	Salt peat	3730 ± 200		4797-3565	-5.66	0.81	Pardi et al. (1984)
Piermont Tidal Marsh	41.025	73.900	QC-739	Salt peat	3790 ± 90		4421-3925	-7.71	0.82	Pardi et al. (1984)
Piermont Tidal Marsh	41.025	73.900	QC-261	Salt peat	4610 ± 110		5586-4974	-8.35	0.81	Pardi et al. (1984)
Piermont Tidal Marsh	41.025	73.900	QC-740	Salt peat	4300 ± 280		5589-4101	-9.37	0.83	Pardi et al. (1984)
Piermont Tidal Marsh	41.025	73.900	QC-741	Salt peat	4720 ± 120		5710-5048	-9.71	0.83	Pardi et al. (1984)
Piermont Tidal Marsh	41.025	73.900	QC-742	Salt peat	5320 ± 170		6441-5667	-11.16	0.82	Pardi et al. (1984)
Piermont Tidal Marsh	41.025	73.900	QC-808	Salt peat	5480 ± 140		6555-5933	-11.16	0.84	Pardi et al. (1984)
Piermont Tidal Marsh	41.025	73.900	QC-734	Salt peat	1420 ± 120		1563-1063	-1.46	0.81	Pardi et al. (1984)
Piermont Tidal Marsh	41.025	73.900	QC-735	Salt peat	2000 ± 110		2306-1706	-3.06	0.81	Pardi et al. (1984)
Piermont Tidal Marsh	41.025	73.900	QC-211	Salt peat	2300 ± 160		2742-1950	-2.81	0.80	Pardi et al. (1984)
Piermont Tidal Marsh	41.025	73.900	QC-736	Salt peat	2550 ± 140		2958-2320	-4.56	0.81	Pardi et al. (1984)

Piermont Tidal Marsh	41.025	73.900	QC-732	Salt peat	2990 ± 100		3388-2882	-4.56	0.81	Pardi et al. (1984)
Piermont Tidal Marsh	41.025	73.900	QC-730	Salt peat	3050 ± 100		3455-2959	-5.26	0.81	Pardi et al. (1984)
Piermont Tidal Marsh	41.025	73.900	QC-738	Salt peat	3320 ± 140		3921-3221	-6.74	0.82	Pardi et al. (1984)
Piermont Tidal Marsh	41.025	73.900	QC-262	Salt peat	3460 ± 100		3975-3475	-4.86	0.81	Pardi et al. (1984)
Marine Limiting										
Piermont	41.136	73.894		C. vir	3510 ± 35		3412-3048	-11.40	0.12	Slagle et al. (2006)
Piermont	41.093	73.886		C. vir	2655 ± 35		2335-2003	-11.97	0.11	Slagle et al. (2006)
Piermont	41.056	73.896		C. vir	2955 ± 45		2728-2354	-6.57	0.12	Slagle et al. (2006)
Piermont	41.056	73.896		C. vir	3375 ± 35		3262-2864	-8.54	0.12	Slagle et al. (2006)
Piermont	41.048	-73.896		C. vir	3500 ± 40		3402-3022	-8.18	0.12	Slagle et al. (2006)
Westway	40.726	74.011	QC-1184	Marine shell	5540 ± 160		6189-5435	-23.25	0.59	Pardi et al. (1984)
Terrestrial Limiting										
Constitution Island	41.406	73.948	QC-1040	basal peat	6030 ± 290		7477-6287	-6.85	0.56	Pardi et al. (1984)
Cedar Pond Brook Marsh	41.225	73.967	QC-771	Wood	2890 ± 130		3348-2768	-2.02	0.54	Pardi et al. (1984)
Constitution Island	41.406	73.942	QC-691	Fresh peat	2320 ± 500		3559-1283	0.03	0.54	Pardi et al. (1984)
Constitution Island	41.406	73.942	QC-690	Peat	1440 ± 100		1558-1146	-1.02	0.54	Pardi et al. (1984)
Piermont Tidal Marsh	41.025	73.900	QC-731	Wood	3530 ± 110		4145-3489	-3.93	0.53	Pardi et al. (1984)
Roa Hook	41.299	73.947	QC-566	Wood	4660 ± 100		5593-5049	-5.74	0.54	Pardi et al. (1984)
Roa Hook	41.299	73.947	QC-565	Wood	5470 ± 140		6544-5928	-7.47	0.54	Pardi et al. (1984)
Roa Hook	41.299	73.947	QC-573	wood	6230 ± 120		7419-6807	-9.67	0.54	Pardi et al. (1984)
Roa Hook	41.299	73.947	QC-722	Wood	2360 ± 100		2719-2153	-1.22	0.54	Pardi et al. (1984)
Westway	40.726	74.012	QC-1026	Peat	9170 ± 230		11087-9681	-21.87	0.64	Pardi et al. (1984)
Westway	40.725	74.011	QC-1029	Peat	8190 ± 130		9477-8729	-18.18	0.63	Pardi et al. (1984)
Westway	40.723	74.016	QC-1028	Peat	8750 ± 170		10222-9486	-20.29	0.67	Pardi et al. (1984)
Barclay	40.717	74.000	L-562	Wood	6500 ± 100		7581-7183	-13.22	0.25	Olson and Broecker (1961)
Westway	40.761	74.013	QC-1183	Organic silt	9540 ± 120		11201-10525	-35.50	0.71	Pardi et al. (1984)
Westway	40.741	74.011	QC-1321	Organic silt	7920 ± 200		9395-8371	-23.36	0.65	Pardi et al. (1984)
Westway	40.724	74.016	QC-1380	Organic silt	8960 ± 270		11052-9432	-20.27	0.64	Pardi et al. (1984)
Westway	40.726	74.016	QC-1389	Organic silt	7650 ± 190		8991-8051	-20.44	0.62	Pardi et al. (1984)
Westway	40.725	74.016	QC-1374	Organic silt	8690 ± 190		10231-9309	-23.36	0.65	Pardi et al. (1984)
Piermont Tidal Marsh	41.025	73.900	QC-809	Peat	6840 ± 230		8162-7294	-10.47	0.59	Pardi et al. (1984)
Long Island										
Index Points										
Caumsett Marsh	40.942	73.481	QC-689	Salt peat	780 ± 120		926-548	-0.84	0.92	Pardi et al. (1984)
Caumsett Marsh	40.942	73.481	QC-687	Salt peat	660 ± 120		904-482	-2.04	0.92	Pardi et al. (1984)
Caumsett Marsh	40.942	73.481	QC-688	Salt peat	760 ± 140		953-515	-2.05	0.92	Pardi et al. (1984)
College Point Marsh	40.796	73.831	QC-267	Salt peat	5650 ± 170		6848-6008	-12.76	0.82	Pardi et al. (1984)
College Point Marsh	40.796	73.831	QC-265	Salt peat	6370 ± 100		7469-7017	-18.11	0.82	Pardi et al. (1984)
College Point Marsh	40.796	73.831	QC-269	Salt peat	8100 ± 100		9302-8644	-19.81	0.84	Pardi et al. (1984)
College Point Marsh	40.796	73.831	QC-266	Salt peat	7120 ± 240		8393-7517	-17.76	0.83	Pardi et al. (1984)
Eatons Neck	40.949	73.395	QC-679	Salt peat	1585 ± 110		1720-1292	-1.34	0.91	Cinquemani et al. (1982)
Eatons Neck	40.949	73.395	QC-681	Salt peat	370 ± 120		642-0	-0.64	0.92	Cinquemani et al. (1982)
Eatons Neck	40.949	73.395	QC-682	Salt peat	2520 ± 85		2752-2360	-4.84	0.92	Cinquemani et al. (1982)
Mt. Sinai Harbor	40.949	73.031	QC-190	Salt peat	2180 ± 100		2357-1903	-4.57	1.01	Cinquemani et al. (1982)
Pelham Bay Park	40.868	73.793	QC-295	Salt peat	1800 ± 90		1927-1527	-1.99	0.92	Pardi et al. (1984)
Roosevelt Ave	40.800	73.800	QC-306	Salt peat	7980 ± 390		9766-7982	-15.51	0.82	Pardi et al. (1984)
Cedar Beach Suffolk Co	40.617	73.383	QC-314	Salt peat	5060 ± 120		6177-5585	-10.59	0.74	Pardi and Newman (1980)
Wantagh- Nassau Co	40.650	73.517	QC-315	Salt peat	1020 ± 100		1172-732	-1.61	0.74	Pardi and Newman (1980)
Wantagh- Nassau Co	40.650	73.517	QC-316	Salt peat	300 ± 90		518-0	-0.76	0.74	Pardi and Newman (1980)
LI- south shore	41.023	72.603		Salt peat	7585 ± 125		8637-8057	-16.98	0.79	Field et al. (1979)
NY- Riverhead	40.900	72.617	L-863A	Salt peat	930 ± 150		1175-565	-1.19	0.54	Redfield (1967)
Shelter Island	41.046	72.314	QC-1084	Salt peat	850 ± 150		1057-545	-1.23	0.55	Pardi et al. (1984)
Terrestrial Limiting										
Gardiners Bay	41.192	72.192	I-1663	Undiff peat	6575 ± 125		7670-7260	-11.87	0.80	Field et al. (1979)
Pelham Bay	40.870	73.790	C-943	Stump	2830 ± 220		3452-2364	-1.88	0.16	Redfield and Rubin (1962)
Riverhead	40.900	72.617	I-2077	Fresh peat	8070 ± 130		9398-8596	-2.77	0.42	Redfield (1967)
Shelter Island	41.046	72.314	QC1083A&B	Peat	3590 ± 130		4288-3560	-5.96	0.42	Pardi et al. (1984)
South Long Island	40.748	72.447	I-7434	Fresh peat	5585 ± 110		6627-6131	-10.39	0.80	Field et al. (1979)
NY/NJ Border	40.460	74.180	QC-1399	Organic sediment	2700 ± 150		3207-2363	-0.88	0.16	Pardi et al. (1984)
New Jersey										
Index Points										
Brigantine City- NJ	39.426	74.390	Y-1284	Salt peat	5890 ± 100		6951-6453	-12.95	0.77	Stuiver and Daddario (1963)
Brigantine NWR	39.483	74.424	Y-1281	Salt peat	3000 ± 90		3387-2929	-4.65	0.77	Stuiver and Daddario (1963)
Brigantine NWR	39.479	74.419	Y-1282	Salt peat	3830 ± 100		4517-3929	-7.35	0.77	Stuiver and Daddario (1963)
Brigantine NWR	39.454	74.405	Y-1283	Salt peat	4760 ± 80		5643-5315	-10.25	0.78	Stuiver and Daddario (1963)
Brigantine NWR	39.485	74.426	Y-1331	Salt peat	1890 ± 40		1922-1720	-2.55	0.77	Stuiver and Daddario (1963)
Great Bay	39.561	74.349		Salt peat	3035 ± 120		3475-2879	-4.05	0.77	Psuty et al. (1986)
Great Bay	39.522	74.324		Salt peat	4495 ± 125		5565-4843	-8.35	0.78	Psuty et al. (1986)
Great Bay	39.522	74.324		Salt peat	4175 ± 145		5264-4256	-8.35	0.78	Psuty et al. (1986)
Sea Island City	39.200	74.700	QC-850	Salt peat	920 ± 160		1177-559	-1.31	0.80	Cinquemani et al. (1982)
Sea Island City	39.200	74.700	QC-850A	Salt peat	2260 ± 100		2695-1993	-3.51	0.80	Cinquemani et al. (1982)
Sea Island City	39.200	74.700	QC-851	Salt peat	2345 ± 100		2715-2149	-2.81	0.80	Cinquemani et al. (1982)
Sea Island City	39.200	74.700	QC-853	Salt peat	2760 ± 100		3204-2720	-4.76	0.80	Cinquemani et al. (1982)
Sea Island City	39.200	74.700	QC-854	Salt peat	3440 ± 110		3981-3445	-5.51	0.81	Cinquemani et al. (1982)
Sea Island City	39.200	74.700	QC-855	Salt peat	3960 ± 110		4816-4092	-7.36	0.81	Cinquemani et al. (1982)
Sea Island City	39.180	74.730	QC-852	Salt peat	2260 ± 100		2695-1993	-3.51	0.80	Pardi et al. (1984)
Brigantine Marsh	39.420	74.354		Salt peat	240 ± 50	-13.2	462-0	-1.70	0.68	Donnelly et al. (2004)
Edwin B Forsythe NWR	39.495	74.418		Salt peat	1249 ± 13	-10.1	1263-1147	-2.43	0.58	This publication
Edwin B Forsythe NWR	39.495	74.418		Salt peat	1502 ± 14	-1.7	1407-1349	-2.70	0.58	This publication
Edwin B Forsythe NWR	39.495	74.418		Salt peat	1188 ± 30	-28.7	1228-1004	-2.23	0.58	This publication
Edwin B Forsythe NWR	39.495	74.418		Salt peat	1541 ± 14	-14.6	1379-1517	-2.93	0.58	This publication
Edwin B Forsythe NWR	39.495	74.418		Salt peat	319 ± 13	-12	452-308	-1.52	0.58	This publication
Edwin B Forsythe NWR	39.495	74.418	OS-66514	Salt peat	1550 ± 25	-14.4	1521-1383	-3.07	0.58	This publication
Edwin B Forsythe NWR	39.495	74.418	OS-66518	Salt peat	950 ± 30	-13.78	926-794	-2.09	0.58	This publication
Cheesequake Marsh	40.400	74.300	QC-842	Salt peat	2080 ± 160		2457-1625	-3.32	0.85	Cinquemani et al. (1982)
Cheesequake Marsh	40.400	74.300	QC-844	Salt peat	1210 ± 185		1510-738	-2.62	0.85	Cinquemani et al. (1982)
Cheesequake Marsh	40.400	74.300	QC-847	Salt peat	1960 ± 130		2306-1572	-2.85	0.85	Cinquemani et al. (1982)
Little Egg Inlet- NJ	39.412	74.123	GX-2966	Salt peat	7600 ± 300		9239-7799	-30.15	1.53	Field et al. (1979)
Great Bay	39.549	74.342		Salt peat	3050 ± 95		3448-2972	-6.95	0.78	Psuty et al. (1986)
Great Bay	39.510	74.320	OS-34136	Salt peat	1200 ± 35		1257-1009	-1.45	0.31	Miller et al. (2009)
Great Bay	39.510	74.320	OS-34134	Salt peat	2890 ± 30		3156-2926	-5.11	0.31	Miller et al. (2009)

Island Beach	39.803	74.094	GX-19017	Salt peat	5625 ± 200		6883-5947	-10.38	0.67	Miller et al. (2009)
Core 127	39.417	74.256		Salt peat	7690 ± 50		8581-8401	-17.37	0.60	Miller et al. (2009)
Core 127	39.417	74.256		Salt peat	7130 ± 100		8171-7749	-17.62	0.60	Miller et al. (2009)
Brigantine Marsh	39.420	74.354		Salt peat	210 ± 50	-12.4	426-0	-0.85	0.68	Donnelly et al. (2004)
Brigantine Marsh	39.420	74.354		Salt peat	340 ± 40	-15.1	488-308	-0.96	0.68	Donnelly et al. (2004)
Brigantine Marsh	39.420	74.354		Salt peat	1420 ± 40	-19.6	1386-1284	-2.60	0.68	Donnelly et al. (2004)
Brigantine Marsh	39.420	74.354		Salt peat	450 ± 50	-15.4	617-319	-0.82	0.68	Donnelly et al. (2004)
Whale Beach	39.184	74.671	BETA-131489	Sa	230 ± 40		428-0	-0.94	0.79	Donnely et al. (2001)
Whale Beach	39.184	74.671	BETA-129433	Sa	60 ± 40		266-0	-0.57	0.79	Donnely et al. (2001)
Whale Beach	39.184	74.671	BETA-128149	Sa	210 ± 40		420-0	-0.55	0.79	Donnely et al. (2001)
Whale Beach	39.184	74.671	BETA-131490	Sa	220 ± 40		426-0	-0.66	0.79	Donnely et al. (2001)
Whale Beach	39.184	74.671	BETA-129432	Sa	110 ± 40		274-0	-0.66	0.79	Donnely et al. (2001)
Whale Beach	39.184	74.671	BETA-124176	Sa	290 ± 50		490-0	-0.89	0.79	Donnely et al. (2001)
Whale Beach	39.184	74.671	BETA-124177	Sa	300 ± 40		475-289	-0.79	0.79	Donnely et al. (2001)
Cheesequake Marsh	40.400	74.300	QC-845	Salt peat	4820 ± 95		5741-5319	-10.95	0.86	Cinquemani et al. (1982)
Whale Beach	39.184	74.671	BETA-123305	Sa	560 ± 50		653-513	-1.27	0.79	Donnely et al. (2001)
Marine Limiting										
Rainbow Island	39.305	74.585	GX-30879	Elphidium spp.	2580 ± 30		2235-1921	-4.54	0.18	Miller et al. (2009)
Rainbow Island	39.305	74.585	GX-30880	Elphidium spp.	2880 ± 30		2646-2314	-5.15	0.18	Miller et al. (2009)
Rainbow Island	39.305	74.585	GX-30881	Elphidium spp.	3770 ± 40		3658-3376	-6.98	0.19	Miller et al. (2009)
Rainbow Island	39.304	74.588	GX-31527	Elphidium spp.	2330 ± 70		1957-1561	-3.60	0.18	Miller et al. (2009)
Rainbow Island	39.304	74.588	GX-31526	Elphidium spp.	2960 ± 70		2720-2340	-5.18	0.19	Miller et al. (2009)
Cheesequake Marsh	40.439	74.273		Marine shell	4330 ± 460		5446-3122	-10.29	0.59	Psuty et al. (1986)
Terrestrial Limiting										
Great Bay	39.549	74.342		Undiff peat	6380 ± 355		7933-6477	-7.89	0.55	Psuty et al. (1986)
Great Bay	39.510	74.320	OS-3415	Undiff peat	7340 ± 35		8287-8027	-7.14	0.19	Miller et al. (2009)
Island Beach	39.803	74.094	GX-19018	Undiff peat	4532 ± 58		5442-4976	0.40	0.18	Miller et al. (2009)
Core 3	39.664	74.099		Undiff peat	8800 ± 170		10242-9502	-3.80	1.09	Miller et al. (2009)
Cheesequake Marsh	40.400	74.300	QC-896	Undiff peat	7320 ± 185		8508-7756	-11.24	0.59	Cinquemani et al. (1982)
Cheesequake Marsh	40.439	74.273		Cedar peat	6610 ± 215		7930-7020	-10.99	0.59	Psuty et al. (1986)
Cheesequake Marsh	40.439	74.273		Undiff peat	7735 ± 195		9087-8163	-11.79	0.59	Psuty et al. (1986)
Cheesequake Marsh	40.435	74.281		Cedar peat	6020 ± 215		7413-6403	-7.59	0.59	Psuty et al. (1986)
Union Beach	40.446	74.161		Undiff peat	660 ± 110		897-497	-0.59	0.58	Psuty et al. (1986)
Union Beach	40.446	74.161		Undiff peat	2695 ± 145		3201-2363	-0.54	0.58	Psuty et al. (1986)
Inner Delaware										
Index Points										
Leipsic River	39.253	75.460	Beta-118799	Salt peat	970 ± 80		1055-727	-1.51	0.79	Nikitina et al. (2000)
Leipsic River	39.251	75.469	GrN-18995	Salt peat	1160 ± 50		1232-960	-2.81	0.79	Nikitina et al. (2000)
Leipsic River	39.429	75.457	Beta-118800	Salt peat	1770 ± 60		1857-1543	-3.13	0.79	Nikitina et al. (2000)
Leipsic River	39.251	75.469	GrN-18994	Salt peat	2030 ± 80		2302-1818	-3.14	0.79	Nikitina et al. (2000)
Leipsic River	39.249	75.469	Beta-118803	Salt peat	2070 ± 80		2308-1870	-2.79	0.79	Nikitina et al. (2000)
Leipsic River	39.235	75.436	Beta-118802	Salt peat	2880 ± 70		3244-2810	-5.25	0.79	Nikitina et al. (2000)
Leipsic River	39.248	75.469	GrA-9719	Salt peat	3320 ± 40		3676-3452	-5.66	0.79	Nikitina et al. (2000)
Leipsic River	39.243	75.442	Beta-117237	Salt peat	3430 ± 70		3865-3483	-6.86	0.79	Nikitina et al. (2000)
Leipsic River	39.246	75.470	GrA-9698	Salt peat	3485 ± 40		3861-3641	-8.54	0.79	Nikitina et al. (2000)
Leipsic River	39.247	75.469	GrA-9693	Salt peat	3530 ± 40		3912-3694	-7.23	0.79	Nikitina et al. (2000)
Leipsic River	39.247	75.469	GrN-18993	Salt peat	3660 ± 30		4084-3900	-6.61	0.79	Nikitina et al. (2000)
Port Mahon	39.125	75.321	I-5955	Salt peat	4090 ± 100		4851-4299	-8.31	0.85	Belknap (1975)
Leipsic River			Beta-117239	Salt peat	4490 ± 80		5318-4872	-11.52	0.79	Nikitina et al. (2000)
Port Mahon	39.125	75.321	I-5955	Salt peat	2020 ± 110		2307-1721	-5.18	0.58	Marx (1981)
Port Mahon	39.180	75.403	TEM-173	Salt peat	2490 ± 80		2739-2361	-6.06	0.60	Marx (1981)
Bowers	39.052	75.390	P-1686	Salt peat	1950 ± 55		2036-1736	-4.50	0.80	Belknap (1975)
Bowers	39.052	75.390	P-1688	Spartina	2999 ± 59		3348-3004	-6.02	0.85	Belknap (1975)
Bowers	39.056	75.394	I-5927	Salt peat	5205 ± 110		6273-5723	-16.54	0.86	Belknap (1975)
Sheppards Island	38.922	75.313	I-5930	Salt peat	5345 ± 110		6391-5905	-14.10	1.15	Belknap (1975)
St Jones River	39.071	75.431	Beta-176159	Organic sediment	3930 ± 80	-15.6	4781-4095	-6.54	0.80	Leorri et al. (2006)
Slaughter Beach	38.905	75.296	I-9230	Salt peat	720 ± 80		793-539	-1.36	0.85	Kraft (1976)
Smyrna	39.302	75.598	DC-3_c	Salt peat	1370 ± 110		1519-1059	-2.71	0.81	Rogers and Pizzuto (1994)
Sheppards Island	38.926	75.322	I-9228	Salt peat	1690 ± 85		1813-1409	-2.37	0.85	Kraft (1976)
Bowers	39.049	75.388	P-1687	Salt peat	1952 ± 45		2003-1743	-2.21	0.85	Belknap (1975)
Slaughter Beach	38.886	75.265	I-5205	Spartina	2560 ± 95		2844-2356	-3.43	0.79	Belknap (1975)
St Jones River	39.082	75.445	Beta-176158	Organic sediment	4170 ± 40	-18.2	4835-4577	-9.14	0.80	Leorri et al. (2006)
St Jones River	39.073	75.423	Beta-176160	Organic sediment	2790 ± 40	-14.2	2988-2784	-7.34	0.80	Leorri et al. (2006)
Bowers	39.051	75.394	P-1685	Spartina	3314 ± 63		3691-3403	-5.85	0.81	Belknap (1975)
Marine Limiting										
Offshore Bowers	39.087	75.228	I-6674	Marine shell	2685 ± 90		2428-1906	-11.50	0.52	Belknap (1975)
Offshore Bowers	39.087	75.228	I-6675	Marine shell	2855 ± 90		2687-2141	-11.67	0.51	Belknap (1975)
Terrestrial Limiting										
Smyrna	39.320	75.483	I-6589	Peat	6835 ± 115		7931-7497	-13.80	0.63	Belknap (1975)
Sheppards Island	38.929	75.319	I-9229	Peat	285 ± 75		508-0	1.07	0.61	Kraft (1976)
Port Mahon	39.136	75.403	TEM-148	Stump	3450 ± 100		3972-3468	-5.48	0.60	Ramsey and Baxter (1996)
Smyrna	39.243	75.584		Fresh peat	3515 ± 85		4072-3574	-1.08	0.54	Rogers and Pizzuto (1994)
Port Mahon	39.177	75.408	I-5929	Peat	2945 ± 95		3352-2870	-4.67	0.61	Belknap (1975)
Bowers	39.056	75.394	I-5994	Peat	7730 ± 125		8978-8328	-20.79	0.65	Belknap (1975)
St Jones River	39.082	75.445	Beta-179205	Peat	230 ± 60	-25	460-0	-0.63	0.52	Leorri et al. (2006)
St Jones River	39.090	75.458	Beta-177401	Plant	3790 ± 40	-25.2	4376-3994	-7.13	0.52	Leorri et al. (2006)
Outer Delaware										
Index Points										
Horse Island	38.672	75.134	Beta-118808	Salt peat	170 ± 80		426-0	-0.80	0.65	Nikitina et al. (2000)
Horse Island	38.672	75.134	Beta-118807	Salt peat	960 ± 50		961-745	-1.52	0.65	Nikitina et al. (2000)
Offshore Rehoboth	38.649	75.021	I-5204	Salt peat	7500 ± 135		8545-8023	-20.19	0.72	Belknap (1975)
Great Marsh	38.786	75.172	Beta-14681	Salt peat	80 ± 60		274-0	-0.80	0.75	Ramsey and Baxter (1996)
Wolf Glade	38.764	75.097	TEM-158	Spartina	280 ± 60		496-0	-0.94	0.76	Ramsey and Baxter (1996)
Great Marsh	38.786	75.171	Beta-14683	Salt peat	670 ± 70		725-539	-1.20	0.75	Ramsey and Baxter (1996)
Wolf Glade	38.765	75.099	TEM-164	Spartina	690 ± 100		892-512	-1.33	0.76	Ramsey and Baxter (1996)
Wolf Glade	38.764	75.098	TEM-163	Spartina	750 ± 70		897-555	-1.73	0.76	Ramsey and Baxter (1996)
Wolf Glade	38.768	75.106	TEM-165	Spartina	760 ± 70		900-558	-1.79	0.76	Ramsey and Baxter (1996)
Great Marsh	38.785	75.171	Beta-14684	Salt peat	930 ± 80		969-689	-1.38	0.75	Ramsey and Baxter (1996)
Wolf Glade	38.764	75.098	TEM-162	Spartina	930 ± 90		1048-680	-1.15	0.76	Ramsey and Baxter (1996)
Great Marsh	38.786	75.172	Beta-14682	Salt peat	950 ± 90		1052-690	-1.05	0.75	Ramsey and Baxter (1996)

Wolf Glade	38.761	75.096	TEM-157	Spartina	940 ± 120		1166-664	-1.55	0.76	Ramsey and Baxter (1996)
Wolf Glade	38.768	75.106	TEM-166	Spartina	980 ± 120		1170-682	-1.27	0.76	Ramsey and Baxter (1996)
Wolf Glade	38.764	75.097	TEM-161	Spartina	1100 ± 90		1260-798	-1.48	0.76	Ramsey and Baxter (1996)
Wolf Glade	38.764	75.097	TEM-160	Spartina	1150 ± 80		1262-930	-1.94	0.76	Ramsey and Baxter (1996)
Great Marsh	38.785	75.171	Beta-14685	Salt peat	1150 ± 80		1262-930	-1.29	0.75	Ramsey and Baxter (1996)
Great Marsh	38.785	75.171	Beta-14686	Salt peat	1370 ± 60		1387-1175	-1.47	0.75	Ramsey and Baxter (1996)
Great Marsh	38.785	75.171	Beta-14687	Salt peat	1650 ± 70		1712-1390	-1.75	0.75	Ramsey and Baxter (1996)
Horse Island	38.670	75.130	I-8118	Spartina	690 ± 85		772-530	-0.96	0.64	Belknap (1975)
Rehoboth Bay	38.645	75.072	R-4114	Salt peat	3780 ± 170		4786-3690	-6.40	0.66	Belknap (1975)
Rehoboth Bay	38.637	75.069	R-4113	Salt peat	3130 ± 170		3805-2871	-4.58	0.72	Belknap (1975)
Rehoboth Bay	38.645	75.072	R-4114_a	Salt peat	3520 ± 160		4241-3405	-5.78	0.71	Belknap (1975)
Rehoboth Bay	38.645	75.072	R-4114_b	Salt peat	3890 ± 170		4822-3892	-5.91	0.76	Belknap (1975)
Rehoboth Bay	38.669	75.070	R-4100_b	Salt peat	4860 ± 180		5991-5053	-9.23	0.73	Belknap (1975)
Rehoboth Bay	38.669	75.068	R-4101_c	Salt peat	6190 ± 190		7459-6639	-13.68	0.67	Belknap (1975)
Wolf Glade	38.760	75.100	I-8119	Spartina	920 ± 90		1043-677	-1.90	0.81	Belknap (1975)
Wall Island	38.802	75.204	I-4353	Salt peat	1990 ± 100		2300-1706	-3.91	0.81	Belknap (1975)
Lewes	38.778	75.174	I-4625	Salt peat	2330 ± 100		2713-2127	-5.07	0.81	Belknap (1975)
Wolf Glade	38.753	75.119	GX-16215	Sp	2945 ± 190		3578-2720	-6.38	0.58	Fletcher et al. (1993)
Wolf Glade	38.753	75.119	GX-16217	Salt peat	3130 ± 200		3829-2849	-7.01	0.58	Fletcher et al. (1993)
Wolf Glade	38.753	75.119	GX-16216	Salt peat	3195 ± 200		3890-2880	-6.68	0.58	Fletcher et al. (1993)
Wolf Glade	38.753	75.119	GX-16218	Salt peat	3465 ± 185		4283-3271	-7.31	0.58	Fletcher et al. (1993)
Wolf Glade	38.756	75.117	GX-15829	Salt peat	3630 ± 40		4082-3840	-7.68	0.59	Fletcher et al. (1993)
Wolf Glade	38.753	75.119	GX-16219	Salt peat	3620 ± 215		4522-3404	-7.38	0.58	Fletcher et al. (1993)
Wolf Glade	38.756	75.117	GX-15830	Sp	3870 ± 200		4838-3728	-8.38	0.59	Fletcher et al. (1993)
Wolf Glade	38.756	75.117	GX-15831	Salt peat	3860 ± 175		4820-3836	-8.98	0.59	Fletcher et al. (1993)
Wolf Glade	38.754	75.116	GX-15837	Jg	4210 ± 85		4961-4453	-9.08	0.59	Fletcher et al. (1993)
Wolf Glade	38.756	75.117	GX-15833	Sp/Ds	4420 ± 170		5574-4574	-9.78	0.59	Fletcher et al. (1993)
Cape Henlopen	38.783	75.078	Beta-5154	Sa	6360 ± 140		7561-6945	-16.52	0.64	Ramsey and Baxter (1996)
Cape Henlopen	38.785	75.094	R-4103	Salt peat	7050 ± 220		9144-7510	-19.46	0.77	Belknap (1975)
Rehoboth Bay	38.669	75.068	R-4101_a	Salt peat	250 ± 140		502-0	-1.00	0.72	Belknap 1975
Rehoboth Bay	38.669	75.070	R-4100_a	Salt peat	350 ± 130		630-0	-0.80	0.63	Belknap 1975
Wolf Glade	38.753	75.119	GX-16214	Salt peat	1775 ± 150	-21.1	2038-1352	-4.33	0.58	Fletcher et al. (1993)
Wolf Glade	38.754	75.120	GX-16221	Salt peat	1885 ± 170	-20.1	2302-1414	-4.05	0.58	Fletcher et al. (1993)
Wolf Glade	38.754	75.120	GX-16220	Sa	1910 ± 245	-19.7	2451-1301	-2.40	0.65	Fletcher et al. (1993)
Wolf Glade	38.754	75.116	GX-15835	Salt peat	2095 ± 205	-26.5	2699-1571	-3.98	0.58	Fletcher et al. (1993)
Wolf Glade	38.754	75.120	GX-16222	Sp	3250 ± 175	-15.7	3903-3001	-5.96	0.58	Fletcher et al. (1993)
Wolf Glade	38.755	75.116	GX-16223	Sp	3460 ± 205	-19.4	4380-3254	-4.93	0.58	Fletcher et al. (1993)
Wolf Glade	38.754	75.116	GX-15836	Salt peat	3805 ± 170	-26.7	4800-3718	-8.08	0.59	Fletcher et al. (1993)
Marine Limiting										
Rehoboth Bay	38.669	75.070	R-4100	Mercenaria	2180 ± 150		1941-1259	-6.83	0.60	Belknap (1975)
Rehoboth Bay	38.669	75.068	R-4101	Cyrtopleura/Tagelus	2630 ± 190		2660-1670	-6.86	0.60	Belknap (1975)
Offshore Rehoboth	38.663	75.058	Beta-5157	Unidentified Shells	3310 ± 90		3208-2722	-8.91	0.53	Ramsey and Baxter (1996)
Rehoboth Beach	38.756	75.082	R-4104_a	C. vir	1950 ± 200		1801-917	-7.32	0.60	Belknap (1975)
Rehoboth Beach	38.756	75.082	R-4104_d	Unidentified Shells	3010 ± 180		3042-2108	-8.43	0.80	Belknap (1975)
Terrestrial Limiting										
Offshore Rehoboth	38.663	75.050	BETA-5158	Wood	6220 ± 90		7407-6885	-10.86	0.51	Ramsey and Baxter (1996)
Lewes	38.789	75.159	I-5206	Undiff peat	330 ± 90		532-0	-0.18	0.59	Belknap (1975)
Lewes	38.781	75.174	I-4799	Undiff peat	2580 ± 95		2849-2363	-4.08	0.59	Belknap 1975
Wolf Glade	38.754	75.116	GX-15838	Sc/Sr	4350 ± 85	-26.8	5289-4665	-7.98	0.54	Fletcher et al 1993
Wolf Glade	38.755	75.116	GX-16224	Undiff peat	4745 ± 245	-26.6	5995-4833	-8.88	0.54	Fletcher et al 1993
Inner Chesapeake										
Index Points										
Blackwater	38.400	76.100	QC-861	Salt peat	2485 ± 125		2846-2208	-3.64	0.34	Cinquemani et al 1982
Blackwater	38.400	76.100	QC-862	Salt peat	2650 ± 180		3240-2334	-4.12	0.33	Cinquemani et al 1982
Blackwater	38.400	76.100	QC-860	Salt peat	2835 ± 140		3357-2730	-3.34	0.34	Cinquemani et al 1982
Blackwater	38.400	76.100	QC-863	Salt peat	3745 ± 120		4436-3729	-5.57	0.35	Cinquemani et al 1982
Radcliffe Creek	39.000	76.100	QC-859	Salt peat	1230 ± 155		1411-795	-1.92	0.33	Cinquemani et al 1982
Radcliffe Creek	39.000	76.100	QC-857	Salt peat	3365 ± 145		4059-3265	-5.17	0.35	Cinquemani et al 1982
Radcliffe Creek	39.000	76.100	QC-856	Salt peat	4505 ± 115		5465-4855	-10.87	0.36	Cinquemani et al 1982
Marine Limiting										
Patuxtent River	38.331	76.378	OS-18535	Shell	580 ± 35	-1.37	296-111	-10.27	0.67	Colman et al. (2002)
Patuxtent River	38.331	76.378	OS-18661	Shell	905 ± 60	-1.18	627-429	-10.40	0.67	Colman et al. (2002)
Patuxtent River	38.331	76.378	OS-20057	Shell	860 ± 40	-0.41	543-418	-11.02	0.67	Colman et al. (2002)
Patuxtent River	38.331	76.378	OS-18534	Shell	1210 ± 45	-7.57	871-665	-11.32	0.67	Colman et al. (2002)
Patuxtent River	38.331	76.378	OS-18413	Shell	780 ± 40	-5.35	491-315	-9.77	0.67	Colman et al. (2002)
Patuxtent River	38.331	76.378	OS-18411	Shell	750 ± 45	-1.25	476-295	-10.06	0.67	Colman et al. (2002)
Patuxtent River	38.331	76.378	OS-18410	Shell	675 ± 45	-0.91	436-246	-10.34	0.67	Colman et al. (2002)
Town Point	38.544	76.427	OS-15674	Shell	1010 ± 85	-0.14	725-471	-25.63	0.67	Colman et al. (2002)
Town Point	38.544	76.427	OS-15676	Shell	605 ± 40	-0.59	355-119	-25.73	0.67	Colman et al. (2002)
Town Point	38.544	76.427	OS-15675	Forams	1220 ± 80	-2.14	921-638	-26.33	0.67	Colman et al. (2002)
Town Point	38.544	76.427	OS-15684	Forams	1310 ± 80	-2.1	1014-682	-26.83	0.67	Colman et al. (2002)
Town Point	38.544	76.427	OS-15683	Forams	1200 ± 75	-2.08	905-633	-26.95	0.67	Colman et al. (2002)
Town Point	38.544	76.427	OS-15677	Forams	1190 ± 70	-2.04	894-633	-27.23	0.67	Colman et al. (2002)
Town Point	38.544	76.427	OS-19508	Forams E.e.	1050 ± 180		957-299	-27.23	0.67	Colman et al. (2002)
Town Point	38.544	76.427	OS-17874	Forams E.s.	1320 ± 195	-2.54	1251-541	-27.23	0.67	Colman et al. (2002)
Town Point	38.544	76.427	OS-15682	Shell	2100 ± 80	-0.24	1875-1492	-27.83	0.67	Colman et al. (2002)
Town Point	38.544	76.427	OS-17881	Forams E.e	2090 ± 30	-2.18	1771-1562	-28.03	0.67	Colman et al. (2002)
Town Point	38.544	76.427	OS-17884	Forams E.s.	2090 ± 55	-2.3	1809-1529	-28.03	0.67	Colman et al. (2002)
Town Point	38.544	76.427	OS-15686	Forams	1290 ± 75	-2.07	973-674	-28.13	0.67	Colman et al. (2002)
Town Point	38.544	76.427	OS-15687	Shell	1850 ± 80	0.32	1580-1251	-28.13	0.67	Colman et al. (2002)
Town Point	38.544	76.427	OS-15685	Forams	2090 ± 70	-1.39	1847-1506	-28.33	0.67	Colman et al. (2002)
Town Point	38.544	76.427	OS-15690	Forams	2570 ± 70	-0.97	2418-2049	-28.45	0.67	Colman et al. (2002)
Town Point	38.544	76.427	OS-15678	Gastropod	1130 ± 80	-0.07	857-542	-29.03	0.67	Colman et al. (2002)
Town Point	38.544	76.427	CAMS-43708	Shell	640 ± 50		413-143	-26.15	0.67	Colman et al. (2002)
Town Point	38.544	76.427	CAMS-43709	Shell	1160 ± 40		788-638	-27.54	0.67	Colman et al. (2002)
Town Point	38.544	76.427	CAMS-43710	Shell	1980 ± 50		1677-1403	-28.62	0.67	Colman et al. (2002)
Town Point	38.538	76.430	OS-18409	Shell	625 ± 35	-0.72	366-142	-23.11	0.67	Colman et al. (2002)
Town Point	38.538	76.430	OS-18532	Shell	535 ± 35	-1.04	266-0	-23.88	0.67	Colman et al. (2002)
Town Point	38.538	76.430	OS-18660	Shell	815 ± 45	-0.4	516-332	-24.20	0.67	Colman et al. (2002)
Town Point	38.538	76.430	OS-18533	Shell	3030 ± 35	0.13	2886-2723	-26.14	0.67	Colman et al. (2002)
Town Point	38.538	76.430	OS-21266	Forams	3090 ± 90	-0.81	3125-2703	-26.83	0.67	Colman et al. (2002)
Town Point	38.538	76.430	OS-18662	Shell	3360 ± 100	-0.73	3446-2937	-26.88	0.67	Colman et al. (2002)

Mayo	38.878	76.446	OS-18412	Shell	1400 ± 40	-2.68	1052-854	-9.32	0.66	Colman et al. 2002
Mayo	38.878	76.446	OS-18900	Shell	1260 ± 30	-3.36	893-723	-9.28	0.66	Colman et al. 2002
Mayo	38.878	76.446	OS-18528	Shell	1520 ± 40	-2.97	1174-958	-9.52	0.66	Colman et al. 2002
Mayo	38.878	76.446	OS-18524	Shell	1750 ± 35	-5.32	1375-1234	-10.18	0.66	Colman et al. 2002
Mayo	38.878	76.446	OS-18523	Shell	1880 ± 35	-2.43	1517-1332	-10.54	0.66	Colman et al. 2002
Mayo	38.878	76.446	OS-18902	Shell	1970 ± 30	-2.01	1615-1412	-10.94	0.66	Colman et al. 2002
Mayo	38.878	76.446	OS-18527	Shell	2050 ± 45	-1.79	1748-1505	-11.25	0.66	Colman et al. 2002
Mayo	38.878	76.446	OS-18901	Shell	2030 ± 35	-2.05	1696-1506	-11.33	0.66	Colman et al. 2002
Mayo	38.878	76.446	OS-18529	Shell	2230 ± 50	-2.29	1957-1700	-11.70	0.66	Colman et al. 2002
Mayo	38.878	76.446	OS-18526	Shell	2290 ± 35	-2.4	1996-1805	-11.92	0.66	Colman et al. 2002
Mayo	38.878	76.441	OS-21262	Shell	2780 ± 75	-3.14	2701-2332	-12.47	0.66	Colman et al. 2002
Mayo	38.878	76.441	OS-20056	Shell	3760 ± 55	-1.63	3849-3547	-13.90	0.66	Colman et al. 2002
Mayo	38.879	76.440	OS-20052	Shell	4410 ± 45	-1.3	4769-4422	-14.40	0.77	Colman et al. 2002
Mayo	38.879	76.440	OS-20054	Shell	5240 ± 55	-2.02	5719-5471	-14.75	0.77	Colman et al. 2002
Mayo	38.879	76.440	OS-20053	Oyster	5340 ± 40	-2.75	5832-5598	-14.75	0.77	Colman et al. 2002
Mayo	38.879	76.440	OS-20055	Oyster	6060 ± 55	-3.52	6628-6348	-15.33	0.77	Colman et al. 2002
Mayo	38.879	76.440	OS-21270	Shell	6850 ± 110	-4.26	7557-7160	-16.01	0.77	Colman et al. 2002
Mayo	38.879	76.440	OS-25830	Oyster	7180 ± 40	-4.66	7735-7564	-16.26	0.77	Colman et al. 2002
Mayo	38.887	76.392	OS-19213	Shell	320 ± 60	-0.65	121-0	-28.06	0.66	Colman et al. 2002
Mayo	38.887	76.392	OS-19212	Shell	325 ± 60	-0.04	124-0	-28.56	0.66	Colman et al. 2002
Mayo	38.887	76.392	OS-19216	Shell	325 ± 30	-0.4	52-0	-29.17	0.66	Colman et al. 2002
Mayo	38.887	76.392	OS-19940	Shell	555 ± 35	-0.6	278-0	-29.88	0.66	Colman et al. 2002
Mayo	38.887	76.392	OS-19215	Shell	725 ± 55	-0.87	471-273	-30.54	0.66	Colman et al. 2002
Mayo	38.887	76.392	OS-19214	Shell	1150 ± 85	-1.03	883-555	-31.71	0.66	Colman et al. 2002
Mayo	38.887	76.392	OS-21226	Shell	610 ± 30	-0.87	311-139	-30.10	0.66	Colman et al. 2002
Mayo	38.887	76.392	OS-21381	Shell	745 ± 35	-0.57	464-299	-30.83	0.66	Colman et al. 2002
Mayo	38.887	76.392	OS-21382	Shell	1150 ± 40	-0.68	780-634	-31.69	0.66	Colman et al. 2002
Mayo	38.887	76.392	OS-21227	Shell	1240 ± 30	-1.29	880-701	-31.99	0.66	Colman et al. 2002
Mayo	38.887	76.392	OS-21383	Shell	1600 ± 35	-0.9	1251-1064	-32.87	0.66	Colman et al. 2002
Mayo	38.887	76.392	OS-21384	Shell	2050 ± 40	-1.73	1728-1512	-33.79	0.66	Colman et al. 2002
Mayo	38.887	76.392	OS-21228	Shell	2210 ± 35	-0.77	1901-1704	-34.47	0.66	Colman et al. 2002
Mayo	38.887	76.392	OS-21229	Shell	2500 ± 35	-0.74	2290-2058	-34.94	0.66	Colman et al. 2002
Mayo	38.887	76.392	OS-21385	Shell	4230 ± 40	-0.18	4440-4185	-35.34	0.66	Colman et al. 2002
Mayo	38.887	76.392	OS-21230	Shell	5530 ± 40	-0.7	6020-5781	-36.18	0.66	Colman et al. 2002
Mayo	38.887	76.392	OS-21231	Shell	5690 ± 40	-0.14	6208-5976	-37.45	0.67	Colman et al. 2002
Mayo	38.887	76.392	OS-21232	Shell	5960 ± 40	-0.08	6463-6280	-38.74	0.67	Colman et al. 2002
Mayo	38.887	76.392	OS-21233	Shell	5980 ± 40	0.02	6485-6290	-39.14	0.67	Colman et al. 2002
Mayo	38.887	76.392	OS-21488	Shell	6250 ± 35	-0.74	6801-6603	-41.54	0.67	Colman et al. 2002
Mayo	38.887	76.392	OS-21386	Shell	6290 ± 35	-3.73	6850-6649	-43.21	0.68	Colman et al. 2002
Mayo	38.887	76.392	OS-21489	Shell	8670 ± 45	-3.53	9457-9229	-44.10	0.68	Colman et al. 2002
Mayo	38.887	76.392	OS-21387	Oyster	6660 ± 45	-1.04	7298-7072	-44.10	0.68	Colman et al. 2002
Mayo	38.887	76.392	OS-21388	Shell	7050 ± 40	-1.49	7611-7448	-44.21	0.68	Colman et al. 2002
Mayo	38.887	76.392	OS-21389	Shell	7100 ± 45	-1.5	7663-7486	-44.36	0.68	Colman et al. 2002
Potomac River	38.028	76.220	CAMS-39237	Shell	540 ± 50	0.1	276-0	-23.38	0.70	Colman et al. 2002
Potomac River	38.028	76.220	CAMS-43711	Shell	990 ± 40		643-512	-24.20	0.68	Colman et al. 2002
Potomac River	38.028	76.220	CAMS-39238	Gastropod	1240 ± 50	0.1	896-681	-26.06	0.68	Colman et al. 2002
Potomac River	38.028	76.220	OS-15679	Shell	540 ± 30	0.01	266-0	-22.76	0.68	Colman et al. 2002
Potomac River	38.028	76.220	OS-15680	Shell	885 ± 35	-0.29	555-440	-23.56	0.68	Colman et al. 2002
Potomac River	38.028	76.220	OS-15681	Shell	1150 ± 25	0.01	753-648	-24.06	0.68	Colman et al. 2002
Potomac River	38.028	76.220	OS-17242	Forams	1230 ± 30	-1.72	870-690	-24.24	0.68	Colman et al. 2002
Potomac River	38.028	76.220	OS-15689	Shell	1530 ± 70	0.1	1236-933	-24.92	0.68	Colman et al. 2002
Potomac River	38.028	76.220	OS-17508	Forams	2450 ± 256	-2.41	2723-1515	-25.26	0.68	Colman et al. 2002
Potomac River	38.028	76.220	OS-17241	Forams	2400 ± 85	-1.94	2280-1846	-25.87	0.68	Colman et al. 2002
Potomac River	38.031	76.215	OS-21487	Shell	855 ± 25	-0.42	522-439	-24.16	0.68	Colman et al. 2002
Potomac River	38.031	76.215	OS-21670	Shell	4100 ± 45	0.11	4296-3984	-25.83	0.68	Colman et al. 2002
Potomac River	38.031	76.215	OS-21671	Shell	4470 ± 45	-0.13	4798-4521	-27.69	0.68	Colman et al. 2002
Potomac River	38.031	76.215	OS-25826	Shell	4590 ± 55	0.14	4952-4627	-28.83	0.68	Colman et al. 2002
Potomac River	38.031	76.215	OS-21664	Shell	6130 ± 55	0.2	6698-6420	-29.72	0.68	Colman et al. 2002
Potomac River	38.031	76.215	OS-21665	Shell	6430 ± 65	0.18	7113-6746	-30.29	0.68	Colman et al. 2002
Potomac River	38.031	76.215	OS-25827	Shell	6540 ± 45	0.7	7171-6924	-30.96	0.68	Colman et al. 2002
Potomac River	38.031	76.215	OS-21666	Shell	9150 ± 65	-8.09	10144-9697	-30.96	0.68	Colman et al. 2002
Potomac River	38.031	76.215	OS-25828	Shell	8150 ± 55	-1.94	8853-8474	-31.55	0.68	Colman et al. 2002
Potomac River	38.031	76.215	OS-21667	Shell	7080 ± 60	0.37	7666-7446	-31.88	0.68	Colman et al. 2002
Potomac River	38.031	76.215	OS-25829	Shell	8930 ± 65	-7.27	9802-9460	-33.49	0.69	Colman et al. 2002
Potomac River	38.031	76.215	OS-21668	Shell	9400 ± 100	-9.66	10504-9963	-33.57	0.69	Colman et al. 2002
Potomac River	38.053	76.221	OS-21669	Shell	9350 ± 70	-7.57	10393-9958	-22.72	0.68	Colman et al. 2002
Potomac River	38.053	76.221	OS-21486	Shell	9670 ± 50	-10.62	10631-10414	-23.29	0.68	Colman et al. 2002
Eastern Shore										
Index Points										
Oyster	37.287	75.917		Salt peat	1461 ± 31		1398-1303	-1.35	0.26	Engelhart et al. (2009)
Magothy Bay	37.145	75.946		Seed in salt peat	2213 ± 18	-27.8	2316-2152	-2.69	0.26	Engelhart et al. (2009)
Magothy Bay	37.145	75.946		Salt peat	1598 ± 14	-21.1	1532-1416	-2.15	0.26	Engelhart et al. (2009)
Boxtree Farm	37.396	75.867		Salt peat	1537 ± 23	-22.6	1518-1366	-1.62	0.26	Engelhart et al. (2009)
Metompkin Island	37.750	75.560	B-1952	Juncus peat	4620 ± 80		5582-5048	-7.02	0.47	Finkelstein and Ferland (1987)
Assawoman Island	37.810	75.520	B-2662	Juncus peat	3580 ± 60		4078-3700	-5.83	0.47	Finkelstein and Ferland (1987)
Custis Neck	37.622	75.678	GrN-16341	HM peat	4470 ± 50		5303-4891	-8.46	0.47	van de Plassche (1990)
Custis Neck	37.622	75.678	GrN-16340	HM peat	4445 ± 40		5286-4878	-8.42	0.47	van de Plassche (1990)
Custis Neck	37.622	75.678	GrN-16339	HM peat	4430 ± 40		5279-4871	-8.00	0.47	van de Plassche (1990)
Metompkin Island	37.750	75.560	W-4788	Juncus peat	2200 ± 80		2347-2003	-2.87	0.47	Finkelstein and Ferland (1987)
Assawoman Island	37.810	75.520	B-2659	Sa	650 ± 60		683-539	-1.11	0.44	Finkelstein and Ferland (1987)
Assawoman Island	37.810	75.520	B-2660	Sa	700 ± 60		732-552	-0.80	0.44	Finkelstein and Ferland (1987)
Metomkin Island	37.750	75.560	B-2663	Sa	1180 ± 60		1261-967	-1.25	0.44	Finkelstein and Ferland (1987)
Metomkin Island	37.750	75.560	B-1951	Sa	1660 ± 70		1719-1393	-1.88	0.44	Finkelstein and Ferland (1987)
Magothy Bay	37.150	75.900	B-1948	Sp	1430 ± 80		1520-1182	-1.03	0.44	Finkelstein and Ferland (1987)
Marine Limiting										
Parramore Island	37.580	75.650	W-4792	C. vir	600 ± 60		397-0	-2.57	0.44	Finkelstein and Ferland (1987)
Parramore Island	37.580	75.650	B-1955	C. vir	1380 ± 90		1130-727	-1.66	0.44	Finkelstein and Ferland (1987)
Parramore Island	37.580	75.650	W-4787	C. vir	2900 ± 110		2888-2342	-5.16	0.44	Finkelstein and Ferland (1987)
Hog Island	37.430	75.760	B-2664	C. vir	450 ± 50		226-0	-1.30	0.44	Finkelstein and Ferland (1987)
Hog Island	37.430	75.760	B-2665	C. vir	890 ± 50		607-430	-1.40	0.44	Finkelstein and Ferland (1987)
Cobb Island	37.350	75.810	B-1957	C. vir	890 ± 60		624-413	-1.99	0.44	Finkelstein and Ferland (1987)
Cobb Island	37.350	75.810	B-1958	C. vir	610 ± 70		419-0	-1.54	0.44	Finkelstein and Ferland (1987)
Terrestrial Limiting										

Wachapreague	37.580	75.650	ML-191	Undiff peat	2550 ± 70		2767-2365	-1.92	0.53	Newman and Rusnak (1965)
Wachapreague	37.580	75.650	ML-192	Undiff peat	5120 ± 145		6260-5592	-5.17	0.53	Newman and Rusnak (1965)
Wachapreague	37.580	75.650	ML-193	Undiff peat	3160 ± 195		3835-2871	-3.73	0.54	Newman and Rusnak (1965)
Wachapreague	37.580	75.650	ML-193	Undiff peat	3390 ± 75		3834-3464	-3.73	0.54	Newman and Rusnak (1965)
Wachapreague	37.580	75.650	ML-194	Undiff peat	4350 ± 75		5284-4728	-6.26	0.53	Newman and Rusnak (1965)
Magothy Bay	37.150	75.900	B-1950	Wood	1740 ± 100		1873-1415	0.10	0.10	Finkelstein and Ferland (1987)
Northern North Carolina										
Index Points										
Frisco	35.260	75.520	OS-39722	Salt peat	205 ± 40		310-0	-0.71	0.70	Horton et al. (2009)
Hatteras Island	35.230	75.680	Beta-187692	Salt peat	250 ± 40	-26.3	436-0	-0.86	0.54	Horton et al. (2009)
Hatteras Island	35.520	75.480	OS-54058	Salt peat	265 ± 35	-22.49	456-0	-0.54	0.20	Horton et al. (2009)
Northern Outer Banks	35.970	75.660	Beta-187694	Salt peat	1580 ± 40	-23	1548-1382	-1.78	0.20	Horton et al. (2009)
Pamlico Sound	35.220	75.660	Beta-187689	Salt peat	500 ± 40	-26.6	630-496	-0.66	0.54	Horton et al. (2009)
Sand Point	35.880	75.680	OS-43066	Salt peat	185 ± 30	-24.28	300-0	-0.56	0.20	Kemp (unpublished)
Sand Point	35.880	75.680	OS-43067	Salt peat	900 ± 50	-27.27	927-727	-1.14	0.20	Kemp (unpublished)
Sand Point	35.880	75.680	OS-43068	Salt peat	1520 ± 40	-25.55	1521-1333	-1.84	0.54	Kemp (unpublished)
Sand Point	35.880	75.680	OS-43069	Salt peat	1920 ± 45	-21.98	1986-1734	-2.28	0.20	Kemp (unpublished)
Sand Point	35.880	75.680	OS-43070	Salt peat	2090 ± 35	-22.92	2151-1951	-2.38	0.20	Kemp (unpublished)
Sand Point	35.880	75.680	OS-43071	Salt peat	2420 ± 35	-26.52	2599-2349	-2.70	0.20	Kemp (unpublished)
Sand Point	35.880	75.680	OS-43266	Salt peat	2470 ± 45	-25.47	2715-2363	-3.00	0.20	Kemp (unpublished)
Sand Point	35.880	75.680	OS-58902	Salt peat	315 ± 25	-27.33	461-305	-0.69	0.20	Kemp (unpublished)
Sand Point	35.880	75.680	OS-58897	Salt peat	535 ± 30	-26.67	632-512	-0.81	0.20	Kemp (unpublished)
Sand Point	35.880	75.680	OS-58901	Salt peat	910 ± 30	-27	917-743	-1.26	0.20	Kemp (unpublished)
Sand Point	35.880	75.680	OS-58896	Salt peat	1000 ± 25	-14.08	964-800	-1.40	0.20	Kemp (unpublished)
Sand Point	35.880	75.680	OS-58713	Salt peat	1080 ± 30	-13.26	1057-933	-1.50	0.20	Kemp (unpublished)
Sand Point	35.880	75.680	OS-58712	Salt peat	1190 ± 30	-13.4	1230-1006	-1.71	0.20	Kemp (unpublished)
Sand Point	35.880	75.680	OS-58711	Salt peat	1600 ± 25	-13.28	1539-1413	-1.99	0.20	Kemp (unpublished)
Sand Point	35.880	75.680	OS-58710	Salt peat	2120 ± 25	-13.78	2287-2003	-2.50	0.20	Kemp (unpublished)
Sand Point	35.880	75.680	OS-62716	Salt peat	2620 ± 45	-20.65	2849-2543	-2.67	0.20	Kemp (unpublished)
Kitty Hawk	36.050	75.700	Beta-168063	Salt peat	9720 ± 40	-24.6	11231-10889	-30.37	1.10	Mallinson et al. (2005)
Kitty Hawk	36.050	75.700	OS-36176	Salt peat	9930 ± 45	-25.48	11603-11235	-30.37	1.10	Mallinson et al. (2005)
Kitty Hawk	36.050	75.710	OS-36174	Salt peat	9460 ± 40	-14.64	11062-10576	-35.76	1.10	Mallinson et al. (2005)
Buxton	35.260	75.520	BETA-183551	Salt peat	160 ± 30	-25.1	286-0	-0.42	0.20	Horton et al. (2009)
Salvo	35.650	75.460	OS-39790	Salt peat	200 ± 35	-27.43	306-0	-0.43	0.20	Horton et al. (2009)
Sand Point	35.880	75.680	OS-63287	Salt peat	2550 ± 70	-26.26	2770-2360	-3.11	0.20	Kemp (unpublished)
Sand Point	35.880	75.680	OS-64687	Salt peat	615 ± 35	-26.65	658-546	-0.77	0.20	Kemp (unpublished)
Sand Point	35.880	75.680	OS-64688	Salt peat	2410 ± 35	-27.45	2698-2346	-2.49	0.20	Kemp (unpublished)
Sand Point	35.880	75.680	OS-64813	Salt peat	1390 ± 110	-27.97	1523-1067	-1.42	0.20	Kemp (unpublished)
Sand Point	35.880	75.680	OS-64689	Salt peat	2410 ± 40	-28.58	2699-2345	-2.68	0.20	Kemp (unpublished)
Kitty Hawk	36.020	75.720	Beta-168060	Plant frags	7830 ± 50	-28	8853-8455	-15.37	1.10	Mallinson et al. (2005)
Marine Limiting										
Albemarle Sound	36.110	76.070	Beta-90661	Crassostrea shell	6140 ± 80		6612-6204	-15.06	0.51	Horton et al. (2009)
Albemarle Sound	36.110	76.070	Beta-90671	Crassostrea shell	2880 ± 60		2689-2245	-6.68	0.51	Horton et al. (2009)
Albemarle Sound	36.110	76.070	Beta-90672	Cyrtopleura/Tegalus shell	4200 ± 100		4383-3759	-9.11	0.51	Horton et al. (2009)
Albemarle Sound	36.110	76.070	Beta-90674	Cyrtopleura shell	4810 ± 40		5049-4679	-8.99	0.11	Horton et al. (2009)
Albemarle Sound	36.050	75.690		Mactra/Mercenaria shell	5225 ± 105		5642-5066	-11.88	0.11	Horton et al. (2009)
Albemarle Sound	36.050	75.690		Ensis shell	5600 ± 110		6104-5566	-13.37	0.11	Horton et al. (2009)
Croatan Sound	35.890	75.720	Beta-115591	Crassostrea shell	4480 ± 80		4767-4155	-7.91	0.11	Horton et al. (2009)
Croatan Sound	35.880	75.710	Beta-115593	Macoma shell	3610 ± 50	-5.3	3486-3120	-6.01	0.51	Horton et al. (2009)
Croatan Sound	35.920	75.750	Beta-115595	Cyrtopleura shell	4010 ± 150		4225-3403	-6.46	0.51	Horton et al. (2009)
Croatan Sound	35.920	75.750	Beta-115596	Crassostrea shell	4540 ± 80		4799-4275	-7.95	0.11	Horton et al. (2009)
Croatan Sound	35.920	75.740	Beta-115597	Cyrtopleura shell	3670 ± 50	-0.6	3559-3211	-7.13	0.51	Horton et al. (2009)
Croatan Sound	35.920	75.740	Beta-115598	Nassarius shell	3810 ± 50		3722-3364	-7.68	0.51	Horton et al. (2009)
Croatan Sound	35.900	75.730	Beta-119895	Mya shell	4130 ± 60		4173-3721	-7.66	0.51	Horton et al. (2009)
Nags Head	36.150	75.330	W-1402	C. virginica dredge	8130 ± 400	0	9419-7657	-34.00	0.51	Emery et al. (1967)
Pea Island	35.750	75.320		Donax shells	5618 ± 100	0	6090-5584	-24.00	0.51	Sears (1973)
Pamlico Sound	35.450	75.490	Beta-201772	Chione cancellata shell	1760 ± 40	0.1	1282-990	-3.70	0.11	Horton et al. (2009)
Pamlico Sound	35.470	75.530	Beta-205450	Chione cancellata shell	2070 ± 40	-0.1	1595-1301	-4.94	0.51	Horton et al. (2009)
Roanoke Sound	35.950	75.650	Beta-95296	Articulated Crassostrea	1900 ± 60		1468-1116	-4.16	0.11	Horton et al. (2009)
Salvo	35.520	75.480	OS-53608	Chione cancellate	1900 ± 30	1.62	1399-1161	-2.91	0.51	Horton et al. (2009)
SNL-113A-63	35.460	75.570	OS-39293	Petricola sp.	7780 ± 45	-2.4	8217-7927	-18.38	0.51	Stanton (2008)
SNL-161C-90	35.460	75.570	OS-39198	C. virginica	6580 ± 40	-2.34	7084-6721	-13.38	0.51	Stanton (2008)
SNL-163B-28	35.460	75.570	OS-39195	C. virginica	8210 ± 40	-2.7	8650-8360	-18.48	0.51	Stanton (2008)
SNL-164D-93	35.460	75.570	OS-39196	C. virginica	8980 ± 35	-1.41	9605-9340	-24.98	0.51	Stanton (2008)
Terrestrial Limiting										
Albemarle Sound	36.110	76.070	Beta-90666	Wood	6060 ± 60	-30.7	7157-6749	-8.71	0.51	Horton et al. (2009)
Buxton	35.160	75.310	OS-39792	Undiff peat	315 ± 35	-27.77	472-302	0.53	0.51	Horton et al. (2009)
Broad Creek	35.850	75.620	I-8988	Paleosol	2505 ± 90		2750-2356	-1.78	0.51	Horton et al. (2009)
Broad Creek	35.860	75.630	I-9208	Paleosol	3545 ± 100		4141-3577	-1.78	0.51	Horton et al. (2009)
Broad Creek	35.870	75.640	I-8990	Paleosol	5315 ± 110		6312-5770	-1.93	0.51	Horton et al. (2009)
Broad Creek	35.870	75.640	I-9253	Fresh peat	2290 ± 110		2703-2009	-1.79	0.51	Horton et al. (2009)
Southern North Carolina										
Index Points										
Tump Point	34.970	76.380	OS-59677	Salt peat	350 ± 30	-14.35	493-315	-0.36	0.20	Kemp (unpublished)
Tump Point	34.970	76.380	OS-59728	Salt peat	385 ± 35	-26.16	509-317	-0.47	0.20	Kemp (unpublished)
Tump Point	34.970	76.380	OS-59676	Salt peat	915 ± 35	-25.6	921-743	-0.67	0.20	Kemp (unpublished)
Tump Point	34.970	76.380	OS-59675	Salt peat	1350 ± 30	-26.8	1313-1183	-0.97	0.20	Kemp (unpublished)
Wilmington	34.100	78.000	QC793A	Salt peat	3390 ± 110	0	3901-3387	-3.03	0.59	Cinquemani et al. (1982)
Jarrett Bay	34.800	76.490		Salt peat	701 ± 230	-25	1170-0	-0.73	0.25	Spaur and Snyder (1999)
Jarrett Bay	34.800	76.490		Salt peat	2130 ± 161	-23	2682-1712	-1.91	0.25	Spaur and Snyder (1999)
Tump Point	34.970	76.380	OS-59697	Salt peat	1650 ± 35	-14.15	1689-1417	-1.19	0.20	Kemp (unpublished)
Croatan National Forest	34.700	77.100	QC-801	Salt peat	1180 ± 190		1414-698	-0.77	0.58	Cinquemani et al. (1982)
Croatan National Forest	34.700	77.100	QC-802	Salt peat	1735 ± 110		1890-1402	-1.27	0.58	Cinquemani et al. (1982)
Wilmington	34.100	78.000	QC-799	Salt peat	1385 ± 130		1546-988	-0.93	0.59	Cinquemani et al. (1982)
Wilmington	34.100	78.000	QC-793B	Salt peat	3395 ± 110		3905-3389	-3.43	0.60	Cinquemani et al. (1982)
Wilmington	34.100	78.000	QC-794	Salt peat	3600 ± 115		4240-3592	-4.23	0.60	Cinquemani et al. (1982)
Wilmington	34.100	78.000	QC-796	Salt peat	3870 ± 175		4821-3845	-5.53	0.63	Cinquemani et al. (1982)
Wilmington	34.100	78.000	QC-797	Salt peat	5675 ± 250		7156-5922	-8.03	0.60	Cinquemani et al. (1982)
Marine Limiting										
Pamlico Sound	34.980	76.200	OS-54866	Argopecten	835 ± 30	0.16	450-146	-2.25	0.11	Horton et al. (2009)
Pamlico Sound	34.900	76.260	OS-53604	Elphidium	1670 ± 30	-1.57	1187-919	-2.91	0.51	Culver et al. (2007)

Terrestrial Limiting										
Cape Fear Arch	33.590	77.880	GX-2965	Undiff peat	10000 ± 300		12637-10701	-24.64	0.51	Field et al. (1979)
Jarrett Bay	34.800	76.490		Fresh peat	3330 ± 263	-27	4282-2880	-2.01	0.19	Spaur and Snyder (1999)
Jarrett Bay	34.800	76.490		Fresh peat	5710 ± 142	-28	6856-6214	-2.43	0.19	Spaur and Snyder (1999)
Northern South Carolina										
Index Points										
Murrells Inlet	33.580	79.000	GX-16569	Salt peat	4090 ± 235	-24.4	5291-3975	-3.02	0.93	Gayes et al. (1992)
Pee Dee River	33.400	79.200	QC-602	Salt peat	3690 ± 150		4434-3638	-3.41	0.95	Cinquemani et al. (1982)
Pee Dee River	33.400	79.200	QC-603	Salt peat	2630 ± 110		2957-2363	-2.61	0.95	Cinquemani et al. (1982)
Pee Dee River	33.400	79.200	QC-813	Salt peat	5625 ± 130		6737-6129	-6.60	0.95	Cinquemani et al. (1982)
Pee Dee River	33.400	79.200	QC-814	Salt peat	6140 ± 200		7429-6555	-6.59	0.97	Cinquemani et al. (1982)
Santee River	33.200	79.400	QC-595	Salt peat	4420 ± 405		5986-3924	-4.11	0.96	Cinquemani et al. (1982)
Santee River	33.200	79.400	QC-596(1)	Salt peat	3105 ± 85		3554-3068	-3.01	0.95	Cinquemani et al. (1982)
Santee River	33.200	79.400	QC-596(2)	Salt peat	3135 ± 140		3687-2959	-3.01	0.95	Cinquemani et al. (1982)
Murrells Inlet	33.580	79.000	GX-15987	Salt peat	3340 ± 240	-22.6	4235-2961	-3.05	0.93	Gayes et al. (1992)
Pee Dee River	33.400	79.200	QC-604	Salt peat	4680 ± 115		5644-5042	-4.81	0.95	Cinquemani et al. (1982)
Terrestrial Limiting										
Santee River	33.200	79.400	QC-597	Paleosol	4550 ± 150		5583-4857	-3.22	0.65	Cinquemani et al. (1982)
Murrells Inlet	33.580	79.000	GX-16476	Peat	4550 ± 150	-28.4	2732-1616	-0.11	0.63	Gayes et al. (1992)
Murrells Inlet	33.580	79.000	GX-16477	Wood	2510 ± 140	-28.2	2919-2181	-0.21	0.63	Gayes et al. (1992)
Murrells Inlet	33.580	79.000	GX-16568	Peat	3460 ± 155	-27.5	4148-3378	-2.13	0.63	Gayes et al. (1992)
Murrells Inlet	33.580	79.000	GX-16571	Peat	2355 ± 140	-27.8	2748-2060	-0.12	0.63	Gayes et al. (1992)
Murrells Inlet	33.580	79.000	GX-16572	Peat	8575 ± 270	-27.3	10272-8790	-1.43	0.63	Gayes et al. (1992)
Murrells Inlet	33.580	79.000	GX-15988	Peat	9035 ± 245	-27.8	11059-9527	-2.51	0.63	Gayes et al. (1992)
Murrells Inlet	33.580	79.000	GX-16480	Peat	9510 ± 285	-29	11762-9944	-2.57	0.63	Gayes et al. (1992)
Southern South Carolina										
Index Points										
Combahee River	32.700	80.700	QC-589	Salt peat	5400 ± 115		6401-5933	-4.10	1.02	Cinquemani et al. (1982)
Combahee River	32.700	80.700	QC-593	Salt peat	5280 ± 115		6297-5753	-3.95	1.02	Cinquemani et al. (1982)
Combahee River	32.700	80.700	QC-594	Salt peat	5620 ± 140		6743-6025	-3.58	1.02	Cinquemani et al. (1982)
Combahee River	32.700	80.700	QC-609	Salt peat	2880 ± 105		3323-2781	-2.20	1.02	Cinquemani et al. (1982)
Combahee River	32.700	80.700	QC-610_a	Salt peat	3325 ± 130		3895-3265	-2.68	1.02	Cinquemani et al. (1982)
Combahee River	32.700	80.700	QC-828	Salt peat	4425 ± 170		5577-4577	-3.29	1.04	Cinquemani et al. (1982)
Coosawatchie River	32.600	80.900	QC-826	Salt peat	2125 ± 100		2337-1897	-1.28	1.03	Cinquemani et al. (1982)
Coosawatchie River	32.600	80.900	QC-827	Salt peat	730 ± 105		907-533	-0.72	1.03	Cinquemani et al. (1982)
Savannah River	32.100	81.000	QC-599	Salt peat	3095 ± 95		3553-3003	-2.61	1.11	Cinquemani et al. (1982)
Savannah River	32.100	81.000	QC-600	Salt peat	2320 ± 110		2718-2066	-2.41	1.11	Cinquemani et al. (1982)
Savannah River	32.100	81.000	QC-821	Salt peat	2440 ± 130		2776-2156	-3.26	1.11	Cinquemani et al. (1982)
Savannah River	32.100	81.000	QC-825	Salt peat	3130 ± 125		3637-2995	-1.96	1.11	Cinquemani et al. (1982)
Cooper-Wando River	32.900	79.900	QC-584	Salt peat	3100 ± 100		3556-3004	-2.50	0.94	Cinquemani et al. (1982)
Cooper-Wando River	32.900	79.900	QC-586	Salt peat	5005 ± 140		6175-5333	-4.40	0.96	Cinquemani et al. (1982)
Cooper-Wando River	32.900	79.900	QC-587	Salt peat	4290 ± 125		5287-4525	-3.45	0.95	Cinquemani et al. (1982)
Cooper-Wando River	32.900	79.900	QC-588	Salt peat	4135 ± 65		4838-4448	-2.85	0.95	Cinquemani et al. (1982)
Cooper-Wando River	32.900	79.900	QC-611	Salt peat	2150 ± 110		2352-1882	-1.60	0.94	Cinquemani et al. (1982)
Cooper-Wando River	32.900	79.900	QC-613	Salt peat	2330 ± 140		2740-2012	-1.85	1.00	Cinquemani et al. (1982)
Cooper-Wando River	32.900	79.900	QC-702	Salt peat	4665 ± 130		5647-4973	-2.80	0.95	Cinquemani et al. (1982)
Cooper-Wando River	32.900	79.900	QC-703	Salt peat	3100 ± 155		3678-2878	-2.00	0.94	Cinquemani et al. (1982)
Cooper-Wando River	32.900	79.900	QC-704	Salt peat	4755 ± 285		6181-4665	-3.95	0.95	Cinquemani et al. (1982)
Terrestrial Limiting										
Cooper-Wando River	32.900	79.900	QC-583	Stump	2035 ± 105		2311-1739	-0.20	0.62	Cinquemani et al. (1982)
Cooper-Wando River	32.900	79.900	QC-585	Stump	2695 ± 115		3144-2464	-1.20	0.62	Cinquemani et al. (1982)

References

Ablain, M., Cazenave, A., Valladeau, G., and Guinehut, S. (2009). A new assessment of the error budget of global mean sea level rate estimated by satellite altimetry over 1993-2008. *Ocean Science 5*, 193-201.

Aharon, P. (1984). Implications of the coral reef record from New Guinea concerning the astronomical theory of Ice Ages. In "*Milankovitch and Climate: Understanding the response to astronomical forcing*." (A. Berger, J. Imbrie, J. Hays, G. Kukla, and B. Saltzman, Eds.), pp. 379-389. Reidel, Dordrecht.

Allen, P.A. and Allen, J.R. (1990). *Basin Analysis. Principles and Applications*. Blackwell Publishing, Oxford.

Alley, R. B., Clark, P. U., Huybrechts, P., and Joughin, I. (2005). Ice-sheet and sea-level changes. *Science 310*, 456-460.

Andrews, J. E., Greenaway, A. M., and Dennis, P. F. (1998). Combined carbon isotope and C/N ratios as indicators of source and fate of organic matter in a poorly flushed, tropical estuary: Hunts Bay, Kingston Harbour, Jamaica. *Estuarine Coastal and Shelf Science 46*, 743-756.

Angulo, R. J., Lessa, G. C., and de Souza, M. C. (2006). A critical review of mid- to late-Holocene sea-level fluctuations on the eastern Brazilian coastline. *Quaternary Science Reviews* 25, 486-506.

Argus, D. F., Peltier, W. R., and Watkins, M. M. (1999). Glacial isostatic adjustment observed using very long baseline interferometry and satellite laser ranging geodesy. *Journal of Geophysical Research* 104, 29077-29093.

Argus, D. L., and Peltier, W. R. (submitted). Constraining models of postglacial rebound using spacer geodesy: A detailed assesment of model ICE-5G(VM2) and its relatives. *Geophysical Journal International*, submitted.

Atwater, B. F. (1987). Evidence for Great Holocene Earthquakes Along the Outer Coast of Washington-State. *Science* 236, 942-944.

Austin, W. E. N., Bard, E., Hunt, J. B., Kroon, D., and Peacock, J. D. (1995). The C-14

Age of the Icelandic Vedde Ash - Implications for Younger-Dryas Marine Reservoir Age Corrections. *Radiocarbon* 37, 53-62.

Barber, D. C., Dyke, A., Hillaire-Marcel, C., Jennings, A. E., Andrews, J. T., Kerwin, M. W., Bilodeau, G., McNeely, R., Southon, J., Morehead, M. D., and Gagnon, J. M. (1999). Forcing of the cold event of 8,200 years ago by catastrophic drainage of Laurentide lakes. *Nature* 400, 344-348.

Bard, E., Hamelin, B., Arnold, M., Montaggioni, L., Cabioch, G., Faure, G., and Rougerie, F. (1996). Deglacial sea-level record from Tahiti corals and the timing of global meltwater discharge. *Nature* 382, 241-244.

Bard, E., Hamelin, B., and Fairbanks, R. G. (1990a). U-Th ages obtained by mass spectrometry in corals from Barbados: sea level during the past 130 000 years. *Nature* 346, 456-458.

Bard, E., Hamelin, B., Fairbanks, R. G., and Zindler, A. (1990b). Calibration of the 14C timescale over the past 30 000 years using mass spectrometric U-Th ages from Barbados corals. *Nature* 382, 405-410.

Barnett, T. P. (1984). The Estimation of Global Sea-Level Change - a Problem of Uniqueness. *Journal of Geophysical Research-Oceans* 89, 7980-7988.

Barnhardt, W.A., Gehrels, W.R., Belknap, D.F. and Kelley, J.T. (1995). Late Quaternary relative sea-level change in the Western Gulf of Maine: evidence for a migrating glacial forebulge. *Geology* 23, 317-320.

Barrie, J. V., and Conway, K. W. (2002). Rapid sea-level change and coastal evolution on the Pacific margin of Canada. *Sedimentary Geology* 150, 171-183.

Bartlein, P. J., Edwards, M. E., Shafer, S. L., and Barker, E. D. (1995). Calibration of radiocarbon ages and the interpretation of paleoenvironmental records. *Quaternary Research* 44, 417-424.

Bassett, S. E., Milne, G. A., Mitrovica, J. X., and Clark, P. U. (2005). Ice sheet and solid earth influences on far-field sea-level histories. *Science* 309, 925-928.

Behre, K.-E. (2004). Coastal development, sea-level change and settlement history during the later Holocene in the Clay District of Lower Saxony (Niedersachsen), northern Germany. *Quaternary International* 112, 37-53.

Behre, K. E. (2007). A new Holocene sea-level curve for the southern North Sea. *Boreas* 36, 82-102.

Belknap, D.F., 1975, Dating of late Pleistocene and Holocene relative sea levels in coastal Delaware. Thesis, University of Delaware, Newark, 95pp.

Belknap, D. F., and Kraft, J. C. (1977). Holocene Relative Sea-Level Changes and Coastal Stratigraphic Units on Northwest Flank of Baltimore Canyon through Geosyncline. *Journal of Sedimentary Petrology* 47, 610-629.

Belknap, D., Andersen, B., Anderson, R., Anderson, W., Borns Jr, H., Jacobson, G., Kelley, J., Shipp, R., Smith, D., and Stuckenrath Jr, R. (1987). Late Quaternary sea-level changes in Maine. Sea-Level Fluctuations and Coastal Evolution. *SEPM special publication* 41, 71-85.

Belknap, D. F., Shipp, R. C., Stuckenrath, R., Kelley, J. T., and Borns, H. W. (1989). Holocene Sea-Level Change in Coastal Maine. In "*Neotectonics of Maine: Studies in Seismicity, Crustal Warping, and Sea-Level Change*." (W. A. Anderson, and H. W. Borns, Eds.). Maine Geological Survey, Augusta, ME.

Bennike, O., and Bjorck, S. (2002). Chronology of the last recession of the Greenland Ice Sheet. *Journal of Quaternary Science* 17, 211-219.

Bird, M. I., Taylor, D., and Hunt, C. (2005). Palaeoenvironments of insular Southeast Asia during the Last Glacial Period: a savanna corridor in Sundaland? *Quaternary Science Reviews* 24, 2228-2242.

Bloom, A. L. (1964). Peat accumulation and compaction in a Connecticut coastal marsh. *Journal of Sedimentary Research* 34, 599-603.

Bloom, A. L. (1967). Pleistocene Shorelines - a New Test of Isostasy. *Geological Society of America Bulletin* 78, 1477-1494.

Bloom, A. L. (1977). "*Atlas of Sea Level Curves*." International Geological Correlation Programme 61, Cornell University, New York.

Bloom, A. L., and Stuiver, M. (1963). Submergence of Connecticut Coast. *Science* 139, 332-334.

Blum, M. D., Misner, T. J., Collins, E. S., Scott, D. B., Morton, R. A., and Aslan, A. (2001). Middle Holocene sea-level rise and highstand at+2 m, central Texas coast.

Journal of Sedimentary Research 71, 581-588.

Bowen, D. Q. (1978). "*Quaternary Geology: a stratigraphic framework for multidisciplinary work*." Pergamon Press, Oxford.

Bowman, S. (1990). "*Interpreting the past: Radiocarbon dating*." British Museum Press, London.

Bradley, S. L., Milne, G. A., Teferle, F. N., Bingley, R. M., and Orliac, E. J. (2009). Glacial isostatic adjustment of the British Isles: New constraints from GPS measurements of crustal motion. *Geophysical Journal International* 178, 14-22.

Brooks, A. J., Bradley, S. L., Edwards, R. J., Milne, G. A., Horton, B., and Shennan, I. (2008). Postglacial relative sea-level observations from Ireland and their role in glacial rebound modelling. *Journal of Quaternary Science* 23, 175-192.

Cazenave, A., Dominh, K., Guinehut, S., Berthier, E., Llovel, W., Ramillien, G., Ablain, M., and Larnicol, G. (2009). Sea level budget over 2003-2008: A reevaluation from GRACE space gravimetry, satellite altimetry and Argo. *Global and Planetary Change* 65, 83-88.

Chappell, J. (1974). Geology of coral terraces, Huon Peninsula, New Guinea: a study of Quaternary tectonic movements and sea-level changes. *Geological Society of America Bulletin* 85, 553-570.

Chappell, J., Omura, A., Esat, T., McCulloch, M., Pandolfi, J., Ota, Y., and Pillans, B. (1996). Reconciliation of late Quaternary sea levels derived from coral terraces at Huon Peninsula with deep sea oxygen isotope records. *Earth and Planetary Science Letters* 141, 227-236.

Chappell, J., and Polach, H. (1991). Postglacial Sea-Level Rise from a Coral Record at Huon Peninsula, Papua-New-Guinea. *Nature* 349, 147-149.

Chmura, G. L., and Aharon, P. (1995). Stable Carbon-Isotope Signatures of Sedimentary Carbon in Coastal Wetlands as Indicators of Salinity Regime. *Journal of Coastal Research* 11, 124-135.

Church, J. A., and White, N. J. (2006). A 20th century acceleration in global sea-level rise. *Geophysical Research Letters* 33, doi:10.1029/2005GL024826.

Church, J. A., White, N. J., Aarup, T., Wilson, W. S., Woodworth, P. L., Domingues, C.

M., Hunter, J. R., and Lambeck, K. (2008). Understanding global sea levels: past, present and future. *Sustainability Science* 3, 9-22.

Cinquemani, L. J., Newman, W. S., Sperling, J. A., Marcus, L. F., and Pardi, R. R. (1982). Holocene sea level fluctuations, magnitudes and causes. In "*IGCP Annual Meeting*." Columbia, South Carolina.

Clark, J. A. (1980). The Reconstruction of the Laurentide Ice-Sheet of North-America from Sea-Level Data - Method and Preliminary-Results. *Journal of Geophysical Research* 85, 4307-4323.

Clark, J. A., Farrell, W. E., and Peltier, W. R. (1978). Global Changes in Post-Glacial Sea-Level - Numerical-Calculation. *Quaternary Research* 9, 265-287.

Clark, J. A., and Lingle, C. S. (1977). Future sea-leel changes due to West Antarctic ice sheet fluctuations. *Nature* 269, 206-209.

Clark, P. U., Mitrovica, J. X., Milne, G. A., and Tamisiea, M. E. (2002). Sea-level fingerprinting as a direct test for the source of global meltwater pulse IA. *Science* 295, 2438-2441.

Clark, P. U., and Mix, A. C. (2002). Ice sheets and sea level of the Last Glacial Maximum. *Quaternary Science Reviews* 21, 1-7.

Cleaves, E. T., Edwards, J., and Glaser, J. D. (1968). Geologic map of Maryland. Maryland Geological Survey, scale 1:250,000.

Colman, S. M., Baucom, P. C., Bratton, J. F., Cronin, T. M., McGeehin, J. P., Willard, D., Zimmerman, A. R., and Vogt, P. R. (2002). Radiocarbon dating, chronologic framework, and changes in accumulation rates of Holocene estuarine sediments from Chesapeake Bay. *Quaternary Research* 57, 58-70.

Conrad, C. P., and Hager, B. H. (1997). Spatial variations in the rate of sea level rise caused by the present-day melting of glaciers and ice sheets. *Geophysical Research Letters* 24, 1503-1506.

Cram, J. M. (1979). Influence of Continental-Shelf Width on Tidal Range - Paleoceanographic Implications. *Journal of Geology* 87, 441-447.

Daly, R. A. (1934). "The Changing World of the Ice Age." Yale University Press, New Haven.

Davis, J. E., Latychev, K., Mitrovica, J. X., Kendall, R., and Tamisiea, M. E. (2008). Glacial isostatic adjustment in 3-D earth models: Implications for the analysis of tide gauge records along the US east coast. *Journal of Geodynamics* 46, 90-94.

Davis, J. L., and Mitrovica, J. X. (1996). Glacial isostatic adjustment and the anomalous tide gauge record of eastern North America. *Nature* 379, 848-848.

Day, J. W., Gunn, J. D., Folan, W. J., Yanez-Arancibia, A., and Horton, B. P. (2007). Post-glacial coastal margin productivity and the emergence of civilizations. *EOS Transaction AGU* 80, 170-171.

De Deckker, P., and Yokoyama, Y. (2009). Micropalaeontological evidence for Late Quaternary sea-level changes in Bonaparte Gulf, Australia. *Global and Planetary Change* 66, 85-92.

De Rijk, S., and Troelstra, S. R. (1997). Saltmarsh foraminifera from the Great Marshes, Massachusetts: environmental controls. *Palaeogeography Palaeoclimatology Palaeoecology* 130, 81-112.

Denys, L., and Baeteman, C. (1995). Holocene evolution of relative sea level and local mean high water spring tides in Belgium: a first assessment. *Marine Geology* 124, 1-19.

Domingues, C. M., Church, J. A., White, N. J., Gleckler, P. J., Wijffels, S. E., Barker, P. M., and Dunn, J. R. (2008). Improved estimates of upper-ocean warming and multi-decadal sea-level rise. *Nature* 453, 1090-1096.

Donnelly, J. (1998). Evidence of late Holocene post-glacial isostatic adjustment in coastal wetland deposits of eastern North America. *Georesearch Forum* 34, pp. 393–400.

Donnelly, J. P. (2006). A revised late Holocene sea-level record for northern Massachusetts, USA. *Journal of Coastal Research* 22, 1051-1061.

Donnelly, J. P., Cleary, P., Newby, P., and Ettinger, R. (2004). Coupling instrumental and geological records of sea-level change: Evidence from southern New England of an increase in the rate of sea-level rise in the late 19th century. *Geophysical Research Letters* 31, doi:10.1029/2003GL018933.

Donner, J. J. (1964). Pleistocene geology of eastern Long Island, New York. American *Journal of Science* 262, 355-376.

Douglas, B. C. (1991). Global Sea-Level Rise. *Journal of Geophysical Research-Oceans* 96, 6981-6992.

Douglas, B. C. (1995). Global Sea-Level Change - Determination and Interpretation. *Reviews of Geophysics* 33, 1425-1432.

Douglas, B. C. (1997). Global sea rise: A redetermination. *Surveys in Geophysics* 18, 279-292.

Douglas, B. C. (2001). Sea Level Change in the Era of the Recording Tide Gauge. In "*Sea Level Rise: History and Consequences*." (B. C. Douglas, M. S. Kearney, and S. P. Leatherman, Eds.). Academic Press, San Diego.

Douglas, B. C. (2008). Concerning Evidence for Fingerprints of Glacial Melting. *Journal of Coastal Research* 24, 218-227.

Douglas, B. C., Cheney, R. E., and Agreen, R. W. (1983). Eddy Energy of the Northwest Atlantic and Gulf of Mexico Determined from GEOS3 Altimetry. *Journal of Geophysical Research* 88, 9595-9603.

Dyke, A. S. (1987). A Reinterpretation of Glacial and Marine Limits around the Northwestern Laurentide Ice-Sheet. *Canadian Journal of Earth Sciences* 24, 591-601.

Dyke, A. S. (2004). An outline of North American deglaciation with emphasis on central and northern Canada. In "*Quaternary Glaciations - Extent and Chronology, Part II.*" (J. Ehlers, and P. L. Gibbard, Eds.). Elsevier, Amsterdam.

Dyke, A. S., and Prest, V. K. (1987). Late Wisconsinan and Holocene History of the Laurentide Ice Sheet. *Geographie physique et Quaternaire* 41, 237-263.

Dziewonski, A. M., and Anderson, D. L. (1981). Preliminary reference Earth model. *Physics of the Earth and Planetary Interiors* 25, 297-356.

Edwards, R. J. (2006). Mid- to late-Holocene relative sea-level change in southwest Britain and the influence of sediment compaction. *Holocene* 16, 575-587.

Edwards, R. J., Wright, A., and Van de Plassche, O. (2004). Surface distributions of salt-marsh foraminifera from Connecticut, USA: modem analogues for high-resolution sea level studies. *Marine Micropaleontology* 51, 1-21.

Ekman, M. (1991). A Concise History of Postglacial Land Uplift Research (from Its

Beginning to 1950). *Terra Nova* 3, 358-365.

Elliot, G.K., 1972, The Great Marsh, Lewes, Delaware: The physiography, classification and geologic history of a coastal marsh. College of Marine Studies, University of Delware, Technical Report 19, 139pp.

Engelhart, S. E., Horton, B. P., Douglas, B. C., Peltier, W. R., and Tornqvist, T. E. (2009). Spatial variability of late Holocene and 20th century sea-level rise along the Atlantic coast of the United States. *Geology* 37, 1115-1118.

Fairbanks, R. G. (1989). A 17,000-Year Glacio-Eustatic Sea-Level Record - Influence of Glacial Melting Rates on the Younger Dryas Event and Deep-Ocean Circulation. *Nature* 342, 637-642.

Fairbridge, R. W. (1961). Eustatic changes in sea level. *Physics and Chemistry of Earth* 5, 99-185.

Farrell, W. E., and Clark, J. A. (1976). On post-glacial sea level. *Royal Astronomical Society Geophysical Journal* 46, 647-657.

Fenneman, N. M. (1938). "Physiography of the Eastern United States." McGraw-Hill, New York.

Field, M. E., Meisburger, E. P., Stanley, E. A., and Williams, S. J. (1979). Upper Quaternary Peat Deposits on the Atlantic Inner Shelf of the United-States. *Geological Society of America Bulletin* 90, 618-628.

Finkelstein, K. and Ferland, M.A. 1987. Back-barrier response to sea-level rise, Eastern Shore of Virginia. In "*Sea-level fluctuations and coastal evolution*' (Nummedal, D., Pilkey, O.H., Howard, J.D., Eds.), pp. 145-156.

Fisher, J. J. (1968). Barrier Island Formation - Discussion. *Geological Society of America Bulletin* 79, 1421-1426.

Fisher, J. J. (1982). Barrier Islands. In "*The Encyclopedia of Beaches and Coastal Environments*." (M. L. Schwartz, Ed.), pp. 124-133. Hutchinson Ross, Stroudsburg.

Fleming, K., Johnston, P., Zwartz, D., Yokoyama, Y., Lambeck, K., and Chappell, J. (1998). Refining the eustatic sea-level curve since the Last Glacial Maximum using far- and intermediate-field sites. *Earth and Planetary Science Letters* 163, 327-342.

Fletcher, C. H., Knebel, H. J., and Kraft, J. C. (1990). Holocene evolution of an estuarine coast and tidal wetlands. *Geological Society of America Bulletin* 102, 283-297.

Fletcher, C. H., Vanpelt, J. E., Brush, G. S., and Sherman, J. (1993). Tidal Wetland Record of Holocene Sea-Level Movements and Climate History. *Palaeogeography Palaeoclimatology Palaeoecology 102, 177-213.*

Forte, A. M., and Mitrovica, J. X. (1996). New inferences of mantle viscosity from joint inversion of long-wavelength mantle convection and post-glacial rebound data. *Geophysical Research Letters* 23, 1147-1150.

Foyle, A. M., and Oertel, G. F. (1997). Transgressive systems tract development and incised-valley fills within a Quaternary estuary-shelf system: Virginia inner shelf, USA. *Marine Geology* 137, 227-249.

Froede, C. R. (2002). Rhizolith evidence in support of a late Holocene sea-level highstand at least 0.5 m higher than present at Key Biscayne, Florida. *Geology* 30, 203-206.

Gayes, P. T., Scott, D. B., Collins, E. S., and Nelson, D. D. (1992). A Late Holocene Sea-level fluctuation in South Carolina. *SEPM Special Publication* 48, 155-160.

Gehrels, W. R. (1994). Determining Relative Sea-Level Change from Salt-Marsh Foraminifera and Plant Zones on the Coast of Maine, USA. *Journal of Coastal Research* 10, 990-1009.

Gehrels, W. R. (1999). Middle and late holocene sea-level changes in Eastern Maine reconstructed from foraminiferal saltmarsh stratigraphy and AMS C-14 dates on basal peat. *Quaternary Research* 52, 350-359.

Gehrels, W. R. (2000). Using foraminiferal transfer functions to produce high-resolution sea-level records from salt-marsh deposits, Maine, USA. *Holocene* 10, 367-376.

Gehrels, W. R. (in press). Sea-level changes since the Last Glacial Maximum: an appraisal of the IPCC Fourth Assessment Report. *Journal of Quaternary Science*.

Gehrels, W. R., and Belknap, D. F. (1993). Neotectonic History of Eastern Maine Evaluated from Historic Sea-Level Data and C-14 Dates on Salt-Marsh Peats. *Geology* 21, 615-618.

Gehrels, W.R., Belknap, D.F., and Kelley, J.T. (1996). Integrated high-precision analyses

of Holocene relative sea-level changes: Lessons from the coast of Maine. *GSA Bulletin* 108, 1073-1088.

Gehrels, W. R., Belknap, D. F., Pearce, B. R., and Gong, B. (1995). Modeling the Contribution of M(2) Tidal Amplification to the Holocene Rise of Mean High Water in the Gulf of Maine and the Bay of Fundy. *Marine Geology* 124, 71-85.

Gehrels, W. R., Belknap, D. F., Black, S., and Newnham, R. M. (2002). Rapid sea-level rise in the Gulf of Maine, USA, since AD 1800. *Holocene* 12, 383-389.

Gehrels, W. R., Milne, G. A., Kirby, J. R., Patterson, R. T., and Belknap, D. F. (2004). Late Holocene sea-level changes and isostatic crustal movements in Atlantic Canada. *Quaternary International* 120, 79-89.

Gehrels, W. R., Kirby, J. R., Prokoph, A., Newnham, R. M., Achterberg, E. P., Evans, H., Black, S., and Scott, D. B. (2005). Onset of recent rapid sea-level rise in the western Atlantic Ocean. *Quaternary Science Reviews* 24, 2083-2100.

Gehrels, W. R., and Long, A. J. (2007). Quaternary land-ocean interactions: Sea-level change, sediments and tsunami. *Marine Geology* 242, 1-4.

Gonzalez, J. L., and Tornqvist, T. E. (2009). A new Late Holocene sea-level record from the Mississippi Delta: evidence for a climate/sea level connection? *Quaternary Science Reviews* 28, 1737-1749.

Gornitz, V. (1995). A comparison of differences between recent and late Holocene sea-level trends from eastern North America and other selected regions. *Journal of Coastal Research*, 287-297.

Gornitz, V., and Seeber, L. (1990). Vertical Crustal Movements Along the East Coast, North-America, from Historic and Late Holocene Sea-Level Data. *Tectonophysics* 178, 127-150.

Greensmith, J. T., and Tooley, M. J. (1982). I.G.C.P. Project 61. Sea-level movements during the last deglacial hemicycle (about 15,000 years). Final report of the U.K. Working Group. *Proceedings of the Geologists' Association* 93, 1-125.

Groger, M., and Plag, H. P. (1993). Estimations of a global sea level trend: limitations from the structure of the PSMSL global sea level data set. *Global and Planetary Change* 8, 161-179.

Hadjas, I., Zolitschaka, B., Ivy-och, S. D., Beer, J., Leroy, S. A. G., Negendank, J. W., Ramrath, M., and Suter, M. (1995). AMS radiocarbon dating of annually laminated sediments from lake Holzmaar, Germany. *Quaternary Science Reviews* 14, 137-143.

Hanebuth, T., Stattegger, K., and Grootes, P. M. (2000). Rapid flooding of the Sunda Shelf: A late-glacial sea-level record. *Science* 288, 1033-1035.

Harris, M. S., Gayes, P. T., Kindinger, J. L., Flocks, J. G., Krantz, D. E., and Donovan, P. (2005). Quaternary geomorphology and modern coastal development in response to an inherent geologic framework: An example from Charleston, South Carolina. *Journal of Coastal Research* 21, 49-64.

Hatte, C., and Jull, A. J. T. (2007). Plant macrofossils. In "*Encyclopedia of Quaternary Science.*" (S. A. Elias, Ed.), pp. 2958-2965. Elsevier, Amsterdam.

Headlee, T. J., and Carroll, M. (1920). Report of Mosquito Work. In "*Documents of the One Hundred and Forth-Third and One and Forty-Fourth Legislaturs of the State of New Jersey and Seventy-Fifth and Seventy-Sixth Under the New Constitution.*" (S. o. N. Jersey, Ed.). State Gazette Publishing Co., Trenton, NJ.

Hiebert, R. D., and Watts, R. J. (1953). Fast coincidence circuits for H3 and C14 measurements. *Nucleonics* 11, 38-41.

Hobbs, N. B. (1986). Mire morphology and the properties and behavior of some British and foreign peats. *Quarterly Journal of Engineering Geology* 19, 7-80.

Horton, B. P., Corbett, R., Culver, S. J., Edwards, R. J., and Hillier, C. (2006). Modern saltmarsh diatom distributions of the Outer Banks, North Carolina, and the development of a transfer function for high resolution reconstructions of sea level. *Estuarine Coastal and Shelf Science* 69, 381-394.

Horton, B. P., and Edwards, R. J. (2006). Quantifying Holocene sea-level change using intertidal foraminifera: lessons for the British Isles. *Cushman Foundation for Foraminiferal Research Special Publication*, 40, 97p.

Horton, B. P., Gibbard, P. L., Milne, G. M., Morley, R. J., Purintavaragul, C., and Stargardt, J. M. (2005). Holocene sea levels and palaeoenvironments, Malay-Thai Peninsula, southeast Asia. *Holocene* 15, 1199-1213.

Horton, B. P., Peltier, W. R., Culver, S. J., Drummond, R., Engelhart, S. E., Kemp, A. C., Mallinson, D., Thieler, E. R., Riggs, S. R., Ames, D. V., and Thomson, K. H. (2009).

Holocene sea-level changes along the North Carolina Coastline and their implications for glacial isostatic adjustment models. *Quaternary Science Reviews* 28, 1725-1736.

Horton, B. P., and Shennan, I. (2009). Compaction of Holocene strata and the implications for relative sea-level change on the east coast of England. *Geology* 37, 1083-1086.

Hughen, K., Baillie, M., Bard, E., Bayliss, A., Beck, J., Bertrand, C., Blackwell, P., Buck, C., Burr, G., and Cutler, K. (2004). Marine04 Marine radiocarbon age calibration, 26-0 ka BP. *Radiocarbon* 46, 1059-1086.

IPCC. (2007). "*Climate Change 2007: The Physical Science Basis. Contribution of Work Group I to the Fourth Assessment. Report of the Intergovernmental Panel on Climate Change* [Solomon, S., D. Qin, M. Manning, Z. Chen, M. Marquis, K.B. Averyt, M. Tignor and H.L. Millers (Eds.)]. Cambridge University Press, Cambridge, United Kingdom and New York, NY, USA.".

Isachsen, Y. W., Landing, E., Lauber, J. M., Richard, L. V., and Rogers, W. B. (2000). "*Geology of New York. A Simplified Account*." New York State Museum, Albany, NY.
Ivins, E. R., Sammis, C. G., and Yoder, C. F. (1993). Deep Mantle Viscous Structure with Prior Estimate and Satellite Constraint. Journal of Geophysical Research-Solid Earth 98, 4579-4609.

Ivins, E. R., Dokka, R. K., and Blom, R. G. (2007). Post-glacial sediment load and subsidence in coastal Louisiana. *Geophysical Research Letters* 34, doi:10.1029/2007GL030003.

Jacobson, H. A., Jacobson, G. L., and Kelley, J. T. (1987). Distribution and Abundance of Tidal Marshes Along the Coast of Maine. *Estuaries* 10, 126-131.

Jansa, L. F. (1986). Paleoceanography and evolution of the North Atlantic Ocean Basin during the Jurassic. In "*The Western North Atlantic Region*." (P. R. Vogt, and B. E. Tucholke, Eds.), pp. 603-616. Geological Society of America, Boulder.

Jardine, W. G. (1975). Chronology of Holocene margine transgression and regression in southwestern Scotland. *Boreas* 4, 173-196.

Jelgersma, S. (1961). Holocene sea-level changes in the Netherlands. *Mededelingen Geologische Stichting Serie C*. VI 7, 1-100.

Jelgersma, S. (1966). Sea-level changes during the last 10 000 years. In "*Royal*

Meteorological Society Proceedings of a Symposium on World Climate 8000-0 BC." pp. 54-81.

Jelgersma, S. (1979). Sea-level changes in the North Sea basin. In "*The Quaternary History of the North Sea: .*" (E. Oele, R. T. E. Schuttenhelm, and A. J. Wiggers, Eds.). Acta Universitatis Upsaliensis Symposia Universitatis Upsaliensis Annum Quingentesimum Celebrantis, 2 pp. 233-248.

Jevrejeva, S., Moore, J. C., Grinsted, A., and Woodworth, P. L. (2008). Recent global sea level acceleration started over 200 years ago? *Geophysical Research Letters* 35, doi:10.1029/2008GL033611.

Jiang, H., Bjorck, S., and Knudsen, K. L. (1997). A palaeoclimatic and palaeoceanographic record of the last 11,000 C-14 years from the Skagerrak-Kattegat, northeastern Atlantic margin. *Holocene* 7, 301-310.

Johnson, B. J., Moore, K. A., Lehmann, C., Bohlen, C., and Brown, T. A. (2007). Middle to late Holocene fluctuations of C3 and C4 vegetation in a Northern New England Salt Marsh, Sprague Marsh, Phippsburg Maine. *Organic Geochemistry* 38, 394-403.

Jones, G. A., Jull, A. J. T., Linick, T. W., and Donahue, D. J. (1989). Radiocarbon Dating of Deep-Sea Sediments - a Comparison of Accelerator Mass-Spectrometer and Beta-Decay Methods. *Radiocarbon* 31, 105-116.

Kaye, C. A. (1976). The geology and early history of the Boston area of Massachusetts (U. S. G. Survey, Ed.), pp. 78.

Kaye, C. A. (1982). Bedrock and Quaternary geology of the Boston area, Massachusetts. *Geological Society of America Reviews in Engineering Geology* 5, 25-40.

Kaye, C. A., and Barghoorn, E. S. (1964). Late Quaternary Sea-Level Change and Crustal Rise at Boston, Massachusetts, with Notes on the Autocompaction of Peat. *Geological Society of America Bulletin* 75, 63-80.

Kelley, J. T. (1987). An inventory of environments and classification of Maine's estuarine coastline. In "*A Treatise on Glaciated Coastlines.*" (P. Rosen, and D. Fitzgerald, Eds.), pp. 151-176. Academic Press, San Diego.

Kelley, J. T., Belknap, D. F., Jacobson, G. L., and Jacobson, H. A. (1988). The Morphology and Origin of Salt Marshes Along the Glaciated Coastline of Maine, USA. *Journal of Coastal Research* 4, 649-666.

Kelley, J.T., Dickson, S.M., Belknap, D.F. and Stuckenrath, R. (1992). Sea-level change and late Quaternary sediment accumulation on the southern Maine inner continental shelf. In "*Quaternary Coasts of the United States*" (Fletcher, C.J., Wehmiller, J., Eds). 23-34.

Kelley, J. T., Gehrels, W. R., and Belknap, D. F. (1995). Late Holocene Relative Sea-Level Rise and the Geological Development of Tidal Marshes at Wells, Maine, USA. *Journal of Coastal Research* 11, 136-153.

Kemp, A. C., Horton, B. P., Culver, S. J., Corbett, D. R., van de Plassche, O., Gehrels, W. R., Douglas, B. C., and Parnell, A. C. (2009). Timing and magnitude of recent accelerated sea-level rise (North Carolina, United States). *Geology* 37, 1035-1038.

Kemp, A. C., Vane, C., Horton, B. P., and Culver, S. J. (In Press). Stable carbon isotopes as potential sea-level indicators in salt marshes. *The Holocene*.

Kendall, R. A., Mitrovica, J. X., Milne, G. A., Tornqvist, T. E., and Li, Y. X. (2008). The sea-level fingerprint of the 8.2 ka climate event. *Geology* 36, 423-426.

Kiden, P. (1995). Holocene Relative Sea-Level Change and Crustal Movement in the Southwestern Netherlands. *Marine Geology* 124, 21-41.

Kidson, C. (1982). Sea level changes in the Holocene. *Quaternary Science Reviews* 1, 121-151.

Kidson, C. (1986). Sea-level changes in the Holocene. In "*Sea-Level Research: A Manual for the Collection and Evaluation of data*." (O. van de Plassche, Ed.). Geobooks, Norwich.

Klitgord, K. D., Hutchinson, D. R., and Schouten, H. (1988). U.S. Atlantic continental margin; Structural and tectonic framework. In "*The Geology of North America: The Atlantic Continental Margin: U.S.*" (R. E. Sheridan, and J. A. Grow, Eds.). Geological Society of America, Boulder.

Klitgord, K. D., and Schouten, H. (1986). Plate kinematics of the Central Atlantic. In "*The Western North Atlantic Region.*" (P. R. Vogt, and B. E. Tucholke, Eds.), pp. 351-378. Geological Society of America, Boulder.

Knebel, H. J., Fletcher, C. H., and Kraft, J. C. (1988). Late Wisconsinan-Holocene paleogeography of Delaware Bay; a large Coastal Plain estuary. *Marine Geology* 83, 115-

133.

Kraft, J. C. (1971). Sedimentary facies patterns and geologic history of a Holocene marine transgression. *Geological Society of America Bulletin* 82, 2131-2158.

Kraft, J. C. (1979). Processes and morphologic evolution of an estuarine and coastal barrier system. In "*Barrier Islands from the Gulf of St. Lawrence to the Gulf of Mexico.*" (S. P. Leatherman, Ed.), pp. 149-183. Academic Prress, New York.

Kraft, J. C., Chrzastowski, M. J., Belknap, D. F., Toscano, M. A., and Fletcher, C. H. (1987). The transgressive barrier-lagoon coast of Delaware: Morphostratigraphy, sedimentary sequences and responses to relative rise in sea level. In "*Sea Level Fluctuation and Coastal Evolution.*" (D. Nummedal, O. H. Pilkey, and J. D. Howard, Eds.), pp. 129-145. Society of Sedimentary Geology Special Publication 41.

LaForge, L. (1932). "Geology of the Boston area, Massachusetts."

Lamb, A. L., Vane, C. H., Wilson, G. P., Rees, J. G., and Moss-Hayes, V. L. (2007). Assessing δ13C and C/N ratios from organic material archived in cores as Holocene sea level and palaeoenvironmental indicators in the Humber Estuary, UK. *Marine Geology* 244, 109-128.

Lamb, A. L., Wilson, G. P., and Leng, M. J. (2006). A review of coastal palaeoclimate and relative sea-level reconstructions using delta C-13 and C/N ratios in organic material. *Earth-Science Reviews* 75, 29-57.

Lambeck, K. (2002). Sea level change from mid-Holocene to recent time: an Australian example with global implications. In "*Glacial isostatic adjustment and the earth system*". (J. X. Mitrovica, and L. L. A. Vermeersen, Eds.), pp. 33-50.

Lambeck, K., Antonioli, F., Purcell, A., and Silenzi, S. (2004). Sea-level change along the Italian coast for the past 10,000 yr. *Quaternary Science Reviews* 23, 1567-1598.

Lambeck, K., and Bard, E. (2000). Sea-level change along the French Mediterranean coast for the past 30,000 years. *Earth and Planetary Science Letters* 175, 203-222.

Lambeck, K., Esat, T. M., and Potter, E. K. (2002). Links between climate and sea levels for the past three million years. *Nature* 419, 199-206.

Lambeck, K., and Purcell, A. (2005). Sea-level change in the Mediterranean Sea since the LGM: model predictions for tectonically stable areas. *Quaternary Science Reviews* 24,

1969-1988.

Larcombe, P., Carter, R.M., Dye, J., Gagan, M.K., and Johnson, D.P. (1995). New evidence for episodic post-glacial sea-level rise, central Great Barrier Reef, Australia. *Marine Geology*, 127, 1-44.

Latychev, K., Mitrovica, J. X., Tromp, J., Tamisiea, M. E., Komatitsch, D., and Christara, C. C. (2005). Glacial Isostatic Adjustment on 3-D Earth Models: A Finite Volume Formulation. *Geophysical Journal International* 161, 421-444.

Lefor, M. W., Kennard, W. C., and Civco, D. L. (1987). Relationships of Salt-Marsh Plant-Distributions to Tidal Levels in Connecticut, USA. *Environmental Management* 11, 61-68.

Leorri, E., Martin, R., and McLaughlin, P. (2006). Holocene environmental and parasequence development of the St. Jones Estuary, Delaware (USA): Foraminiferal proxies of natural climatic and anthropogenic change. *Palaeogeography, Palaeoclimatology, Palaeoecology* 241, 590-607.

Lewis, J. V., and Kummel, H. B. (1915). The Geology of New Jersey (H. B. Kummel, Ed.). Geological Survey of New Jersey, Union Hill, NJ.

Lewis, R. S., and DiGiacomo-Cohen, M. (2000). A Review of the Geologic Framework of the Long Island Sound Basin, With Some Observations Relating to Postglacial Sedimentation. *Journal of Coastal Research* 16, 522-532.

Libby, W. F. (1952). "*Radiocarbon Dating*." University of Chicago Press, Chicago.

Long, A., and Shennan, I. (1994). Sea-level changes in Washington and Oregon and the 'Earthquake deformation cycle'. *Journal of Coastal Research* 10, 825-838.

Long, A. J., Roberts, D. H., and Rasch, M. (2003). New observations on the relative sea level and deglacial history of Greenland from Innaarsuit, Disko Bugt. *Quaternary Research* 60, 162-171.

Long, A. J., Waller, M. P., and Stupples, P. (2006). Driving mechanisms of coastal change: Peat compaction and the destruction of late Holocene coastal wetlands. *Marine Geology* 225, 63-84.

MacMillan, D. (2004). Rate difference between VLBI and GPS reference frame scales. EOS, Trans. Am. geophys. Un, 85(47) Fall Meet. Suppl., G21B-5.

Mallinson, D., Riggs, S., Thieler, E. R., Culver, S., Farrell, K., Foster, D. S., Corbett, D. R., Horton, B., and Wehmiller, J. F. (2005). Late Neogene and Quaternary evolution of the northern Albemarle Embayment (mid-Atlantic continental margin, USA). *Marine Geology* 217, 97-117.

Manspeizer, W., Puffer, J. H., and Cousminer, H. L. (1978). Separation of Morocco and Eastern North-America - Triassic-Liassic Stratigraphic Record. *Geological Society of America Bulletin* 89, 901-920.

Marcos, M., and Tsimplis, M. N. (2007). Forcing of coastal sea level rise patterns in the North Atlantic and the Mediterranean Sea. *Geophysical Research Letters* 34, doi:10.1029/2007GL030641.

Marple, R. and Talwani, P. (2004). Proposed Shenandoah Fault and East-Coast Stafford Fault System and their implications for U.S. Tectonics. *Southeastern Geology* 43, 57-80.

Massey, A. C., Gehrels, W. R., Charman, D. J., Milne, G. A., Peltier, W. R., Lambeck, K., and Selby, K. A. (2008). Relative sea-level change and postglacial isostatic adjustment along the coast of south Devon, United Kingdom. *Journal of Quaternary Science* 23, 415-433.

Massey, A. C., and Taylor, G. K. (2007). Coastal evolution in south-west England, United Kingdom: An enhanced reconstruction using geophysical surveys. *Marine Geology* 245, 123-140.

Maul, G. A., and Martin, D. M. (1993). Sea level rise at Key West, Florida, 1846-1992: America's longest instrument record. *Geophysical Research Letters* 20, 1955-1958.

Mazzotti, S., Lambert, A., Courtier, N., Nykolaishen, L., and Dragert, H. (2007). Crustal uplift and sea level rise in northern Cascadia from GPS, absolute gravity and tide gauge data. *Geophysical Research Letters* 34, doi:10.1029/2008JC004835.

McConnell, R. K. (1968). Viscosity of the mantle from relaxation time spectra of isostatic adjustment. *Journal of Geophysical Research* 73, 7089-7105.

McGregor, H. V., Gagan, M. K., McCulloch, M. T., Hodge, E., and Mortimer, G. (2008). Mid-Holocene variability in the marine C-14 reservoir age for northern coastal Papua New Guinea. *Quaternary Geochronology* 3, 213-225.

McLean, R. (1984). Coastal landforms: sea-level history and coastal evolution. *Progress*

in Physical Geography 8, 431-442.

Mencher, E., Copeland, R. A., and Payson, H. (1968). Surficial Sediments of Boston Harbor Massachusetts. *Journal of Sedimentary Petrology* 38, 79-86.

Miller, K. G., Sugarman, P. J., Browning, J. V., Horton, B. P., Stanley, A., Kahn, A., Uptegrove, J., and Aucott, M. (2009). Sea-level rise in New Jersey over the past 5000 years: Implications to anthropogenic changes. *Global and Planetary Change* 66, 10-18.

Miller, L., and Douglas, B. C. (2004). Mass and volume contributions to twentieth-century global sea level rise. *Nature* 428, 406-409.

Miller, L., and Douglas, B. C. (2006). On the rate and causes of twentieth century sea-level rise. *Philosophical Transactions of the Royal Society a-Mathematical Physical and Engineering Sciences* 364, 805-820.

Milne, G. A., Gehrels, W. R., Hughes, C. W., and Tamisiea, M. E. (2009). Identifying the causes of sea-level change. *Nature Geoscience* 2, 471-478.

Milne, G. A., Long, A. J., and Bassett, S. E. (2005). Modelling Holocene relative sea-level observations from the Caribbean and South America. *Quaternary Science Reviews* 24, 1183-1202.

Milne, G. A., and Mitrovica, J. X. (1996). Postglacial sea-level change on a rotating Earth: First results from a gravitationally self-consistent sea-level equation. *Geophysical Journal International* 126, F13-F20.

Milne, G. A., and Mitrovica, J. X. (2008). Searching for eustasy in deglacial sea-level histories. *Quaternary Science Reviews* 27, 2292-2302.

Milne, G. A., Mitrovica, J. X., and Schrag, D. P. (2002). Estimating past continental ice volume from sea-level data. *Quaternary Science Reviews* 21, 361-376.

Milne, G. A., Shennan, I., Youngs, B. A. R., Waugh, A. I., Teferle, F. N., Bingley, R. M., Bassett, S. E., Cuthbert-Brown, C., and Bradley, S. L. (2006). Modelling the glacial isostatic adjustment of the UK region. *Philosophical Transactions of the Royal Society a-Mathematical Physical and Engineering Sciences* 364, 931-948.

Mitchell, J. K., and Soga, K. (2005). "*Fundamentals of soil behaviour.*" Wiley, New York.

Mitchum, G. T. (1998). Monitoring the stability of satellite altimeters with tide gauges.

Journal of Atmospheric and Oceanic Technology 15, 721-730.

Mitrovica, J. X., and Forte, A. M. (1997). The Radial Profile of Mantle Viscosity: Results from the Joint Inversion of Convection and Post -Glacial Rebound Observables. *Journal of Geophysical Research* 102, 2751-2769.

Mitrovica, J. X., and Forte, A. M. (2004). A new inference of mantle viscosity based upon joint inversion of convection and glacial isostatic adjustment data. *Earth and Planetary Science Letters* 225, 177-189.

Mitrovica, J. X., Gomez, N., and Clark, P. U. (2009). The Sea-Level Fingerprint of West Antarctic Collapse. *Science* 323, 753-753.

Mitrovica, J. X., and Milne, G. A. (2002). On the origin of late Holocene sea-level highstands within equatorial ocean basins. *Quaternary Science Reviews* 21, 2179-2190.

Mitrovica, J. X., and Peltier, W. R. (1991). On postglacial geoid subsidence over the equatorial oceans. *Journal of Geophysical Research* 96, 20053-20071.

Mitrovica, J. X., and Peltier, W. R. (1992). Constraints on Mantle Viscosity from Relative Sea-Level Variations in Hudson-Bay. *Geophysical Research Letters* 19, 1185-1188.

Mitrovica, J. X., and Peltier, W. R. (1995). Constraints on Mantle Viscosity Based Upon the Inversion of Postglacial Uplift Data from the Hudson-Bay Region. *Geophysical Journal International* 122, 353-377.

Mitrovica, J. X., Tamisiea, M. E., Davis, J. L., and Milne, G. A. (2001). Recent mass balance of polar ice sheets inferred from patterns of global sea-level change. *Nature* 409, 1026-1029.

Montaggioni, L. F., Cabioch, G., Camoinau, E., Bard, A., Ribaud-Laurenti, G., Faure, P., Dejardin, P., and Recy, J. (1997). Continous record of reef growth over the past 14ky on the mid-Pacific island of Tahiti. *Geology* 25.

Morner, N. (1976). Eustasy and geoid changes. *Journal of Geology* 84, 123-152.

Murray-Wallace, C. V. (2007). Eustatic sea-level changes since the last glaciation. In "*Encyclopedia of Quaternary Science*." (S. A. Elias, Ed.), pp. 3034-3043. Elsevier, Amsterdam.

Nakada, M., and Lambeck, K. (1989). Late Pleistocene and Holocene sea-level change in

the Australian region and mantle rheology. *Geophysical Journal International* 96, 497-517.

Nakada, M., and Okuno, J. (2003). Perturbations of the Earth's rotation and their implications for the present-day mass balance of both polar ice caps. *Geophysical Journal International* 152, 124-138.

Needell, S. W., and Lewis, R. S. (1984). Geology of Block Island Sound, Rhode Island and New York. U.S. Geological Survey Miscellaneous Field Studies Map MF-1621, scale 1:125,000.

Nelson, A. R. (2007). Tectonic Locations. In "*Encyclopedia of Quaternary Science*." (S. A. Elias, Ed.). Elsevier, Amsterdam.

Nelson, A. R., Jennings, A. E., and Kashima, K. (1996). An earthquake history derived from stratigraphic and microfossil evidence of relative sea-level change at Coos Bay, southern coastal Oregon. *GSA Bulletin* 108, 141-154.

Nerem, R. S., and Mitchum, G. T. (2001). Observation of sea level change from satellite altimetry. In "*Sea Level Rise: History and Consequences*." (B. C. Douglas, M. S. Kearney, and S. P. Leatherman, Eds.). Academic Press, San Diego.

Newell, W. L., Prowell, D., Krantz, D., Powars, D., Mixon, R., Stone, B., and Willlard, D. (In Review). Surficial Geology and Geomorpholy of the Atlantic Coastal Plain. U.S.G.S. Open File Report.

Newman, W. A., and Rosen, P. S. (1990). Differentiation of tills in the Boston Harbor drumlins. In "5h Annual Boston Harbor/Massachusetts Bay Symposium." pp. 24.

Newman, W. S., Cinquemani, L. J., Pardi, R. R., and Marcus, L. F. (1980). Holocene Delevelling of the United States' East Coast. In "*Earth Rheology, Isostasy and Eustasy.*" (N. Morner, Ed.), pp. 449-463. Wiley, New York.

Newman, W. S., Pardi, R. R., and Fairbridge, R. W. (1987). Some considerations of the compilation of Late Quaternary sea-level curves: a North American perspective. In "*Late Quaternary Sea-Level Correlation and Applications*." (D. B. Scott, P. A. Pirazzoili, and C. A. Honig, Eds.). NATO Advanced Science Institute Series. Kluwer Academic Publishers, Dordrecht.

Niering, W. A., and Warren, R. S. (1980). Vegetation Patterns and Processes in New England Salt Marshes. *Bioscience* 30, 301-307.

Nikitina, D. L., Pizzuto, J. E., Schwimmer, R. A., and Ramsey, K. W. (2000). An updated Holocene sea-level curve for the Delaware coast. *Marine Geology* 124, 137-159.

Nouel, F. N., Berthias, J. P., Deleuze, M., Guitart, A., Laudet, P., Piuzzi, A., Pradines, D., Valorge, C., Dejoie, C., Susini, M. F., and Taburiau, D. (1994). Precise Center National d'Etudes Spatiales orbits for TOPEX/POSEIDON: Is reaching 2 cm still a challenge? *Journal of Geophysical Research* 99, 24405-24420.

Nydick, K. R., Bidwell, A. B., Thomas, E., and Varekamp, J. C. (1995). A Sea-Level Rise Curve from Guilford, Connecticut, USA. *Marine Geology* 124, 137-159.

Oldale, R. N., and O'Hara, C. J. (1980). New radiocarbon dates from the inner continental shelf off southeastern Massachusetts and a local sea-level-rise curve for the past 12,000 years. *Geology* 8, 102-106.

Oldale, R. N., and Barlow, R. A. (1986). Geologic map of Cape Cod and the islands. U.S. Geological Survey Miscellaneous Investigations Series Map I-1763, scale 1:100,000.

Olssen, I. U. (1979). Radiometric Dating. In "*Palaeohydrological changes in the temperate zone in the last 15000 years*." (B. E. Berglund, Ed.). Vol. IGCP Project Guide 2.

Ota, Y., and Yamaguchi, M. (2004). Holocene coastal uplift in the western Pacific Rim in the context of late Quaternary uplift. *Quaternary International* 120, 105-117.

Pardi, R.R., Tomecek, L., and Newman, W.S., (1984). Queens College Radiocarbon Measurements IV. *Radiocarbon*, v. 26, p. 412-430.

Pardi, R. R., and Newman, W. S. (1987). Late Quaternary Sea Levels Along the Atlantic Coast of North-America. *Journal of Coastal Research* 3, 325-330.

Paul, M. A., and Barras, B. F. (1998). A geotechnical correction for post-depositional sediment compression: examples from the Forth valley, Scotland. *Journal of Quaternary Science* 13, 171-176.

Peltier, W. R. (1974). The Impulse Response of a Maxwell Earth. *Reviews of Geophysics and Space Physics* 12, 649-669.

Peltier, W. R. (1990). Glacial Isostatic Adjustment and Relative Sea Level Change. In "*Sea Level Change*." (R. Revelle, Ed.), pp. 73-87. National Academy Press, Washington,

D.C.

Peltier, W. R. (1994). Ice-Age Paleotopography. *Science* 265, 195-201.

Peltier, W. R. (1996). Global sea level rise and glacial isostatic adjustment: An analysis of data from the east coast of North America. *Geophysical Research Letters* 23, 717-720.

Peltier, W. R. (1996). Mantle viscosity and ice-age ice sheet topography. *Science* 273, 1359-1364.

Peltier, W. R. (1998). Postglacial variations in the Level of the Sea. Implications for Climate Dynamics and Solid-Earth Geophysics. *Reviews of Geophysics* 36, 603-689.

Peltier, W. R. (1999). Global sea level rise and glacial isostatic adjustment. *Global and Planetary Change* 20, 93-123.

Peltier, W. R. (2001). Global Glacial Isostatic Adjustment and Modern Instrumental Records of Relative Sea Level History. In "*Sea Level Rise: History and Consequences*." (B. C. Douglas, M. S. Kearney, and S. P. Leatherman, Eds.), pp. 65-95. Academic Press, San Diego.

Peltier, W. R. (2002). On eustatic sea level history: Last Glacial Maximum to Holocene. *Quaternary Science Reviews* 21, 377-396.

Peltier, W. R. (2004). Global glacial isostasy and the surface of the ice-age earth: The ice-5G (VM2) model and grace. *Annual Review of Earth and Planetary Sciences* 32, 111-149.

Peltier, W. R. (2005). On the hemispheric origins of meltwater pulse 1a. *Quaternary Science Reviews* 24, 1655-1671.

Peltier, W. R. (2007). History of Earth Rotation. In "*Treatise on Geophysics v.9*" (G. Schubert, Ed.). Elsevier, Oxford.

Peltier, W. R. (2009). Closure of the budget of global sea level rise over the GRACE era: the importance and magnitudes of the required corrections for global glacial isostatic adjustment. *Quaternary Science Reviews* 28, 1658-1674.

Peltier, W. R., and Andrews, J. T. (1976). Glacio isostatic adjustment I: The forward problem. *Geophysical Journal of the Royal Astronomical Society* 46, 605-646.

Peltier, W.R., Argus, D.F., Drummond, R., Gyllencreutz, R., Mangerud, J., Swensen, J-I and Lohne, O.S. (submitted). Space Geodesy Constrains Ice-Age Terminal Deglaciation.

Peltier, W. R., and Drummond, R. (2008). Rheological stratification of the lithosphere: A direct inference based upon the geodetically observed pattern of the glacial isostatic adjustment of the North American continent. *Geophysical Research Letters 35*, doi:10.1029/2008GL034586.

Peltier, W. R., and Fairbanks, R. G. (2006). Global glacial ice volume and Last Glacial Maximum duration from an extended Barbados sea level record. *Quaternary Science Reviews* 25, 3322-3337.

Peltier, W. R., Farrell, W. E., and Clark, J. A. (1978). Glacial isostasy and relative sea level: a global finite element model. *Tectonophysics* 50, 81-110.

Peltier, W. R., and Jiang, X. H. (1996). Mantle viscosity from the simultaneous inversion of multiple data sets pertaining to postglacial rebound. *Geophysical Research Letters* 23, 503-506.

Peltier, W. R., Shennan, I., Drummond, R., and Horton, B. (2002). On the postglacial isostatic adjustment of the British Isles and the shallow viscoelastic structure of the Earth. *Geophysical Journal International* 148, 443-475.

Peltier, W. R., and Tushingham, A. M. (1989). Global Sea-Level Rise and the Greenhouse-Effect - Might They Be Connected. *Science* 244, 806-810.

Peltier, W. R., and Tushingham, A. M. (1991). Influence of Glacial Isostatic-Adjustment on Tide-Gauge Measurements of Secular Sea-Level Change. *Journal of Geophysical Research-Solid Earth and Planets* 96, 6779-6796.

Pirazzoli, P. A. (1996). "*Sea-Level Changes*." John Wiley & Sons, Chichester, UK.

Pizzuto, J. E., and Schwendt, A. E. (1997). Mathematical modeling of autocompaction of a Holocene transgressive valley-fill deposit, Wolfe Glade, Delaware. *Geology* 25, 57-60.

Psuty, N. P. (1986). Holocene sea level in New Jersey. *Physical Geography* 7, 156-167.

Rahmstorf, S., Cazenave, A., Church, J. A., Hansen, J. E., Keeling, R. F., Parker, D. E., and Somerville, R. C. J. (2007). Recent climate observations compared to projections. *Science* 316, 709-709.

Rampino, M. R., and Sanders, J. E. (1981). Evolution of the barrier islands of southern Long Island, New York. *Sedimentology* 28, 37-47.

Ramsey, K. W., and Baxter, S. J. (1996). Radiocarbon dates from Delaware: A Compilation. Delaware Geological Survey, Newark.

Redfield, A. C. (1958). The Influence of the Continental Shelf on the Tide of the Atlantic Coast of the United-States. *Journal of Marine Research* 17, 432-448.

Redfield, A. C. (1967). Postglacial Change in Sea Level in Western North Atlantic Ocean. *Science* 157, 687.

Redfield, A. C. (1972). Development of a New England Salt Marsh. *Ecological Monographs* 42, 201-&.

Redfield, A. C., and Rubin, M. (1962). Age of Salt Marsh Peat and Its Relation to Recent Changes in Sea Lev at Barnstable Massachusetts. *Proceedings of the National Academy of Sciences of the United States of America* 48, 1728-&.

Reimer, P., and Reimer, R. (2001). A marine reservoir correction database and on-line interface. *Radiocarbon* 43, 461-463.

Reimer, P. J., Baillie, M. G. L., Bard, E., Bayliss, A., Beck, J. W., Bertrand, C. J. H., Blackwell, P. G., Buck, C. E., Burr, G. S., Cutler, K. B., Damon, P. E., Edward, R. L., Fairbanks, R. G., Friedrich, M., Guilderson, T. P., Hogg, A. G., Hughen, K. A., Kromer, B., McCormac, G., Manning, S., Bronk Ramsey, C., Reimer, R. W., Remmele, S., Southon, J. R., Stuiver, M., Talamo, S., Taylor, F. W., van der Plicht, J., and Weyhenmeyer, C. E. (2004). IntCal04 terrestrial radiocarbon age calibration, 0-26 cal kyr BP. *Radiocarbon* 46, 1029-1058.

Renssen, H., Seppa, H., Heiri, O., Roche, D. M., Goosse, H., and Fichefet, T. (2009). The spatial and temporal complexity of the Holocene thermal maximum. *Nature Geoscience* 2, 411-414.

Richardson, C. J., Reiss, P., Hussain, N. A., Alwash, A. J., and Pool, D. J. (2005). The restoration potential of the Mesopotamian marshes of Iraq. *Science* 307, 1307-1311.

Riggs, S., and Belknap, D. F. (1988). Upper Cenozoic processes and environments of continental margin sedimentation: eastern United States. In "*The Atlantic Continental Margin*." (R. E. Sheridan, and J. A. Grow, Eds.). Geological Society of America, Boulder, CO.

Riggs, S. R. (2002). Life at the edge of North Carolina's coastal system: the geologic controls. In "*Life at the Edge of the Sea: Essays on North Carolina's Coast and Coastal Culture*." (C. Beal, and C. Pirioli, Eds.), pp. 63-95. Coastal Carolina Press.

Riggs, S. R., and Ames, D. V. (2003). Drowning of North Carolina: Sea-Level Rise and Estuarine Dynamics. NC Sea Grant Program, Raleigth, NC, publication no. UNC-SC-03-04, 152pp.

Rignot, E., Box, J. E., Burgess, E., and Hanna, E. (2008). Mass balance of the Greenland ice sheet from 1958 to 2007. *Geophysical Research Letters* 35, doi:10.1029/2008GL035417.

Rinterknecht, V. R., Clark, P. U., Raisbeck, G. M., Yiou, F., Bitinas, A., Brook, E. J., Marks, L., Zelcs, V., Lunkka, J. P., Pavlovskaya, I. E., Piotrowski, J. A., and Raukas, A. (2006). The last deglaciation of the southeastern sector of the Scandinavian Ice Sheet. *Science* 311, 1449-1452.

Roe, H. M., and van de Plassche, O. (2005). Modern pollen distribution in a Connecticut saltmarsh: Implications for studies of sea-level change. *Quaternary Science Reviews* 24, 2030-2049.

Rohling, E. J., Grant, K., Hemleben, C., Siddall, M., Hoogakker, B. A. A., Bolshaw, M., and Kucera, M. (2008). High rates of sea-level rise during the last interglacial period. *Nature Geoscience* 1, 38-42.

Rostami, K., Peltier, W. R., and Mangini, A. (2000). Quaternary marine terraces, sea-level changes and uplift history of Patagonia, Argentina: comparisons with predictions of the ICE-4G (VM2) model of the global process of glacial isostatic adjustment. *Quaternary Science Reviews* 19, 1495-1525.

Sabadini, R., Yuen, D. A., and Boschi, E. (1982). Polar Wandering and the Forced Responses of a Rotating, Multilayered, Viscoelastic Planet. *Journal of Geophysical Research* 87, 2885-2903.

Scott, D. B., and Greenberg, D. A. (1983). Relative Sea-Level Rise and Tidal Development in the Fundy Tidal System. *Canadian Journal of Earth Sciences* 20, 1554-1564.

Sella, G. F., Stein, S., Dixon, T.H., Craymer, M., James, T.S., Mazzotti, S. and Dokka, R. (2007). Observation of glacial isostatic adjustment in "stable" North America with GPS.

Geophysical Research Letters 34, doi:10.1029/2006GL027081.

Shaw, J., Gareau, P., and Courtney, R. C. (2002). Palaeogeography of Atlantic Canada 13-0 kyr. *Quaternary Science Reviews* 21, 1861-1878.

Shennan, I. (1980). "Flandrian Sea-level Changes in the Fenland." University of Durham.

Shennan, I. (1982). Interpretation of Flandrian sea-level data from the Fenland, England. *Proceedings of the Geologists' Association* 93, 53-63.

Shennan, I. (1986). Flandrian sea-level changes in the Fenland. II: Tendencies of sea-level movement, altitudinal changes, and local and regional factors. *Journal of Quaternary Science* 1, 155-179.

Shennan, I. (1987). Sea-level changes in the North Sea. In "*Sea-level Changes*." (M. J. Tooley, and I. Shennan, Eds.), pp. 109-151. Basil Blackwell, Oxford.

Shennan, I. (1989). Holocene crustal movements and sea-level changes in Great Britain. *Journal of Quaternary Science* 4, 77-89.

Shennan, I. (2009). From exploration to hypothesis testing - thirty-five years of IGCP sea-level research. IGCP495 Annual Meeting, Myrtle Beach, SC.

Shennan, I., Coulthard, T., Flather, R., Horton, B., Macklin, M., Rees, J., and Wright, M. (2003). Integration of shelf evolution and river basin models to simulate Holocene sediment dynamics of the Humber Estuary during periods of sea-level change and variations in catchment sediment supply. *Science of the Total Environment* 314, 737-754.

Shennan, I., Hamilton, S., Hillier, C., Hunter, A., Woodall, R., Bradley, S., Milne, G., Brooks, A., and Bssett, S. (2006). Relative sea-level observations in western Scotland since the Last Glacial Maximum for testing models of glacial isostatic land movements and ice-sheet reconstructions. *Journal of Quaternary Science* 21, 601-613.

Shennan, I., Hamilton, S., Hillier, C., and Woodroffe, S. (2005). A 16,000-year record of near-field relative sea-level changes, northwest Scotland, United Kingdom. *Quaternary International* 133-34, 95-106.

Shennan, I., and Horton, B. (2002). Holocene land- and sea-level changes in Great Britain. *Journal of Quaternary Science* 17, 511-526.

Shennan, I., Horton, B., Innes, J., Gehrels, R., Lloyd, J., McArthur, J., and Rutherford, M.

(2000). Late Quaternary sea-level changes, crustal movements and coastal evolution in Northumberland, WK. *Journal of Quaternary Science* 15, 215-237.

Shennan, I., Lambeck, K., Horton, B., Innes, J., Lloyd, J., McArthur, J., and Rutherford, M. (2000). Holocene isostasy and relative sea-level changes on the east coast of England. Holocene Land–Ocean Interaction and Environmental Change around the North Sea, 275–298.

Shennan, I., Milne, G., and Bradley, S. (2009). Late Holocene relative land- and sea-level changes: Providing information for stakeholders. *GSA Today* 19, 52-53.

Shennan, I., Peltier, W. R., Drummond, R., and Horton, B. (2002). Global to local scale parameters determining relative sea-level changes and the post-glacial isostatic adjustment of Great Britain. *Quaternary Science Reviews* 21, 397-408.

Sherman, D. J. (2005). North America, Coastal Geomorphology. In "*Encyclopedia of Coastal Science.*" (M. L. Schwartz, Ed.). Springer, Dordrecht, The Netherlands.

Sholtz, C. (2002). "*The Mechanics of Earthquakes and Faulting*." Cambridge University Press, Cambridge.

Siddall, M., Stocker, T. F., and Clark, P. U. (2009). Constraints on future sea-level rise from past sea-level change. *Nature Geoscience* 2, 571-575.

Simpson, M. J. R., Milne, G. A., Huybrechts, P., and Long, A. J. (2009). Calibrating a glaciological model of the Greenland ice sheet from the Last Glacial Maximum to present-day using field observations of relative sea level and ice extent. *Quaternary Science Reviews* 28, 1631-1657.

Skempton, A. W. (1970). The consolidation of clays by gravitational compaction. *Quarterly Journal of the Geological Society of London* 125, 373-412.

Slagle, A.L., Ryan, W.B.F., Carbotte, S.M., Bell, R., Nitsche, F.O. and Kenna, T. (2006). Late-stage estuary infilling controlled by limited accomodation space in the Hudson River. *Marine Geology* 232, 181-202.

Smith, A. J. (1985). A Catastrophic Origin for the Paleovalley System of the Eastern English-Channel. *Marine Geology* 64, 65-75.

Snay, R., Cline, M., Dillinger, W., Foote, R., Hilla, S., Kass, W., Ray, J., Rohde, J., Sella, G., and Soler, T. (2007). Using global positioning system-derived crustal velocities to

estimate rates of absolute sea level change from North American tide gauge records. *Journal of Geophysical Research-Solid Earth* 112, doi:10.1029/2006JB004606.

Spaur, C.C., and Snyder, S.W., 1999, Coastal wetlands evolution at the leading edge of the marine trangression: Jarrett Bay, North Carolina. J*ournal of the Elisha Mitchell Scientific Society*, v. 115, p. 20-46.

Spojlaric, N., and Jordan, R. R. (1966). Generalized Geologic Map of Delaware. Delaware Geological Survey.

Stanley, D. J. (1988). Subsidence in the Northeastern Nile Delta - Rapid Rates, Possible Causes, and Consequences. *Science* 240, 497-500.

Stanley, H. R. (1979). Geos-3 Project. *Journal of Geophysical Research* 84, 3779-3783.

Stocchi, P., and Spada, G. (2009). Influence of glacial isostatic adjustment upon current sea level variations in the Mediterranean. *Tectonophysics* 474, 56-68.

Stone, J. O., Balco, G. A., Sugden, D. E., Caffee, M. W., Sass, L. C., Cowdery, S. G., and Siddoway, C. (2003). Holocene deglaciation of Marie Byrd Land, West Antarctica. *Science* 299, 99-102.

Stuiver, M., and Borns, H.W. (1975). Late Quaternary Marine Invasion in maine: Its Chronology and Associated Crustal Movement. *GSA Bulletin* 86, 99-104.

Stuiver, M., and Daddario, J. J. (1963). Submergence of the New Jersey Coast. *Science* 142, 951.

Stuiver, M., Reimer, P. J., and Reimer, R. (2005). Radiocarbon calibration program revision 5.0.1.

Suess, H. E. (1970). Bristlecone pine calibration of the radiocarbon time-scale 5000 BC to present. In "*Radiocarbon variations and absolute chronology*." (I. U. Olssen, Ed.). John Wiley & Sons, London.

Summerfield, M. A. (1991). "*Global Geomorphology*." Longman, Harlow, England.

Sun, H., Grandstaff, D., and Shagam, R. (1999). Land subsidence due to groundwater withdrawal: potential damage of subsidence and sea level rise in southern New Jersey, USA. *Environmental Geology* 37, 290-296.

Szabo, B. J. (1985). Uranium-Series Dating of Fossil Corals from Marine-Sediments of Southeastern United-States Atlantic Coastal-Plain. *Geological Society of America Bulletin* 96, 398-406.

Tamisiea, M. E., Mitrovica, J. X., Milne, G. A., and Davis, J. L. (2001). Global geoid and sea level changes due to present-day ice mass fluctuations. *Journal of Geophysical Research* 106, 30809-30864.

Tapley, B. D., Ries, J. C., Davis, G. W., Eanes, R. J., Schutz, B. E., Shum, C. K., Watkins, M. M., Marshall, J. A., Nerem, R. S., Putney, B. H., Klosko, S. M., Luthcke, S. B., Pavlis, D., Williamson, R. G., and Zelensky, N. P. (1994). Precision orbit determination for TOPEX/Poseidon. *Journal of Geophysical Research* 99, 24383-24404.

Teal, J., and Peterson, S. (2009). The Use of Science in the Restoration of Northeastern U.S. Salt Marshes. In "*Human Impacts on Salt Marshes: A Global Perspective.*" (B. R. Silliman, E. D. Grosholz, and M. D. Bertness, Eds.). University of California Press, Berkeley.

Teferle, F. N., Bingley, R. M., Orliac, E. J., Williams, D. P., Woodworth, P. L., McLaughlin, D., Baker, T. F., Shennan, I., Milne, G. A., Bradley, S. L., and Hansen, D. N. (2009). Crustal motions in Great Britain: evidence from continous GPS, absolute gravity and Holocene sea level data. *Geophysical Journal International* 178, 23-46.

Thom, B. G., and Chappell, J. (1975). Holocene sea levels relative to Australia. *Search* 6, 90-93.

Thom, B. G., and Roy, P. S. (1985). Relative sea levels and coastal sedimentation in Southeast Australia in the Holocene. *Journal of Sedimentary Research* 55, 257-264.

Thompson, W. B. (2001). Deglaciation of western Maine. In "*Deglacial history and relative sea-level changes, northern New England and adjacent Canada*." (T. K. Weddle, and M. J. Retelle, Eds.). Geological Society of America Special Paper, 351, 109-123.

Thompson, W. G., Varekamp, J. C., and Thomas, E. (2000). Fault motions along the eastern border fault, Hartford Basin, CT, over the past 2800 years. EOS Transactions, American Geophysical Union 1999 Spring Meeting, 80, 18, Supplement, S86.

Thornbury, W. D. (1965). "*Regional Geomorphology of the United States.*" John Wiley & Sons, New York.

Tooley, M. J. (1974). Sea-level changes during the last 9000 years in northwest England.

The Geographic Journal 140, 18-42.

Tooley, M. J. (1978). "*Sea-level changes: northwest England during the Flandrian Stage*." Clarendon Press, Oxford.

Tornqvist, T. E., de Jong, A. F. M., Oosterbaan, W. A., and van der Borg, K. (1992). Accurate dating of organic deposits by AMS 14C measurement of macrofossils. *Radiocarbon* 34, 566-577.

Törnqvist, T., Bick, S., González, J., van der Borg, K., and de Jong, A. (2004). Tracking the sea-level signature of the 8.2 ka cooling event: New constraints from the Mississippi Delta. *Geophysical Research Letters* 31, L23309.

Tornqvist, T. E., Gonzalez, J. L., Newsom, L. A., van der Borg, K., de Jong, A. F. M., and Kurnik, C. W. (2004). Deciphering Holocene sea-level history on the US Gulf Coast: A high-resolution record from the Mississippi Delta. Geological Society of America Bulletin 116, 1026-1039.

Tornqvist, T. E., Bick, S. J., van der Borg, K., and de Jong, A. F. M. (2006). How stable is the Mississippi Delta? *Geology* 34, 697-700.

Tornqvist, T. E., Wallace, D. J., Storms, J. E. A., Wallinga, J., Van Dam, R. L., Blaauw, M., Derksen, M. S., Klerks, C. J. W., Meijneken, C., and Snijders, E. M. A. (2008). Mississippi Delta subsidence primarily caused by compaction of Holocene strata. *Nature Geoscience* 1, 173-176.

Toscano, M. A., and Macintyre, I. G. (2003). Corrected western Atlantic sea-level curve for the last 11,000 years based on calibrated C-14 dates from Acropora palmata framework and intertidal mangrove peat. *Coral Reefs* 22, 257-270.

Tuniz, C., Bird, J. R., Fink, D., and Herzog, G. F. (1998). "*Accelerator Mass Spectrometry: Ultrasensitive Analysis for Global Science.*" CRC Press, Boca Raton, FL.

Turney, C. S. M., and Brown, H. (2007). Catastrophic Early Holocene sea level rise, human migration and the Neolithic transition in Europe. *Quaternary Science Reviews* 26, 2036-2041.

Tushingham, A. M., and Peltier, W. R. (1991). Ice-3G: A New Global Model of Late Pleistocene Deglaciation Based Upon Geophysical Predictions of Post-Glacial Relative Sea Level Change. *Journal of Geophysical Research: Solid Earth* 96, 4497-4523.

Tushingham, A. M., and Peltier, W. R. (1992). Validation of the Ice-3g Model of Wurm-Wisconsin Deglaciation Using a Global Data-Base of Relative Sea-Level Histories. *Journal of Geophysical Research-Solid Earth* 97, 3285-3304.

Uehara, K., Scourse, J. D., Horsburgh, K. J., Lambeck, K., and Purcell, A. P. (2006). Tidal evolution of the northwest European shelf seas from the Last Glacial Maximum to the present. *Journal of Geophysical Research-Oceans* 111, -.

van de Plassche, O. (1979). Sea-level research in the provinces of south Holland, Netherlands. In "*1978 international symposium of coastal evolution in the Quaternary*." pp. 534-551, Sao Paulo, Brazil.

van de Plassche, O. (1980). Compaction and other sourcs of error in obtaining sea-level data: Some results and consequences. *Eiszeitalter und Gegenwart* 30, 171-181.

van de Plassche, O. (1986). "*Sea-level research: a manual for the collection and evaluation of data.*" Geobooks, Norwich.

van de Plassche, O. (1990). Mid-Holocene sea-level change on the eastern shore of Virginia. *Marine Geology* 91, 149-154.

van de Plassche, O. (1991). Late Holocene sea-level fluctuations on the shore of Connecticut inferred from transgressive and regressive overlap boundaries in salt-marsh deposits. *Journal of Coastal Research Special Issue* 11, 159-179.

van de Plassche, O., van der Borg, K., and de Jong, A. F. M. (2002). Relative sea-level rise across the EAstern Border fault (Brandford, Connecticut): evidence against seismotectonic movements. *Marine Geology* 184, 61-68.

van de Plassche, O., van der Borg, K., and de Jonge, A. F. M. (1998). Sea level-climate correlation during the past 1400 yr. *Geology* 26, 319-322.

van Heteren, S., Huntley, D. J., van de Plassche, O., and Lubberts, R. K. (2000). Optical dating of dune sand for the study of sea-level change. *Geology* 28, 411-414.

Velicogna, I. (2009). Increasing rates of ice mass loss from the Greenland and Antarctic ice sheets revealed by GRACE. *Geophysical Research Letters* 36, doi:10.1029/2009GL040222.

Velicogna, I., and Wahr, J. (2002). Post Glacial rebound and Earth's Viscosity Structure From GRACE. *Journal of Geophysical Research* 107, doi:10.1029/2001JB001735.

Velicogna, I., and Wahr, J. (2006). Acceleration of Greenland ice mass loss in spring 2004. *Nature* 443, 329-331.

Vink, A., Steffen, H., Reinhardt, L., and Kaufmann, G. (2007). Holocene relative sea-level change, isostatic subsidence and the radial viscosity structure of the mantle of northwest Europe (Belgium, the Netherlands, Germany, southern North Sea). *Quaternary Science Reviews* 26, 3249-3275.

Virginia Division of Mineral Resources (1993). Geologic map of Virginia. Scale 1:500,000.

Vogel, J. S., Southon, J. R., Nelson, D. E., and Brown, T. A. (1984). Performance of catalytically condensed carbon for use in accerlator mass spectrometry. *Nuclear Instruments and Methods in Physics Research B* 5, 289-293.

Vries, H. L. D. (1958). Variation in concentration of radiocarbon with time and location on earth. *Kon. Ned. Akad. Wetenschap. Proc.* B6, 95-102.

Wahr, J., Molenaar, M., and Bryan, F. (1998). Time-Variability of the Earth's Gravity Field: Hydrological and Oceanic Effects and Their Possible Detection Using GRACE. *Journal of Geophysical Research* 103, 30205-30230.

Wake, L., Milne, G., and Leullette, E. (2006). 20th Century sea-level change along the eastern US: Unravelling the contributions from steric changes, Greenland ice sheet mass balance and Late Pleistocene glacial loading. *Earth and Planetary Science Letters* 250, 572-580.

Walcott, R. I. (1972). Past sea levels, eustasy and deformation of the Earth. *Quaternary Research* 2.

Walker, H. J., and Coleman, J. M. (1987). Atlantic and Gulf Coast province. In "*Geomorphic Systems of North America.*" (W. L. Grad, Ed.), pp. 51-110. Geological Society of America, Boulder, Colorado.

Waller, M. P., and Long, A. J. (2003). Holocene coastal evolution and sea-level change on the southern coast of England: a review. *Journal of Quaternary Science* 18, 351-359.

Watt, D. E., and Ramsden, D. (1964). "*High Sensitivity Counting Techniques*." Pergamon Press, New York.

Widmann, M. (2009). Palaeoclimate: Delayed Holocene warming. *Nature Geoscience* 2, 380-381.

Willis, J. K., Chambers, D. P., and Nerem, R. S. (2008). Assessing the globally averaged sea level budget on seasonal to interannual timescales. *Journal of Geophysical Research-Oceans* 113, doi:10.1029/2007JC004517.

Wilson, G. P., Lamb, A. L., Leng, M. J., Gonzalez, S., and Huddart, D. (2005). Variability of organic delta C-13 and C/N in the Mersey Estuary, UK and its implications for sea-level reconstruction studies. *Estuarine Coastal and Shelf Science* 64, 685-698.

Winker, C.D., and Howard, J.D. (1977). Correlation of tectonically deformed shorelines on the southern Atlantic Coastal Plain. *Geology* 5, 123-127.

Winkler, M. G. (1992). Development of parabolic dunes and interdunal wetlands in the Provincelands, Cape Cod National Seashore. In "*Quaternary Coasts of the United States: Marine and Lacustrine Systems*." (C. H. Fletcher, and J. F. Wehmiller, Eds.), pp. 57-64. SEPM, Tulsa, Oklahoma.

Wolf, D., Klemann, V., Wunsch, J., and Zhang, F. P. (2006). A reanalysis and reinterpretation of geodetic and geological evidence of glacial-isostatic adjustment in the Churchill region, Hudson Bay. *Surveys in Geophysics* 27, 19-61.

Wood, M. E., Kelley, J. T., and Belknap, D. F. (1989). Patterns of Sediment Accumulation in the Tidal Marshes of Maine. *Estuaries* 12, 237-246.

Woodroffe, S. A. (2006). "Holocene relative sea-level changes in Cleveland Bay, North Queensland, Australia." Durham University.

Woodroffe, S. A., and Horton, B. P. (2005). Holocene sea-level changes in the Indo-Pacific. *Journal of Asian Earth Sciences* 25, 29-43.

Woodworth, P. L., and Player, R. (2003). The Permanent Service for Mean Sea Level: An Update to the 21st Century. *Journal of Coastal Research* 19, 287-295.

Woodworth, P. L., Shaw, S. M., and Blackman, D. L. (1991). Secular Trends in Mean Tidal Range around the British-Isles and Along the Adjacent European Coastline. *Geophysical Journal International* 104, 593-609.

Wu, P., and Peltier, W. R. (1983). Glacial Isostatic-Adjustment and the Free Air Gravity-Anomaly as a Constraint on Deep Mantle Viscosity. *Geophysical Journal of the Royal*

Astronomical Society 74, 377-449.

Yamaguchi, H., Yoshinori, O., and Kogure, K. (1985). Volume change characteristics of undisturbed fibrous peat. *Soils and Foundations* 25, 119-134.

Yin, J. J., Schlesinger, M. E., and Stouffer, R. J. (2009). Model projections of rapid sea-level rise on the northeast coast of the United States. *Nature Geoscience* 2, 262-266.

Yokoyama, Y., Esat, T. M., and Lambeck, K. (2001). Late glacial sea-level change deduced from uplifted coral terraces of Huon Peninsula, Papua New Guinea. Quaternary International 83, 275-283.

Yokoyama, Y., Lambeck, K., De Deckker, P., Johnston, P., and Fifield, L. K. (2000). Timing of the Last Glacial Maximum from observed sea-level minima. *Nature* 406, 713-716.

Yu, S. Y., Berglund, B. E., Sandgren, P., and Lambeck, K. (2007). Evidence for a rapid sea-level rise 7600 yr ago. *Geology* 35, 891-894.

Ziegler, P. A. (1982). Faulting and Graben Formation in Western and Central-Europe. *Philosophical Transactions of the Royal Society of London Series a-Mathematical Physical and Engineering Sciences* 305, 113-143.

Zong, Y., and Tooley, M. J. (1996). Holocene sea-level changes and crustal movements in Morecambe Bay, NW England. *Journal of Quaternary Science* 11, 430-458.

Zong, Y. Q. (2004). Mid-holocene sea-level highstand along the southeast coast of China. *Quaternary International* 117, 55-67.

Index